DOCTOR OF PHILOSOPHY

The Synthesis of Biologically Active Guanidines

Harper, Philip

Award date:
2016

Awarding institution:
Bangor University

The Synthesis of Biologically Active Guanidines

A thesis presented for the degree of

Doctor of Philosophy

in the

School of Chemistry

by

Philip Mark Harper

Prifysgol Bangor University

Declaration and Consent

Details of the Work

I hereby agree to deposit the following item in the digital repository maintained by Bangor University and/or in any other repository authorized for use by Bangor University.

Author Name: ……

Title: ……..……..……

Supervisor/Department: .....

Funding body (if any): .....

Qualification/Degree obtained: ……

This item is a product of my own research endeavours and is covered by the agreement below in which the item is referred to as "the Work". It is identical in content to that deposited in the Library, subject to point 4 below.

Non-exclusive Rights

Rights granted to the digital repository through this agreement are entirely non-exclusive. I am free to publish the Work in its present version or future versions elsewhere.

I agree that Bangor University may electronically store, copy or translate the Work to any approved medium or format for the purpose of future preservation and accessibility. Bangor University is not under any obligation to reproduce or display the Work in the same formats or resolutions in which it was originally deposited.

Bangor University Digital Repository

I understand that work deposited in the digital repository will be accessible to a wide variety of people and institutions, including automated agents and search engines via the World Wide Web.

I understand that once the Work is deposited, the item and its metadata may be incorporated into public access catalogues or services, national databases of electronic theses and dissertations such as the British Library's EThOS or any service provided by the National Library of Wales.

I understand that the Work may be made available via the National Library of Wales Online Electronic Theses Service under the declared terms and conditions of use (http://www.llgc.org.uk/index.php?id=4676). I agree that as part of this service the National Library of Wales may electronically store, copy or convert the Work to any approved medium or format for the purpose of future preservation and accessibility. The National Library of Wales is not under any obligation to reproduce or display the Work in the same formats or resolutions in which it was originally deposited.

Statement 1:

This work has not previously been accepted in substance for any degree and is not being concurrently submitted in candidature for any degree unless as agreed by the University for approved dual awards.

Signed …….. (candidate)

Date ……..

Statement 2:

This thesis is the result of my own investigations, except where otherwise stated. Where correction services have been used, the extent and nature of the correction is clearly marked in a footnote(s).

All other sources are acknowledged by footnotes and/or a bibliography.

Signed ……. (candidate)

Date …….

Statement 3:

I hereby give consent for my thesis, if accepted, to be available for photocopying, for inter-library loan and for electronic storage (subject to any constraints as defined in statement 4), and for the title and summary to be made available to outside organisations.

Signed ……. (candidate)

Date …….

Statement 4:

Choose **one** of the following options

a) I agree to deposit an electronic copy of my thesis (the Work) in the Bangor University (BU) Institutional Digital Repository, the British Library ETHOS system, and/or in any other repository authorized for use by Bangor University and where necessary have gained the required permissions for the use of third party material.	
b) I agree to deposit an electronic copy of my thesis (the Work) in the Bangor University (BU) Institutional Digital Repository, the British Library ETHOS system, and/or in any other repository authorized for use by Bangor University when the approved **bar on access** has been lifted.	
c) I agree to submit my thesis (the Work) electronically via Bangor University's e-submission system, however I **opt-out** of the electronic deposit to the Bangor University (BU) Institutional Digital Repository, the British Library ETHOS system, and/or in any other repository authorized for use by Bangor University, due to lack of permissions for use of third party material.	

Options B should only be used if a bar on access has been approved by the University.

In addition to the above I also agree to the following:

1. That I am the author or have the authority of the author(s) to make this agreement and do hereby give Bangor University the right to make available the Work in the way described above.

2. That the electronic copy of the Work deposited in the digital repository and covered by this agreement, is identical in content to the paper copy of the Work deposited in the Bangor University Library, subject to point 4 below.

3. That I have exercised reasonable care to ensure that the Work is original and, to the best of my knowledge, does not breach any laws – including those relating to defamation, libel and copyright.

4. That I have, in instances where the intellectual property of other authors or copyright holders is included in the Work, and where appropriate, gained explicit permission for the inclusion of that material in the Work, and in the electronic form of the Work as accessed through the open access digital repository, *or* that I have identified and removed that material for which adequate and appropriate permission has not been obtained and which will be inaccessible via the digital repository.

5. That Bangor University does not hold any obligation to take legal action on behalf of the Depositor, or other rights holders, in the event of a breach of intellectual property rights, or any other right, in the material deposited.

6. That I will indemnify and keep indemnified Bangor University and the National Library of Wales from and against any loss, liability, claim or damage, including without limitation any related legal fees and court costs (on a full indemnity bases), related to any breach by myself of any term of this agreement.

Signature: …… Date : …….

Contents

Acknowledgements

I would firstly like to thank my supervisor Dr Paddy Murphy for his invaluable help, support and patience over the duration of my BSc, MSc and during my PhD and for the write up period for this thesis. I would also like to thank all members of the research group especially Matthew Buck and Dr Dan Evans for their technical input and for the fun we have had over the past few years. Thanks must also go to Dr M. Jaffar at Morvus Technology Ltd for the help and support early in the PhD project. Thanks also go to Morvus and the ESF for making this PhD position possible through their funding. I would also like to thank the support staff at Bangor University including the general office staff and the technicians, especially Gwynfor Davies for the loan of glassware and chemicals, often at a second's notice.

A special thank you must also go to Prof Roberto Berlinck at the University of Sao Paulo for giving me the opportunity to synthesise two new natural products and to Professor Tempone who evaluated one of them against various diseases.

In addition I would like to thank my family and friends for their support and friendship during this project.

Finally I would like to say thank you to my wife Enlli and to my daughter Lois for your help, encouragement and support during my PhD.

Abstract

Several new alkyl (**147**, **161** and **167**) and alkoxy-methyl derivatives (**171**, **175**) were prepared as analogues of the anti-tumour agent tirapazamine (**38**). These were prepared in an attempt to couple them to the pro-drug delivery agent **52**.

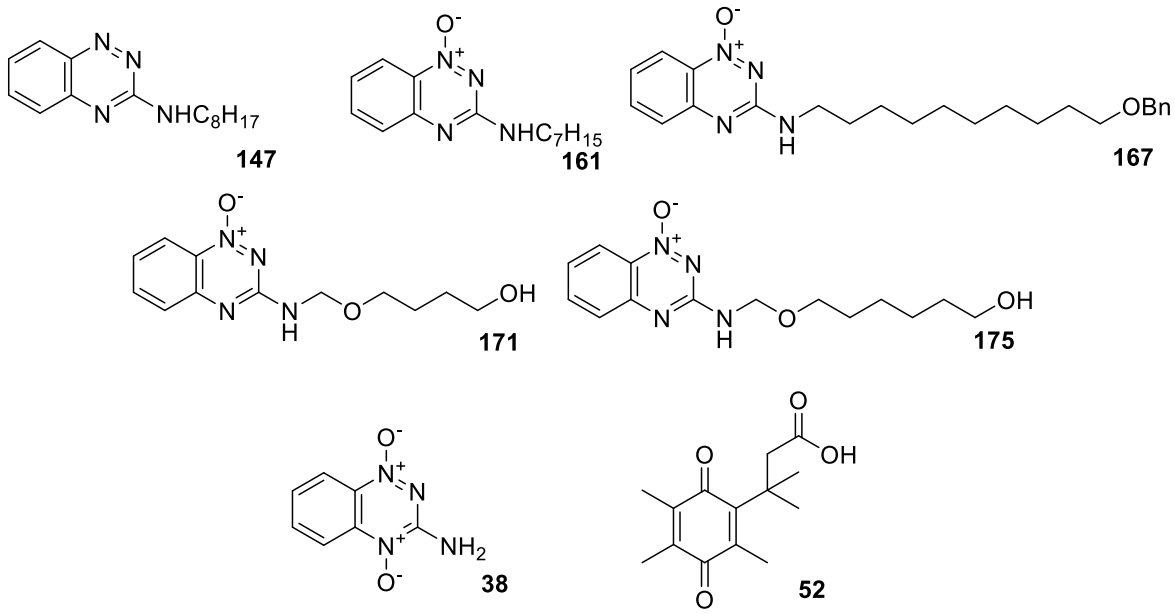

The bicyclic guanidine natural product monalidine A (**186**) was prepared as its hydrochloride salt from 2-undecanone *via* a novel 3-step synthesis. The biological activity of monalidine A (**186**) and one of its synthetic precursors were evaluated against *Leishmaniasis infantum* and *Trypanosoma cruzi*. Research towards the total synthesis of the tricyclic arbusculidine A (**187**) from cucumber aldehyde is reported.

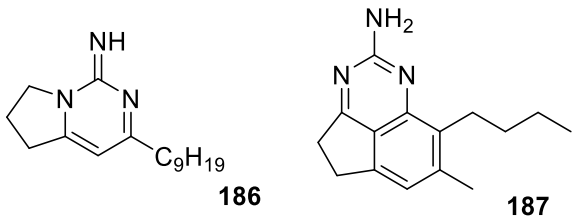

Abbreviations

Ac	Acetyl
ADEPT	Antibody-directed enzyme pro-drug therapy
ATP	Adenosine triphosphate
b	Broad
Bn	Benzyl
Caco-2 cells	Heterogeneous human epithelial colorectal adenocarcinoma cells
d	Doublet
DCC	*N*,*N*'-Dicyclohexylcarbodiimide
DCU	Dicyclohexylurea
DEAD	Diethyl azodicarboxylate
DIBAL	Diisobutylaluminium hydride
DIPEA	Diisopropylethylamine
DMAP	4-Dimethylaminopyridine
DMF	Dimethylformamide
DMSO	Dimethyl sulfoxide
DNA	Deoxyribonucleic acid
EDC	1-Ethyl-3-(3-dimethylaminopropyl) carbodiimide
EtOAc	Ethyl acetate
GDEPT	Gene-directed enzyme pro-drug therapy
HIV	Human immunodeficiency virus
IMS	Industrial methylated spirits
IR	Infrared spectroscopy
J	Coupling constant
KHT Tumour	Kinase Human T cell
LAH	Lithium aluminium hydride
μM	Micromolar
m	Multiplet
MEK	methylethylketone
MeOH	Methanol

m.p.	Melting point
MS	Mass spectrometry
NADPH	Nicotinamide adenine dinucleotide phosphate
NBS	*N*-Bromosuccinimide
NCS	*N*-Chlorosuccinimide
NCTC cells	Mouse fibroblast cells
NHS	*N*-Hydroxysuccinimide
NMR	Nuclear magnetic resonance
PCC	Pyridinium chlorochromate
PFP	Pentafluorophenol
PPTS	Pyridinium *p*-toluenesulfonate
PTSA	*p*-Toluenesulfonic acid monohydrate
Py	Pyridine
q	Quartet
RNA	Ribonucleic acid
s	Singlet
succ	Succinimide
t	Triplet
TAP	Tumour activated pro-drug
TBAF	Tetra-*n*-butylammonium fluoride
t-BuOK	Potassium *tert*-butoxide
THF	Tetrahydrofuran
THP	Tetrahydropyranyl
TLC	Thin layer chromatography
TPZ	Tirapazamine
TsCl	*p*-Toluenesulfonyl chloride
WHO	World Health Organisation

Section A:

Novel Anti Cancer Pro-drugs

1.0 Introduction

1.1 Cancer

Cancer is a leading cause of death globally, accounting for 8.2 million deaths in 2012, with the total number of cases expected to rise from 14 million to 22 million within the next two decades.[1]

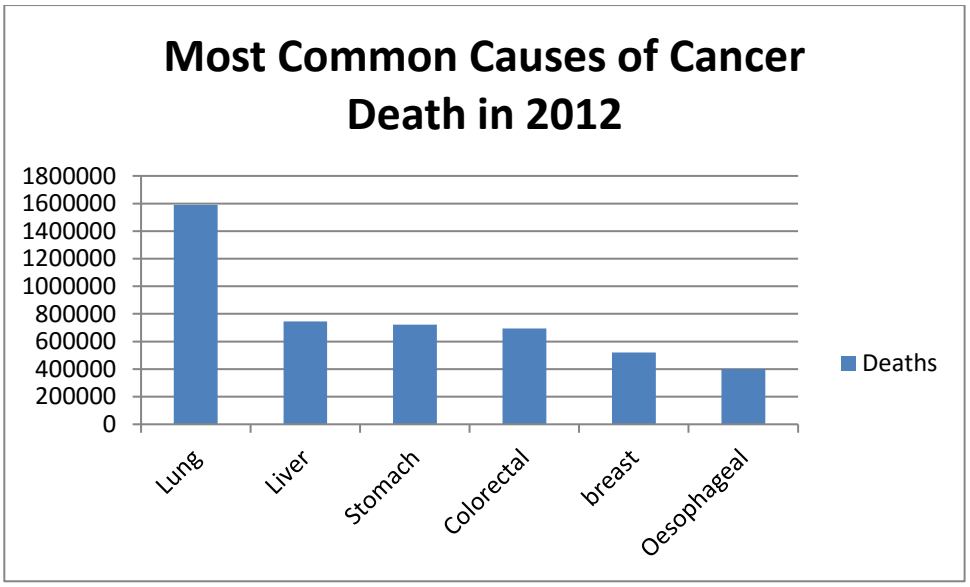

Figure 1. Leading cancer deaths 2012.

According to the World Health Organization, cancer arises from the transformation of a single normal cell into a tumour cell through a multi stage process. As well as being the result of genetic factors, there are three major categories of external agents;

- Ultraviolet and ionizing radiation
- Chemical carcinogens including tobacco smoke and asbestos
- Biological carcinogens including infections caused by viruses, bacteria and parasites

The aim of current cancer treatments is to either cure or treat cancer, prolonging life, while improving the patient's quality of life. The three main treatments for cancer include radiotherapy, surgery and chemotherapy, usually in a combination of the three. This thesis is concerned only with cancer chemotherapy.

1.2 Pro-drug Therapy

Pro-drug technology is a concept that was first proposed by Albert and Harper in the 1950's[2,3]

A pro-drug is a compound that, on administration, must undergo chemical conversion by metabolic processes before becoming an active pharmacological agent. Currently around 10 % of the world's approved medicines can be described as pro-drugs, including the non-steroidal anti-inflammatory drug aspirin (**1**) and the antihistamine fexofenadine (**2**) (Figure 2).

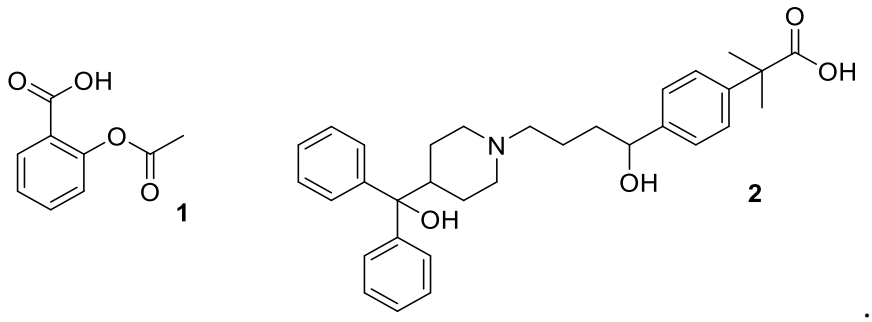

Figure 2. The analgesic aspirin and the antihistamine fexofenadine can be described as pro-drugs.

There are two main classes of pro-drugs: carrier linked pro-drugs and bioprecursor pro-drugs. In the case of carrier linked pro-drugs, the active molecule (the drug) is temporarily linked to a carrier or pro-moiety *via* a bio-reversible covalent linkage. Once inside the body, the carrier linked pro-drug undergoes biotransformation, releasing the parent drug and the carrier. A bioprecursor pro-drug is transformed metabolically by hydration (e.g. lactones), oxidation (e.g. dexpanthenol (**3**)) or reduction (e.g. sulindac (**4**)) to the active agents.[4,5,6]

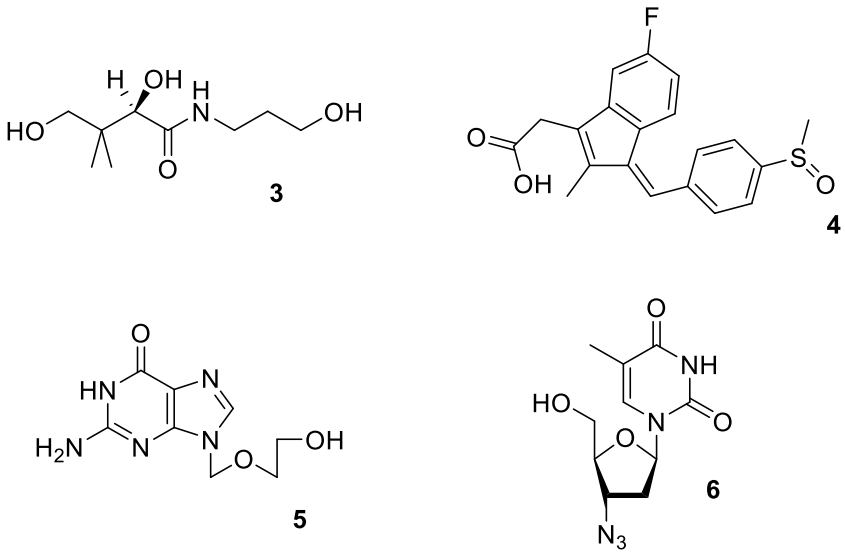

Figure 3. Type I pro-drugs.

Based on the site of conversion into the pharmacologically active agent, the pro-drugs can be additionally classified into two groups.

The first group consists of type I, which are those that are metabolised intracellularly. These can be divided into type IA, for example acyclovir (**5**) and zidovudine (**6**), which are metabolised at the cellular targets of their therapeutic actions, whereas type IB pro-drugs, including carbamazepine (**7**) and primidone (**8**)**,** are converted into parent drugs by specific metabolic tissues such as the liver.

The second group, Type II, are those metabolised extracellularly, and are divided into three groups. Firstly type IIA are metabolised in the milieu of the gastrointestinal fluid, for example loperamide oxide (**9**). Secondly, type IIB are metabolised within the circulatory system and/or other extracellular fluid compartments, for example aspirin (**1**) and bambuterol (**10**). Lastly type IIC are metabolised near or inside the therapeutic target cells, including XP-23829 (**11**).

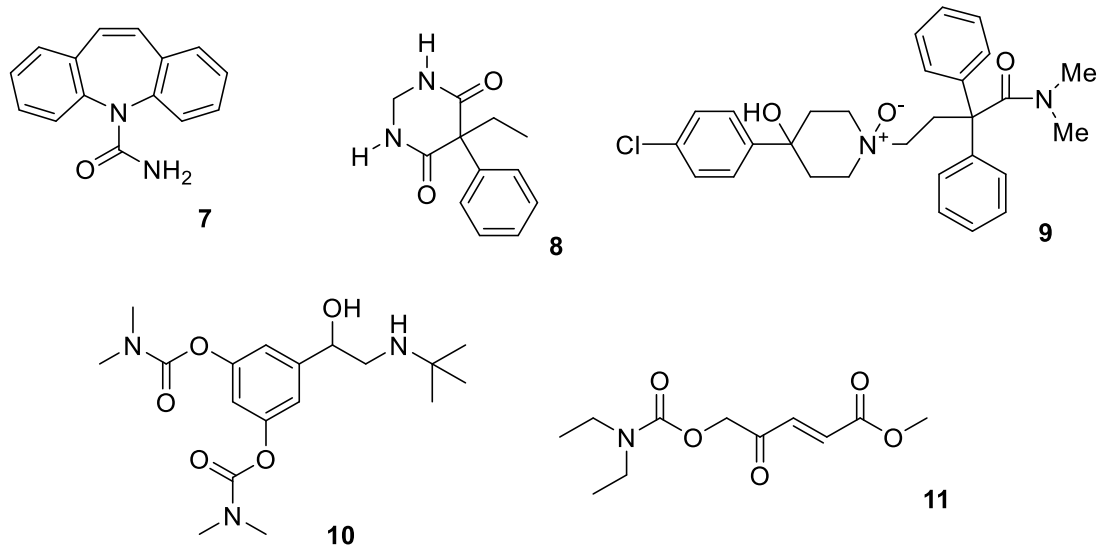

Figure 4. Type II pro-drugs.

Esters of active agents with carboxyl, hydroxyl or thiol functionalities and phosphate esters of hydroxyl or amine functionalities are the most commonly used pro-drugs. Approximately half of the pro-drugs currently available on the market are activated *via* enzymatic hydrolysis by the ubiquitous esterases that are present throughout the body.[4,7]

1.3. Pro-drugs in Cancer Chemotherapy

Chemotherapy is one of the primary treatments for cancer. The majority of anticancer drugs currently in use inhibit proliferation or arrest the cell cycle at a certain phase. Existing oncostatic drugs show poor selectivity, and as a consequence affect not only neoplastic cells but also rapidly proliferating normal cells, including the bone marrow, gut and hair follicles. The lack of selectivity and associated toxicity of anticancer drugs reduces their effectiveness for long term use.

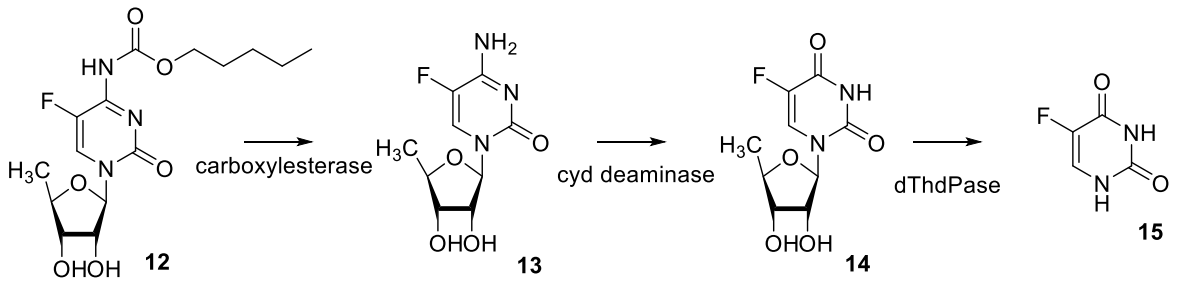

Scheme 1. The activation of capecitabine (**12**) in neoplastic cells.

One promising approach to producing more effective and selective cancer chemotherapy agents is to utilise pro-drug technology. An anticancer pro-drug should be transported to neoplastic cells, where it will undergo transformation by native or recombinant enzymes.[8] Capecitabine (**12**) is a triple pro-drug of 5-fluorouracil (**15**) approved for the therapy of solid tumours, including breast cancer and colorectal cancer, and may be considered a pioneer of anticancer pro-drugs.[4] Following oral administration, capecitabine (**12**) is rapidly and extensively absorbed then metabolised by hepatic carboxyesterases, giving 5-deoxy-5-fluorocytidine (**13**). This intermediate is then converted into 5-fluorouridine (**14**) by cytidine deaminase in the liver and tumour tissues, which is in turn eventually converted by thymine phosphoylases in the tumour tissue into highly cytotoxic 5-fluorouracil (**15**).[9]

Anticancer pro-drugs can be designed to target specific molecules that are overexpressed in tumour cells in comparison to normal cells including:-

- Enzyme-activated pro-drugs antibody-directed enzyme pro-drug therapy (ADEPT) and gene-directed enzyme pro-drug therapy (GDEPT).
- Targeting ligand-conjugating pro-drugs, antibody-drug conjugates, peptide-drug conjugates, aptamer-drug conjugates and folic acid-drug conjugates
- Enzyme cleavable pro-drugs
- Membrane transporter associated pro-drugs
- Polymeric pro-drugs

The work described in this thesis relates to hypoxia-selective tumour activated pro-drugs (known as hypoxia-TAP).

1.4. Tumour Activated Anti-cancer Pro-drugs

There are several classes of tumour activated pro-drugs (TAPs) which have been explored as anti-cancer agents. Each of these classes is activated by reductases present under hypoxic conditions (Scheme 2).

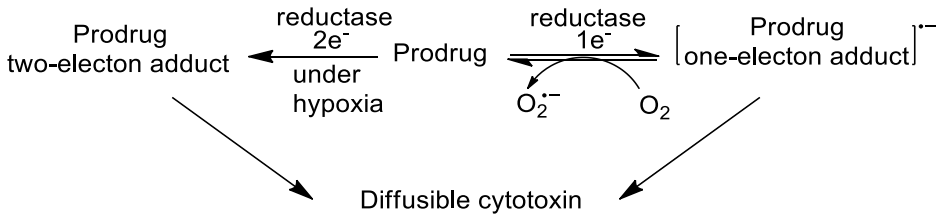

Scheme 2. Typical hypoxic reduction of tumour activated pro-drugs.

1.4.1. Quinones

Quinones were amongst the earliest compounds explored as hypoxia selective TAP, and are known to undergo single-electron reduction by cytochrome C P-450, the cytochrome reductase giving the semiquinone radical.[10] This anionic radical is oxidized back to the quinone by molecular oxygen in normal healthy perfused cells, allowing for increased selectivity.

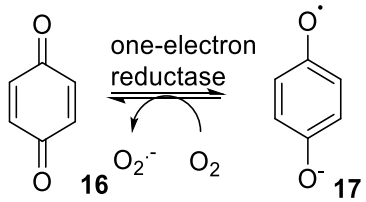

Figure 5. The oxidation of the semiquonone radical with molecular oxygen.[10]

Early studies explored the use of leaving groups on the 2-position with the aim of producing reactive quinone methide intermediates. Compounds such as 2-(hydroxymethyl)-1,4-napthoquone *N*-methylcarbamate (**18**) and more recent analogues such as (**19**) have shown poor hypoxic selectivity (Figure 6).[11]

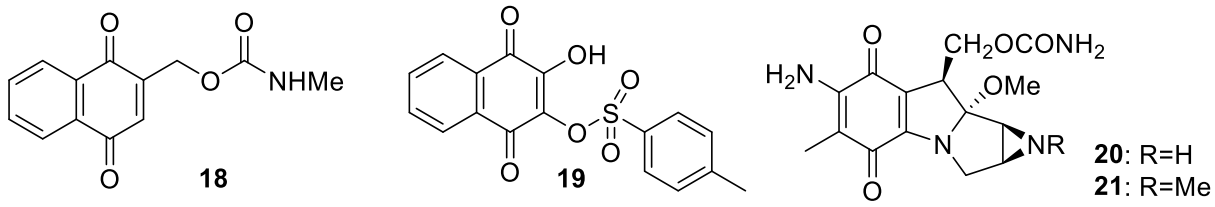

Figure 6. Examples of tumour activated quinones.

However, the first clinical agent identified as a hypoxic selective TAP was the natural product mitomycin C (**20**), although only slight hypoxic selectivity was observed.[11,12] Porfiromycin (**21**), an analogue of (**20**), displayed much higher levels of selectivity, with cytotoxicity being produced by a fragmentation process following reduction, which leads to cross-linked DNA *via* two guanine bases.[13] A clinical study found porformomycin (**21**) to be useful when used in conjunction with radiotherapy in head and neck cancer.[14] A potential drawback, however, is that quinones are good substrates for two electron reductases including DT diphosphorase (DTD, NQO1 and NAD(P)H) which may result in the non-selective conversion to the active agent. Aziridinylquinones such as diaziquone (AZQ) (**22**), which are simple analogues of (**20**), appear to be activated primarily by DTD (Figure 7).

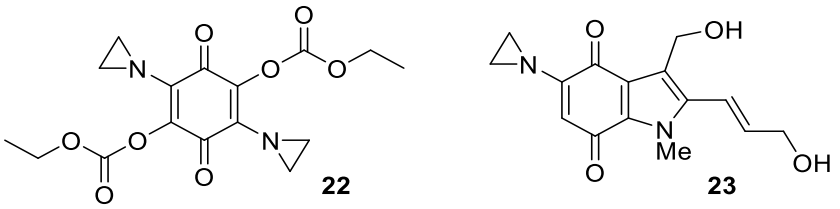

Figure 7. Further tumour activated anticancer pro-drugs.

In a similar series of analogues, there appeared to be a correlation between the rate of reduction and an increase in cytotoxicity in HT-29 cells.[15] As a result a large amount of study was conducted into utilizing DTD (an enzyme which is over-expressed in some tumours) to activate quinone-based drugs. The best example of these drugs is indoloquinone EO9 (**23**). However, clinical testing of EO9 yielded disappointing results attributed to varying activity levels of DTD in clinical tumours, as well as the short half-life of the active drug.[11,16,17]

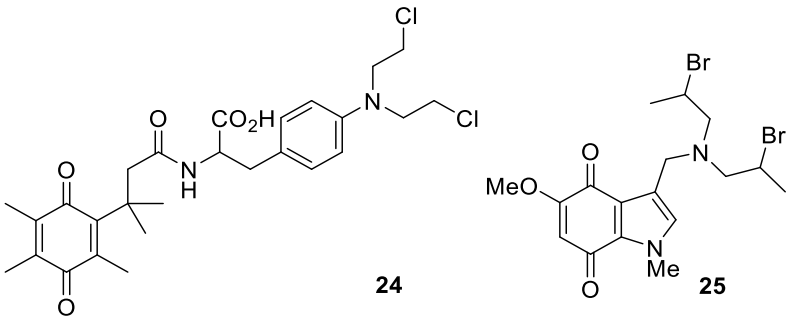

Figure 8. Further tumour activated quinone anticancer pro-drugs.

In the past, quinones have also been used as triggers to release active drugs (effectors).[11,18] Compounds such as **24** (Figure 8), which expels melphalan (**27**), (a nitrogen mustard) *via* reductively-induced cyclolactonisation (Scheme 3), and **25** where reduction causes a direct C-N cleavage resulting in the release of an aliphatic mustard are examples of this triggered release.[11,19]

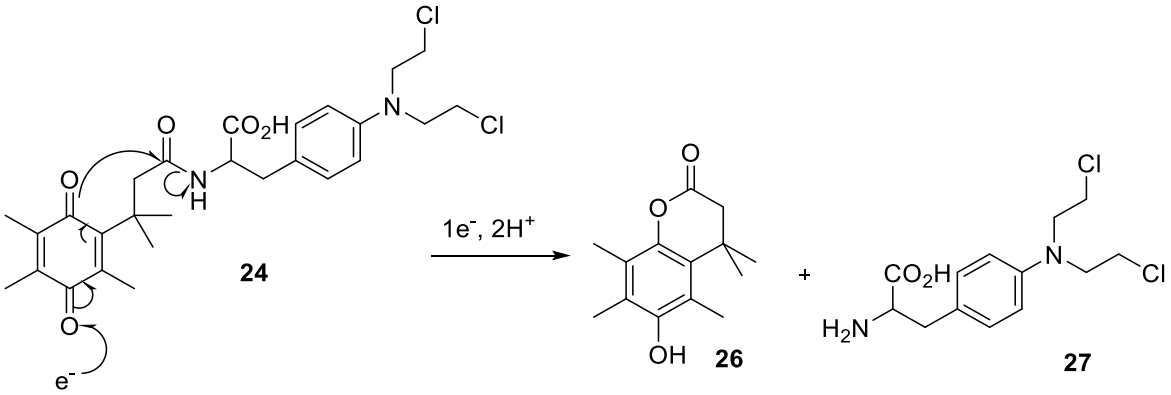

Scheme 3. The reductive release of melphalan from quinone **24**.

1.4.2. Nitroaromatic Compounds

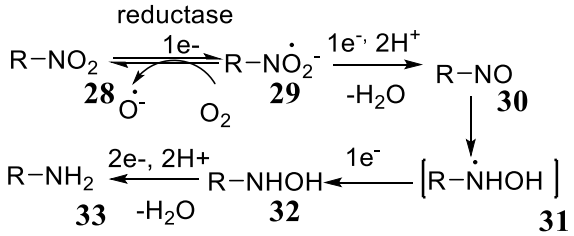

Scheme 4. Mechanistic pathway of the reductive activation for a nitroaromatic drug.

Nitroaromatic compounds were also studied extensively as anti-cancer pro-drugs. These compounds undergo up to six one-electron transfer reductions (Scheme 4). Starting from **28**, the first step gives the nitro-anion radical **29**, which is re-oxidized by the molecular oxygen present in normoxic tissues to regenerate the parent compound. However, in hypoxic

tissue, further reduction processes produce first the nitroso compound **30**, which then is reduced to the hydroxylamine radical **31**, and after subsequent reductions to amine **33**. Amine **33** is the cytotoxic species that is responsible for cell death.[20]

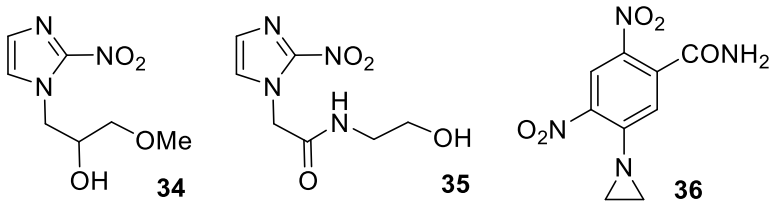

Figure 9. Nitroaromatic anticancer pro-drugs.

Of the nitroaromatic class of pro-drugs, the 2-nitroimidazoles such as misonidazole **34** and etanidazole **35** (Figure 9) have been studied most extensively as oxygen-mimetic radiosensitisers. They are also selectively metabolised under hypoxic conditions to give various ill-defined alkylating species. Unfortunately, they are only weakly cytotoxic and are moderately selective to hypoxic cells of normal oxygenated tissue culture.[21–24] A further nitroaromatic hypoxia- activated pro-drug is dinitrobenzamide 5-(1-aziridinyl)-2,4-dinitrobenzamide (CB1954) (**36**), which has been used widely for gene therapy.[25]

1.4.3. Aliphatic *N*-oxides

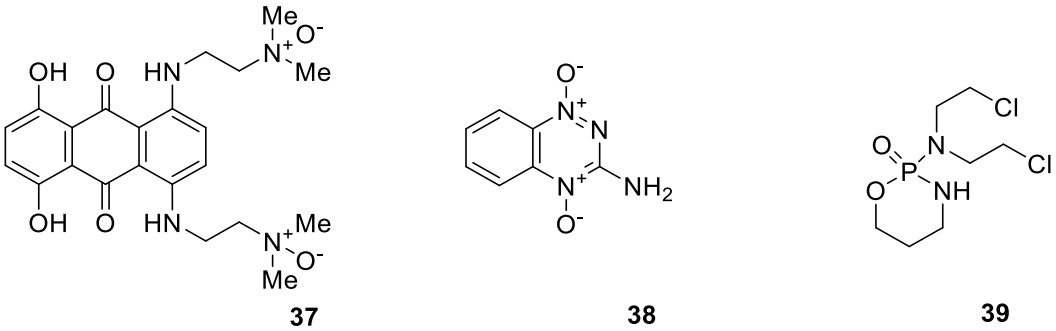

Figure 10. AQ4N, Tirapazamine and cyclophosmamide.

Aliphatic *N*-oxides are among the most widely used anticancer drugs (Figure 10). Polycyclic agents with cationic tertiary amine side chains allow for good cell uptake and binding of DNA. They are excellent cytotoxins, but these properties are dependent on cationic side chains, and are not present in the *N*-oxides.[11, 26] Enzymatic reduction of aliphatic *N*-oxides into the corresponding tertiary amines is inhibited by the presence of

oxygen, possibly due to competition of the drug and oxygen at the active site of the enzyme. Therefore, aliphatic *N*-oxides have been explored extensively as hypoxia selective tumour activated pro-drugs.[27, 28] The drug AQ4N (**37**) (Figure 10) is probably the best representative of the class, but was found to not be significantly active as a sole agent. However, combined with radiation (which kills oxygenated cells) and by increasing the hypoxic fraction of tumours by either clamping blood vessels or by using vasodilators, the drug becomes therapeutically useful.[26] In combination with cyclophosphamide, the effectiveness of **37** against murine tumour models was superior compared to similar combinations of tirapazamine (**38**) and cyclophosphamide (**39**).[29]

Other *N*-oxide derivatives of DNA intercalating agents have been realised as hypoxia selective agents, including nitracine *N*-oxide (**40**) (Figure 11). **40** has a lower DNA-binding efficiency and better distributive properties when compared to nitracine (**41**), which is a very potent cytotoxin with only moderate selectivity.[11,30,31] These improved properties of the *N*-oxide are attributed to it being a *bis*-bioreductive compound requiring two separate reductive steps for full activation. However, **40** was found to have low diffusion rates and low activity against KHT tumours, due to its metabolism, which occurred too rapidly outside the target cells. Studies have been conducted to improve **40** by lowering its reduction potential through chromophore substitution and by changing the steric environment of the *N*-oxide.[32] Neither of these approaches were successful in improving the *in vivo* activity of the drug.[11,33]

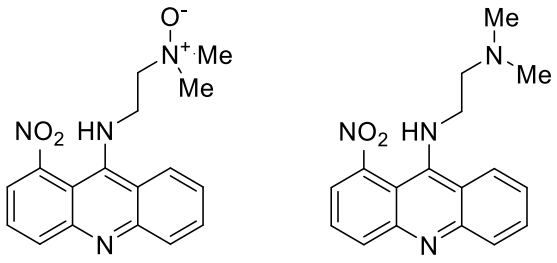

40 **41**

Figure 11. Nitracine *N*-oxide and nitracine.

1.4.4. Aromatic *N*-oxides

Aromatic *N*-oxides are similar to aliphatic *N*-oxides. The cytotoxicity of the drug is masked by being in the *N*-oxide form. The best known example of this class is tirapazamine (**38**), which was probably the first clinically useful tumour-activated pro-drug (see section 1.7).[11,34] Related compounds such as the quinoxalinecarbonitrile 1,4-di-oxides are also potent and highly selective hypoxia specific pro-drugs. In these compounds, for example **42**

to **49** (Figure 12), the nitrogen at the 2-position of the benzotriazaine unit in **36** (TPZ) (Figure 12) is replaced with a C-CN unit. Structural studies which encompassed the relationship between chemical structure and biological activity revealed that hypoxic selectivity is maintained even when the 3-amino group is replaced by H or NHR, but not when replaced with Cl **42**. However, soluble analogues such as **43** remain potent and retain their hypoxic selectivity. The 2-quinoxalinecarbonitrile-1,4-dioxide **45** was found to be relatively potent but not as selective as expected. This low selectivity was thought to be due to the presence of the rigid aniline moiety at the 3 position of the quinoxaline ring. The same effect was noted in the case of arylpiperazines also.[11,35] This type of amine is different from the aliphatic (*N*,*N*-dialkylamino)alkylamino chains present in compounds **46**, **47** and **48** have, in addition shown activity against tuberculosis in in-vitro screens, although it is unclear[5] as to whether their hypoxic selectivity has a part to play in this.[11,35] Other compounds such as the imidazo(1,2-α)quinoxaline *N*-oxides **49** are activated by P450 reductase and cytochrome *b*5 reductase, and lead to DNA strand cleavage.[11,36]

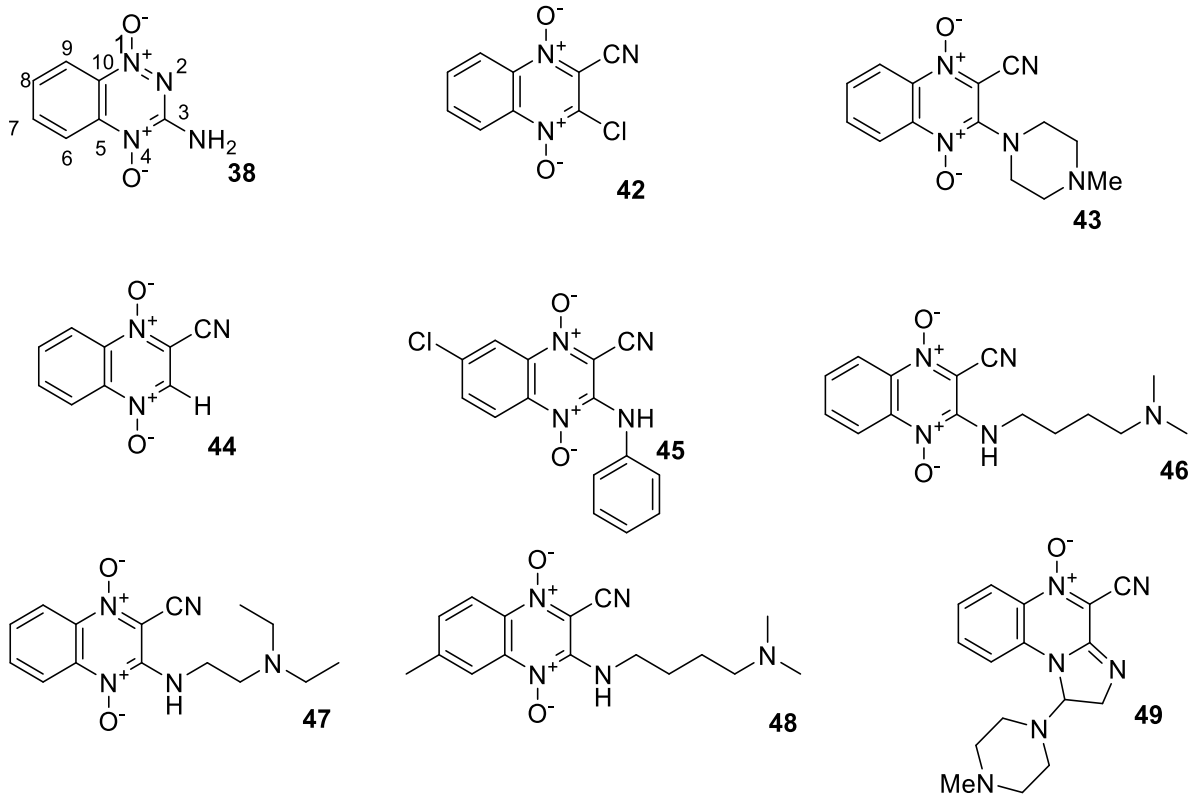

Figure 12. Tirapazamine (**38**) and the quinoxalinecarbonitriles **42-49.**

1.5. Quinone Release Strategies

It has been shown that quinones can undergo a two electron reduction by hQNO1 to form hydroquinones, which are then able to cyclise, leading to the release of a therapeutic

agent which is coupled to the quinone through the carboxylic acid group as an ester or an amide. The basis of the research by the Murphy group[37] follows findings[38] by Milstein and Cohen, who studied the kinetics of lactonisation for a series of *o*-hydroxyhydrocinnamic acids **50a-d** (Table 1).

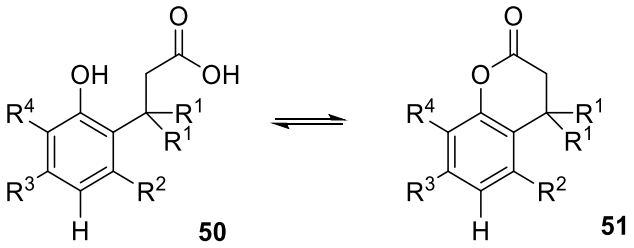

a $R^1 = R^2 = R^3 = R^4 = H$
b $R^1 = H$; $R^2 = R^3 = R^4 = CH_3$
c $R^1 = CH_3$; $R^2 = R^3 = R^4 = H$
d $R^1 = R^2 = R^3 = R^4 = CH_3$

Scheme 5. Lactonisation of o-hydroxyhydrocinnamic acids.[38]

Entry	Compound	No. of methyl groups in trimethyl lock positions	Relative Rate	Lactone (%)*
	50			
1	**A**	0	1	3.6
2	**B**	1	6.7	38.3
3	**C**	2	4.4×10^3	96.2
4	**D**	3	3.4×10^{11}	>99.0

Table 1. Effect of the trimethyl lock on the relative rates of lactonisation
*At 30 °C, in 20% dioxane, μ = 0.3 M.

Their research investigated the effect of structural differences on the rate of lactonisation of the lactone system **50** (Scheme 5).[38] Initially, they found that the addition of methyl substituent at the R^2 position in **50a** to give **50b**, **(**entry 2) resulted in a 6.7 fold increase in the rate of lactonisation when compared to the unsubstituted **50a**. The addition of two methyl substituents at the R^1 position **50c**, (entry 3) had a marked effect, increasing the relative rate of lactonisation by 4.4×10^3 when compared to **50a**. A combination of both

these modifications, in which both the R^1 and R^2 positions **50d**, (entry 4) have methyl substituents, led to a 3.4 x 10^{11} increase in the relative rate of lactonisation when compared to **50a**. This system was referred to as the "trimethyl lock", and its effect on the rate of lactonisation became of great interest as a trigger for molecular release in chemistry, biology, and pharmacology.[39] This effect has its basis in what is variously called the "Thorpe–Ingold effect" or the "*gem*-dimethyl effect" or "angle compression", which is where increasing the size of two substituents on a tetrahedral center leads to enhanced rates of reaction between the other two substituents. The effect was first reported by Beesley, Thorpe and Ingold in 1915 as part of a study of cyclization reactions.[37,40] In the case of the lactones **51** (Scheme 5), this placement of increasing numbers of methyl substituents increases steric crowding, and favours a conformation which is favourable towards the formation of the lactones by cyclisation, in particular for lactone **51d**.[38]

In 1989, Carpino *et al.* studied the cyclisation of esters and amides derived from the acid **52** (Scheme 6). They prepared a number of compounds **52a-f,** which were then reduced with sodium dithionite to give their respective hydroquinone intermediates **53a-f**, which then underwent cyclisation to give the lactone **26**, releasing the molecule "R-H" (Scheme 6).[37]

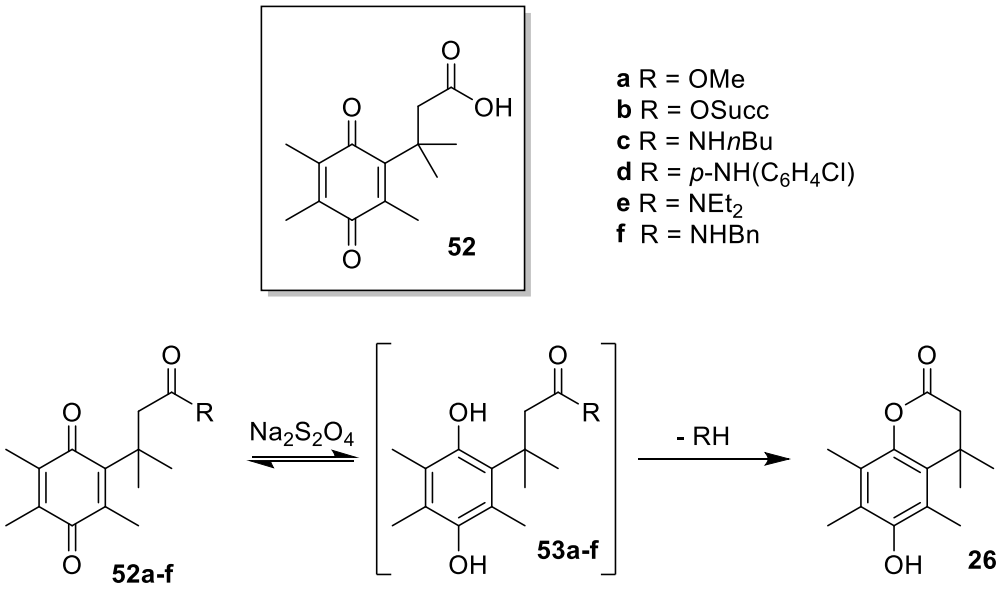

Scheme 6. Reduction of trimethyl-locked quinones to the respective hydroxyquinone and lactone **26**.

All of these compounds showed fast or relatively fast cyclisation half-lives ($t_{1/2}$), which was thought to be due to the presence of the trimethyl lock. Carpino also suggested that if quinones such as **52** were to be used as a drug delivery system (R = drug), the rate of

cyclisation could be tailored to give faster or slower release rates by changing the substituents.[37]

1.5.1. A Redox Activated Drug Delivery System

The release of a drug entity from the benzoquinone **52** has been represented by numerous studies, and forms the basis of this research. Reduction of **52** at the quinone center by a reductase such as hNQO1 results in the production of the hydroquinone **53**, which then undergoes cyclisation to form the lactone **26** and the active drug (Scheme 7).[39]

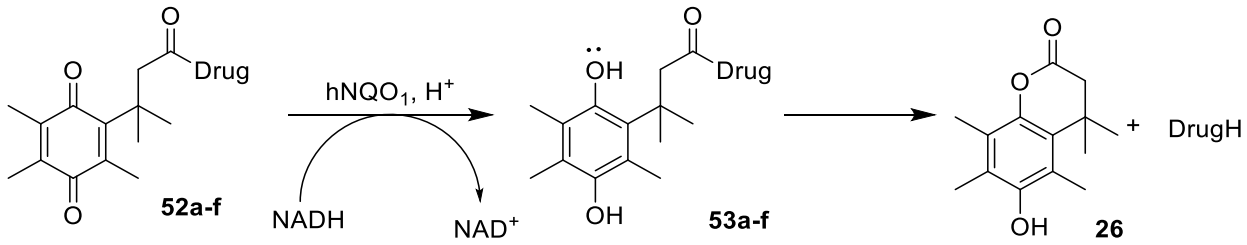

Scheme 7. General enzymatic mechanism of benzoquinone drug delivery system.

Since hNQO1 is overexpressed in hypoxic tumour tissues, it is hoped that the drug will be selectively activated in these regions. However, hNQO1 is also present in many normal cells, including the kidneys, bone marrow and endothelial cells, as well as stomach and bronchial epithelia. This redo benzoquinone drug-delivery system was designed to improve the therapeutic index of a given compound, and should not release the drug unless the quinone 'trigger' is reduced to give the hydroquinone **53**. This increase in selectivity reduces general toxicity and therefore any side effects associated with chemotherapeutic agents.[41] Research has also been carried out to develop protease-,[42] esterase-[43,44] and phosphatase-[43] activated pro-drugs. However, this thesis will focus on redox-activated delivery systems only.

Although many different functional groups have been investigated, our interest lies with mustards and guanidines as the drug substituents, and these will be discussed in the following sections.[37]

1.6. Nitrogen Mustards

The "so-called" nitrogen mustards of the general form **54** were first reported in 1942, and are analogues of the sulfur mustard gas **55**, which was used as a chemical weapon in World War I.[45]

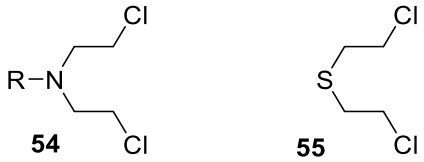

Figure 13. Mustards are powerful DNA alkylating agents.

These mustards are powerful DNA alkylating agents (Scheme 8) and have been extensively used in cancer chemotherapy.[46] Chlorine is a good leaving group, facilitating nucleophilic attack of the nitrogen in the mustard **54**, which cyclises to form an aziridinium ion **57**.[37] This strained three membered ring system readily undergoes alkylation, preferentially at the N-7 position of guanine **56**, to form the monoalkylation adduct **58**.[37] Minor alkylations can also occur at other sites such as the N-3 position of adenine.[37,47] This process is then repeated with the cyclisation of the adduct **58**, to form the aziridinium ion **59**, which undergoes alkylation to give the crosslinked DNA **60**. These bifunctional adducts can generate an interstrand crosslink that is as much as 100 fold more cytotoxic than its monofunctional adduct.[37] Crosslinking can occur between two complementary strands of DNA (interstrand) or on the same strand of DNA (intrastrand) (Figure 19).[37]

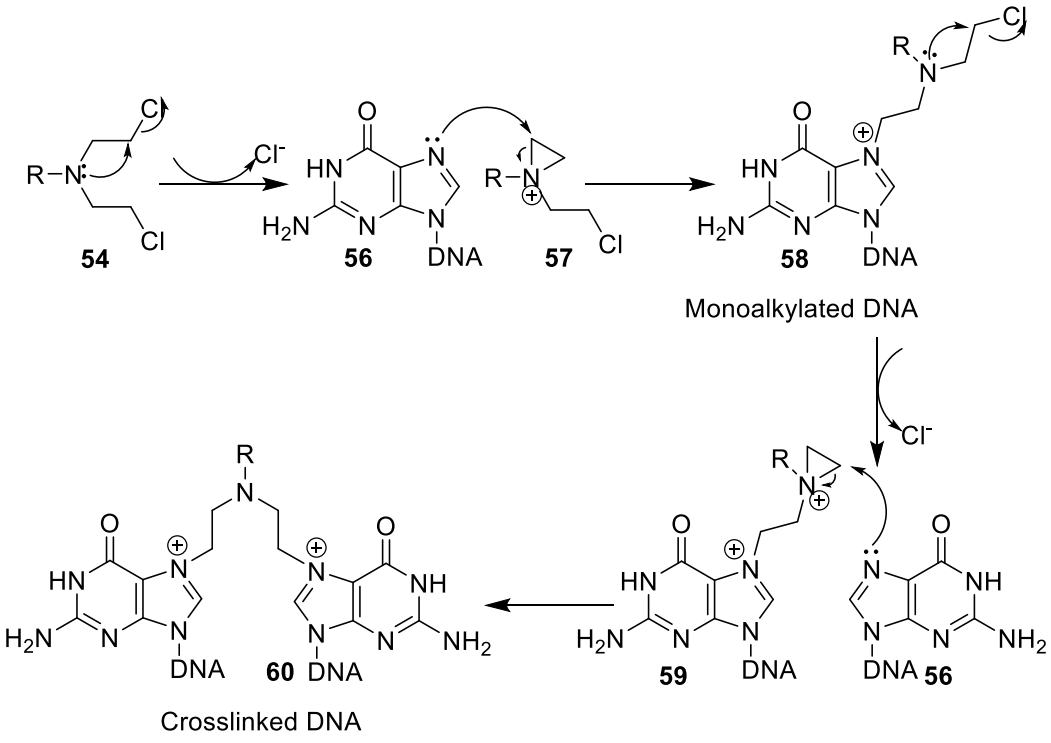

Scheme 8. DNA crosslinking by a nitrogen mustard.

Interstrand crosslinks are essential for maximal cell killing,[37] since they prevent two opposing strands in DNA from separating during replication or transcription. The end result

is the inhibition of DNA synthesis. There has been found to be a direct correlation between interstrand crosslinking and cytotoxicity.[48]

The simplest member of the nitrogen mustard family is mechlorethamine (**61**) (Figure 15)[47], which was the first clinically useful anti-tumour substance.[47] The problem is that mechlorethamine **61** reacts rapidly with biological material and water, making it highly vesicant (causing severe skin, eye and mucosal pain and irritation) and chemically labile. To overcome these problems, the methyl group in **61** has been replaced with an aromatic ring (Figure 16). This lowers its reactivity, giving more time for its absorption and distribution before DNA alkylation and allows for oral administration.

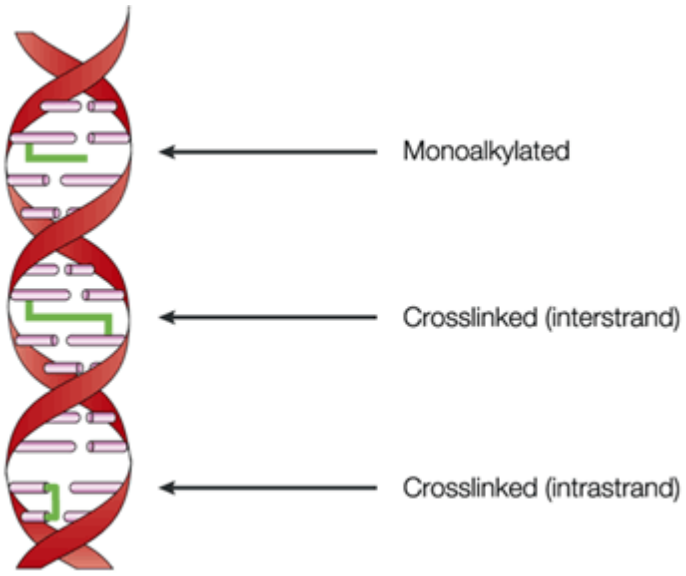

Figure 14. Mustards cause crosslinking between complimentary strands of DNA.[37]

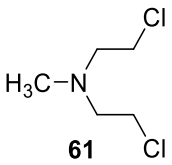

61

Figure 15. The nitrogen mustard mechlorethamine.

However, the simplest aromatic mustard **62** is insoluble in water. Although its carboxylic acid analogue **63** is soluble, it is inactive.[37] To overcome this solubility issue a considerable amount of research has been carried out, developing more water-soluble *N*-mustards.[49,50] It was found that the addition of alkyl spacers gave water-soluble active compounds such as chlorambucil **64** and melphalan **27** (Figure 16).[37]

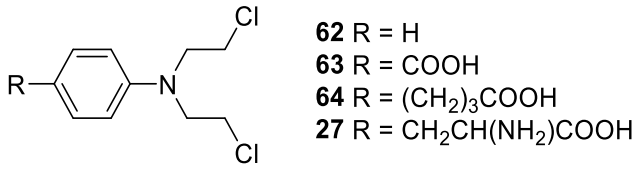

Figure 16. Aromatic nitrogen mustards.

For over 50 years, chlorambucil **64** has been used in the treatment of chronic lympocytic leukemia.[51] Melphalan **27** is used in certain types of bone marrow tumours, including multiple myeloma,[37] and cancers such as ovarian, breast[52] and colorectal.[37,53]

1.6.1. Strategies to Improve the Biological Potential of Mustards

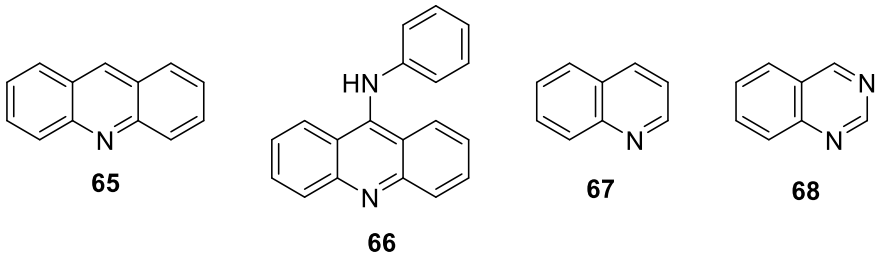

Figure 17. DNA-affinic molecules which have been linked to mustard residues.

Mustard compounds have a number of drawbacks for cancer chemotherapy.[54] Their high reactivity means that they are chemically unstable.[54] This lowers their therapeutic efficacy, since they react with other cellular components such as proteins, inducing severe side effects.[55] One strategy has been to design and synthesise DNA-directed alkylating agents by linking the *N*-mustard residue to DNA-affinic molecules such as acridines **65**[56,56,57], 9- anilinoacridines **66**[54,55,57,58] quinolines **67**[50,59,60] or quinazolines **68**[50] (Figure 17).

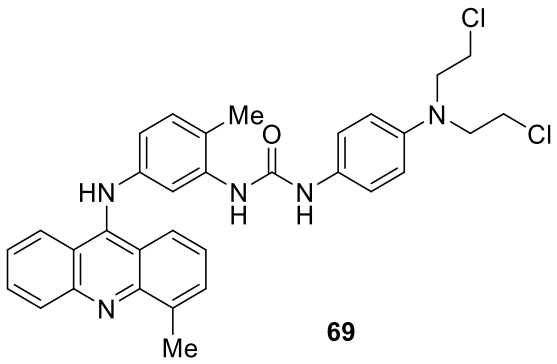

Figure 18. The 9-anilinoacridine *N*-mustard derivative **69**.

These conjugates exhibit higher cytotoxicity and potency than their corresponding untargeted *N*-mustard derivatives.[55] The 9-anilinoacridine derivative **69** (Figure 18) was

found to possess potent therapeutic efficacy against human xenografts *in vivo,* and has the capability to induce DNA interstrand crosslinking in tumour cells[54,61]

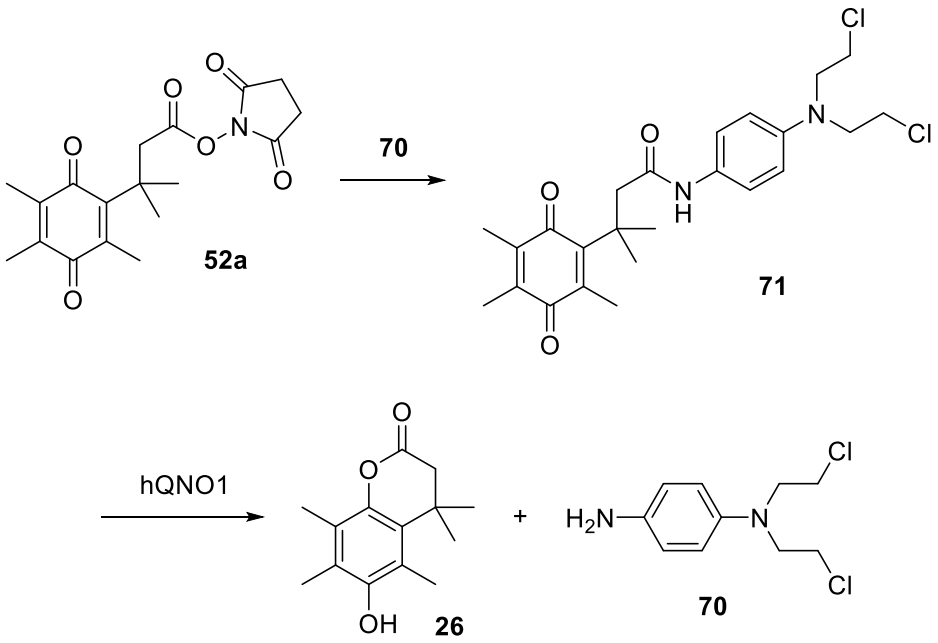

Scheme 9. The synthesis and activation of Volpatos mustard.[41]

Another strategy to minimise side effects is to prepare *N*-mustard pro-drugs,[37,62–66] which can be activated selectively at the tumour site by enzymatic hydrolysis. Previous researchers[67] used the benzoquinone drug delivery system **52** (Scheme 9) to synthesise a methyl ester of melphalan with a trimethyl lock. This was attached *via* an amide linker to the quinone, to give the pro-drug **24**[37,68] and was investigated as a method of increasing the oral absorption of the methyl ester melphalan across the intestine. The uptake, accumulation, activation and transport of the pro-drug **24** was determined using Caco-2 cell monolayers, and results showed potential for improving intestinal drug delivery.[67]

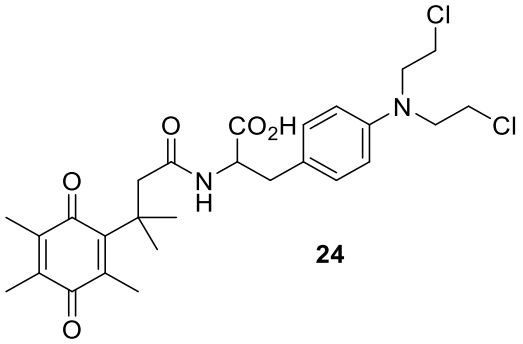

Figure 19. The methyl ester of melphalan with a trimethyl lock.

In 2007 Volpato *et al.* prepared the pro-drug **71** using the aniline mustard **70** according to scheme 9. The pro-drug was obtained by reacting **52** with NHS and DCC to give the activated ester **52a**, which was then reacted with **70** to give the pro-drug **71**. The aim of their experiment was to show that **71** could be reduced by hNQO1 to release the aniline mustard **70**. HPLC of the reaction progress showed that **71** was reduced to give the unstable hydroquinone, which underwent spontaneous cyclisation to produce the lactone **26** and the mustard **70**. Later chemoselectivity studies found **71** to be selectively toxic to cells that overexpress hNQO1.[41]

1.7. Tirapazamine

In 1955[69] Ambramovitch and Schofield reported the use of the Bamberger triazine synthesis to produce benzo-1,2,4-triazines such as **76** (Scheme 10).[69]

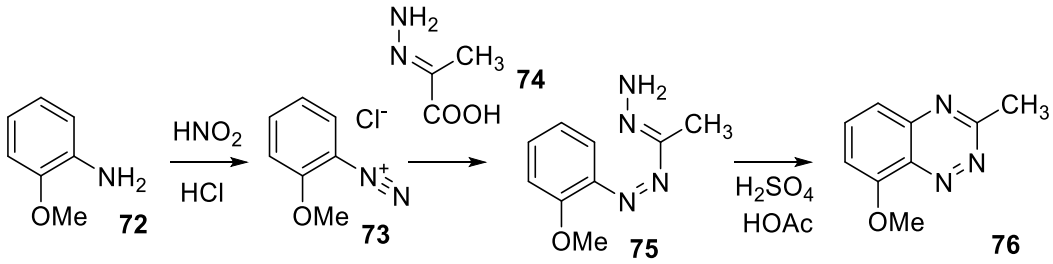

Scheme 10. Bamberger triazine synthesis.

Inspired by the lack of knowledge about the benzotriazines and by the apparent anti-malarial activity and potential antibiotic properties of the 1,2,4-benzotriazines and their *N*-oxides, Schofield reported the synthesis of further substituted 1,2,4-benzotriazines. Around 1957 Schofield undertook experiments which involved the oxidation of benzo-1,2,4-triazines in order to produce the corresponding *N*-oxide derivatives.[70] Schofield found that an amino group must be present on the 3 position in order for oxidation to occur. It was also found that further oxidation of the *N*-oxide **77** with peracetic acid gave the di-oxide which is now known as tirapazamine (**38**).[70]

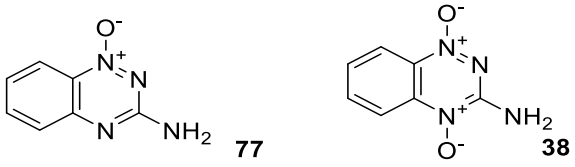

Figure 20. 3-Amino-1,2,4-benzotriazine-1-oxide **77** and TPZ (**38**).

However, it was not until the mid-1980s, that Brown and Lee discovered that TPZ (**38**) killed cancer cells at extremely low concentrations of oxygen, and that its differential selectivity for hypoxic cells over aerobic cells was much larger than that of any other drug at the time. They also showed that the concentration of TPZ required under aerobic conditions to produce equal cell kills was in the range of 50-300 µM compared to that of mitomycin C (**20**) (page 11), which is in the range of 1-5 µM.[34] TPZ (**38**) appears to be a good substrate for a broad range of intercellular reductases that allow for TPZ (**38**) to undergo single electron reductions. This in turn allows for TPZ (**38**) to be protonated, and to produce a neutral radical that is capable of abstracting hydrogen atoms from macromolecules, including DNA, where it results in both single and double strand breaks. However, under aerobic conditions, oxygen can remove the additional electron from the radical, and back-oxidise it to its non-toxic parent molecule TPZ.

TPZ (**38**) has since been the studied in numerous clinical trials as a single agent. Although TPZ (**38**) gave good activities within *in-vitro* studies as a sole agent, poor activities were observed when using TPZ (**38**) as a sole agent in *in-vivo* studies. This is thought to be due to the rapid metabolism of TPZ (**38**) outside the cell nucleus and poor cell penetration. However, in combinations with radiation and cisplatin (**78**), the reported activities in head and neck cancer were encouraging.[72]

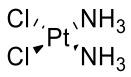

78

Figure 21. Cisplatin (**78**).

Subsequently, a large amount of research to improve the cell penetrative properties of TPZ (**38**) has been conducted.[73]

A study[74] into the benzotriazine-1,4-dioxide series of TPZ analogues demonstrated that neutral non-charged analogues allowed for increased tissue diffusion coefficients, which were measured using multicellular layer cultures of analogues with increased lipophilicity. In the same study[74] an evaluation of a series of 3-aminoalkylamino-benzotriazine-1,4-dioxides was reported, concluding that substituents on the benzene ring of the analogue can be used to predictably tailor the reduction potential. Highest values for hypoxic cytotoxicity ratios were achieved by adding electron-donating substituents to the benzene ring. In addition, compounds such as **79-83** (Figure 21) demonstrated good cell penetration when compared to TPZ, due to an increase in the lipophilic nature of the R group present on the

NH_2.[75] Denny also found that the removal of hydrogen bond donors at the NH-R 3-position could further increase tissue diffusion coefficients, but alkyl substituents such as in **79** raised the reduction potentials. This could be countered further by adding electron donating substituents onto the benzene ring such as in **80** and **83**.[73,75]

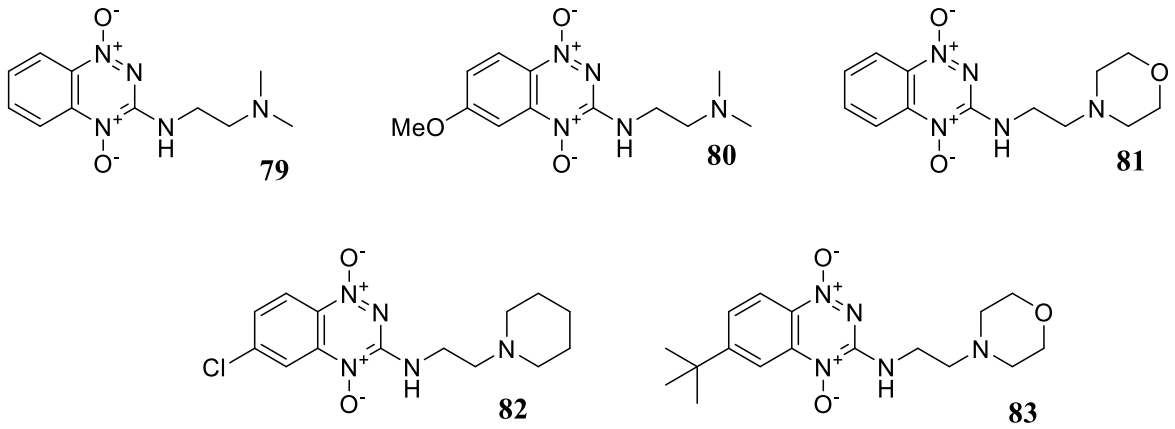

Figure 22. The benzotriazine-1,4-dioxide TPZ analogues reported by Denny.[74]

Denny also reported the preparation of forty novel TPZ analogues which all contained the 1,2,4-benzotriazine core, with the goal of increasing the knowledge of the structure activity relationship (SAR) of these compounds. Various factors were considered, relating to modifications of the triazine-ring substituents and their effect on the 1-electron reduction potential, the overall cytotoxicity, and any hypoxic selectivity.[22] The structures reported by Denny in 2008 were novel tricyclic analogues of TPZ (**38),** with a range of structures incorporating cycloalkyl, oxygen- and nitrogen-containing rings which were fused in a linear or angular fashion to the benzotriazine core (Figure 23). These compounds also contained a range of lipophilic side chains which could be considered neutral and charged at physiological pH. The resulting tirapazamine analogues displayed hypoxia-selective cytotoxicity *in vitro*. The compounds containing fused cycloalkyl rings in combination with either the 3-aminoalkyl or 3-alkyl substituents, such as in **84** were sufficiently electron–donating to allow for the one -electron potential to be in an appropriate range for optimal hypoxic metabolism. The stronger electronic and polar influence of the "oxa" rings (e.g. **85**) were more difficult to balance electronically, which often led to poor reductive properties. The use of amine-containing substituents (e.g. **86**) increased aqueous solubility, but provided either unstable analogues or analogues with only modest activity. The lipophilic nature of the cycloalkyl rings also increased lipophilicity, and led to increased diffusion coefficients, which combined with weakly basic morpholine side chains, gave the best balance of solubility and increased diffusion.

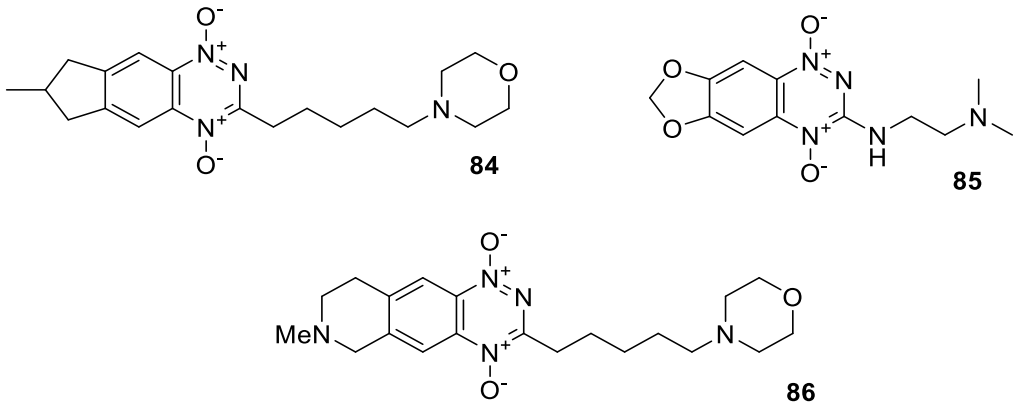

Figure 23. Fused ring derivatives of tirapazamine (**38**).[73]

Analogues **87-96** (Figure 24) were found to give modest cell kill values with high hypoxic cytotoxicity differentials. The analogues all contain solubilising groups that are attached *via* the 3-alkyl substituent or the 7-position of the indane ring. The analogues show improved lipophilic properties, and benefit from balanced electron-donating effects derived from the fused rings.

Following this work, studies by Denny in 2012[76] into multicellular layer culturing of CEN209 (**97**) (Figure 25) demonstrated that it possessed greater diffusion coefficients when compared to TPZ (**38**)**,** indicating greater cell penetrative properties.[76] The morpholine derivative **97** was also found to show the greatest selectivity and increased cytotoxicity in xenograft models when compared to other analogues, due to improved lipophilic properties, as well as balanced reduction potentials. In 2012, phase I clinical evaluation started through Cantella Therapeutics and Cancer Research UK.[77] However, the selectivity and cytotoxicity levels were still below that of TPZ (**38**).

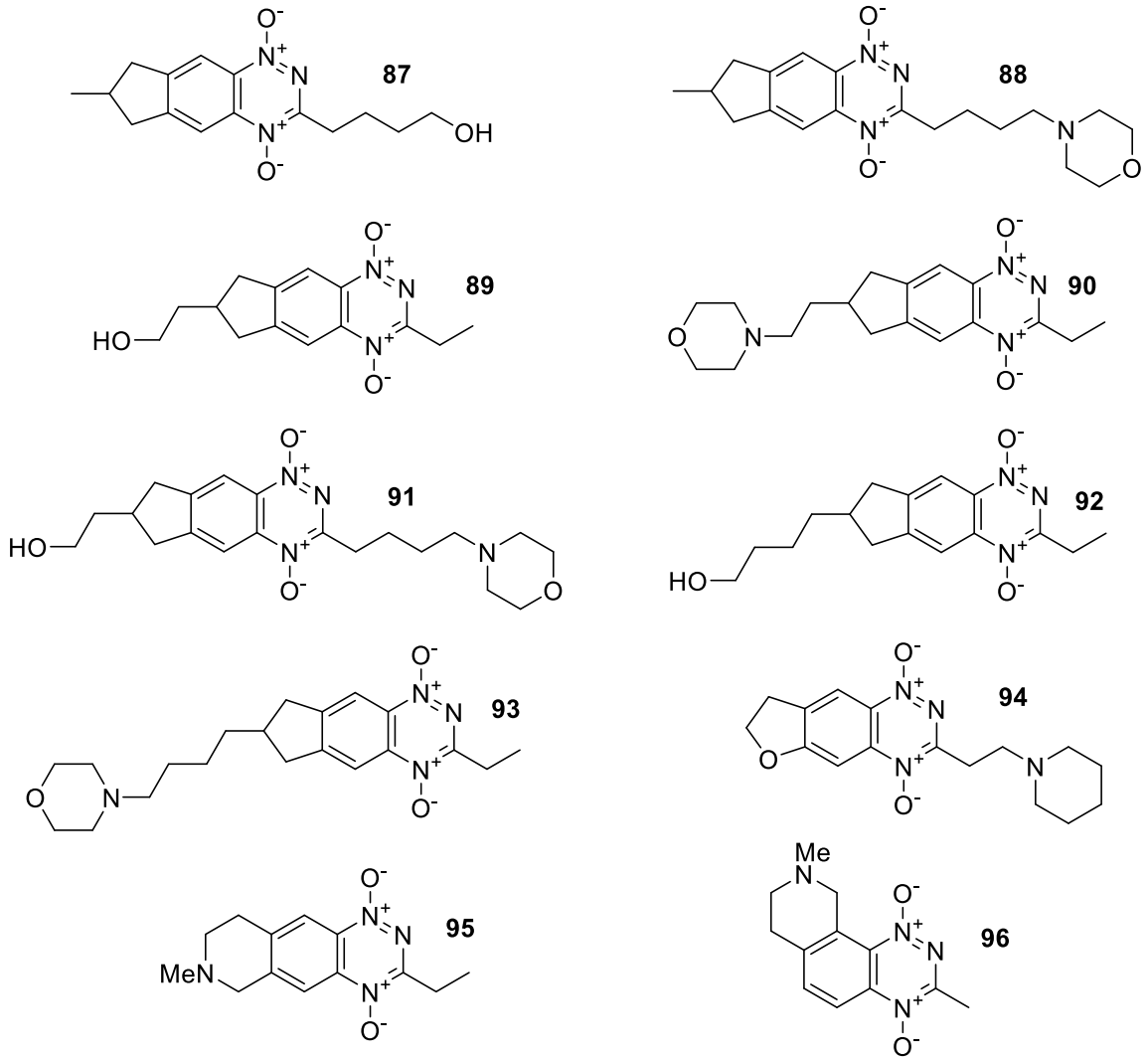

Figure 24. Compounds prepared by Denny which showed modest cell kill values and high cytotoxicity differentials.[22,73,76]

In 2008 the Murphy group started to explore methods of releasing **38** into hypoxic cells using pro-drug technology.[37]

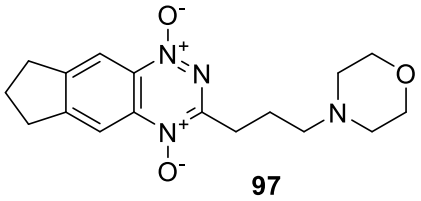

Figure 25. CEN209.

1.8. Previous Work by the Murphy Group

In conjunction with MORVUS technology, research was undertaken with the aim of using quinones such as **52** (page 17) an **104** to deliver nitrogen mustards and substituted guanidines selectively into hypoxic tumours.[37]

1.8.1. Background to the Study

Previous work[37] on the benzoquinone pro-drug delivery system within the Murphy research group concentrated primarily on producing the quinone **105**. In this analogue of **52** the geminal methyl groups have been replaced by a benzene ring, giving a modified but still conformationally locked backbone. The rationale behind this modification was that by replacing the methyl groups with a six-membered aromatic ring, the release rates of various drugs could be tailored as desired. The release rates and activities of the pro-drugs derived from **105** could then be compared to those of **52**.[37]

Compound **105** was prepared in 6 steps from commercially available trimethyl hydroxyquinone **98** (Scheme 11).

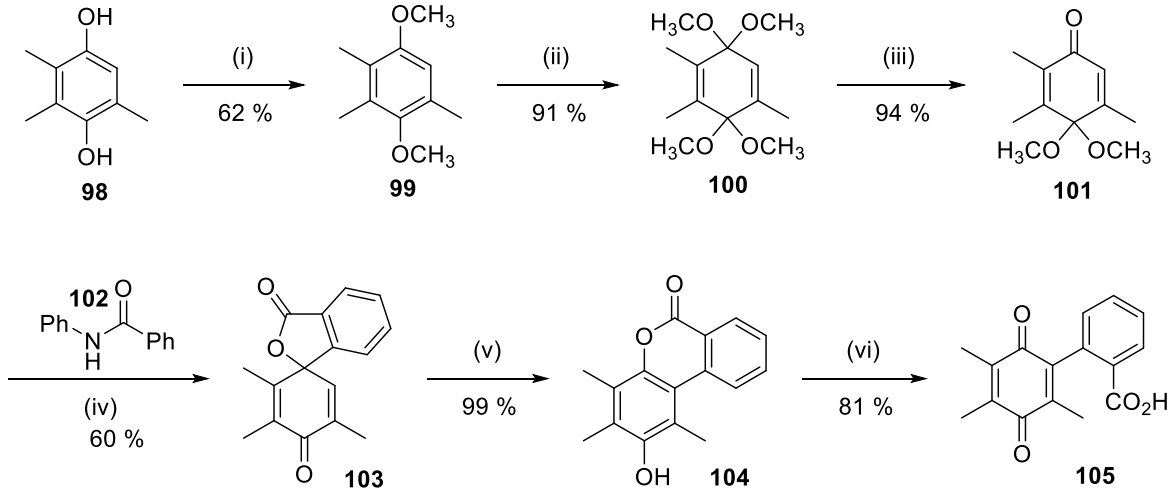

Scheme 11. (i) K_2CO_3, MEK, MeI, 65 °C, 72 h (ii) 2 % KOH, MeOH, <5 °C, 1 h, 1.6 A (iii) CH_3CO_2H (aq., 2 %) acetone, 0 °C, 25 min then r.t, 1.5 h (iv) 0.6 equiv., 1.5 equiv. *n*-BuLi, THF, -78 °C, 30 min then 0 °C, 1.5 h then -78 °C, 4 h (v) CF_3CO_2H, $(CF_3CO)_2O$, H_2SO_4, Δ, 4.5 h (vi) NBS, aqueous acetonitrile.[37]

Both quinones (**50** and 104) were converted into guanidine derivatives. Three guanidine derivatives, **106-108,** were prepared from **52** *via* reaction of the guanidine derivatives **109-111** with the activated ester **52a.** Similarly, three analogous guanidine

derivatives **112-114** were prepared from the acid **105** via the activated ester **115** (scheme 12).

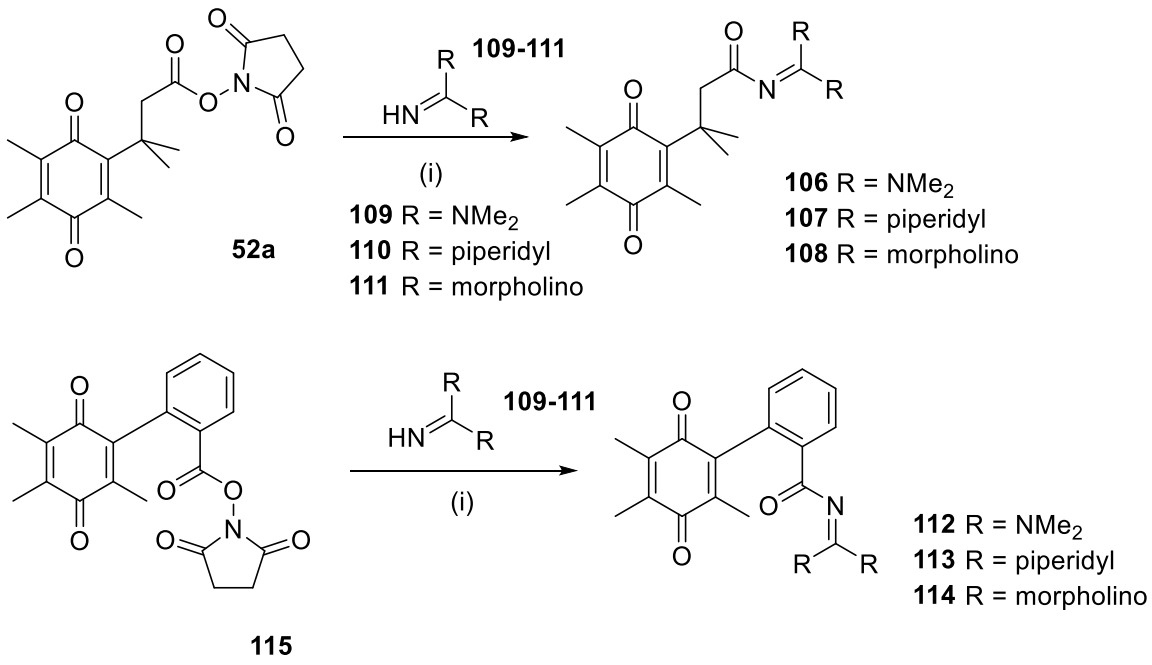

Scheme 12. Guanidine pro-drugs based on quinone acids.

The previously studied aniline-mustard derivative **71** was also prepared using the methodology reported by Volpato,[41] and an attempt was also made to prepare the analogous phenyl-substituted aniline mustard **116** (scheme 13). However, **117** was formed, in which the amine nucleophile has reacted with the imide carbonyl group, causing the succinimide to be ring-opened and to become incorporated into the final molecule instead of being displaced.[37]

I the previous work, the release and cyclisation of **106** and **112** were studied with an enzymatic assay. It was found that the "phenyl" locked pro-drug **112** showed potential with very similar reaction rates to **106**. The cyclisation of **106**, occurring at 2.74 µM/min was similar to **112**, which had a cyclisation rate of 2.26 µM/min.[37]

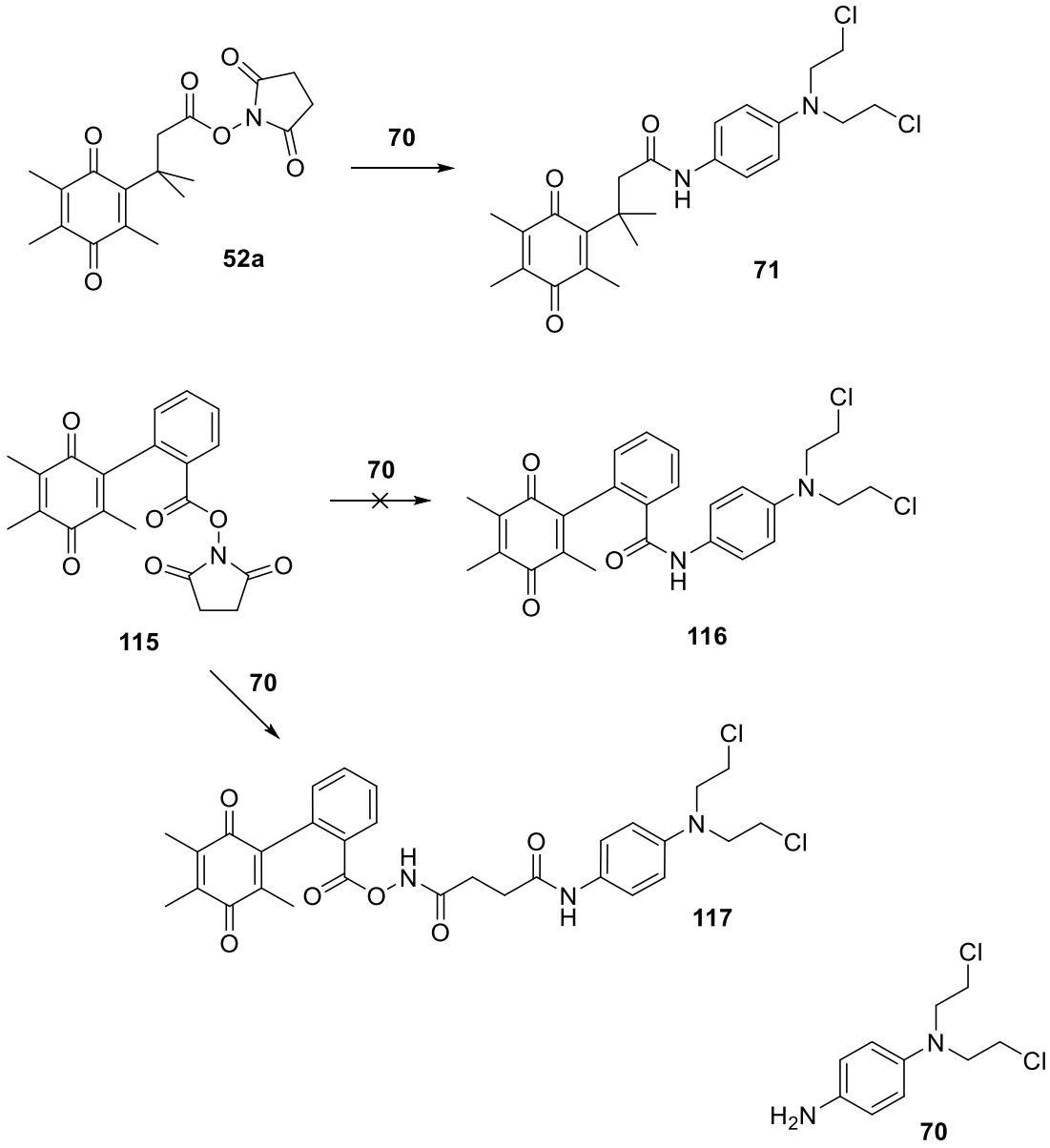

Scheme 13. Synthesis of mustards **71** and **117**.

It was also postulated that benzoquinone drug delivery systems could be used to deliver the drug TPZ (**38**)**,** increasing its selectivity and bioavailability. Subsequently, attempts were made to couple TPZ (**38**) to the benzoquinone **52** (scheme 14). Due to the poor solubility of TPZ, the reaction required the use of dimethylformamide, and after 72 hours there was no evidence of reaction. In addition to the poor solubility, the two *N*-oxide groups deactivate the NH_2 group of the 3-position, preventing nucleophilic substitution.[37]

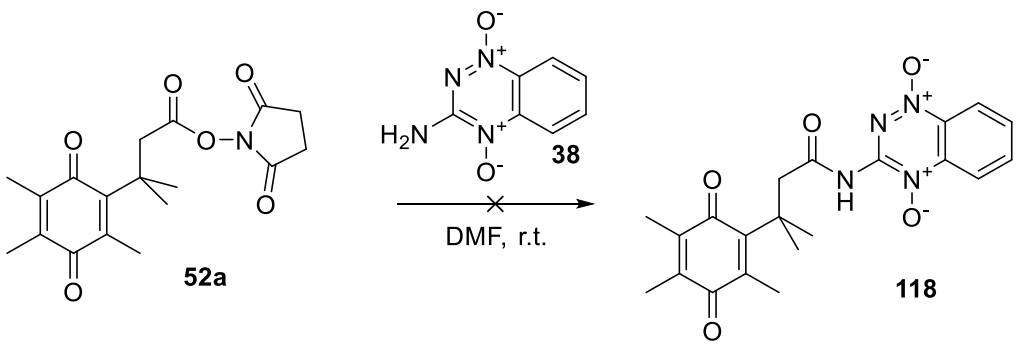

Scheme 14. A failed attempt to conjugate tirapazamine to activated ester **52a**.

1.9. Aims

The primary aim of the first project is to investigate the preparation of a tirapazamine containing pro-drugs such as **118**. The previous attempts by Martin[1] using the NHS ester **52a** failed but changing the reaction conditions, for example by increasing the temperature or by varying solvent conditions will be explored. If unsuccessful, other coupling methods will be attempted, including EDC and HOBT at a range of temperatures. If a direct amide bond cannot be formed methodologies will be explored into the modification of TPZ itself to allow for coupling either at the benzotriazine core or on a functionalised linker. Once a successful method has been developed, analogues incorporating the newly-developed benzoic lock, for example **119**, will be prepared from the carboxylic acid **105**. The series of compounds prepared by Martin[1] has not yet been completely evaluated in any biological trials. One major stumbling block was the inability to prepare the mustard derivative **116**. Therefore a new method is required and other coupling methods will be explored. As with the preparation of **118**, coupling agents such as HOBT will be used as an alternative coupling agent to NHS, as we can speculated that the HOBT will be displaced more easily and no ring-opening reaction is possible. Once completed, the whole range of compounds, including the guanidine derivatives **106** to **108** and **112** to **114**, together with the mustards **71** and **116**, will be submitted to the research group of Professor Roger Phillips at Huddersfield University for activity studies (Scheme 15).

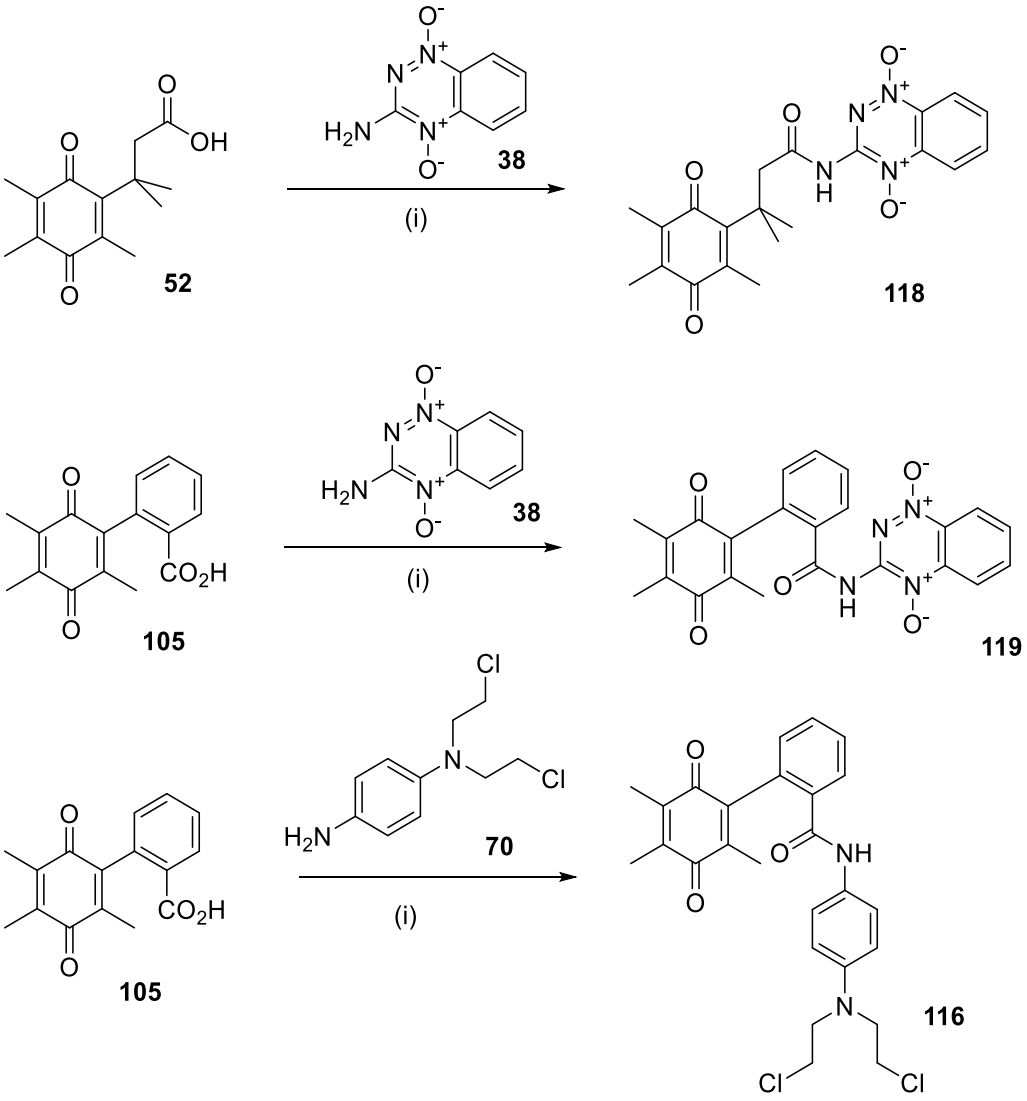

Scheme 15. Aims of the current study (i) EDC, HOBT or DCC, PFP, THF.

2.0 Results and Discussion - Anticancer Pro-drugs

2.1. An Effective Synthesis of the Phenyl Mustard Standard 115

As mentioned in the introduction, the mustard pro-drug **116** is required in order to biologically evaluate the guanidine pro-drugs prepared by Martin[37]. However, attempts to couple the activated phenyl quinone **115** to the aromatic mustard **70** have proven unsuccessful, and produced the linked mustard **117** instead (Scheme 16).

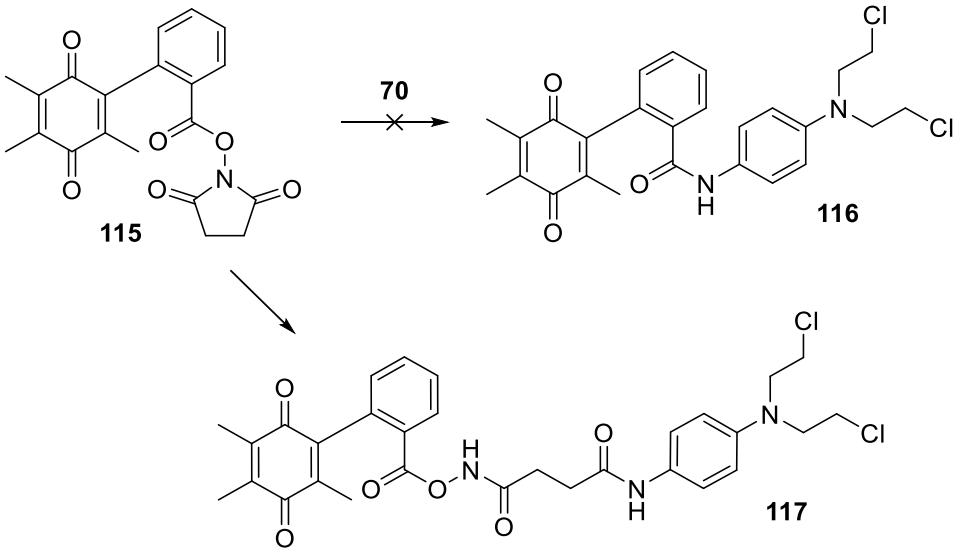

Scheme 16. The unsuccessful coupling of **115** to **70**.

The plan was to investigate other coupling methods for **105** to the mustard **70**.

The first method to be explored was to react **105** with **70** using EDC and HOBT to activate the acid.

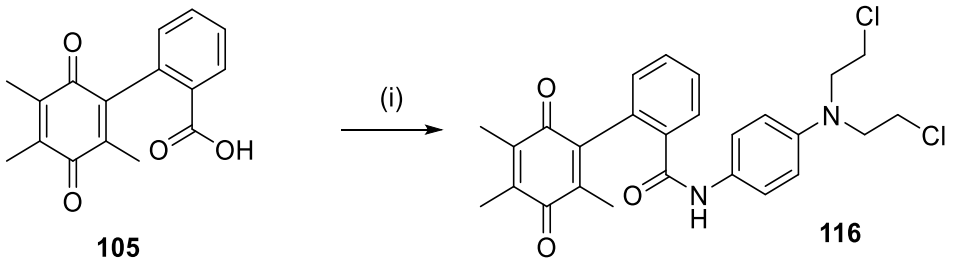

Scheme 17. The planned preparation of pro-drug **116** (i) **70**, THF, r.t, 48 hrs.

Before these experiments could be carried out, the preparation of fresh quinone **105** and mustard **70** was required.

The preparation of **105** was carried out according to Martin's[37] method, as shown in scheme 18. The first step was the methylation of trimethyl hydroquinone **98,** using iodomethane with 2-butanone as solvent and with potassium carbonate as a base, to give **99** as a colourless oil which solidified on standing. The overall yield of the reaction was 65 %, which is comparable to the yield reported by Martin. Then dimethoxytrimethyl hydroquinone **99** was dissolved in 2% methanolic potassium hydroxide. Using a platinum anode and a reticulated carbon cathode, current of 1.0 A was passed through the solution for 2 h (the power supply which was used by Martin was not available and the delivery of a current of 1.6 A not possible) while keeping the temperature below 5 ˚C with an ice bath. Within 2 h the solution became brown, and the solvent was removed by rotary evaporation. The residue was diluted with water and extracted with diethyl ether. Drying and evaporation of the solvent gave **100** as a yellow solid in 87 % yield. The product was used without further purification.

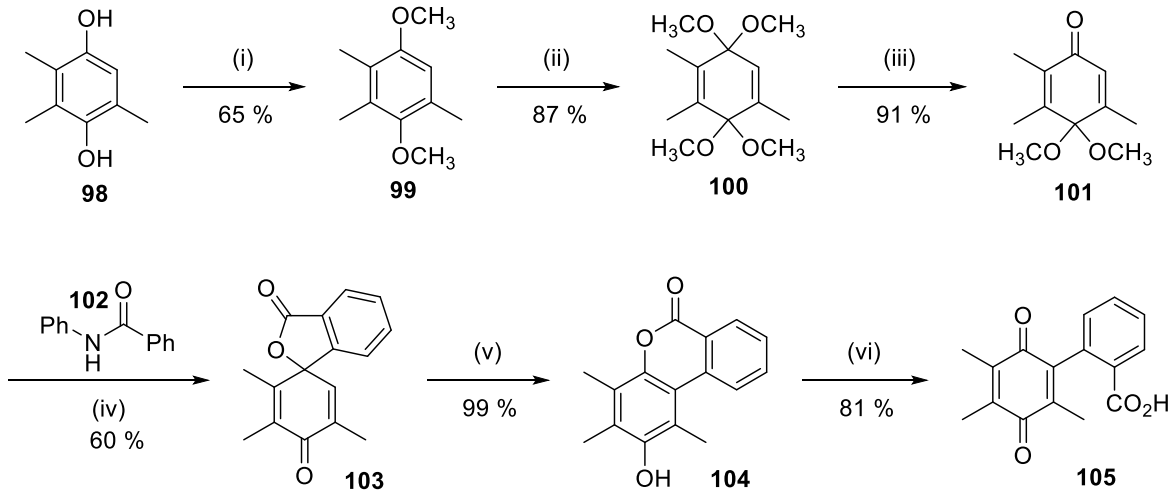

Scheme 18. (i) K_2CO_3, MEK, MeI, 65 °C, 72 h (ii) 2% KOH, MeOH, <5 °C, 2 h, 1.0 Amp (iii) CH_3CO_2H (aq., 2%) acetone, 0 °C, 25 min then r.t, 1.5 h (iv) 0.6 equiv. *N*-phenylbenzamide, 0.95 equiv. *n*-BuLi, THF, -78 °C, 30 min then 0 °C, 1.5 h then -78 °C, 4 h (v) CF_3CO_2H, $(CF_3CO)_2O$, H_2SO_4, Δ, 4.5 h (vi) 1.36 equiv. NBS, aqueous acetonitrile.[37]

Treatment of **100** with chilled acetic acid, followed by aqueous work up with sodium hydrogen carbonate, gave **101** as a pale yellow solid with a 91 % yield. Again the product was used without further purification. Next the quinone **101** was converted into the lactone **103**. It had been found by Martin[37] that residual *N*-phenylbenzamide **102** was impossible to separate from the lactone **103**, and interfered with the subsequent rearrangement of **103** to **104**. Hence, 0.93 equivalents of phenylbenzamide were used with respect to the ketone **101** to ensure that it would all be consumed. *n*-Butyllithium was added drop-wise to a cooled (-78 ˚C) solution of *N*-phenylbenzamide in anhydrous THF, and the resulting mixture was

stirred at -78 ˚C for 30 min and then at 0 ˚C for 1 h. This solution was then cooled (-78 ˚C) before adding a solution of monoketal **101**, and the reaction was allowed to reach r.t. overnight. An aqueous work up was carried out, involving the acidification of the reaction mixture by washing with 3M hydrochloric acid. This hydrolysed the remaining ketal-protecting group and effected lactonisation. Purification by dissolving in hot diethyl ether and precipitation with methanol gave the lactone **103** as a white solid with a yield of 60 %. Lactone **103** was then rearranged by heating at reflux with a combination of trifluoroacetic acid, trifluoroacetic anhydride and sulfuric acid, to give **104**. After work up, the crude product was recrystallized from dichloromethane and hexane to give lactone **104** as white crystals in a 99 % yield. Finally, a ring opening of **104** mediated by NBS in aqueous acetonitrile was carried out to give the quinone acid **105** in 81 % yield as a yellow oil after column chromatography. The yield compares well to the 77 % yield reported by Martin.

It is worth noting that on scale –up, this reaction can be problematic, as appreciable amounts of the by-product **120** can form, which arises *via* an intramolecular bromolactonisation of the quinone acid.

In all cases, the compounds **99-105** gave identical spectroscopic data to the previously prepared compounds.

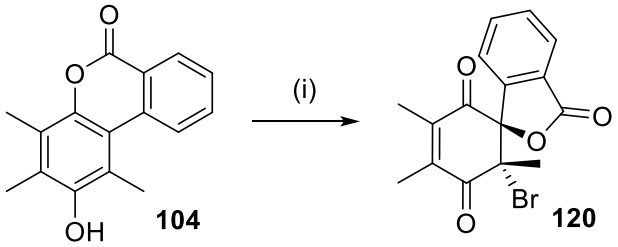

Scheme 19. By-product from the oxidation of **104** (i) 1.36 equiv. NBS, aqueous MeCN.

Quantities of the mustard **70** were also required. The first step was prepared by the method provided by the partner company Morvus (Scheme 20), after which the preparation was continued according to the method reported by Martin.[37]

The synthesis started with the reaction of 2,2-iminoethanol **122** with 4-fluoro-1-nitrobenzene **121** in a sealed tube at 130 ˚C for 17 h, which gave a 73% yield of **123** as yellow crystals, after recrystallization from ethyl acetate. Then the diol **123** was heated at reflux with thionyl chloride in dichloromethane and pyridine for 1h. After work up, the crude product was purified by column chromatography, to yield **124** as yellow crystals with a yield of 46% .[37] Analysis of the ^{1}H NMR data for **124** showed two triplets at

δ_H 3.69 (4H, t, *J* = 6.8 Hz, 2 x CH_2) and 3.87 (4H, t, *J* = 6.8 Hz, 2 x CH_2). The product had a melting point of 91–94 ˚C, which is in accordance with the literature value (lit. 95-96 °C).[37] However, the sample appeared to be contaminated with two lower running spots, and it was not possible to separate these by-products even on repeated chromatography. Martin had reported two by-products- the mono-chlorinated product **125** and the dioxathiazocane 2-oxide **126**[37] (Figure 26).

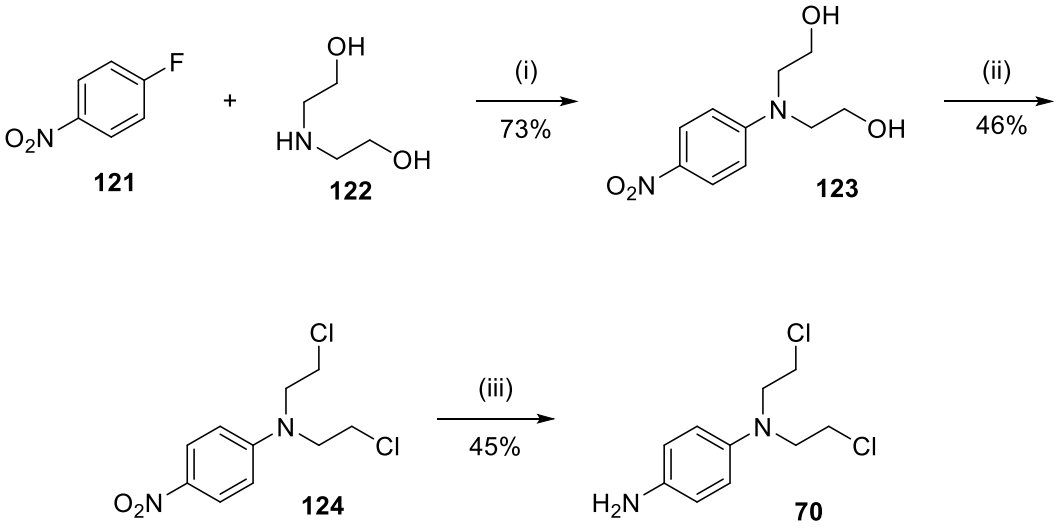

Scheme 20. Preparation of mustard **70**. (i) Sealed tube 130 ˚C, 17 h (ii) pyridine, $SOCl_2$, CH_2Cl_2, reflux (iii) 5% Pd/C, H_2.

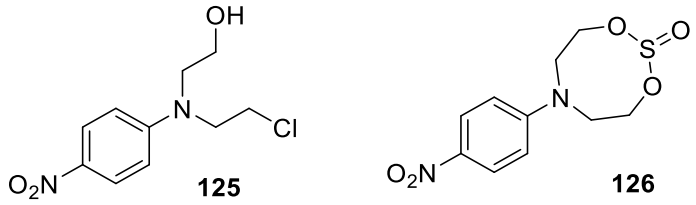

Figure 26. Likely impurities in the mustard **70**.[37]

As these impurities did not seem to cause any problems for Martin, it was decided that the synthesis would be continued without further purification of **124**. Hydrogenation of the nitro group with 5 % palladium on charcoal was carried out, followed by filtration through Celite©, and washing with methanol to ensure complete product recovery. Chromatography of the crude brown material gave an inseparable mixture of products, which was predominately (estimated 90%) the desired product **70** (by ^{1}H NMR analysis), with a yield of 45 % compared to the yield of 68 % reported by Martin. Analysis by ^{1}H NMR spectroscopy showed the appearance of a broad singlet at around δ 5.13, with an integral of 2, indicating the formation of the aniline NH_2.

Due to the poor quality of **70**, a cleaner synthetic method was desired. It was decided that the thionyl chloride step was the initial cause of the presence of inseparable by-products. Thionyl chloride is highly reactive, and generates HCl as it reacts. In 2011, Wang[78] reported a two stage chlorination of **123,** where the diol is firstly mesylated then treated with sodium chloride to give **124** (Scheme 21).

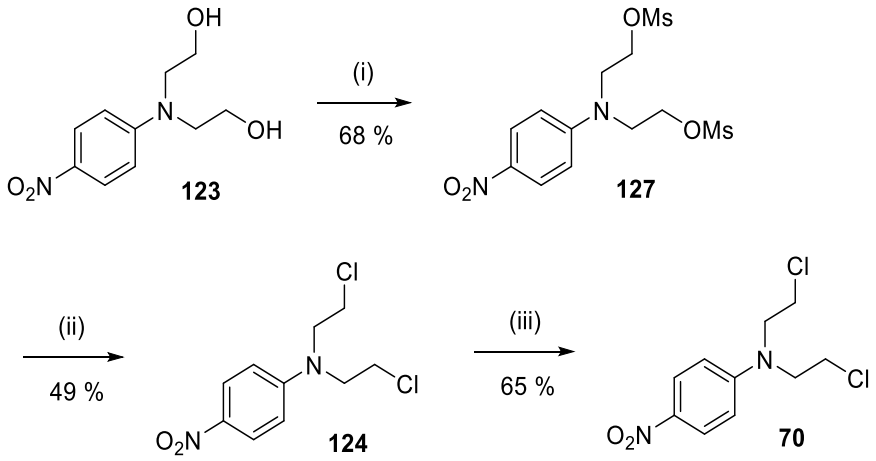

Scheme 21. (i) $MeSO_2Cl$, NEt_3 (ii) DMF, NaCl, reflux (iii) 5% Pd/C, H_2.

Thus, diol **123** was reacted with methane sulfonyl chloride in ethyl acetate with triethylamine to remove the HCl formed in the reaction. Filtration of the reaction product to remove precipitated triethylamine hydrochloride, followed by evaporation and recrystallization using hot ethanol with ethyl acetate, gave the product **127** in 68 % yield (Wang 89 %).[78] Analysis by ^{1}H NMR spectroscopy showed the disappearance of the resonance for the alcohol proton at δ_H 3.28 (2H, b s, 2 x OH) ppm and the appearance of a singlet at 2.98 (6H, s, 2 x Me) ppm for the mesylate.[78] The dimesylate **127** was then dissolved in anhydrous DMF with 3.3 equivalents of sodium chloride and heated at reflux for 15 minutes. After work up and chromatography, **124** was obtained as a yellow crystalline solid, with a yield of 49 %. Comparison of the data with the previously prepared samples indicated that the impurities previously observed were not present in the new material. The overall yield of 36 % over two steps is lower than the 46 % yield from the thionyl chloride route, however, improved product purity is desirable for the continued synthesis. Finally hydrogenation of **124,** using the previously employed method followed by column chromatography, gave pure mustard **70** in a 65 % yield.

In order to circumvent the problems associated with the ring-opening of the succinimide ring in the [37], the *in situ* preparation of the HOBT ester **128** was carried out (scheme 22). HOBT and EDCI were added to the acid **105** in THF. After 3 h, the mustard

70 was added, and the reaction was stirred for an additional 48 hours. Purification by flash chromatography gave **116** in 33 % yield as a brown gum. Analysis of **116** by ^{13}C NMR spectroscopy showed the required 26 carbons. Similarly, analysis by ^{1}H NMR spectroscopy showed a triplet at δ_H 3.61 (4H, t, *J* = 6.5 Hz, 2 x CH_2) ppm and a triplet at 3.70 (4H, t, *J* = 6.5 Hz, 2 x CH_2) ppm, corresponding to methylene signals of the mustard groups. Signals at δ_H 6.67 (2H, d, *J* = 8.6 Hz, CH) and 7.32 (2H, d, *J* = 8.6 Hz, 2 x CH) ppm were indicative of the para-disubstituted aromatic ring, whilst those at δ_H 7.16 (1H, dd, *J* = 1.2, 7.6 Hz, CH), , 7.47-7.56 (2H, m, 2 x CH, NH), and 7.70 (1H, b d, *J* = 7.7 Hz, CH) ppm corresponded to those of the phenyl locking ring. Final confirmation of the structure of **116** was obtained by high resolution mass spectrometry, with a mass of 485.1387 Da being observed for the [M+H^+] ion. This is in good agreement with the required mass of 485.1399.

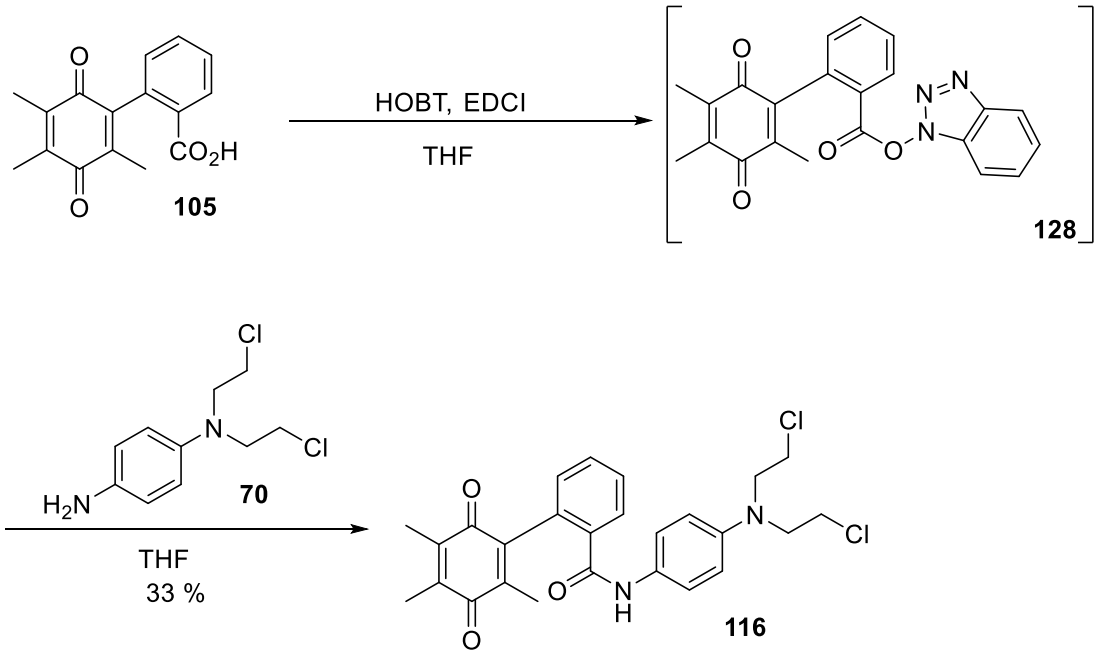

Scheme 22. Synthesis of the phenyl mustard pro-drug **116**.

2.2. Tirapazamine Based Pro-drugs

As previously noted, initial attempts at the preparation of the pro-drug **118,** in which tirapazamine **(38)** has been coupled to the pro-drug quinone system *via* the activated ester **52a,** proved unsuccessful[37] (Scheme 23). As suggested by Martin, there appear to be two possible reasons for this. These are firstly that the presence of the two *N*-oxy groups may deactivate the NH_2 on the 3-position towards nucleophilic substitution in the conjugation step, and secondly the poor solubility of tirapazamine **1** under the reaction conditions. Because of this, it was decided that these hypotheses should be investigated in the hope of developing a new synthetic strategy for **118**.

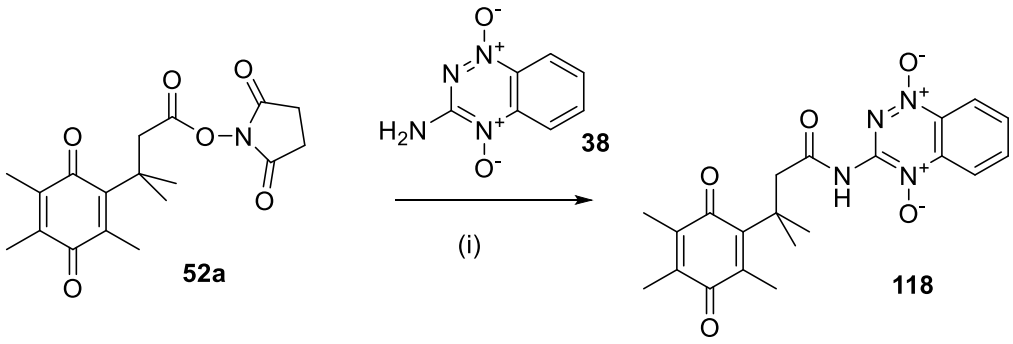

Scheme 23. (i) DMF, r.t. **118,** 0 %.[37]The quinone acid **52** was prepared from trimethyl-1,4-dihydroxyquinone (**98**) *via* a literature method (scheme 24).[41] The first step was the reaction of trimethyl-1,4-dihydroxyquinone (**98**) with dimethylacrylate (**129**) in methanesulfonic acid, to give a brown semi-solid residue. Repeated recrystallisation from chloroform/petroleum ether gave the lactone **26** as a purple/gray solid in a yield of 88 %.[41] The lactone **26** was then converted into the quinone acid **52** using NBS in aqueous acetonitrile. After extraction with diethyl ether, the resulting orange/red solid was recrystallised from ethyl acetate, to give the quinone **52** as a bright yellow solid with a yield of 99 %.[41] The activated ester **52a** was then prepared by reacting the quinone with NHS and DCC in anhydrous THF. The resulting mixture was filtered repeatedly to remove precipitated DCU. Evaporation of the solvent gave a pale orange solid, which was recrystallised from ethyl acetate to give an amorphous solid **52a**. This material still contained DCU, and was used without further purification.[54] In all cases the compounds **98**, **26**, **52** and **52a** were found to have identical spectroscopic data to that reported in the literature (Scheme 24).[54]

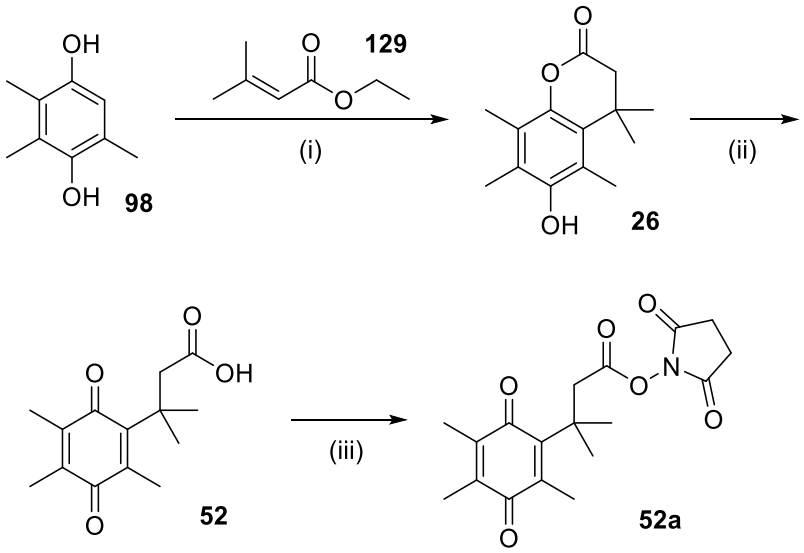

Scheme 24. (i) CH_3SO_3H, 3h, 70 ˚C; 88 %. (ii) NBS, MeCN, 99 %. (iii) DCC, NHS, THF, 0 ˚C.

With the activated ester **52a** in hand, attempts were made to prepare the pro-drug **118** by coupling with tirapazamine (**38**). In the first attempt, the activated ester was stirred with **117** in anhydrous DMF in the dark at varying temperatures of 40-80 ˚C. The reactions were checked by TLC on a regular basis, but no evidence of reaction was observed, as the starting ester **52a** was still present and no other products were apparent. On work up, analysis of the crude material by NMR spectroscopy gave no evidence for formation of the amide **118**, and only the parent acid **52** was isolated on purification. This is thought to have arisen from hydrolysis of **52a**, but the possibility cannot be discounted that it might have arisen from the decomposition of **118**.

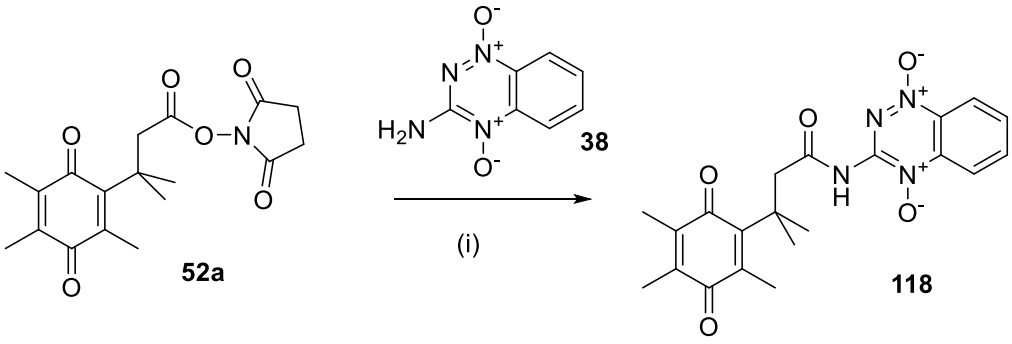

Scheme 25. DMF, 40-80 ˚C.

As was previously suggested, the NH_2 group on the 2-position is deactivated due to the two *N*-oxide groups of the triazine core of **38**, and as a result could be less nucleophilic. An alternative explanation might be that the product is unstable, and the product **118** undergoes hydrolysis on work up and on silica during analysis by TLC.

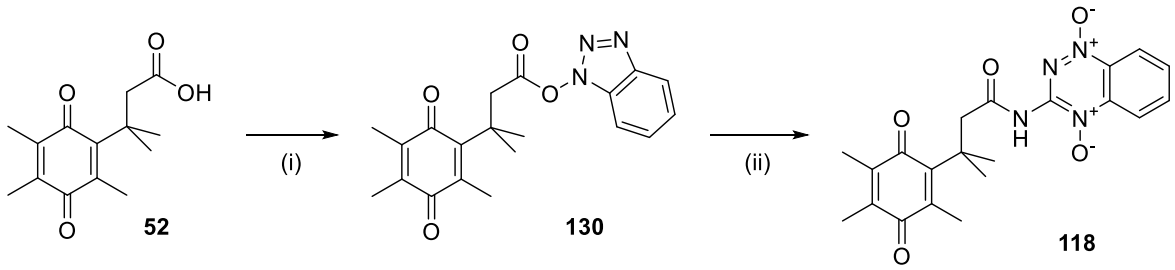

Scheme 26. (i) DCC, HOBT, DMF, r.t., 12h (ii) **38**, DMF, r.t.

In order to investigate these theories, alternative coupling methods were explored. Firstly the NHS was substituted for HOBT. The HOBT ester of **52** was prepared by stirring the acid with DCC and HOBT in dry DMF for 12 h (scheme 26). The activated ester was not isolated, but on completion of the reaction, which was monitored by TLC, tirapazamine (**38**) was added dissolved in further DMF. This reaction proved to be unsuccessful, as evidenced by both TLC and NMR spectroscopy of the products. The reaction was repeated at temperatures of 40, 60 and 80 ˚C over 12-48 hours, and again no evidence for the formation of **118** was observed (Scheme 26).

The coupling was also attempted using a mixed anhydride (Scheme 27), and the carboxylic acid **52** was converted into the carbonic acid anhydride **131** by reaction with isopropyl chloroformate in the presence of *N*-methyl piperidine. Once full consumption of **52** had been observed *via* analysis by TLC, the anhydride **131** was stirred with tirapazamine (**38**) in anhydrous DMF at -15 ˚C and allowed to warm to r.t. overnight. Again, analysis by TLC indicated that no reaction had occurred, and the desired product **118** was not apparent from the analysis of the NMR spectroscopy data of the crude reaction product.

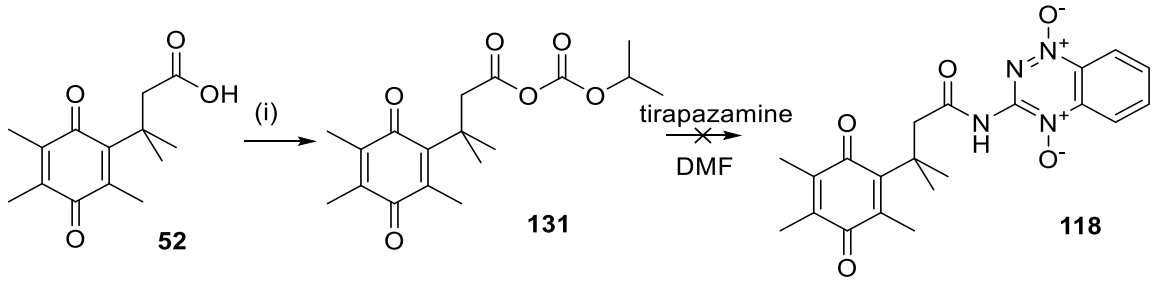

Scheme 27. (i) *iso*-Propylchloroformate, *N*-methyl piperidine, DMF, 0˚C.

The final attempt was carried out according to scheme 28, where the quinone acid was converted into the acid chloride **132** by heating under reflux with neat thionyl chloride for 30 minutes. Once the reaction was complete, excess thionyl chloride was removed under vacuum, and a solution of tirapazamine (**38**) in anhydrous DMF was added. The reaction was stirred at 0 ˚C for 1 hour, then at r.t. overnight. Again after work up, TLC analysis and

the crude NMR spectroscopy data indicated that the desired product **118** had not been formed.

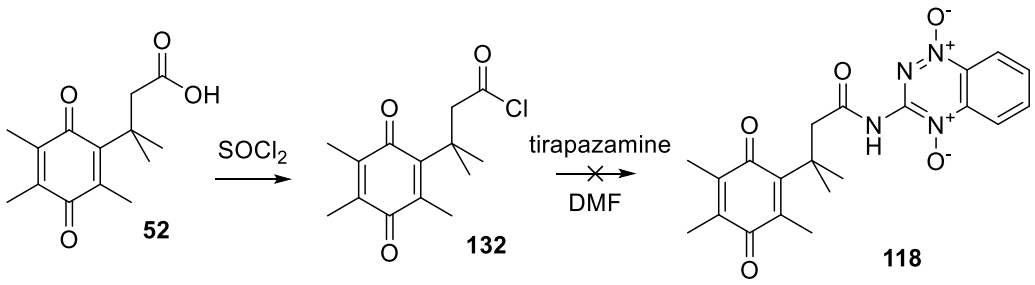

Scheme 28. Attempted acid chloride coupling of **52** to TPZ (**38**).

As this work was unsuccessful, it was decided that attempts would be made to couple the acid **52** to the *N*-oxide 3-amino-1,2,4-benzotriazine-1-oxide (**77**)**,** to give the analogous structure **133** (Scheme 28). The use of **77** was considered to be useful as a pro-drug for several reasons. Firstly **77**, which was found during biological trials and might in itself have useful activity, is a known metabolite of tirapazamine (**38**).[80] Secondly it might be possible to convert **133** into **118** by chemical oxidation, either *in situ* or indeed *in vivo*. In addition, a practical consideration is that **77**might show improved solubility over tirapazamine (**38**), allowing a wider range of solvents to be used in the coupling reactions. Also the lower oxidation level of **77** might lead to the amine at position 3- having a greater nucleophilicity than in **38**.

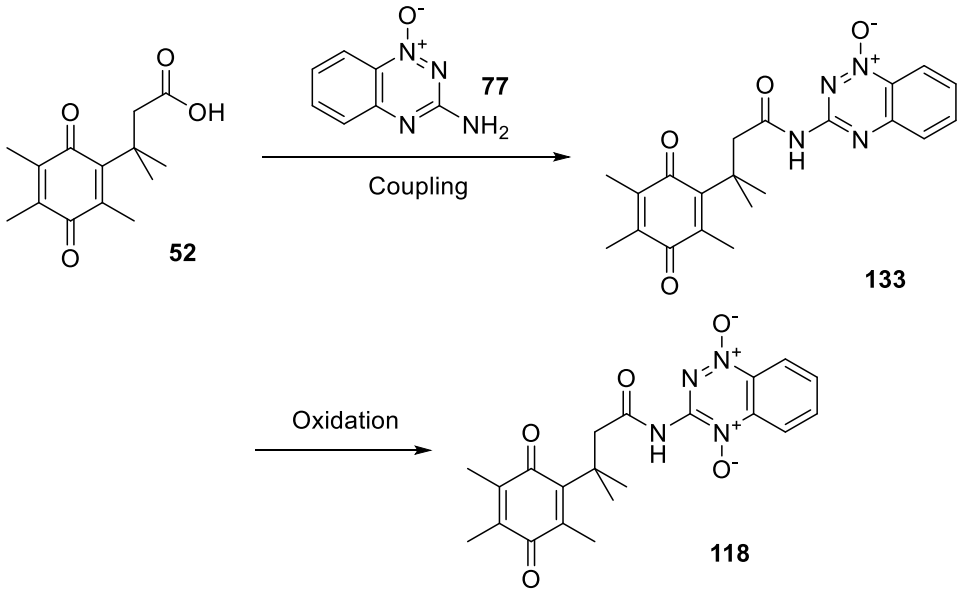

Scheme 29. Proposed preparation of **118** via **133**.

The required triazine **77** was prepared via the heterocyclisation of 2-aminonitrobenzene (**134**) and cyanamide (**135**), using a procedure described by Mason and Tenant which afforded the desired product in a yield of 86 % (Scheme 30).[81]

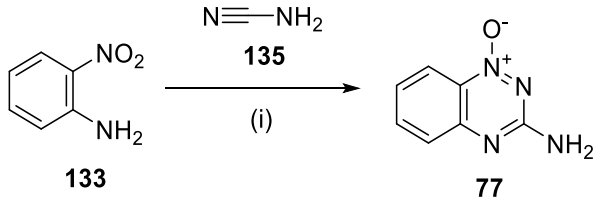

Scheme 30. (i) 100 ˚C then conc. HCl at 100 ˚C followed by 16 M NaOH at 100 ˚C, 86 %.

The triazine **77** was found to be much more soluble at r.t. than TPZ (**38**) in a range of solvents, including pyridine and THF as well as DMF. With **77** in hand, an attempt was made to react it with the activated ester **52a** in anhydrous DMF, but the product **133** was not formed, as evidenced by TLC and the NMR spectroscopy data of the crude reaction product.

The preparation of **133** was also attempted by using the methods investigated in the coupling of acid **52** to TPZ (**38**). Unfortunately, none of these methods appeared to give any evidence for the formation of **133**.

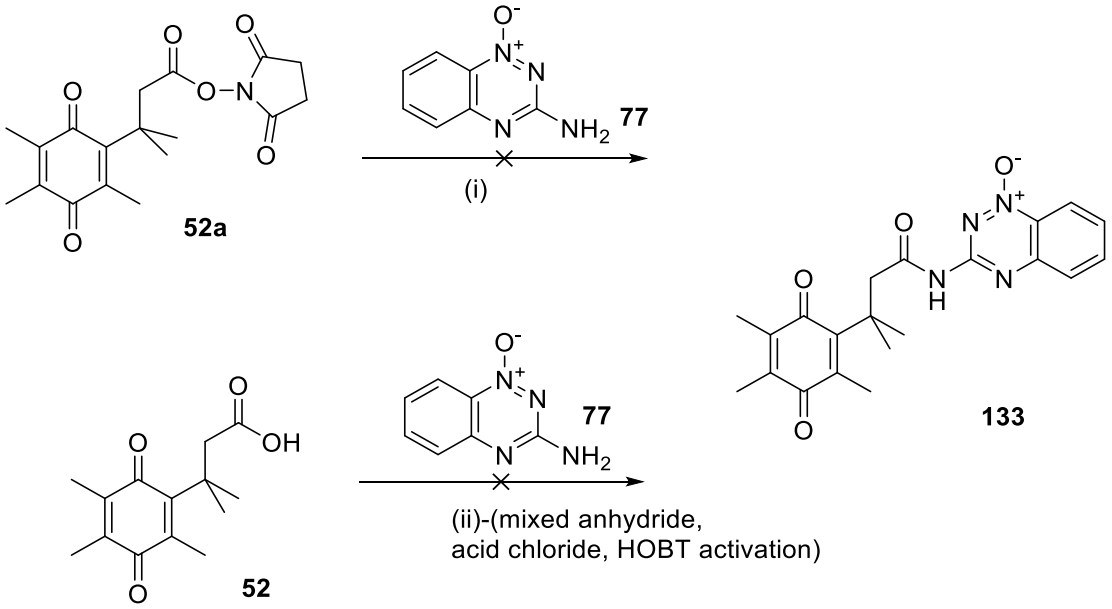

Scheme 31. Attempts to couple **52a** with **77** were unsuccessful.

Similar couplings with unoxidised triazine **136** were next attempted. This, again, is a known metabolite of TPZ (**38**) found to be formed in biological studies, and might have activity in itself.[81] Again the reason behind this was that it was hoped that without the oxide groups present in TPZ, the amino group would show increased nucleophilicity and higher

solubility. An attempt was made to prepare **136** *via* a literature method that reported the reduction of **77** with sodium dithionite ($Na_2S_2O_4$)(Scheme 32).[80]

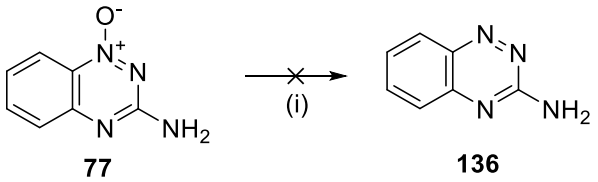

77 136

Scheme 32. (i) $Na_2S_2O_4$, EtOH, H_2O, reflux, 67 %.[80]

In the first attempt, **77** was dissolved in aqueous ethanol, along with 5 equivalents of sodium hydrosulfite, before heating at reflux for 1 hour, as described by Boyd[80]. On this occasion the desired product was not formed, with 86 % of the starting material recovered.

Another research group had prepared **134**[81] by adding sodium hydrosulfite portion-wise over 1 h or until **77** had disappeared by TLC. This method was also failed to produce **136**, again with most of the starting material being recovered. It is known that heating sodium dithionite in aqueous conditions in the presence of dissolved oxygen leads to its decomposition to sodium bisulfate and sodium bisulfite.

Therefore a third reaction was carried out, where a solution of **77** in aqueous ethanol was extensively degassed by bubbling argon through the solution, and the reaction was performed under a positive argon atmosphere. The solution was heated to reflux, and portions of dithionite (each 2 eqv.) were added every 30 minutes. After 2 additions there was no indication of the formation of the desired product, with a 91 % recovery of the starting material.

The synthesis of 1,2,4-triazine systems such as **138** by the reaction of nitroaromatics with guanidine hydrochloride and lithium *t*-butoxide has been reported (Scheme 33).[73]

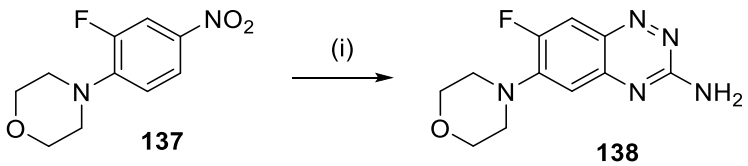

137 138

Scheme 33. (i) Guanidine hydrochloride, THF, LiH, *t*-butanol (cat.), 60 ˚C.[82]

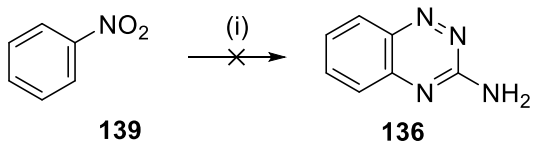

139 136

Scheme 34. (i) Guanidine hydrochloride, DMSO, LiH, *t*-butanol (cat.), 100 ˚C.

Thus, attempts were made to produce **136** from nitrobenzene (**139**) using this method, but no product was isolated. It was assumed that nitrobenzene was less reactive towards nucleophilic substitution than **137** due to the absence of the electron-withdrawing fluorine substituent. Therefore the reaction solvent was changed from THF to DMSO, allowing the reaction to be heated at a higher temperature, and on repeating this reaction, TLC indicated the formation of a new spot, indicating the possible formation of **136**. However, after an extractive work up, no product was obtained as evidenced by NMR spectroscopy. It was observed that during work up the aqueous phase became yellow in colour, which might suggest that the product was being transferred to the aqueous phase. The literature[57] preparation of **138** suggested that the addition of the crude reaction mixture to saturated ammonium sulfate would result in the precipitation of the product. In practice the addition of the reaction mixture to 30 mL of ammonium sulfate solution caused a lumpy black precipitate to form, from which no product was obtained.[82]

Next, the reaction conditions were modified by using potassium *t*-butoxide in anhydrous THF, instead of lithium hydride (which required an aqueous work up to decompose excess reagent). On completion, the crude residue was purified by column chromatography, which gave the desired product **136** in a low yield (~2 %), while the *N*-oxide **77** was formed in 48% yield. Unfortunately, both products co-eluted with a brown by-product which was inseparable even on repeated column chromatography. It was postulated that the red colour of the reaction is formed as a result of the basic nature of the reaction conditions, and it was thought that the crude reaction mixture could be neutralised by quenching with saturated ammonium hydrochloride solution. However, as mentioned earlier, aqueous work ups were problematic as the product appeared to be soluble in the aqueous phase. To counter this issue, saturated ammonium hydrochloride solution was added dropwise until the reaction mixture was neutral, and excess water was then removed by drying with magnesium sulfate followed by filtration washing with copious amounts of dichloromethane. These measures proved successful giving **136** in 30 % yield after chromatography, together with the *N*-oxide **77** in 52 % yield. The solubility of **136** in a range of solvents including tetrahydrofuran and ethyl acetate was much improved compared to **77** and TPZ (**38**).

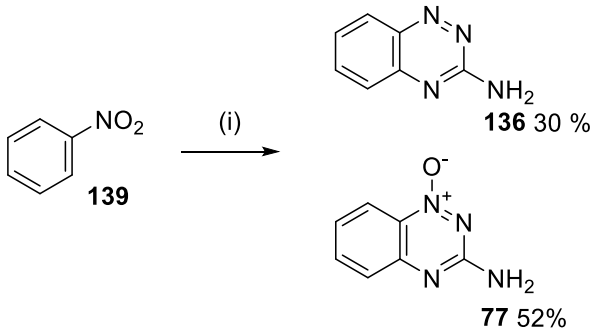

Scheme 35. (i) *t*-BuOK, guanidine hydrochloride, THF, 60 ˚C, 12 h.

Attempts were made to form the quinone-conjugated derivative **140** by reacting triazine **136** with the activated ester **52a** (scheme 36). However, this reaction was unsuccessful as evidenced by TLC and NMR spectroscopy of the crude reaction mixture. The preparation of **140** was also attempted from acid **52** and triazine **136** using all the methods investigated for the coupling of acid **52** to TPZ (**38**). The unchanged starting materials were identified in each case with no evidence of the formation of the coupling product **140**.

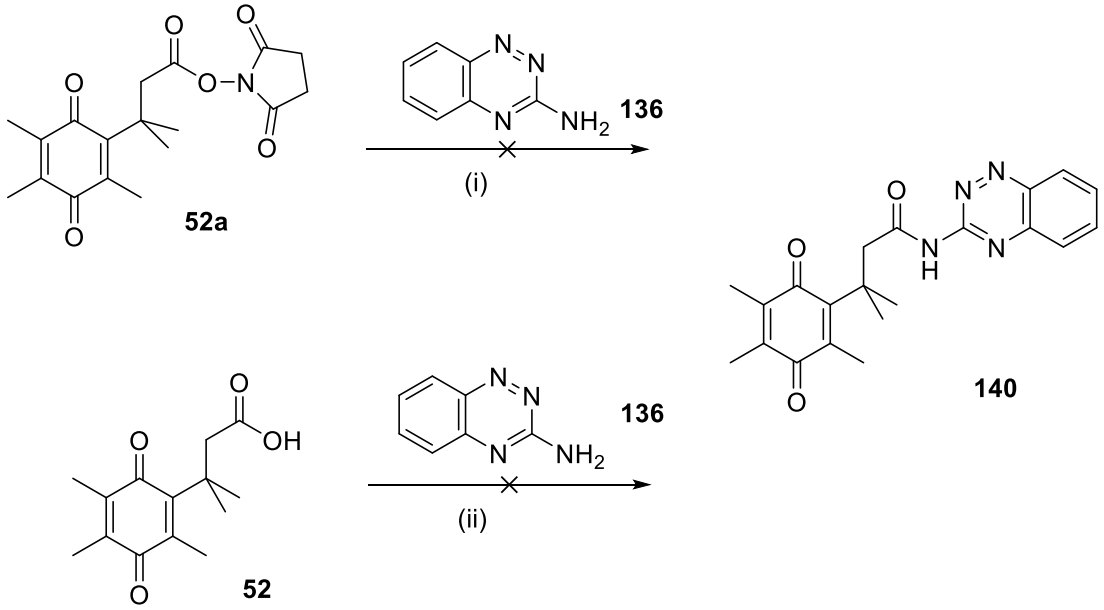

Scheme 36. (i) DMF, r.t., 48h (ii) mixed anhydride, HOBT activation.

At this stage of the research, attempts had been made to couple tirapazamine (**38**) and its deoxy-analogues **77** and **136** to the quinone acid **52**. However, all of these attempts had failed. It is speculated that the amine present on the 3-position of the heterocycle is not nucleophilic enough to mediate this coupling. As this methodology had failed, an alternative

strategy for the incorporation of the TPZ moiety into a pro-drug delivery system was required.

2.3. Preparation of *N*-alkylated Tirapazamine Derivatives

The two main problems associated with the incorporation of tirapazamine (**38**) and its analogues into the quinone pro-drug delivery system were perceived to be low solubility of the reactants and poor nucleophilicity of the amino group. It was postulated that the addition of an alkyl chain to the amino group could help to improve solubility and might possibly improve the nucleophilic nature of the amino function.[22,73] It is noteworthy that no simple *N*-alkyl TPZ analogues have been reported in the literature, although in 1959 Mueller reported the synthesis of the triazine **145** from **77** in 4 steps. No biological activity data has been reported for this compound (Scheme 37).[83]

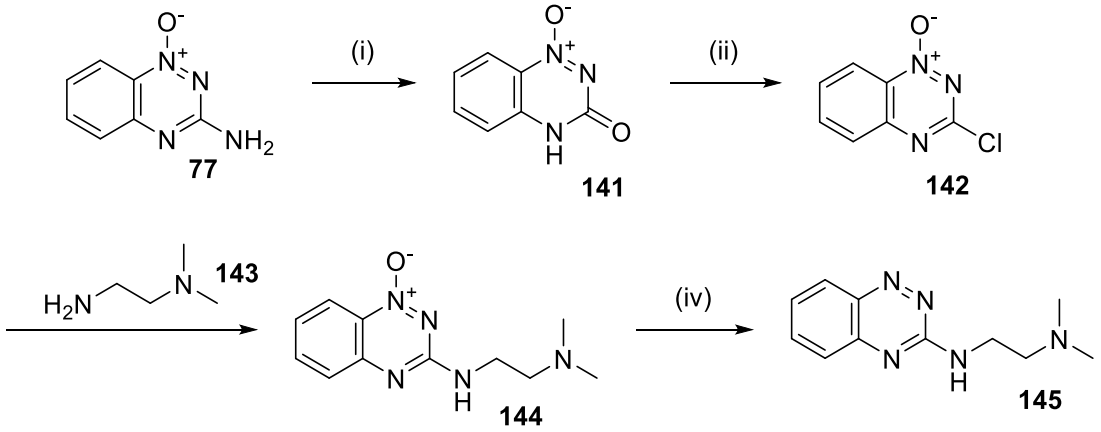

Scheme 37. (i) H_2SO_4, $NaNO_3$, (ii) $POCl_3$, (iii) ethylene glycol, DME, reflux, (iv) NH_4Cl, Zn[83].

Therefore a test reaction was carried out in which nitrobenzene (**139**) was reacted with 1-octylguanidine hemisulfate (**146**) and *t*-BuOK in anhydrous THF for 20 hours. On completion, the reaction products were quenched with water and extracted with chloroform, to give **147** as a yellow solid in 30% yield after column chromatography. Analysis by NMR spectroscopy confirmed the structure of **147**, with the ^{13}C NMR data showing the required 15 carbons and the presence of a characteristic NH signal at 6.00 ppm in the ^{1}H NMR spectrum. Final confirmation of the structure of **147** was given by high resolution mass spectroscopy, with a mass of 259.1917 being observed for [M+H$^+$], which is in agreement with the required mass. The alkylated derivative **147** was found to be soluble in a wide range of solvents including diethyl ether, THF, ethyl acetate and dichloromethane.

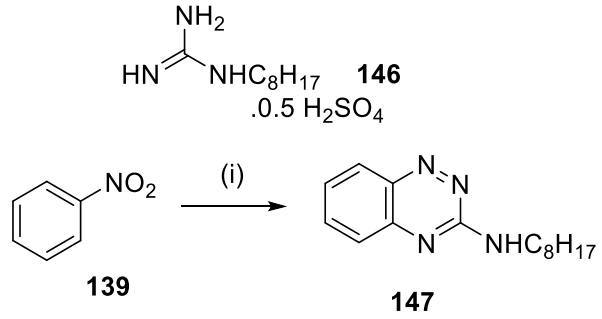

Scheme 38. (i) *t*-BuOK, $PhNO_2$, THF, 65 ˚C, 30 %.

Several attempts were made to couple the alkylated analogue **147** with the quinone **52** to produce the pro-drug **148** (Scheme 39).

In the first attempt the analogue **147** was stirred in anhydrous THF with the activated ester **52a**. Analysis by TLC showed **52a** to be consumed and new spots had formed. However, isolation of the new spots revealed them to be the starting quinone **52**, which is a hydrolysis product of **52a** and the activated quinone **50a** itself. Multiple attempts using these reagents at a range of temperatures from ambient to 60 ˚C also proved unsuccessful, with no evidence for the formation of the desired product. Similar attempts at the coupling of **147** with the previously-employed mixed anhydride **131** in the presence of methylpiperidine were also unsuccessful (Scheme 39).

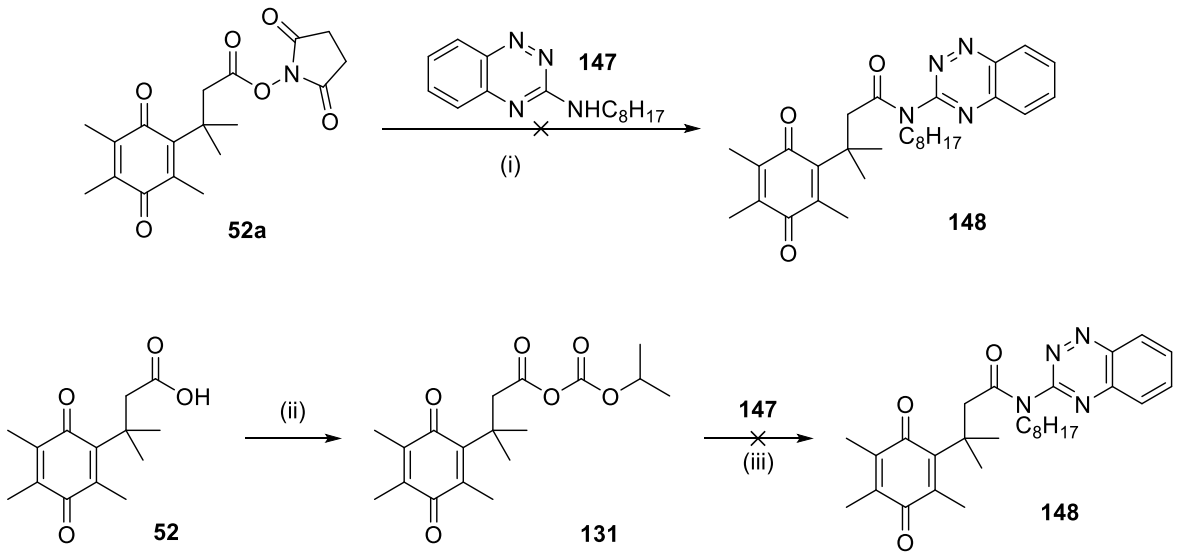

Scheme 39. (i) THF, r.t.-60 ˚C, 0%. (ii) Isopropyl chloroformate, NEt_3, THF, -5 ˚C (iii) **147**, MeCN, r.t., 16 hrs.

There are two possible explanations as to why this reaction failed. Firstly, the octyl chain on the 3-position might make the amine too bulky and thus prevent the coupling occurring, and secondly the addition of the alkyl group might not have had an appreciable activating effect, leaving the system largely unreactive.

Although this approach proved unsuccessful as a method for direct conjugation at the three position, the preparation of **147** offered the possibility of incorporating a functionalised alkyl chain in which a pendant alcohol group is present. This could allow for esterification with the acid **52** to give a candidate pro-drug. For example, the reaction of nitrobenzene (**139**) with the guanidine alcohol **149** would give the analogue **150** which could then be linked to the quinone **52** *via* an ester bond to give the pro-drug **151** (Scheme 40).

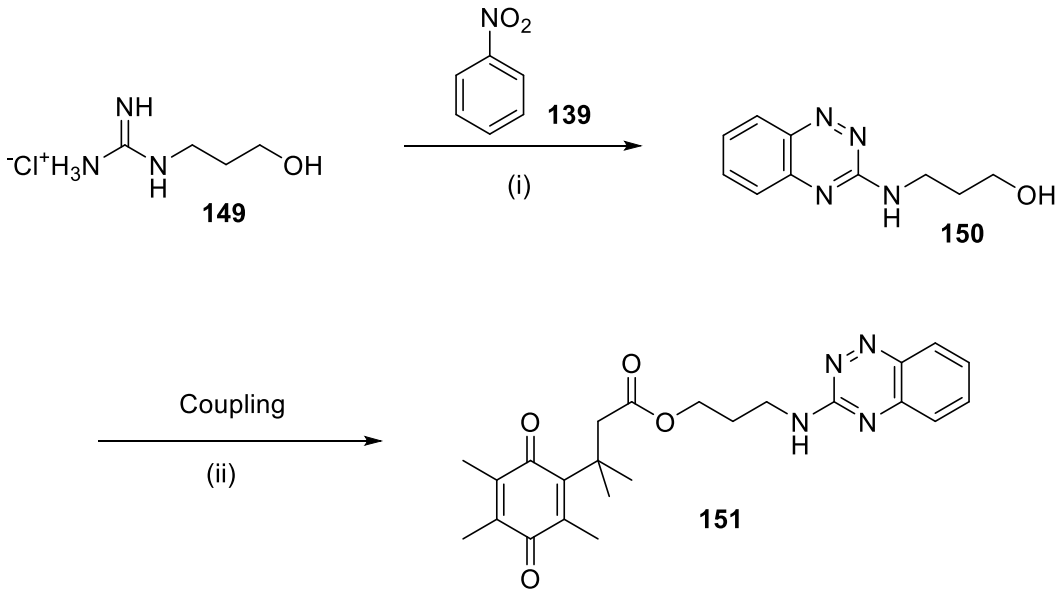

Scheme 40. Planned synthesis of **151** (i) *t*-BuOK, THF, 60 ˚C. **(**ii) HOBT, DMAP, THF,

r.t.The desired guanidine **149** was prepared using a method reported by Nowak, which was by the reaction of 3-amino propan-1-ol (**153**) with 1*H*-pyrazole-1-carboximidamide hydrochloride (**152**) (scheme 41).[84] The reaction requires the presence of a mild base, and initially triethylamine was used and the reaction was carried out in DMF. It is possible to carry out the reaction in ethanol but reaction times are longer and the respective yields are lower.[84] Due to the potentially very hygroscopic nature of the product, it was decided that an aqueous work up was not possible. Therefore on completion, the reaction products were cooled to r.t. and diethyl ether was added, which precipitated an oil. Analysis by NMR spectroscopy indicated that the product **149** had been formed, as evidenced by a signal at 159.7 ppm in the carbon spectrum corresponding to the guanidinium carbon. However, analysis by NMR spectroscopy also indicated that the product was contaminated by DMF and triethylamine hydrochloride, which was thought to have precipitated during the reaction. Attempts to remove these contaminants by trituration with further diethyl ether proved unsuccessful.

The reaction was repeated with DIPEA instead of triethylamine, and in this case the resulting solution was a clear golden yellow colour and no precipitate was formed. The solution was cooled and diluted with diethyl ether and the resulting oil was stirred mechanically with several portions of diethyl ether until ^{1}H NMR spectroscopy indicated the removal of all traces of DMF, giving **149** as a viscous oil which was golden in colour. Compound **149** was used without further purification (Scheme 41).

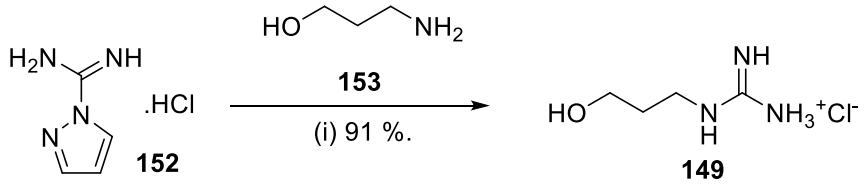

Scheme 41. (i) DIPEA, DMF, 60 ˚C.

Analysis of **149** by NMR spectroscopy confirmed the structure, with the ^{13}C data indicating the required 4 carbons and a signal at 158.9 ppm confirming the presence of a guanidinium species. The ^{1}H NMR spectrum gave an apparent pentet at δ_H 1.75 (2H, J = 6.3 Hz) ppm and two triplets at δ_H 3.26 (2H, J = 6.7 Hz) and δ_H 3.61 (2H, J = 6.0 Hz), confirming the presence of the alkyl chain. The structure of **149** was ultimately confirmed by high resolution mass spectrometry, with a mass of 118.0975 Da being observed for the [M+H^{+}], which is in agreement with the required mass of the guanidinium ion.

With **149** in hand, reaction with nitrobenzene **139** was attempted. However, guanidine **149** was found to be extremely difficult to dissolve in most solvents, and due to the possible instability of DMF under highly basic conditions, the only suitable solvent at this stage appeared to be DMSO.

In the first attempt, nitrobenzene (**139**) was dissolved in anhydrous DMSO in the presence of *t*-BuOK before adding **149** dissolved in further DMSO. The reaction, which was red in colour, was heated at 60 ˚C overnight, and after an extractive work up no product was obtained. Analysis of the aqueous phase by TLC showed that several yellow compounds were present, suggesting that **150** was more soluble in water than in dichloromethane. Other extraction solvents were explored, including ethyl acetate, but no encouraging products were collected.

In an attempt to avoid this aqueous solubility, the reaction was repeated in THF. Nitrobenzene (**139**) and *t*-BuOK were stirred together in THF to produce a red solution. This was then added via cannula to the guanidine **149,** and the mixture was heated at reflux overnight. It was observed that the poorly soluble **149** had completely dissolved within an

hour of heating under reflux (scheme 42). Once the nitrobenzene (**139**) had been fully consumed (as indicated by TLC), the solution was carefully neutralised by adding just enough saturated ammonium chloride solution. The THF was then removed by rotary evaporation and the residue was dissolved in methanol before being filtered and dried. Analysis by NMR spectroscopy and mass spectrometry indicated that the desired compound **150** had not been formed.

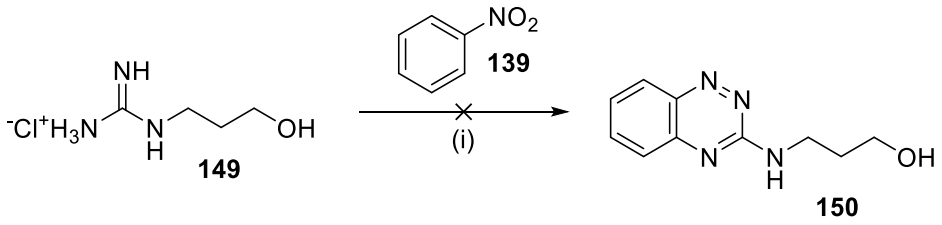

Scheme 42. (i) *t*-BuOK, anhydrous THF, 60 ˚C.

It was postulated that unprotected alcohol might be interfering with the reaction, and in an attempt to address this it was decided that the alcohol should be protected. Silyl protection was chosen due to the ease of its installation and removal, as well as its stability under highly basic conditions. Thus a new synthetic route was put forward, in which the protected guanidine **154** would be prepared before reacting with nitrobenzene (**139**)**.** This would give **155,** which after deprotection would give the target compound **150** (Scheme 43).

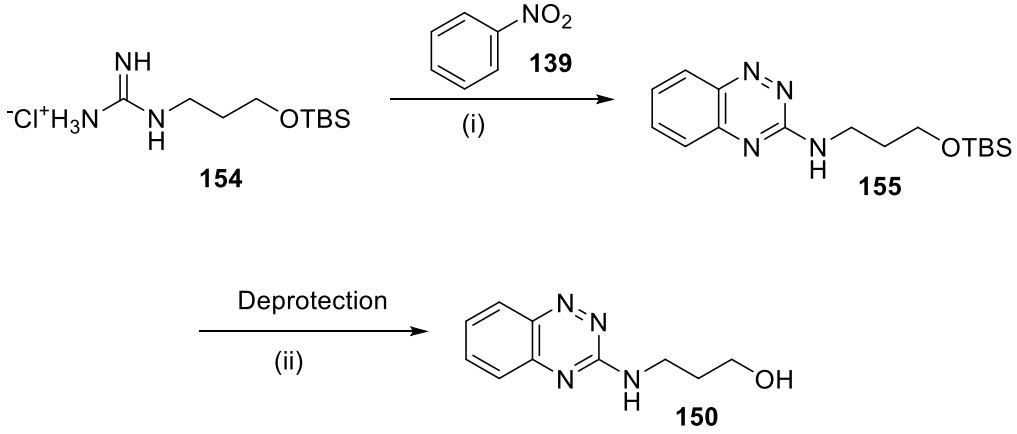

Scheme 43. Planned synthesis of **150** *via* **155** (i) *t*-BuOK, THF, 60 ˚C. (ii) TBAF.

The amine **156** was prepared by the reaction of 3-amino-1-propanol (**153**) with TBSCl and imidazole in dichloromethane, giving the amine in 75 % yield. The next stage was the guanylation of **156** using **152**. It was realised that the silyl group would prevent the precipitation of **154** from DMF using diethyl ether. In order to overcome this obstacle, the reaction was carried out in ethanol. On work up, the ethanol was removed by rotary

evaporation to give a white solid, which on trituration with diethyl ether gave the previously-prepared unprotected guanidine **149**, and not the desired product **154**.

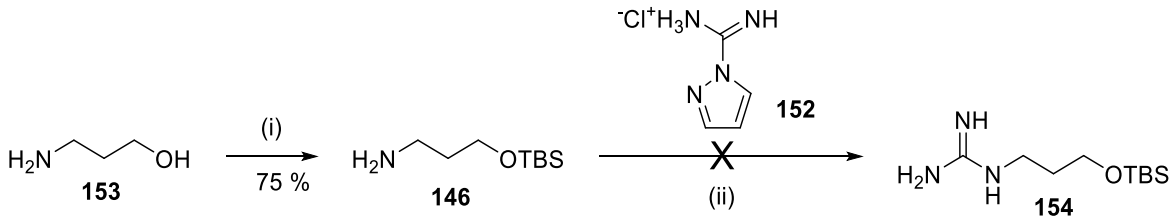

Scheme 44. Attempted synthesis of protected guanidine **154**. (i) CH_2Cl_2, imidazole, TBSCl, 0 ˚C (ii) DIPEA, ethanol, 65 ˚C.

It is likely that the silyl group was hydrolysed, either during the reaction or on standing. Some evidence exists for the hydrolysis of silyl protecting groups by guanidinium residues *via* anchimeric assistance.[85] This involves a hydrogen bonding interaction (**157**) between the lone pair of the oxygen atom and the NH group of the guanidinium group, increasing the susceptibility to nucleophilic attack and thus hydrolysis (Scheme 45). At this point, this route was abandoned.

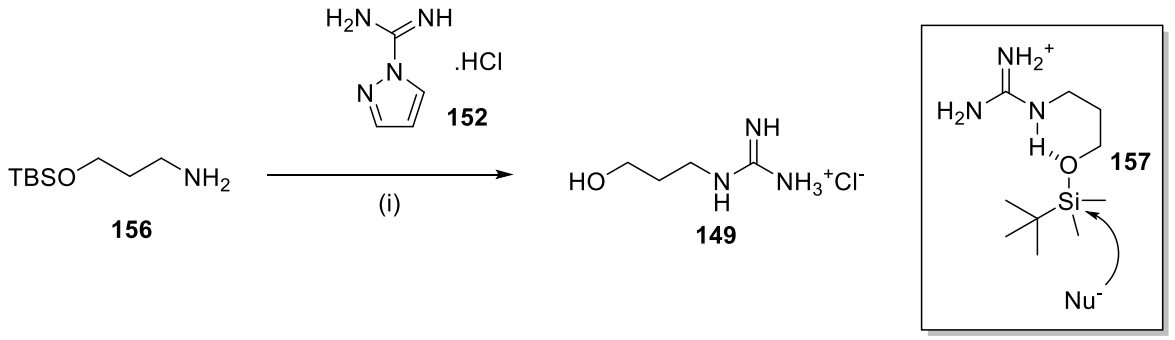

Scheme 45. Hydrogen bonding between the NH and the OTBS may cause the silyl group to be more susceptible to nucleophilic attack.

2.4. The Direct Alkylation Approach

Even though the amino group wasn't sufficiently nucleophilic, Novellino[86] reported the alkylation of a similar heterocycle **158** to give **160** in 54 % yield (Scheme 46).

Alkylation at the 3-position of **77** might allow for the preparation of analogues which allow for the coupling to the quinone **52** *via* ester or amide bonds.

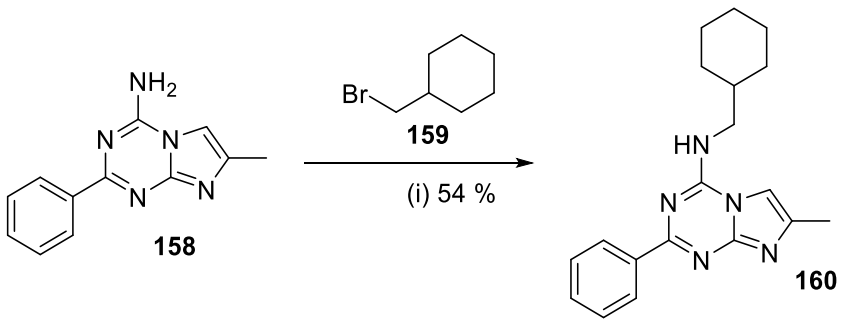

Scheme 46. K_2CO_3, KI (cat.), acetonitrile, reflux, 20 h.[86]

The alkylation of **77** with 1.5 equivalents 1-iodoheptane was attempted under,[86] using potassium carbonate and molecular sieves under reflux for 24 h (scheme 47, table entry 1).

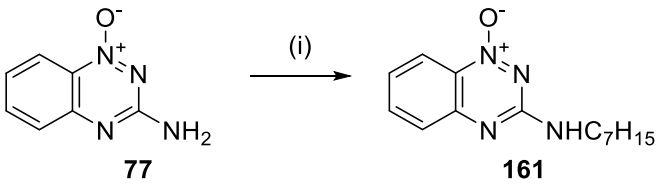

	Solvent	K_2CO_3 eqv.	Iodoheptane eqv.	temperature ˚C	Time	Yield
1	Acetonitrile	1.5	1.5	82	24 h	2%
2	Acetonitrile	1.5	1.5	82	7 d	3%
3	Acetonitrile	1.5	1.5	130	24 h	11%
4	DMF	1.5	1.5	135	24 h	30%
5	DMF	1.5	1.5	125	24 h	27%
6	DMF	1.5	1.5	120	24 h	24%
7	DMF	1	1.5	120	24 h	25%
8	DMF	0.5	1.5	120	24 h	9%
9	Dioxane	1.5	1.5	120	24 h	0%
10	DMF	1.5	1.2	120	24 h	22%
11	DMF	1.5	1	120	24 h	18%

Scheme 47. (i) Iodoheptane, K_2CO_3, reflux.

The theory is that this approach may be advantageous over the method described in section 2.3, in which an alkyl guanidine was reacted with nitrobenzene (**139**). Under these conditions **161** was formed, but in a very low yield of 2 %. Increasing the reaction time did not improve the yield (entry 2). The reason for the low yield was thought to be due to the apparent lack of reactivity of the NH_2 at the 3-position of **77**. Therefore, a range of different solvents and reaction conditions were trialled to allow the reaction to be carried out at a higher temperature.

The first of these reactions involved heating at reflux in acetonitrile in a Carius tube at 100 ˚C for 24 h, which resulted in an improved yield of 11 % (entry 3). It was found that the yield of **161** was increased to 30 % when changing the solvent to DMF and heating at 135 °C for 24 h (entry 4). However, it was apparent that at this temperature other reaction products were being produced and unfortunately it was impossible to separate these products from the desired product **161**, even with repeated chromatography.

In order to counter this problem, the reaction temperature was lowered to 125 ˚C, in the hope that this would be high enough for the reaction to occur without the formation of the contaminants (entry 5). This gave the required product in 27 % yield, but again the product was contaminated with the unknown impurity. The reaction was repeated but at the lower temperature of 120 ˚C, which gave pure **161** in 24 % yield after chromatography (entry 6).

Other attempts at improving the yield included lowering the amount of potassium carbonate, which seemed to have a marginal effect. The use of 0.5 equivalents of potassium carbonate decreased the yield to 9% (entries 7 and 8). The use of dioxane as a solvent was investigated but was unsuccessful (entry 9). Further reactions explored the use of less equivalents of iodoheptane, due to speculation that the excess of reagent might be leading to a doubly alkylated product. A reduction to 1.2 equivalents of iodoheptane and 1.5 equivalents of potassium carbonate in DMF at 120 ˚C gave a similar yield of 22 % (entry 10), where the use of 1.0 equivalent of iodoheptane gave a reduced yield of 18 % (entry 11). In all of these reactions, no evidence for a double alkylated product was observed.Analysis of **161** by NMR spectroscopy confirmed the structure, with the ^{13}C data indicating the required 14 carbons. The ^{1}H NMR spectrum indicated the presence of a triplet at δ_H 0.81 (3H, t, J = 6.6 Hz) ppm for the CH_3 group, a multiplet at δ_H 1.15-1.36 (8H, m, 4 x CH_2) ppm, an apparent pentet at δ_H 1.59 (2H, pentet, J = 7.2 Hz) and an apparent quartet at δ_H 3.44 (2H, q, J = 6.9 Hz) ppm confirming the presence of the alkyl chain. A characteristic broad singlet at δ_H 5.31 ppm was diagnostic for the presence of the NH proton on the ring system. Aromatic protons were also observed at δ_H 7.20 (1H, ddd, J = 1.1, 7.2, 8.3 Hz), 7.51 (1H, ddd, 1.1, 7.2, 8.3 Hz) and 8.25 (1H, bd, J = 8 Hz) ppm. Analysis of the IR spectrum gave a band at 3294 cm^{-1} corresponding to the N-H stretch. Final confirmation of the structure of **161** was obtained from high resolution mass spectrometry, with a mass of 261.1711 being observed for the $[M+H^+]$, which is in good agreement with the required mass of 261.1710. It was also found that slow evaporation of a dichloromethane solution of **161** gave needle-

like crystals which were suitable for X-ray analysis. This confirmed both the structure and the point of alkylation on the ring system. (Figure 27)

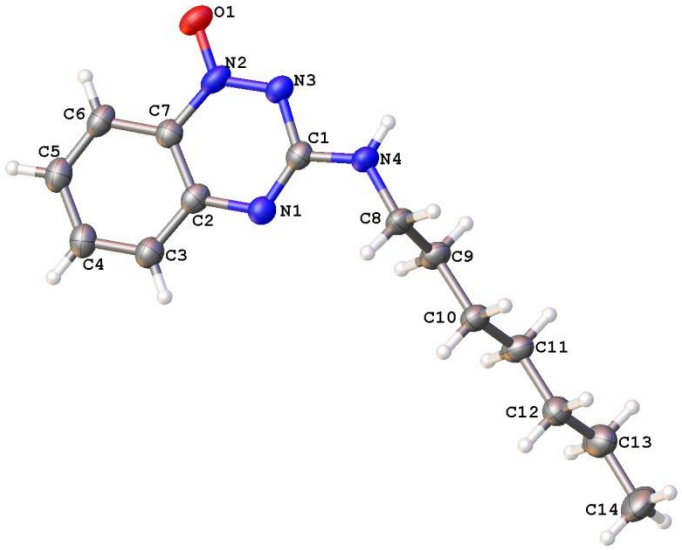

Figure 27. Crystal structure of triazine **161**.

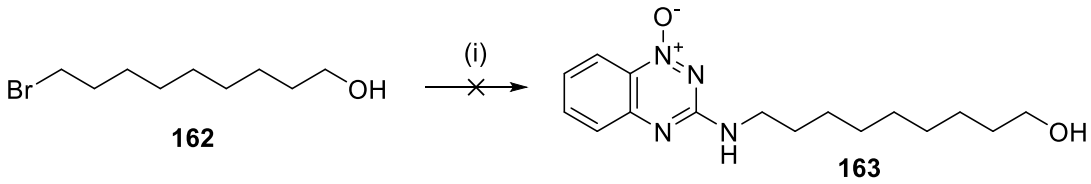

Scheme 48. Attempted Synthesis of **163** i) **77**, DMF, K_2CO_3, KI, 3Å molecular sieves, 120 ˚C, 24-48h.

When compared to the nitrobenzene approach described in section 2.3., this methodology offers the potential to quickly produce a large catalogue of alkylated TPZ derivatives, as halo alkanes are more readily available and easier to prepare. It was also hoped that this method would allow for the preparation of functionalised derivative such as **150,** which would allow coupling to the quinone **52**.

Since pro-drug esters are more suitable, the use of a long chain bromoalcohol might be advantageous. The distance between the two linking functionalities might prevent the possible counterproductive anchimeric assistance. Thus 9-bromo-1-nonanol (**162**) was employed as the alkylating agent with **77**, under the previously employed conditions (scheme 49). **162** and **77** were dissolved in DMF with potassium carbonate and molecular sieves, together with potassium iodide as a catalyst, to effect an *in situ* Finkelstein modification, as suggested by Novellino[86] The reaction was heated at 120 ˚C for 24 h. This reaction gave no

evidence for the formation of the desired product **163**. A repeat of the reaction for 48 h also gave no product. The starting triazine **77** was recovered unchanged in each case.

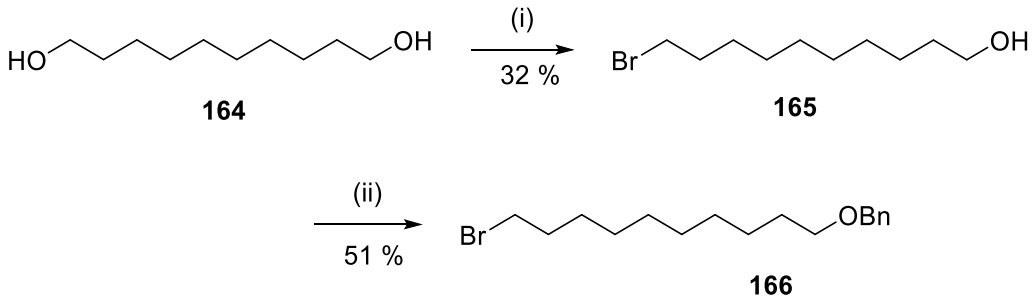

Scheme 49. (i) 48 % aq. HBr, PhMe, reflux, 16 h (ii) NaH, THF 0 ˚C, 1 h, then BnBr, reflux 16 h.

The major difference between using iodoheptane and 9-bromo-1-nonanol is the presence of an unprotected alcohol, which appears to prevent the reaction from proceeding. As a result, the benzyl group was chosen as a robust protecting group. Unfortunately, by this point in the research the donated sample of 9-bromo-1-nonanol (**162**) had been used and no more was available. A large feedstock of decane-1,10-diol (**164**) was found and used instead for the next steps of this particular investigation. The desired protected compound **166** was prepared according to Huws[87] (Scheme 49). Firstly decane-1,10-diol **164** was heated under reflux in 48 % aqueous HBr in toluene, and after column chromatography the pure bromoalcohol **165** was obtained in 32 % yield.[87] Analytical data for **165** was in agreement with that reported by Huws.[87] Alcohol **165** was then treated with sodium hydride and benzyl bromide in THF, to give benzyl ether **166** in 51 % yield. Evidence for the success of the reaction was the presence of signals at δ_H 4.51 (2H, s, CH_2), 7.36-7.35 and 7.31-7.29 (5H, m, Ph) ppm for the benzyl protecting group, which was in agreement with the literature data.[87]

Alkylation of **77** with bromide **166** was carried out under the previously used conditions. This led to the formation of **167** as a yellow solid after chromatography (Scheme 50). The presence of the compound was confirmed by high resolution mass spectrometry of the product, which gave a mass of 409.2598 being observed for [M+H$^+$]. This is in exact agreement with the required mass. However, attempts to purify **167** were difficult, as the material co-ran with several minor impurities. Partial data for the compound was obtained. NMR spectroscopy of **167** confirmed the structure, with the ^{13}C NMR data indicating the presence of 24 carbons, whilst signals in the ^{1}H NMR spectrum at δ_H 1.18-1.41 (12H, m, 6 x CH_2), 1.51-1.75 (4H, m, 2 x CH_2), 3.46 (2H, t, J = 6.6 Hz, NH-C$\underline{H}_2$) and 3.50 (2H, app q, J = 7.0 Hz, $\underline{CH}_2$-OBn) ppm indicated the presence of the alkyl chain, and a singlet at 4.50,

(2H, s, CH_2) ppm indicated the benzyl methylene group. A broad multiplet at δ_H 7.32-7.35 (5H, m, Ph) indicated the aromatic ring of the benzyl group while the presence of the triazine was confirmed by peaks at δ_H, 7.25-7.30 (1H, m, CH), 7.59 (1H, b d, *J* = 8.4 Hz, CH), 7.69 (1H, ddd, *J* = 1.4, 6.9, 8.5 Hz, CH) and 8.26 (1H, dd, *J* = 1.1, 8.7 Hz, CH). Analysis by infrared spectroscopy showed an NH peak at 3307 cm^{-1}.

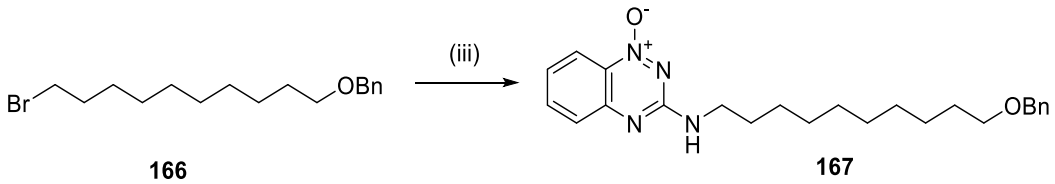

166 167

Scheme 50. (i) K_2CO_3, KI (cat.), **77**, DMF, 120 ˚C, 60%.

The final stage of the synthesis was to deprotect **166** to provide alcohol **168** ready for coupling to the quinone **52**. In the first instance, this was attempted under classical hydrogenation conditions using Pd/C and hydrogen gas. Analysis by TLC indicated the consumption of the starting material **167**. However, the only triazine product that was isolated from the reaction appeared to be amine **77** in an amount which corresponded to 85 % of the **167** used in the reaction. Benzyl alcohol was also identified in the crude reaction mixture using thin layer chromatography. Attempts were also made to deprotect the benzyl group in **167** using HBr in acetic acid.[88] Unfortunately, on heating **167** at reflux with 33% HBr in acetic acid no reaction was observed, thus suggesting that the benzyl group was not susceptible to acid hydrolysis.

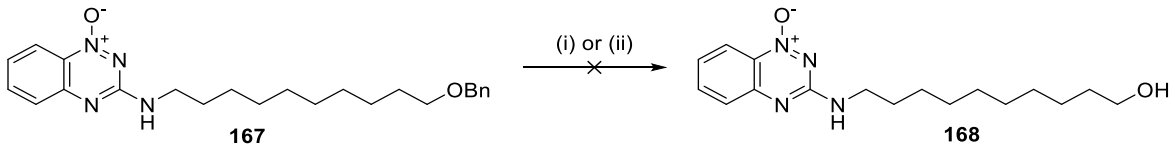

167 168

Scheme 51. (i) H_2, 5% Pd/C in methanol; or (ii) 33 % HBr in acetic acid.

Although it was possible to prepare *N*-alkyl derivatives of TPZ (**38**), these derivatives could not successfully be attached to the quinone pro-drug delivery system. As a result, a new method was required for the preparation of substituted analogues of TPZ (**38**), incorporating a linker that would allow coupling to the quinone acid **52**.

2.5. Alkoxymethyl derivatives of tirapazamine

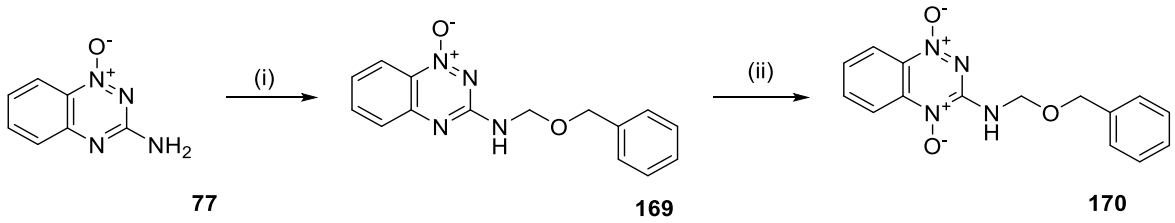

Scheme 52. Yongzhous preparation of **168**: (i) $(CH_2O)_n$, BnOH, acetic acid, (ii) MCPBA, dichloromethane, $NaHCO_3$..

Fortunately, in 2011 Yongzhou et al[89] prepared a range of tirapazamine analogues by reacting **77** with paraformaldehyde and an alcohol. This produced alkoxymethyl derivatives such as **169**. These derivatives were then oxidized using MCPBA to the corresponding 1,4-dioxides, for example **170** (scheme 52).

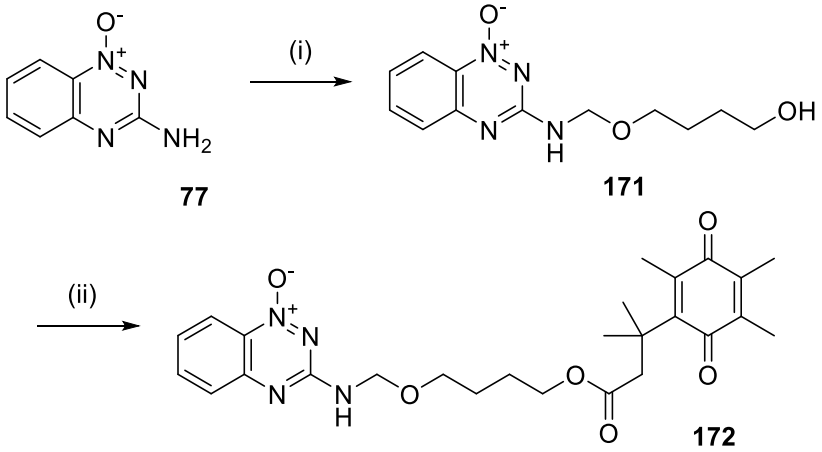

Scheme 53. Proposed preparation of functionalised alkoxy methyl derivatives: (i) $(CH_2O)_n$, butane-1,4-diol, acetic acid, (ii) **77**, DMAP, EDC, THF, r.t.

It was thus proposed that this method could be used to produce an analogue capable of being linked to the quinone **52**. Reacting **77** with a large excess of a diol (for example butane-1,4-diol) should lead to the derivative **171**, and ultimately to the pro-drug **172** (Scheme 53).

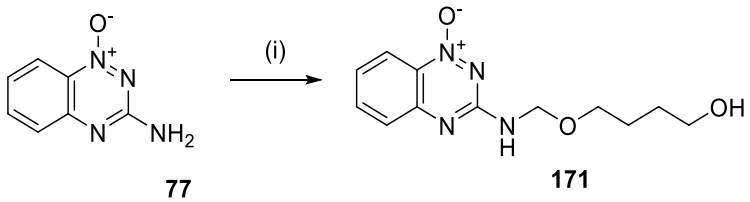

Scheme 54. (i) $(CH_2O)_n$, 1,4-butane-1,4-diol, acetic acid, 5 h, 55 %.

In choosing butane-1,4-diol, it was also hoped that a 4-carbon chain would be long enough to prevent any anchimeric effects from occurring. Thus, reaction of **77** with a large

excess of 1,4-butanediol under the reported conditions gave the desired compound **171**, contaminated with the excess unreacted butane-1,4-diol. Due to the high boiling point of butane-1,4-diol (235 ˚C)[90] evaporation was not an option. Therefore, the crude mixture was poured into water and extracted with chloroform until the organic phase no longer turned yellow. This practice removed a great deal of the diol, giving a bright yellow semi-solid. Attempts were then made to purify **171** by column chromatography. However, the residual diol made this a very difficult process.

Therefore on repeating this reaction, the crude product was dissolved in a minimum of hot chloroform and diethyl ether was added carefully until the solution became turbid. The flask was then stored at -17 ˚C overnight, during which time an amorphous yellow solid was precipitated. The solid was collected by vacuum filtration, then adsorbed onto silica and purified further by column chromatography, to give the target compound in 55 % yield. Analysis of the product **171** by NMR spectroscopy confirmed the structure, with the ^{13}C data indicating the presence of 12 carbons, whilst signals in the ^{1}H NMR spectrum at δ_H 1.75-1.62 (4H, m, 2 x CH_2), 3.67 (4H, apparent bt, J = 6.0 Hz, 2 x CH_2) and 1.93 (1H, b s, OH) ppm indicated the presence of the pendant 4-carbon chain. A broad doublet at δ_H 5.07 (2H, d, J = 7.2 Hz, CH_2) ppm and a broad triplet at δ_H 6.18 (1H, b t, J = 7.2 Hz, NH) ppm are indicative of the methylene and NH groups respectively. Aromatic protons were observed at δ_H 7.37 (1H, b t, J = 7.2 Hz, CH), 7.68 (1H, b d, J = 8.4 Hz, CH), 7.75 (1H, b t, J = 8.1 Hz, CH) and 8.28 (1H, b d, J = 8.5 Hz, CH) ppm. Analysis by infrared spectroscopy showed a broad OH peak at 3295 cm^{-1} and final confirmation of the structure of **171** was obtained from high resolution mass spectrometry, with a mass of 287.1109 being observed for [$M+H^+$], which is in exact agreement with the required mass.

With the derivative **171** in hand, analogues such as **172** might be produced from it. However, an initial test reaction was performed using propanoic acid, largely due to the time and effort required to produce the quinone **52**. Thus the alcohol **171** was reacted with propanoic acid in the presence of EDC and DMAP in anhydrous THF (scheme 55) to give the ester **173** as a yellow solid in 60 % yield. Analysis of **173** by NMR spectroscopy confirmed the structure, with the ^{13}C data indicating the required 15 carbons. The ^{1}H NMR spectrum indicated the presence of a triplet at δ_H 1.03 (3H, t, J = 7.5 Hz, Me) ppm, and a quartet at δ_H 2.19 (2H, q, 7.5 Hz, CH_2) ppm indicated the presence of an ethyl group. Signals at δ_H 1.67-1.55 (4H, m, 2 x CH_2), 3.56 (2H, t, 6.0 Hz, CH_2) and 4.02 (2H, t, J = 6.4 Hz, CH_2) ppm confirmed the presence of the pendant butyl chain, whilst a broad doublet at δ_H

4.86 (2H, d, J = 7.1 Hz, CH_2) and a broad triplet at δ_H 6.84 (1H, b t, NH) confirmed the presence of the methylene and NH groups. Four aromatic protons were observed at δ_H 7.40 (1H, ddd, J = 1.2, 7.0, 8.6 Hz, CH), 7.62 (1H, b d, J = 8.4 Hz, CH), 7.79 (1H, ddd, J = 1.2, 7.0, 8.4 Hz, CH) and 8.21 (1H, dd, J = 1.2, 8.6, Hz, CH) ppm. Analysis using infrared spectroscopy gave bands at 3307 cm^{-1} for the NH stretch and at 1728 cm^{-1} for the ester carbonyl stretch. Final confirmation of structure was obtained by high resolution mass spectrometry, with a mass of 321.1561 being observed for [M+H$^+$], which is in good agreement with the required mass of 321.1557.

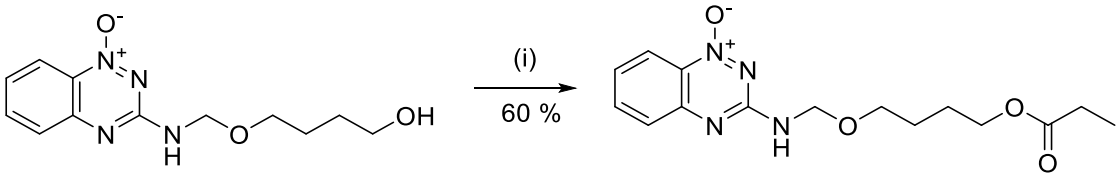

171 **173**

Scheme 55. (i) Propanoic acid, EDC, DMAP, anhydrous THF, r.t., 48 h.

This reaction was then repeated using the quinone **52**, and the analogue **171** (Scheme 56) was successfully produced, with a yield of 39 % after chromatography. Confirmation of the presence of **172** was initially obtained by high resolution mass spectrometry with a mass of 497.2388 Da being observed for the [M+H$^+$] ion, which is in good agreement with the required mass of 497.2386 Da. However, the mass spectrum was complex and it was apparent that a large number of masses were present, due to impurities and possible decomposition products. On analysis of **172** by NMR spectroscopy, it was apparent that the compound underwent decomposition in chloroform to give **171**. This was also apparent by TLC, which suggested that the completed pro-drug was susceptible to acidic hydrolysis. A 2-dimensional TLC study where the plate was immersed in chloroform for 15 minutes also indicated the formation of **171**. The same TLC experiment was performed on **173**, which appeared to be stable in chloroform. This result might suggest that the ester group in **172** is more easily hydrolysed, and this might be an effect related to the previously-observed anchimeric effect act in tandem with the gem-dimethyl effect reported by Levine.[39] A conformer such as **174** might be proposed.

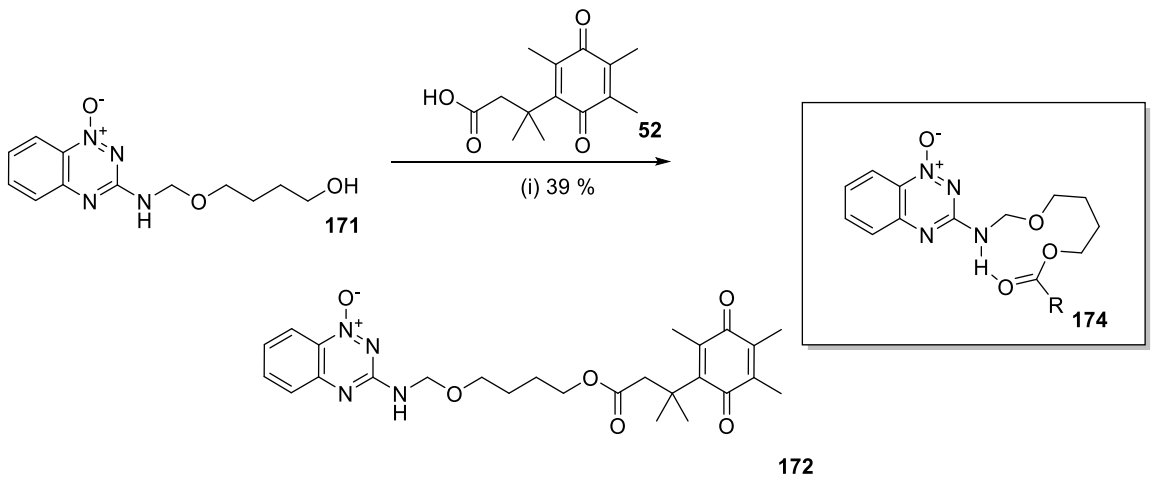

Scheme 56. EDC, DMAP, anhydrous THF, r.t. 48 hrs.

Some improved stability was observed when performing NMR spectroscopy in CD_3CN. However, hydrolysis was still apparent, despite being at a somewhat reduced rate, and it was difficult to obtain a convincing NMR spectrum of the compound.

Given the propensity for **172** to be hydrolysed under mild conditions, there was a concern that the product was being lost during the aqueous work up and during purification by flash chromatography, so the reaction was repeated, using DCC instead of EDC as there would be no aqueous work up. Once the reaction was complete, the solvent was removed under reduced pressure, and the residue was dissolved in the minimum of ethyl acetate and cooled to 0 ˚C. The precipitated DCU was filtered off, and the process was repeated three times more. The crude product was then purified on triethylamine-deactivated silica gel, to give an improved yield of 54 %. Analysis by ^{1}H NMR spectroscopy indicated the presence of **172**. However, the product was contaminated with DCU, and again the ^{1}H NMR spectrum was not convincing as to the formation of a pure product. The ^{1}H NMR spectrum did indicate the presence of 4 singlets for the methyl groups of the quinone portion of the molecule at δ_H 1.46 (6H, s, 2 x Me), 1.98 (3H, s, Me), 1.99 (3H, s, Me) and 2.15 (3H, s, Me), as well as a singlet methylene signal at δ_H 2.95 (2H, s, CH_2) ppm. The signals at δ_H 1.62-1.68 (4H, m, 2 x CH_2), 3.61 (2H, t, J = 5.9 Hz) and 4.01 (2H, t, J = 6.0 Hz) ppm are indicative of the 4-carbon pendant chain, whilst signals at δ_H 5.01 (2H, b d, J = 7.0 Hz, CH_2) and at 7.03 (1H, b t, J = 7.0 Hz) confirm the presence of the methylene linker unit. Aromatic protons were also observed at 7.47 (1H, dt, J = 1.0, 7.3 Hz, CH), 7.68 (1H, b d, J = 9.6 Hz, CH), 7.86 (1H, dt, J = 1.2, 7.1 Hz, CH) and 8.27 (1H, dd, J = 0.7, 8.6 Hz, CH) ppm. Analysis of the sample by ^{13}C-NMR spectroscopy in D_6-DMSO gave a very complex spectrum, indicating

that the compound was not pure and had possibly undergone degradation during or post purification by chromatography.

Following these results, it was speculated that a longer linker might reduce these proposed anchimeric interactions. The proposed study was to prepare the extended analogue **175** from the intermediate alcohol **176** (Scheme 57).

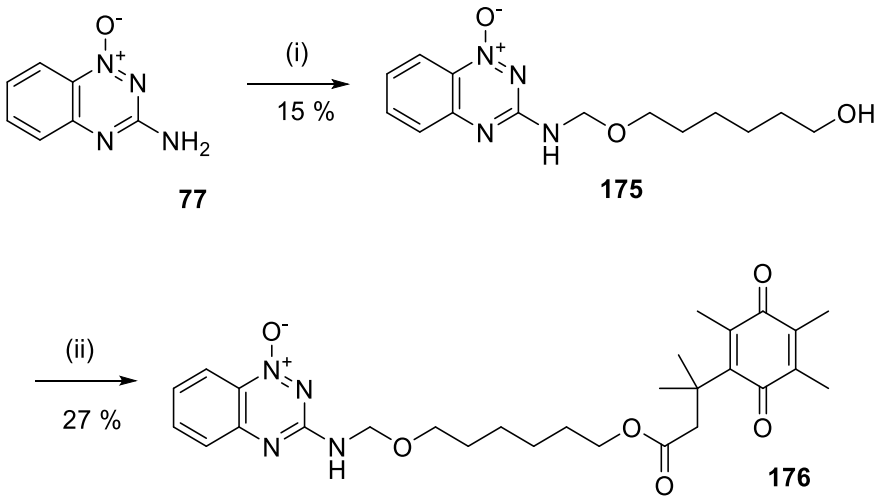

Scheme 57. Hexane-1,6-diol, $(CH_2O)_n$, CH_3CO_2H, 85 ˚C 16 hrs. (ii) **50**, DMAP, DCC, THF, r.t. 48 hrs.

Thus, compound **77** was treated with hexane-1,6-diol in the presence of glacial acetic acid. The reaction was performed in neat hexane-1,6-diol (excess, 32 eqv), and as this solvent melts at 42 ˚C, the reaction was performed at 80 ˚C. Attempts to precipitate the product from the residual hexane-1,6-diol by cooling the mixture proved difficult. Attempts to remove the hexane-1,6-diol by dissolving in ethyl acetate solution and washing with water only removed some of the diol. It was possible to purify the compound by repeated flash chromatography, to give **175** in a yield of only 15 %. However, it was apparent that the final product was still contaminated with traces of diol. Analysis of the product **175** by NMR spectroscopy confirmed the structure, with the ^{13}C data indicating the presence of 14 carbons, whilst signals in the ^{1}H NMR spectrum at δ_H 1.24-1.40 (4H, m, 2 x CH_2), 1.47-1.61 (4H, m, 2 x CH_2), 3.50-3.62 (4H, m, 2 x CH_2), and δ_H 2.07 (1H, b s, OH) ppm indicated the presence of the pendant 6-carbon chain. A broad doublet at δ_H 5.04 (2H, b d, J = 7.1 Hz, CH_2) ppm and a broad triplet at 6.68 (1H, b t, J = 7.1 Hz, NH) ppm are indicative of the methylene and NH groups respectively. Aromatic protons were observed at δ_H 7.32 (1H, ddd, J = 1.2, 7.1, 8.3 Hz, CH), 7.64 (1H, b d, J = 8.1 Hz, CH), 7.70 (1H, ddd, J = 1.2, 7.2, 8.0 Hz, CH) and 8.23 (1H, b d, J = 8.0 Hz, CH) ppm. Analysis by infrared spectroscopy showed a broad OH peak

at 3295 cm,$^{-1}$ and final confirmation of the structure of **175** was obtained from high resolution mass spectroscopy, with a mass of 293.1611 being observed for [M+H^{+}], which is in exact agreement with the required mass.

Pure **175** was then coupled to quinone **52** using DCC and DMAP (Scheme 57), to give the pro-drug **176**, with a yield of 27 % after purification by flash chromatography. NMR data revealed the product **176** to be contaminated with DCU and easily hydrolysed on standing in chloroform. However, analysis of **176** by NMR spectroscopy in CD_3CN confirmed the general structure, with the ^{13}C data indicating the required 26 carbons. The ^{1}H NMR spectrum indicated the presence of 3 singlets for the methyl groups of the quinone portion of the molecule at δ_H 1.38 (6H, s, 2 x Me), 1.89 (3H, s, 2 x Me) and 2.07 (3H, s, Me) ppm, as well as a singlet methylene signal at δ_H 2.86 (2H, s, CH_2) ppm. The signals δ_H 4.90 (2H, d, *J* = 7.0 Hz, CH_2) and at 6.89 (1H, b t, *J* = 7.0 Hz, 1H, NH) confirmed the presence of the methylene linker unit. Aromatic protons were also observed at 7.38 (1H, ddd, *J* = 1.1, 7.0, 8.5 Hz, CH), 7.59 (1H, b d, *J* = 8.5 Hz, CH), 7.77 (1H, ddd, *J* = 1.4, 7.0, 8.5 Hz, CH) and 8.18 (1H, dd, *J* = 1.4, 8.5 Hz, CH) ppm. Analysis by infrared spectroscopy gave bands at 3294 cm^{-1} corresponding to the amine N-H stretch and at 1724 cm^{-1} for the ester carbonyl stretch. Analysis by high resolution mass spectrometry was unsuccessful, indicating the instability of the compound.

In conclusion, a new method has been developed for producing analogues of **77**, with a linker for conjugation, to release quinones such as **52**. The methodology is simple, requiring few steps to the pro-drugs without the need of any protecting groups. However, modifications to the structure are required, as the conjugated esters may be hydrolysed, possibly due to anchimeric effects between the amine on the 3-position and the carbonyl of the ester linker. A further issue which had been foreseen with this approach is that it would probably be difficult to oxidise the final pro-drugs e.g. **172** and **176** due to their instability. Additionally, the pendant alcohol group might competitively oxidise. As a result it was envisaged that it would be preferable to form alkoxy-methyl derivatives directly by reacting tirapazamine (**38**) under the conditions reported by Yongzhou (Scheme 58).[89]

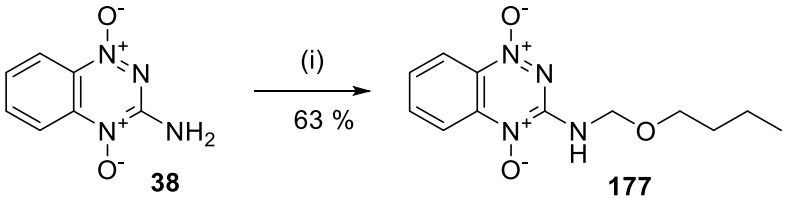

Scheme 58. *n*-Butanol, $(CH_2O)_n$, acetic acid (cat).

Thus, a test reaction was set up where tirapazamine (**38**) was reacted with *n*-butanol and paraformaldehyde in the presence of glacial acetic acid (Scheme 58). It took two hours for TPZ (**38**) to dissolve fully, but after warming the reaction to 80 °C, the solution was bright red in colour. The reaction was monitored by TLC, and once complete the solvent was removed by rotary evaporation. The crude orange product was purified by column chromatography to give the TPZ analogue **177** as an orange powder in a yield of 63 %. Compound **177** had previously been prepared via a two-step method by Yongzhou[89] with a yield of 51 %. Derivative **177** is considerably more soluble than TPZ (**38**), being soluble in solvents such as chloroform and ethyl acetate. This suggests that these analogues are likely to be much more workable than TPZ itself. This result shows that oxidised analogues of **172** and **176** could be produced by this method, negating the need for a late stage oxidation, which may as mentioned prove problematic.

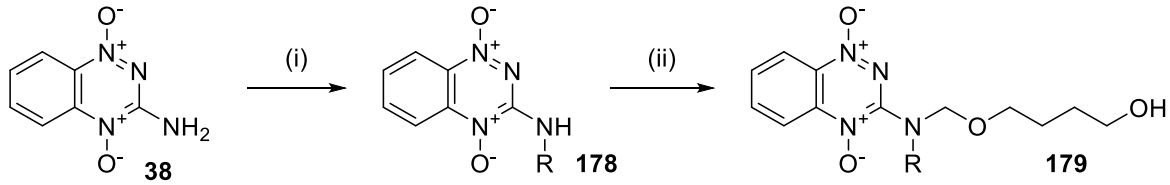

Scheme 59. (i) Alkyl halide, K_2CO_3, DMF, 120 ˚C (ii) Butane-1,4-diol, $(CH_2O)_n$, acetic acid (cat).

Further future work might involve the blocking of the remaining amine function at the 3-position, which would eliminate hydrogen bonding to the carbonyl of the ester. It is proposed that a methodology for achieving this would be first alkylation of the TPZ (**38**) using the methods described in section 2.4, following which the alkylated derivative **178** would be treated with paraformaldehyde and diol as described in this chapter, to give analogues such as **179** (Scheme 59). Due to time constraints, this work could not be carried out during this study.

3.0. Conclusions and future work

The previously unprepared phenyl-locked mustard pro-drug **116** was successfully prepared using a HOBT-based coupling methodology. As part of this work, the quinone **105** was prepared according to a known procedure[37] in a comparable yield. However, an improved method[91] was developed for the synthesis of the aniline mustard **70**, which allowed synthesis without the formation of contaminant by-products (Scheme 60).

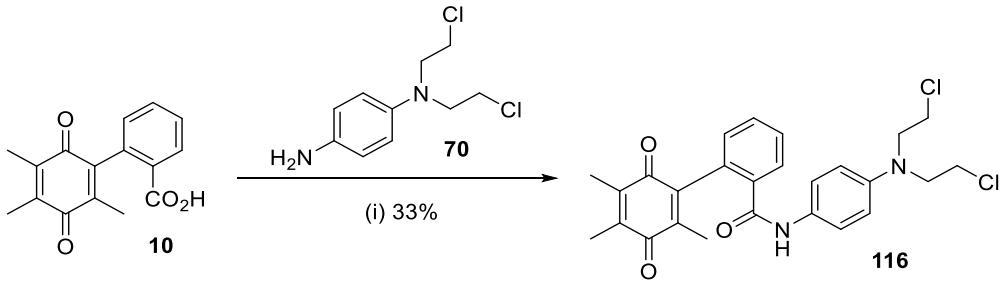

Scheme 60. Synthesis of the pro-drug **116** (i) HOBT, EDCI, THF, r.t., 48 h.

Now that the pro-drug **116** is available, together with a supply of the previously prepared guanidines **109-111** and **112-114** (prepared by Martin),[1] as well as the mustard **71** (also synthesised by Martin)[37] they will be appraised as subjects for NQ01 and have their anticancer activity determined by the research group of Professor Roger Phillips at Huddersfield University.

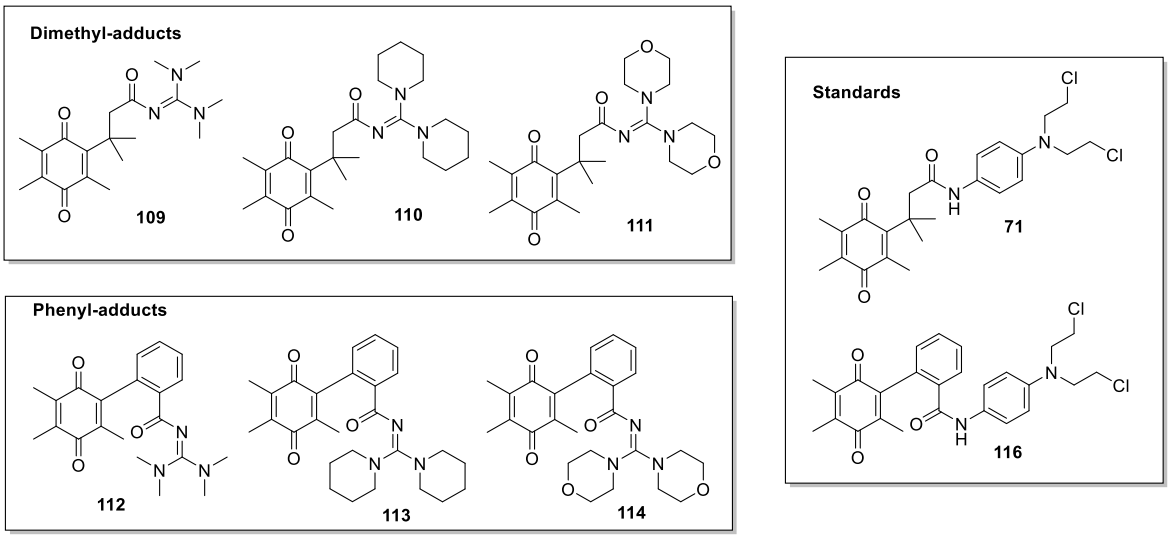

Figure 28. Guanidines and mustards submitted for biological evaluation.

The first section of this thesis also focused on the preparation of several new analogues **147**, **161**, **167**, **171**, **173** and **175** of tirapazamine (**38**) and 3-amino-benzotriazine-1-oxide

77. Attempts were made to couple **171** and **175** to the quinone **52** to give pro-drugs **172** and **176** respectively. However, rapid hydrolysis of these compounds was observed to occur even in mildly acidic conditions, and therefore the absolute confirmation of structure for these was difficult. This undesired hydrolysis is a drawback in terms of suitability of these structures for pro-drug applications. However, by using the methodologies developed throughout the study, there is the potential to generate further, perhaps more stable, analogues of TPZ (**38**). The simplicity and robustness of these methods would also allow the rapid generation of a library of different TPZ analogues (Figure 29).

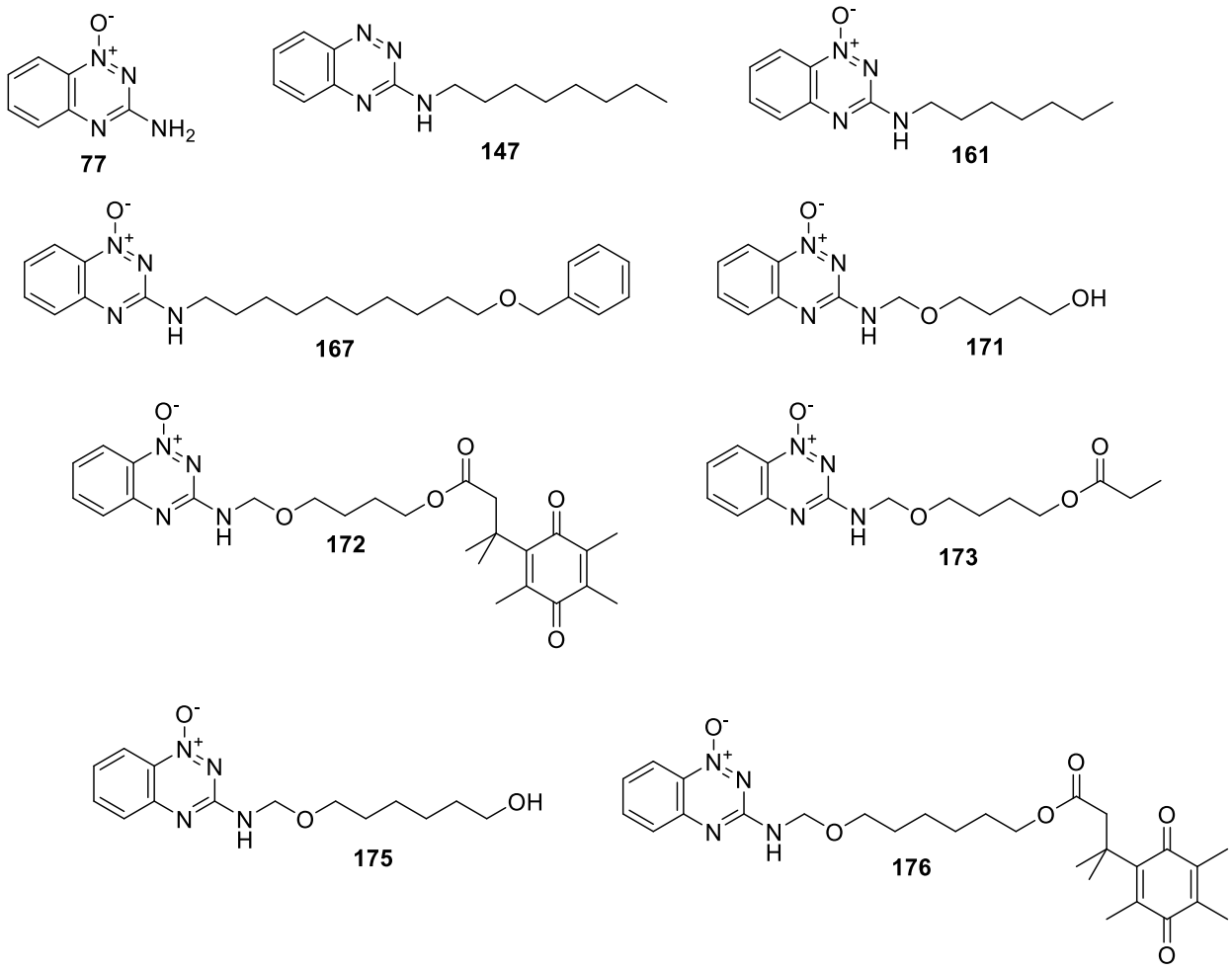

Figure 29 Novel analogues of tirapazamine **1** prepared as part of this study.

Currently none of these compounds have been appraised for activity. The partner company went bankrupt in 2012 and only recently an alternative method for evaluation has been identified.

As part of this work, two proposals have been put forward to overcome synthetic and stability problems. Firstly, the synthesis of TPZ analogues such as **177** directly from **38** by using the methods developed by Yongzhou[89] negates the need for a late-stage oxidation.

Secondly, future work might involve the blocking of the remaining amine function at the 3-position, which would eliminate hydrogen bonding to the carbonyl of the ester. Thus, starting with the alkylation of TPZ (**38**) using the methods described in section 2.4, the alkylated product **178** would then be treated with paraformaldehyde and diol as described in section 2.5, to give analogues such as **179** (Scheme 61).

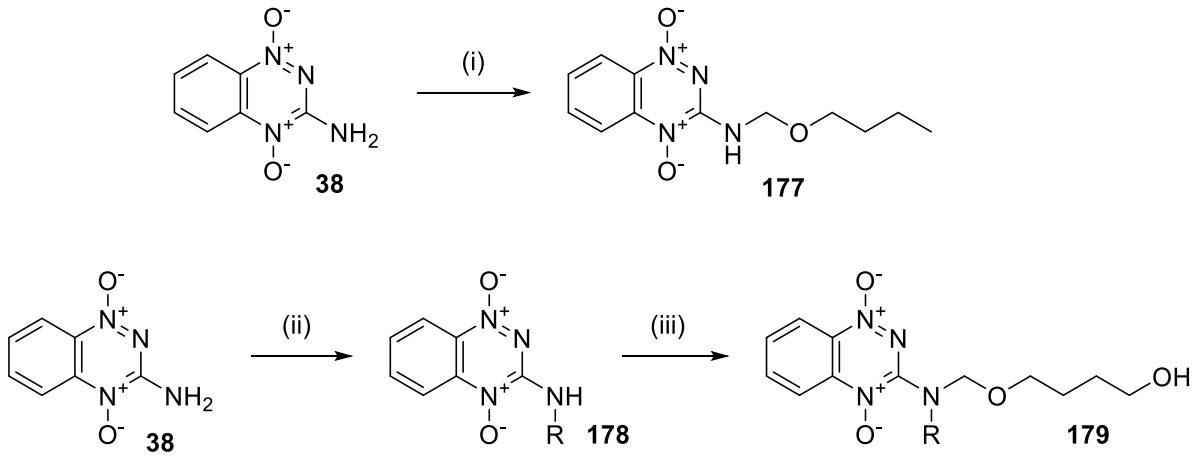

Scheme 61. Future developments of this work: (i) *n*-Butanol, $(CH_2O)_n$, acetic acid (cat). (ii) Alkyl halide, K_2CO_3, DMF, 120 ˚C. (iii) Butane-1,4-diol, $(CH_2O)_n$, acetic acid (cat).

Section B:

The Synthesis of Natural Products from the Sea Sponge *Monarca Arbuscula*.

4.0 Introduction

4.1 Leishmaniasis

Leishmaniasis is a disease caused by a parasite of the order protozoa Leishmania, and is spread by various species of sandfly. The disease can present itself in three forms. These are Cutaneous (the least severe form presented as skin ulcers), mucotaneous (presenting as ulcers of the skin of the mouth and nose), and finally visceral (the most severe form, starting with skin ulcers which are followed by fever and in later stages low red blood cell count, the swelling of the spleen and liver, and death). The disease mostly affects the poorest regions of the world, but is widely spread. Annually, approximately 1.3 million new cases occur and 20,000 to 30,000 people die as a consequence of leishmaniasis (Figure 30).[60,61]

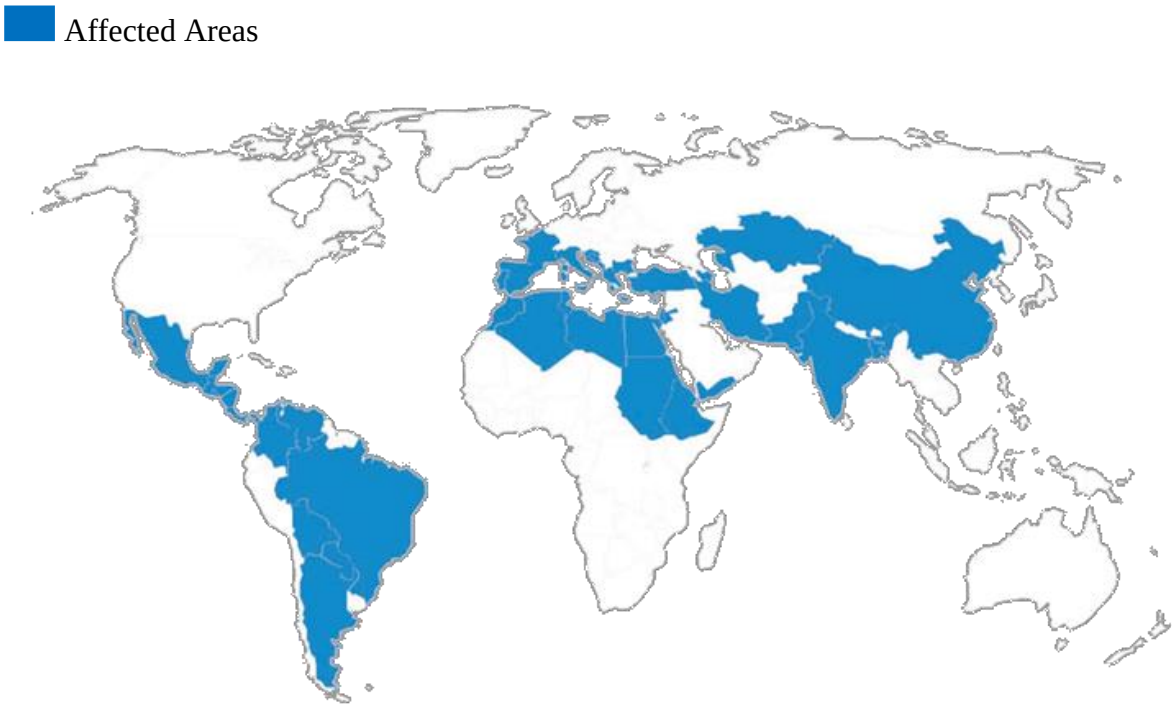

Figure 30. Global Distribution of leishmaniasis.[60]

The skin lesions are reminiscent of leprosy and in many regions the disease is misdiagnosed until it is in its later stages.

Currently there are four main drugs in circulation for the treatment of leishmaniasis (Figure 31); Pentostam (**180**) (Fig 31.) is a pentavalent antimony compound which displays very good activity against visceral leishmaniasis. Unfortunately, the parasite has become resistant to the drug in areas such as India and the Mediterranean. The drug is also

phlebotoxic (toxic to veins), and after several doses of the drug, administration becomes difficult as viable veins become difficult to find.[61]

Paromomycin (**181**) (Fig. 31) is an aminoglycoside antibiotic, and is currently used in Africa in conjuction with pentavalent antimonials. Although the side effects are much milder when compared to other anti-leishmanial drugs, it has shown poor activity as a sole agent.[61]

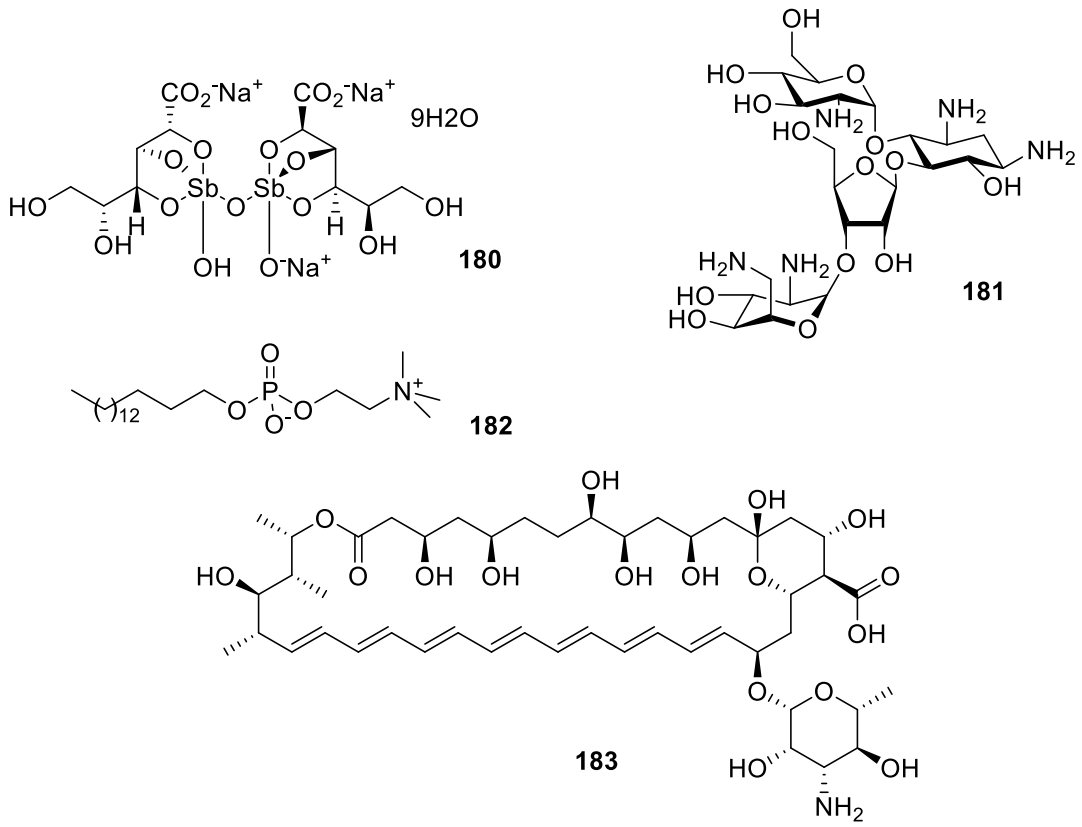

Figure 31. Current anti-leishmanial drugs

Miltefosine **(182)** (Fig. 31) is a phospholipid which is effective against both cutaneous and visceral leishmaniasis, and is the only leishmanial drug to date to be administered orally. Approximately 60 % of patients experience nausea and vomiting, with the effects being more severe towards women and children. The drug is also embryotoxic and has been linked with birth defects. As a consequence, contraception must be taken in conjuction with the drug.[61]

Amphotericin B (**183**) (Fig. 31) was first extracted from the filamentous bacterium *Streptomyces nodosus* in 1955 and has been used extensively as a fungicide. It is effective against visceral leishmanisias in India, South America and the Mediterranean where the disease has become resistant to pentavalent antimonials. Unfortunately, amphotericin B is

well known for its severe side effects, which occur between 1 and 3 hours after infusion and include hypotension, low breathing, rapid breathing and often cardiac arrest and death.[61]

The current treatments for leishmaniasis are far from ideal, displaying severe side effects or low activity and there is a need for a safe and effective treatment which can be administered orally. Controversially, cutaneous leishmaniasis is not a priority on the global agenda, and the development of new treatments is lagging behind.[61]

4.2 The Role of Natural Products in Medicine

Nature has been the source of pharmaceutical compounds on countless occasions throughout human history. Hippocrates (c. 460 – c. 377 BC) left records describing the prescription of powder made from the leaves and bark of the willow tree spirea to alleviate the symptoms of headaches, fevers and pains.[62] However, with modern science allowing a deeper understanding into the pathology of several diseases, attention was shifted from natural products to synthetic targets, which could be created with a specific molecular target in mind. A synthetic approach in turn allowed for high throughput screening technologies supplying a large number of chemical libraries. In the past, combinatorial chemistry allowed the rapid generation of compounds. However, this methodology could only continue for so long, and by 2001 the number of new drugs discovered and licensed in this way had decreased dramatically. Since 2001 there has been a significant new drive to isolate new natural products that may have medicinal applications.[63]

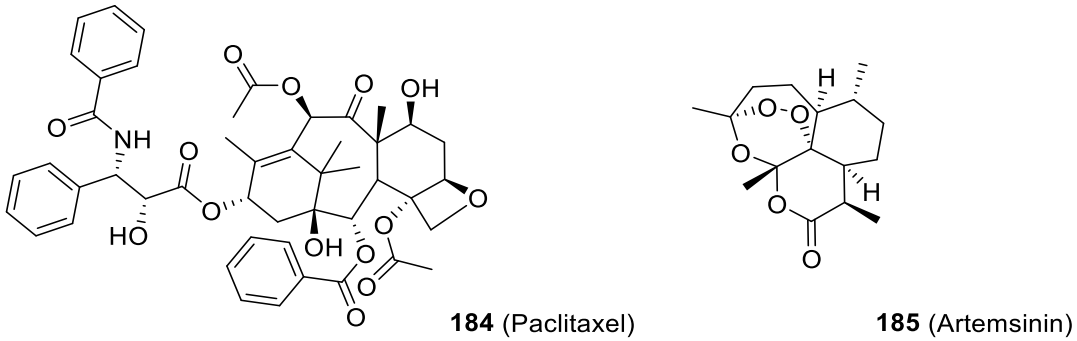

184 (Paclitaxel) **185** (Artemsinin)

Figure 32. Paclitaxel (**184**) and artemisinin (**185**).

The majority of current natural product derived therapies are of terrestrial origin, i.e. plants, bacterial and fungi. For example, both the cancer chemotherapy agent paclitaxel (**184**) **(**isolated from the bark of the pacific yew tree), and the anti-malarial agent artemisinin (**185**) (isolated from *Artemisia anuua)* are plant metabolites (Figure 32).

A natural product is a chemical compound or substance which is produced by a living organism such as plants, animals and microorganisms.[96] Within the field of organic chemistry, the definition of natural products is usually restricted to mean purified organic compounds isolated from natural sources that are produced by the pathways of primary or secondary metabolism. Within the field of medicinal chemistry, the definition is often further restricted to secondary metabolites, Secondary metabolites are not usually biosynthesized by the primary metabolic pathways and have no apparent function in the growth, development or reproduction of the organism.[97] However, they may play a role in many other ecological relationships, including defense against predation and competition for space and food. Compared to non-natural compounds, natural products show high chemical diversity, biochemical specificity, binding efficiency, and have the propensity to interact with biological targets, making them favourable lead structures for drug development. [98–100]

4.3. Marine Natural Products

The ocean is a vast source of new species and, crucially, new natural products, which could hold the key to curing many diseases worldwide. The exploration of marine ecosystems only began in the mid-1970s with the advent of modern snorkelling and the introduction of scuba diving in 1970. Remotely operating vehicles came into use around 1990, further increasing the potential for the exploration of the oceans.[98]

As a result of technical limitations, exploitation of marine organisms started with the collection of larger creatures such as red algae, sponges and soft corals. This resulted in the isolation of many unique compounds.[101] Marine natural products have shown a myriad of biological activity including anti-tumour, anti-microbial and anti-proliferative properties.[100,102–106]

4.3.1. Guanidine Marine Natural Products

Over the years, the work within the Murphy group at Bangor University has been focussed on the synthesis of guanidine-containing marine natural products.[107–112] As a result of their biological properties, guanidine-containing natural products are gaining considerable interest from many research groups.[113] Molecules containing the guanidine and guanidinium structural motif are capable of hydrogen bonding (from the guanidinium ion) with phosphate- and carboxylate-containing molecules. and possess a broad range of biological properties.[108,109,112,114,115]

In 2013 Berlinck and co-workers at the university of Sao Paulo isolated two new guanidine-containing alkaloids from the sea sponge *Monarca arbuscula*, which were monalidine A (**186**) and arbusculidine A (**187**).[116] From 360 g of dry sea sponge, only 1.2 mg of **186** and 0.9 mg of **187** were obtained after several extraction and HPLC purification stages.

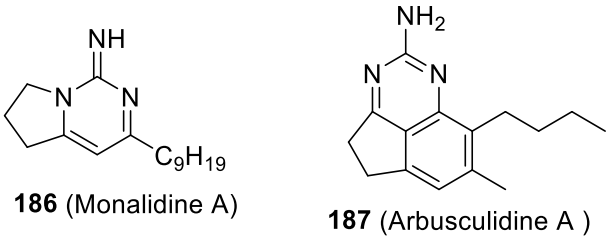

186 (Monalidine A) **187** (Arbusculidine A)

Figure 33. Two new natural products from the sea sponge *Monarca Arbuscula*.[116]

4.4. The Crambine Alkaloids.

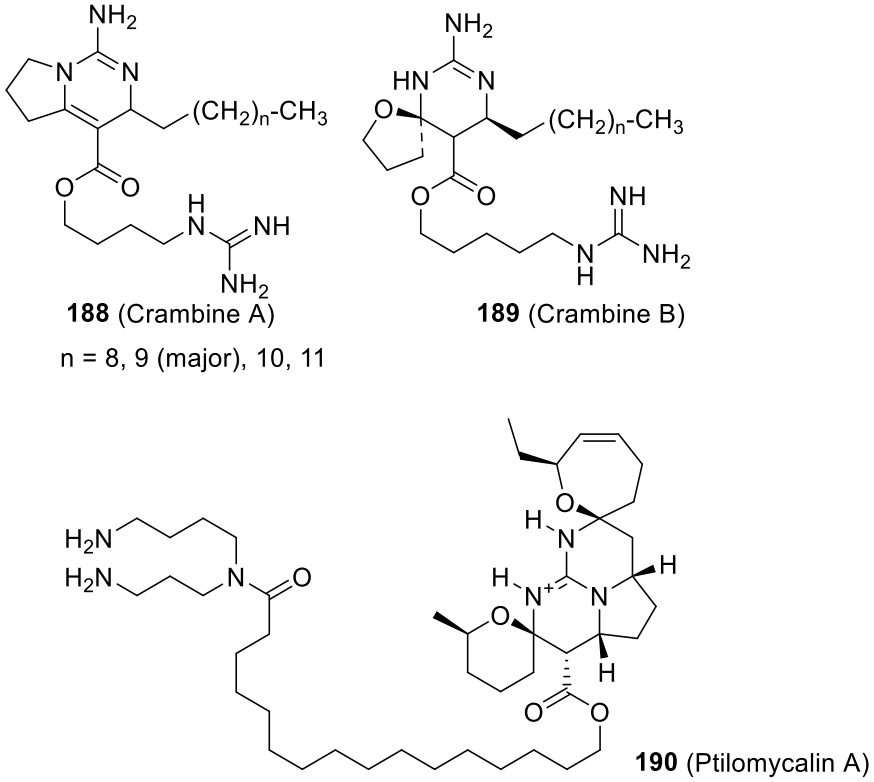

188 (Crambine A) **189** (Crambine B)

n = 8, 9 (major), 10, 11

190 (Ptilomycalin A)

Figure 34. Crambines A and B and ptilomycalin A.

The structure of monalidine A (**186**) is very similar to the structures of the crambines A (**188**) and B (**189**) (figure 34), which were isolated from the Mediterranean sea sponge *Crambe crambe* by Berlinck in 1990.[117,118] The bright red encrusting sea sponge is common along the coasts of the Mediterranean and is generally free from parasites and other epizoites.

Crambe crambe is also capable of causing tissue necrosis of other sponges which may be in physical contact with it.[118]

Dried specimens were extracted with methanol to give a material with high toxicity against the fish *Lebiste reticulatus*, and which inhibited the re-aggregation of cells in other specimens such as the freshwater sponge *Ephydiata fluviatillis*. Berlinck identified **188** and **189** as being *bis*-guandine alkaloids, and speculated that they were biogenetically related to ptilomycalin A (**190**), which was isolated from the Red sea sponges *Ptilocaulis spiculifer* and *Hemimycale columella* in 1989.[118]

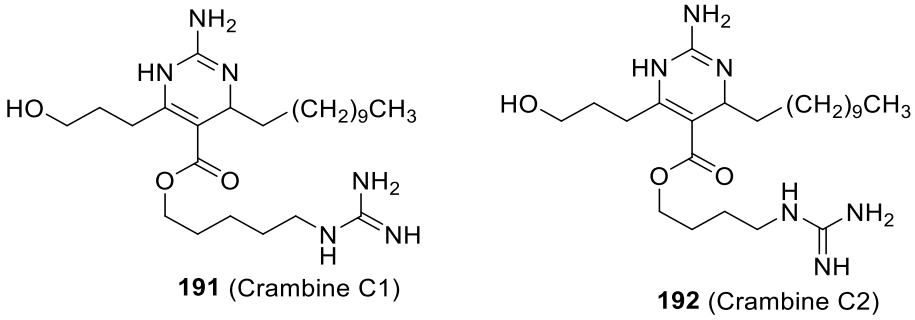

Figure 35. Crambines C1 and C2.

In 1992 Berlinck reported two further extracts from *Crambe*. The alkaloid crambine C1 (**191**) (Figure 35) was found in a specimen taken from Nice in France. It was also found as a minor component from specimens that were collected from Favignana (Italy), together with the second new alkaloid crambine C2 (**192**) (Figure 35). Structural elucidation revealed that crambine C1 (**191**) is an isomer of crambine B (**1192**). Furthermore, C1 (**191**) differs from C2 (**192**) only in the length of the alkyl chain between the ester group and the guanidine.[119]

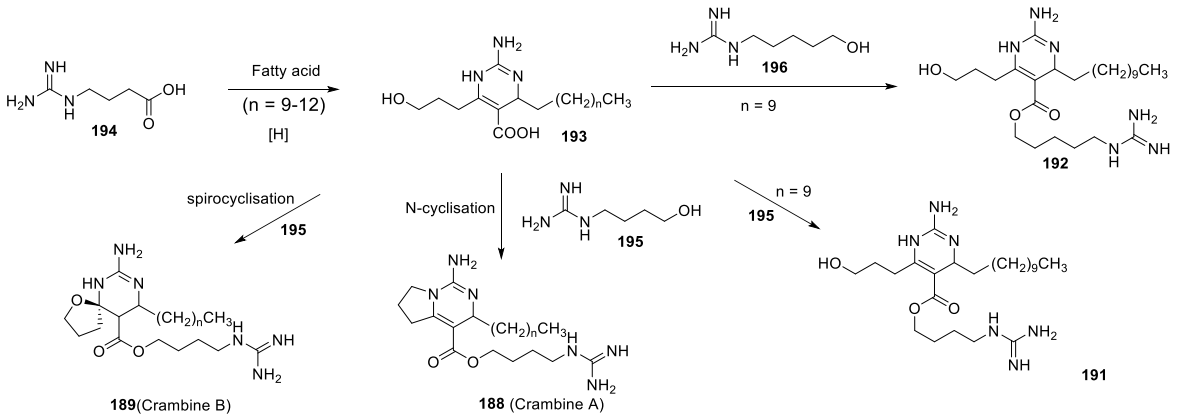

Scheme 62. Proposed Biosynthesis of crambines A and B.[119]

Berlinck speculated that both crambine A (**188**) and crambine B (**189**) are derived from the intermediate **193** (scheme 62), which could be formed by the condensation of fatty acids using a reduced form of γ-guanidinobutyric acid **194**. Guanidine derivative **194** which is found in many marine invertebrates is a degradation product of arginine. Esterification of **193** with a molecule of γ-guanadinobutanol **195** would give the chain found in crambines **188**, **189**, **191** and **192**. Cyclisation of this intermediate **193** leads to crambine A (**188**)**,** whilst spirocyclisation would give the crambine B (**189**). Similarly crambine C1 (**191**) could arise from the esterification of **193** with γ-guanidinopentanol **196** respectively.[80]

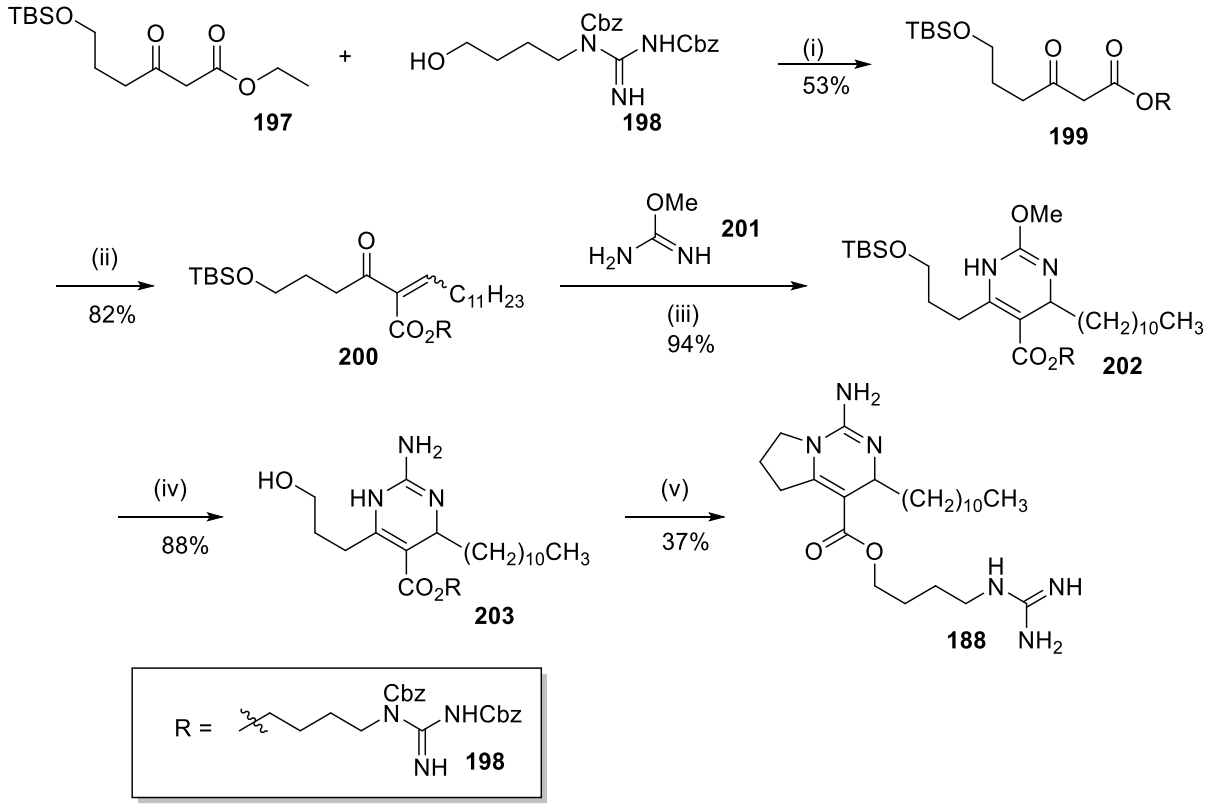

Scheme 63. (i) DMAP, benzene, Δ. (ii) $C_{11}H_{23}CHO$, piperidine. (iii) NH_3, NH_4OAc, MeOH, Δ. (iv) TBAF, THF. (v) a) MsCl, Et_3N, CH_2Cl_2. b) Et_3N, $CHCl_3$, Δ. c) H_2, Pd.[120]

By 1993, both **188** and **189** had been synthesised from ethyl acetoacetate (**195**) in eight steps by Snider, according to scheme 623 (crambine A) and scheme 64 (crambine B).[83] Firstly the protected β-keto ester **197** underwent acyl transfer using DMAP, to give the guanylated ester **199** in a 53 % yield. The fatty acid chain was added by reacting **199** with dodecanal and piperidine to give **200** in 82 % yield. This then underwent condensation with *O*-methylisourea (**201**) to give the pyrimidine **202**. This in turn was converted into the guanidine **203** using ammonia and ammonium acetate, giving a 94 % yield. Ring closure

was then carried out using methanesulfonyl chloride and triethylamine, before hydrogenation to deprotect the guanidine and give crambine A (**188**) in a 37 % yield.

As an alternative method, **203** was cyclised on treatment with triethylamine to give **205**, which on hydrogenation gave crambine B (**189**) in 86 % yield.

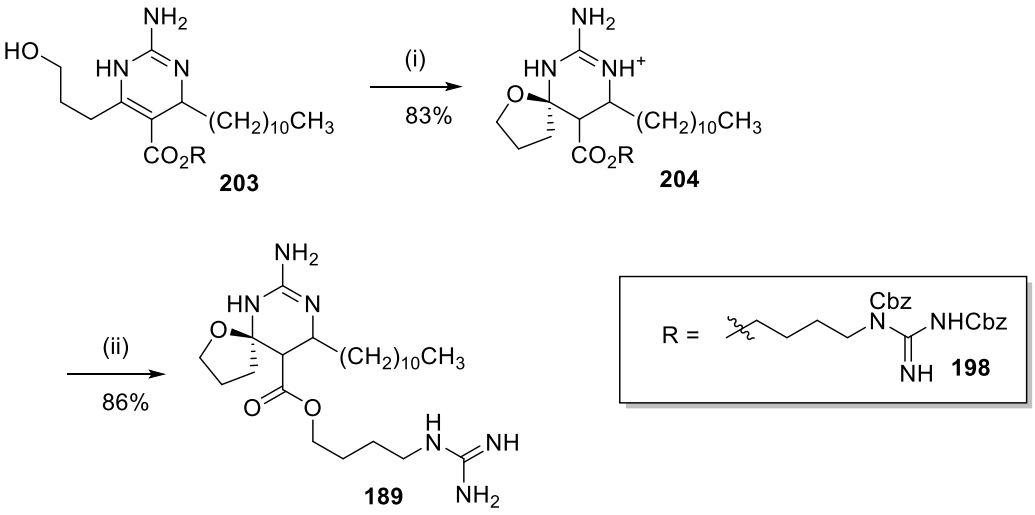

Scheme 64. (i) Et_3N, $CHCl_3$, Δ. (ii) H_2, Pd/C, dichloromethane.[120]

Biological studies performed by Rinehart[121] found that crambines A (**188**) and B (**189**) were cytotoxic to L1210 cells with IC_{50} values of less than 1 µg/mL, showing identical activity to that of the naturally occurring material.

4.5. The Batzelladine Alkaloids

In 1994 Patil *et al.* isolated the batzelladines A-E **205-209** from the sea sponge *Batzella spiculifer,* along with the other previously isolated guanidine metabolites ptilomycaulin A (**190**), crambine A (**188**), crambescidine 900 (**210**), crambescidine 816 (**211**) and ptilocaulin (**212**). Batzelladine A (**205**) and batzelladine B (**206**) were the first-known naturally occurring small molecules to be shown to inhibit the binding of HIVgp-120 to the CD4 receptor, and as a consequence were potential inhibitors of HIV.[122]

As previously noted, monalidine A (**186**) is very similar in structure to crambine A (**188**), and is also a similar structure to the "tethered" ester of batzelladine A (**205**) and batzelladine B (**206**), which share the same bicyclic motif. The major difference, however, is that **186** is devoid of the ester group at the 4-position, which might or might not have a profound effect on its biological activity.

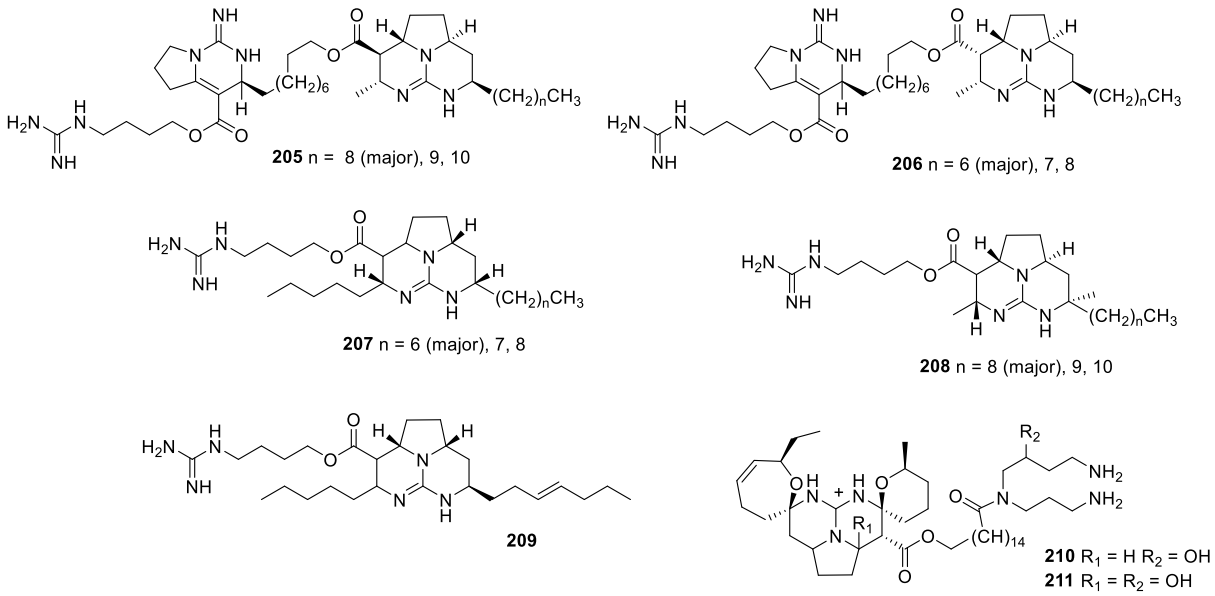

Figure 36. The alkaloids isolated by Patil in 1994.[122]

4.6. Arbusculidine A

The structure of arbusculidine A (**187**) is very similar to those of the family of natural products of which ptilocaulin (**212**) was the first to be isolated, from the sponges *Ptilocaulis aff.* and *P. spiculifer* in 1981.[121]

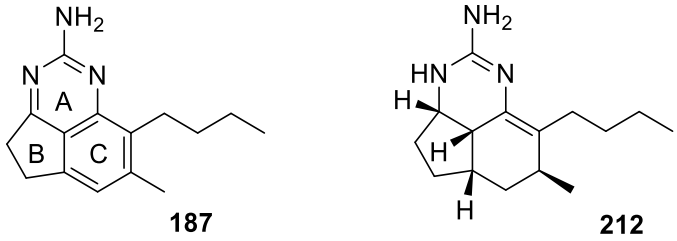

Figure 37. Arbusculidine A (**187**) and ptilocaulin (**212**).

Both arbusculidine A (**187**) and ptilocaulin (**212**) have a tricyclic structure with aliphatic butyl chains on the 4-position and a methyl group on the 5 position. However, in arbusculidne, both 6-membered rings are aromatised and thus devoid of the stereochemistry present in ptilocaulin (**212**)**.** The rings have been arbitrarily assigned A, B and C in order to aid discussion. Thus, arbusculidine A (**187**) appears to be a member of the ptilocaulin family, which is a range of compounds that have been shown to possess diverse biological activity, including anti-parasitic and anti-HIV activity.[121–123] It also appears to be the first compound in the series which is aromatised in both the A- and C-rings.

4.6.1. The Ptilocaulin Family of Alkaloids

In 1981, Rinehart and co-workers isolated the two tricyclic guanidine- containing alkaloids, ptilocaulin (**212**) (Figure 37) and isoptilocaulin (**215**), from two samples of *Ptilocaulis aff. P. Spiculifer* which were collected from slightly different locations and depths.[85] The two compounds were found to be biologically active, ptilocaulin (**212**) being the more active of the two, with an LD_{50} of 0.39 µg/mL (50 % inhibition of cell growth) against L1210 leukemia cells. It also showed strong activities against *Streptococcus pyogenes*, *Pneumoniae faecalis*, *Staphylococcus aureus* and *Escherichia coli*.[121]

Between 1995 and 2008, 19 additional tricyclic alkaloids were isolated from a variety of other marine sponges. Braekman isolated 8b-hydroxyptilocaulin (**226**) from the sponge *Monanchora arbuscula*.[124] In 1996 Capon *et. al.* isolated Mirabilins A-F **219-221**, **231-232** and **213-215** as their *N*-acetyl derivatives from the sponge *Arenochalina mirabilis***.**[123]

In 1997, Patil and Freyer isolated mirabilin B (**220**) along with 8α-hydroxymirabilin B (**224**) and compounds **216** and **217**. Patil named compound **216** 8a,8b-dehydroptilocaulin.[125] However, it was realised by Snider[123] that **216** is in the same oxidation state as ptilocaulin (**212**), resulting in the *dehydro*-prefix being incorrect. Subsequently **216** was renamed 7-*epi*-neoptilocaulin, using the *neo*-prefix to identify a double bond between 8a and 8b as the *iso*-prefix was already in use. Similarly **217** was named 8a-hydroxy-7-*epi*-neoptilocaulin.[123]

In 2001, Capon reported the isolation of mirabilin G (**214**) from the sea sponge *Claritha*.[126] It is worth noting that at this stage only ptilocaulin (**212**) and isoptilocaulin (**215**) had been evaluated for their biological activities.[127]

In 2004 Hamann *et al.* isolated two further tricyclic guanidine alkaloids, 8α-hydroxymirabilin B (**224**) and 8β-hydroxymirabilin B (**225**) as well as mirabilin B (**220**), from the Jamaican sea sponge *Monanchora unguifera*.[127] They were unable to separate **224** and **225**, but managed to obtain **220** as a pure sample. The biological activities of the alkaloids were evaluated and it was found that mirabilin B (**220**) exhibits antifungal activity against *Cryptococcus neoformams*, with an IC_{50} value of 7 µg/mL, and antiprotozoal activity against *Leishmania donovani* with an IC_{50} value of 17 µg/mL. It was also found that a mixture of **224** and **225** was active against the malaria parasite *Plasmodium falciparum* with an IC_{50} of 3.8 µg/mL.[127]

In 2006 Kashman reported the isolation of netamines A-G **227**-**230**, **218**, **222** and **223** from the marine sponge *Beimna laboutei*. Netamines C and D **229** and **230** showed biological activity (Table 2) against three human tumour cells lines: NSCL (A549), colon (HT29) and breast (MDA-MB-231).[128]

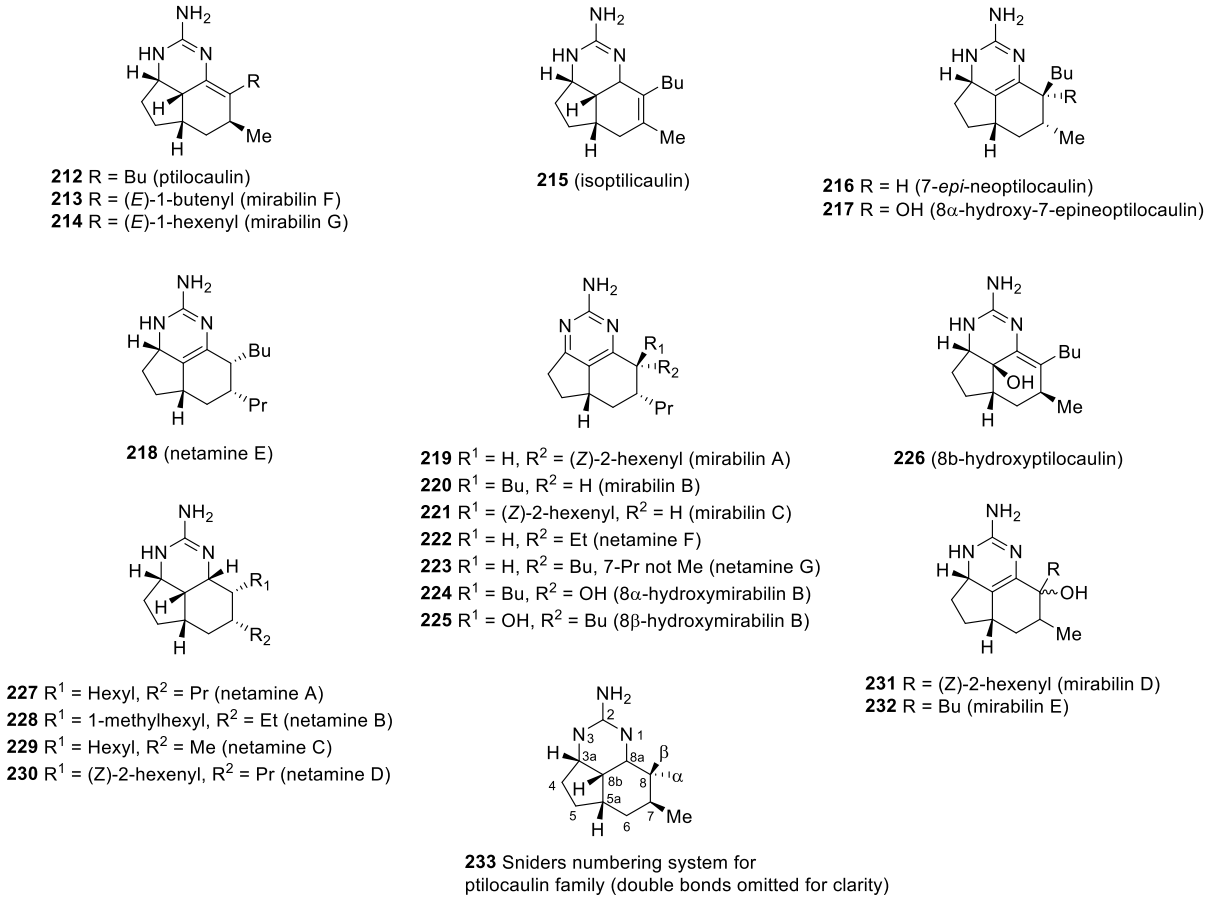

Figure 38. The ptilocaulin family of alkaloids.

Compound	Cell lines/GI_{50} (μM)		
	A549	HT29	MDA-MB-231
229	4.3	2.4	2.6
230	6.6	5.3	6.3

Table 2. Cytotoxicity of netamines C **229** and D **230**.[128]

Most of these tricyclic alkaloids show 7-*epi* stereochemistry, but mirabilin F (**213**), mirabilin G (**214**) and 8b-hydroxyptilocaulin (**226**) share the same C-7 stereochemistry as ptilocaulin (**212**).[123] Mirabilins A (**219**), B (**220**) and C (**221**) and the netamines F (**222**) and G (**223**) are more oxidised and have aromatic 2-aminopyrimidine rings, whereas netamines A-D **227**-**230** are highly reduced, with a tetrahydro-2-aminopyrimidine ring. Hydroxylated metabolites **217**, **226**, **231** and **232** are at the dihydro-2-aminopyrimidine oxidation state

whereas **224** and **225** are at the aromatic 2-aminopyrimidine oxidation state. In the aromatic series or with the double bond between position 8a and position 8b as in the neoptilicaulins, two stereoisomers are possible at C-8. The side chains are in 7-epineoptilocaulin (**216**), mirabilin B (**220**) and mirabilin C (**221**).[123]

It was postulated by Capon that the members of the ptilocaulin family are derived *via* the intramolecular cyclisation of guanidine-substituted polyketides.[123,128] However, in 2008, Snider[123] proposed a biosynthetic pathway to ptilocaulin (**212**), 7-*epi*-neoptilocaulin (**216**) and the batzelladine alkaloids such as batzelladine K (**240**) in which they are biosynthetically related (Scheme 65). He proposed that the conjugate addition of guanidine to the bis-enone **234** results in the guanidinium enolate **235**, which can then undergo an intramolecular Michael addition to give cyclopentane dione **236**. There is considerable synthetic evidence to support conjugate additions leading to *trans,trans*-cyclopentane analogues of **236**.[129,130,117] An intramolecular aldol condensation and imine formation, followed by an epimerisation of H-8b, leads to the key tricyclic intermediate for the ptilocaulin metabolite, **237**.

The most critical step in the biosynthetic pathway for each metabolite is the reduction of **237**, for example the 1,4-reduction of the α,β-unsaturated imine in **237** at the α face gives ptilocaulin (**212**), whilst a 1,2-reduction of the imine at the less hindered β-face gives isoptilocaulin (**215**). In contrast the 1,4-reduction from the β-face followed by isomerisation of the enamine leads to 7-*epi*-neoptilocaulin (**216**).[123]

Intermediate **235**, once protonated, leads to the enone **238**, which, on intramolecular conjugate addition of the guanidine, forms the pyrrolidine **239**. After iminium ion formation and 1,2-reduction, this intermediate gives rise to batzelladine K **240**.

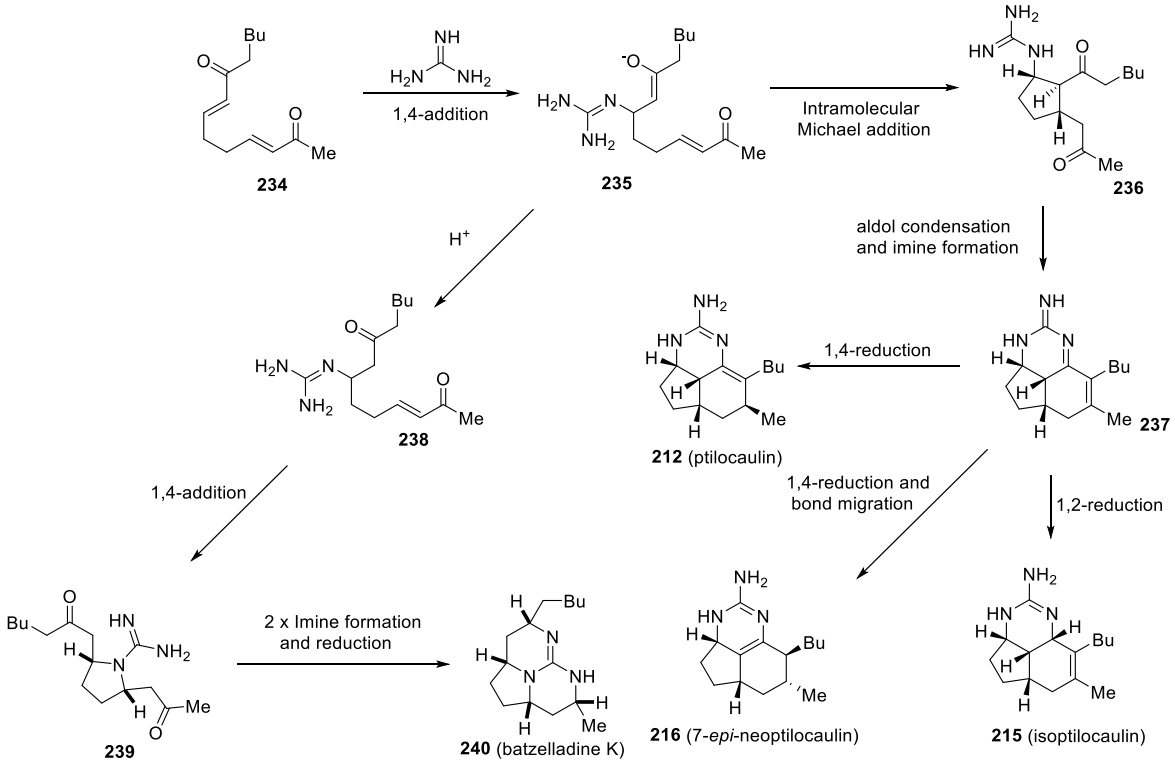

Scheme 65. Hypothesis of the origins of the ptilocaulin alkaloids.[123]

This proposed biosynthesis was put forward by Murphy in 1996, and formed the cornerstone of his synthetic methodology towards the batzelladine alkaloids and their analogues.[110–112]

4.6.2. The Synthesis of the Ptilocaulin Alkaloids

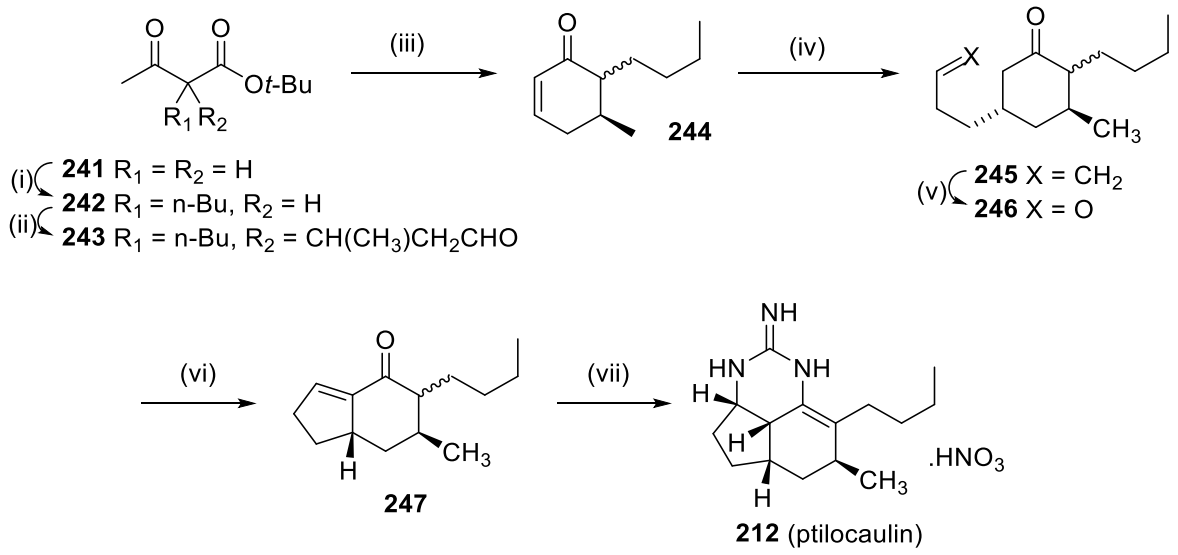

Scheme 66. (i) Na, dioxane, *n*-BuI, 55 %. (ii) Crotonaldehyde, MeOH, -40 ˚C. 39 % (iii) CH_3COOH, H_2O, HCl 25 ˚C, 58 %. (iv) 3-Butenylmagnesium bromide, $CuBr.SMe_2$, 45 %. (v) O_3, MeOH, -78 ˚C, then Me_2S. (vi) HCl, THF, 70 %. (vii) a) Guanidine, Benzene, azeotropic reflux. 35 %. b) HNO_3 1% aqueous.[131]

In 1983, Snider first reported the synthesis of ptilocaulin (**212**) from the β-ketoester **241**, according to scheme 66.[131] *t*-Butyl acetoacetate (**241**) was converted into **242** using sodium and iodobutane in dioxane. This was then reacted with crotonaldehyde to give Michael adduct **243**. Acid-mediated cyclisation, ester hydrolysis and decarboxylation with acetic acid, water and HCl gave the enone **244** as a 1.7:1 mixture of *trans*:*cis* isomers. Conjugate addition of the cuprate prepared from 3-butenylmagnesium bromide and $CuBr:S(CH_3)_2$ to this enone gave **245**, again as a 1.7:1 mixture of isomers. Ozonolysis of **245** gave a quantitative yield of **246** which was cyclised using HCl in THF, to give enone **247** in a 1:1 mixture of isomers in 70 % yield. This enone was heated with guanidine in benzene to bring about the azeotropic removal of water, and after quenching the reaction with nitric acid, ptilocaulin **(212)** was obtained as its nitrate in 35 % yield.

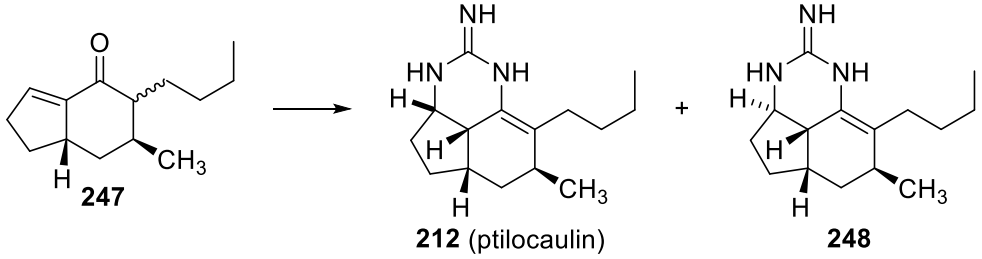

Scheme 67. Synthesis of ptilocaulin **(212)** and the co-crystallising isomer **248**.[132]

Between 1983 and 1998, several syntheses and synthetic approaches to ptilocaulin (**212**) were reported.[123,132] From these studies it was realised that the addition of guanidine to **247** results in the formation of multiple isomers. These minor stereo- or double bond positional isomers were not characterised until Schmalz reported[132] that the compound **248** co-crystallised with ptilocaulin (**212**), allowing its structure to be determined by X-ray crystallography. It is of particular interest that **248** appears to be formed by the presumed kinetic addition of guanidine to the less hindered top face of **247**, while ptilocaulin (**212**) is formed by the thermodynamic addition of guanidine to the more hindered bottom face of **247** (Scheme 67).[132–137]

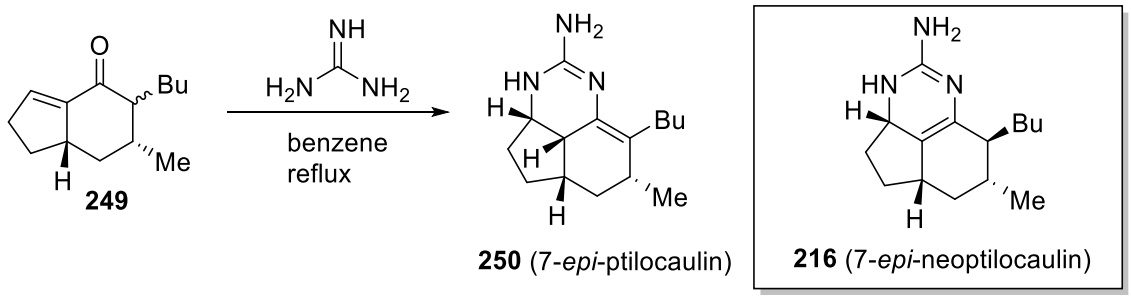

Scheme 68. Hassner's proposed synthesis of 7-*epi*-ptilocaulin (**250**).[123]

In 1986, Hassner prepared the enone **249**. This was treated with guanidine in benzene at reflux to give a compound which he characterized as 7-*epi*-ptilocaulin (**250**) (Scheme 68)**.** The ^{1}H and ^{13}C NMR spectral data of 7-*epi*-ptilocaulin (**250**) in $CDCl_3$ as obtained by Hassner[123] are very similar to those reported in 1997 for 7-*epi*-neoptilocaulin (**216**) in CD_3OD[125]. This suggests that the proposed position of the double bond of Hassner's product **250** is incorrect. However, no definitive conclusions can be drawn because the spectra were recorded in different solvents.[123]

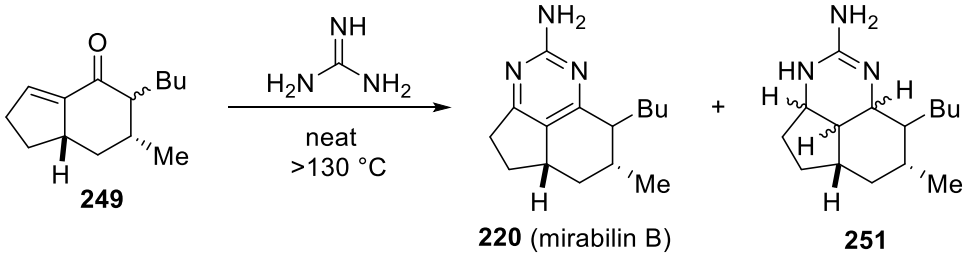

Scheme 69. Hassner's synthesis of mirabilin B.[123]

Hassner also heated **249** with neat guanidine at >130 °C (Scheme 69), resulting in the formation of a disproportionated mixture of an aromatised compound. Snider[123]

concluded that this was most likely to be a mixture of mirabilin B (**220**) and a saturated compound **251** that was one of 16 possible stereoisomers. However, the NMR spectroscopic data for Hassner's compounds were recorded in $CDCl_3$ again, whereas those of natural mirabilin B (**220**) were recorded in CD_3OD, making a direct comparison difficult.[123,125]

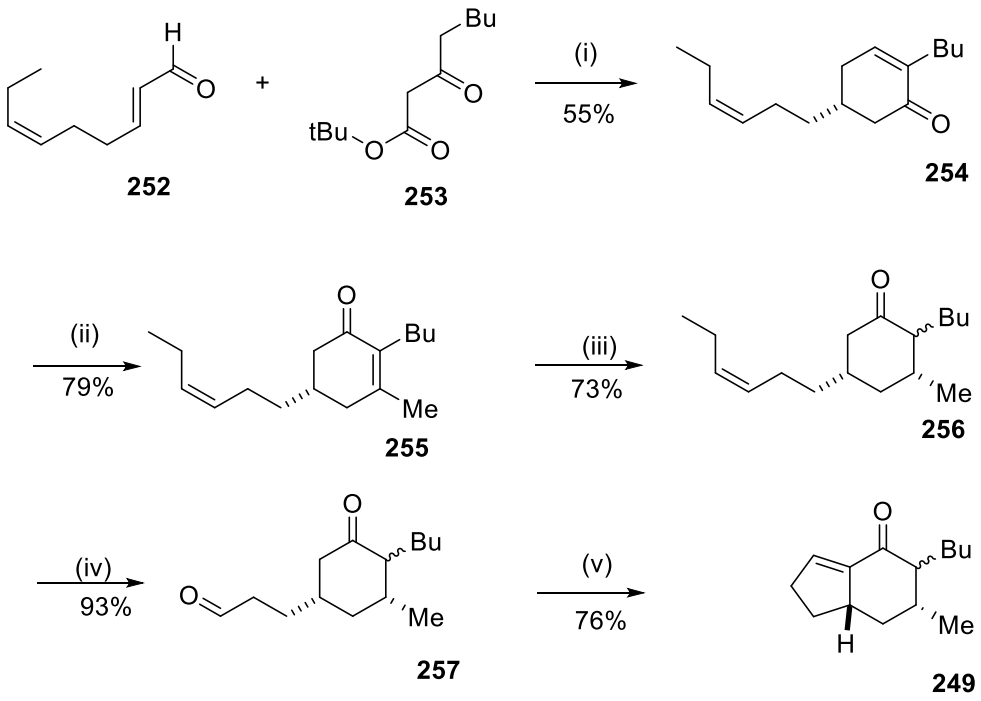

Scheme 70. (i) a) 0.25 eqv. *t*-BuOK, *t*-BuOH, 0°C. b) TsOH, PhMe, 80 °C. (ii) a) $CH_3Li/CeCl_3$ (5 eqv.) THF, -78 °C, 30 min. b) PCC, CH_2Cl_2, 0.8 eqv. NaOAc. (iii) Li, NH_3, *t*-BuOH, THF, -33 °C, 30 min. (iv) O_3, -78 °C, CH_2Cl_2 then Ph_3P. (v) 55 °C, 10 min microwave, 30:1 DME:6 M HCl.[123]

In order to ascertain whether the addition of guanidine to **249** gave 7-*epi*-ptilocaulin (**250**), Snider developed a route to enone **249** with a defined relative stereochemistry at the methyl substituent. A six-step preparation gave indenone **249** as a 4:1 mixture of trans/cis isomers.[123] The synthesis started with the Michael addition of 2*E*,6Z-nonadienal (cucumber aldehyde) (**252**) to the *β*-keto (**253**), followed by an intramolecular aldol condensation mediated by KO*t*Bu in *t*-BuOH. The intermediate keto-ester was then hydrolysed and decarboxylated with TsOH in toluene, to provide cyclohexenone **254**. Addition of MeLi in the presence of cerium chloride gave an intermediate tertiary allylic alcohol. This was then oxidised to the cyclohexanone **255** using PCC. Inspired by the work of House,[138] the Birch reduction of **255** gave **256** as a 10:1 mixture of trans/cis-isomers at the butyl substituient. Ozonolysis of the side chain, followed by the microwave- mediated intramolecular aldol

condensation gave the indenone **249** as a 4:1 mixture of trans/cis isomers at the butyl substituient.[123]

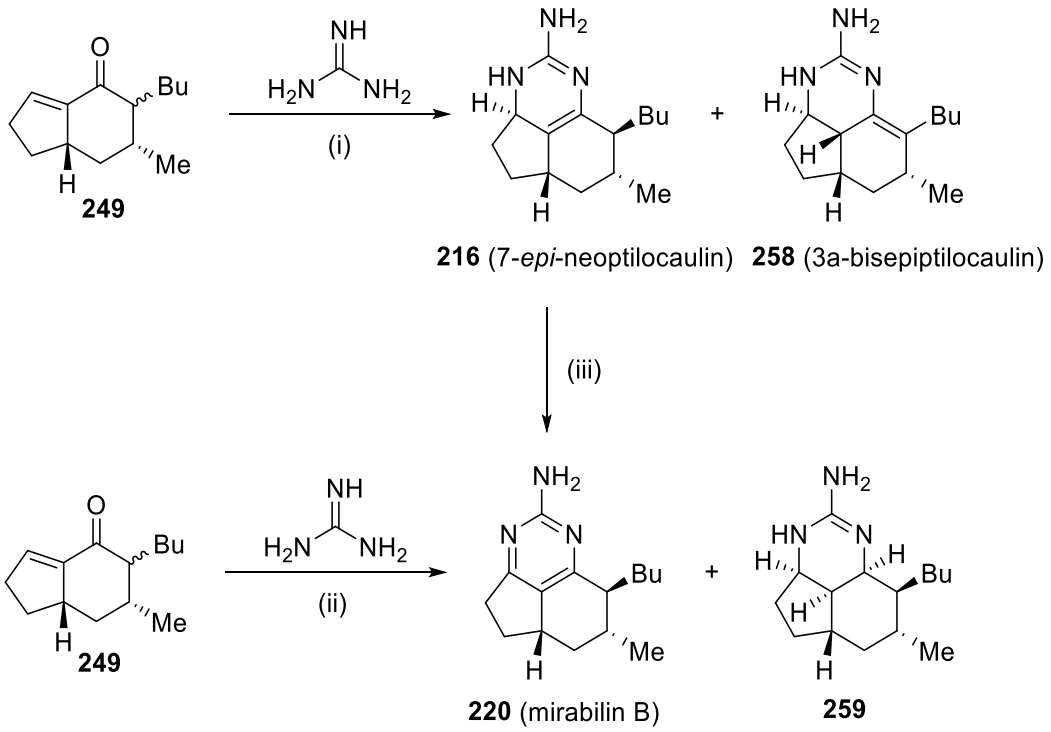

Scheme 71. Snider's synthesis of 7-epineoptilocaulin and mirabilin B (i) MeOH, 24 h, 85 ˚C, then 1 % HNO_3. (ii) Neat, 130 ˚C-140˚C, then 1 % HNO_3. (iii) MnO_2, CH_2Cl_2 55˚C 24 h.

Treatment of **249** with guanidine in methanol at 85 °C led to the formation of 7-epineoptilocaulin (**216)** in 50% yield, together with the formation of the byproduct 3a-bisepiptilocaulin (**258**) in a 10 % yield.[123] This observation supports the proposition that Hassner's original work had also led to the synthesis of 7-epineoptilocaulin (**216**), as NMR spectroscopic data for synthetic **216** in chloroform was identical to that previously reported. Similarly, heating **249** with guanidine in the absence of solvent gave mirabilin B (**2220**) in 39 % yield as described by Hassner, as well as the tricyclic isomer identified as **259** in a 31 % yield.[123] Snider also reported that oxidation of **216** with activated manganese dioxide also gave mirabilin B (**220**) in an 80 % yield.

In order to prepare the alkaloids ptilocaulin (**212**) and isoptilocaulin (**215**), Snider prepared the indenone **261,** in which the cyclohexene double bond was installed by cyclizing the previously prepared **255** without carrying out the Birch reduction. This process gave the indenone **261** in 70% yield, which on treatment with guanidine in methanol gave the intermediate tricyclic iminium ion **237**. The reduction of **237** using sodium borohydride gave an inseparable 1:1 mixture of ptilocaulin (**212**) and isoptilocaulin (**215**) (Scheme 72).

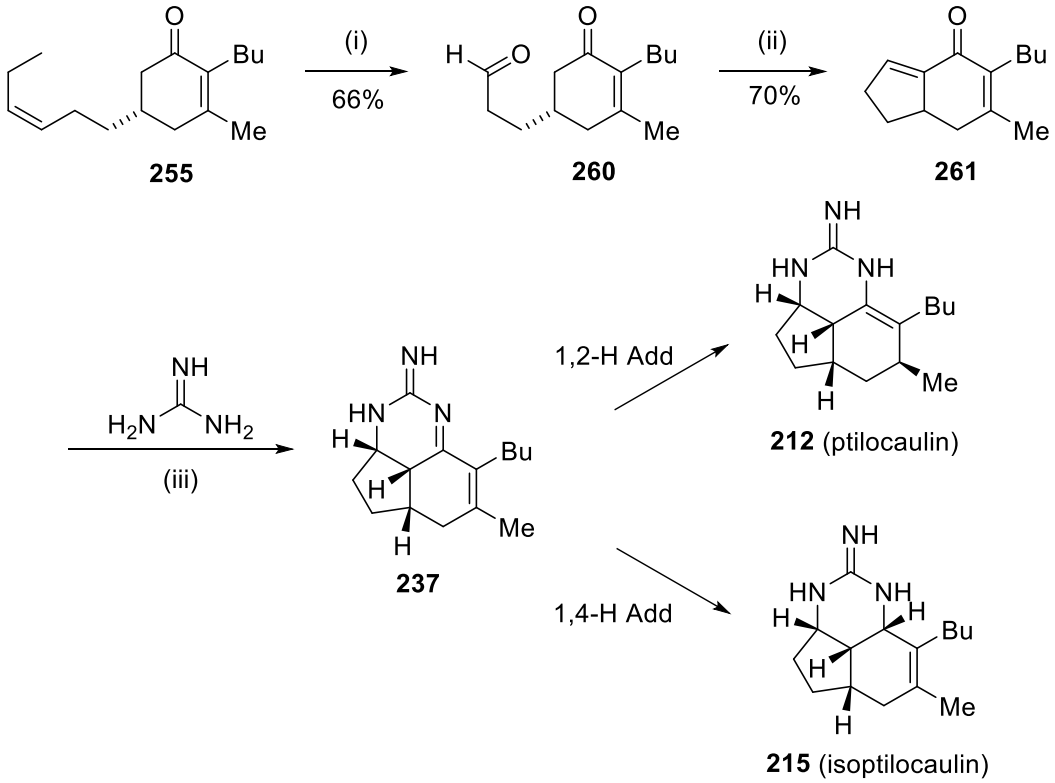

Scheme 72. (i) O_3, -78 ˚C, 99:1 CH_2Cl_2/pyridine. (ii) 55 ˚C, 5 min microwave, 30: 1 DME/6 M HCl. (iii) MeOH, 24 h, 85 ˚C. (iv) a) $NaBH_4$, H_2O, 25 ˚C b) 1 % HNO_3.[123]

Snider also reported the synthesis and structural reassignment of netamines E (**218**) and G (**223**) in an analogous manner, in which the methyl group in the previous synthesis is replaced by an *n*-propyl chain in the key intermediate **265**.[123] Addition of guanidine to **265** under standard conditions led to netamine E (**218**) in 38% yield, whilst oxidation of this intermediate with MnO_2 in dichloromethane led to Netamine G (**223**) in 25% yield over 2 steps (Scheme 73).

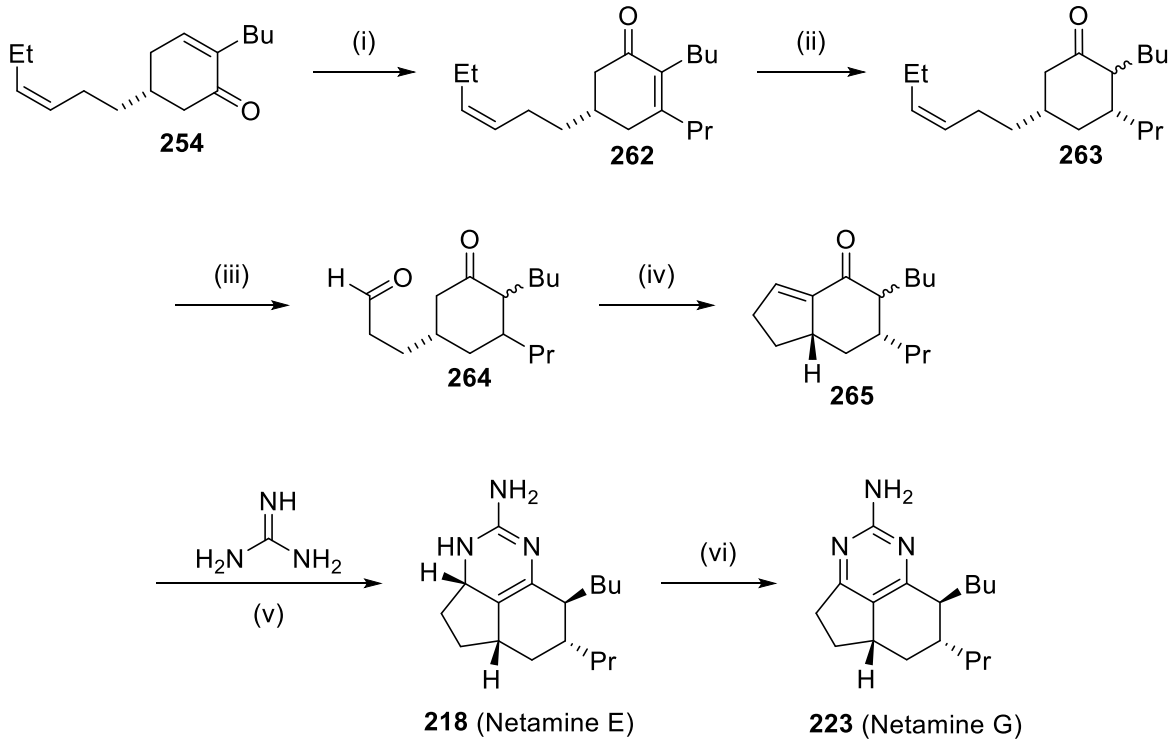

Scheme 73. (i) a) 1: 1 PrMgCl/$CeCl_3$ (5 eqv.) THF, 0 ˚C, 30 min. b) PCC, CH_2Cl_2, 0.8 eqv. NaOAc (ii) Li/NH_3, *t*-BuOH, THF, -33 ˚C, 30 min. (iii) O_3, -78 ˚C, CH_2Cl_2 then Ph_3P (iv) 55 ˚C, 10 min microwave 30: 1 DME/ 6M aq. HCl. (v) MeOH, 24 h, 85 ˚C, 1 % HNO_3 work up (vi) MnO_2, CH_2Cl_2, 55 ˚C, 48 h.[123]

5.0. Results and Discussion

5.1. Synthetic Approaches to Monalidine A (186) and Arbusculidine A (187).

Berlinck reported the recent isolation of the bicyclic alkaloid monalidine A (**186**) and the tricyclic alkaloid arbusculidine A (**187**)**,** which represents the newest member of the ptilocaulin family of alkaloids. This discovery offers the opportunity to embark upon a synthesis of these interesting metabolites. Monalidine A (**186**) is similar in structure to the crambines **188** and **189**. The wide range of activity known for these compounds makes it an ideal target for synthesis.[116–118] Likewise, arbusculidine A (**187**) is structurally similar to the mirabilins and netamine alkaloids, and it is the first of this class to exhibit a fully aromatised B ring, possessing a dihydrocyclopentaquinazoline skeleton.

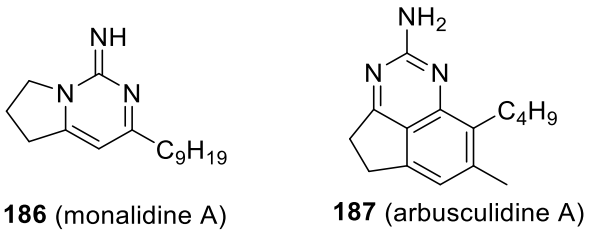

186 (monalidine A) **187** (arbusculidine A)

Figure 39. Monalidine A (**186**) and arbusculidine A (**187**).

5.2. The Synthesis of Monalidine A

5.2.1. Synthesis of Monalidine A

The planned synthesis of monalidine A **(186)** is shown in scheme 74. The proposed synthesis (Scheme 74) is that diketone **268** would be produced *via* the Claisen condensation of commercially available 2-undecanone (**266**) with γ-butyrolactone (**267**), and then treated with guanidine to form the pyrimidine **269**. The cyclisation of **269** could then be effected *via* the corresponding mesylate **270** by cyclisation under basic conditions,[120] to give the target compound monalidine A (**186**).

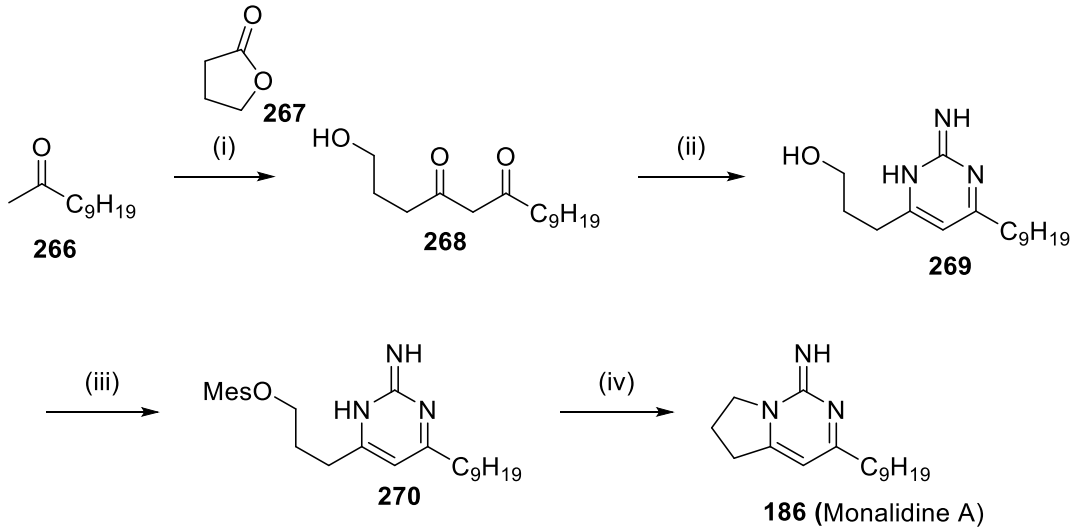

Scheme 74. Proposed synthesis of monalidine A: (i) Claisen condensation. (ii) Guanidine. (iii) MsCl, base. (iv) NEt_3, reflux.

The diketone **268** was prepared by modification of a previously reported procedure by Detty *et al.*, which was used to prepare structurally related compounds.[102] He reported that the reaction of methyl ketones with γ-butyrolactone (**267**) under basic conditions gave the 1,3-diketone **268** in 61-95 % yields (Scheme 75).

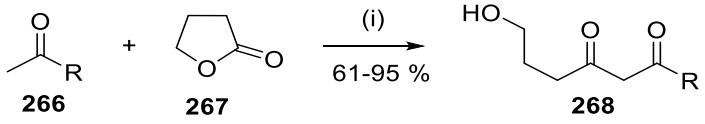

Scheme 75. (i) NaH, ethanol (cat.), diethyl ether, 15 ˚C.

Therefore, the reaction of 2-undecanone (**266**) with γ-butyrolactone (**267**) was attempted under the conditions described by Detty, which gave **268** in a low 6 % yield (Table 3, entry 1). It was found that the major product (48 %) was **271**, which is formed by the dehydration of **268**, presumably under basic conditions (Scheme 76). Attempts at an acid hydrolysis of **271** by heating under reflux with aqueous HCl proved unsuccessful. Therefore the original reaction was repeated, but the work up was modified by omitting the quench with ethanol, as it was felt that this might generate excess sodium ethoxide and promote the cyclisation. Work up with 10 % aqueous ammonium sulfate solution gave an improved yield of 20 % (entry 2).

Next, the use of the less basic trifluoroethoxide ion (pK_a ca 12.5) was investigated. Under these conditions it was found that yields in the range 28-36 % were obtained (entry 3). At this point it was speculated that the solid reaction components not mixing sufficiently

might be a factor that could be causing lower yields. . A further attempt at the reaction in which mechanical stirring was used gave the diketone **268** over three attempts in yields of 46-51 % (entry 4) (Scheme 76).

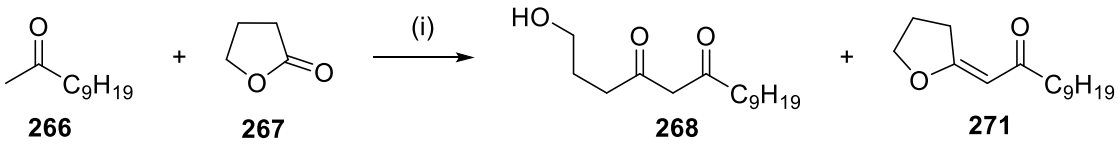

Scheme 76. (i) NaH, EtOH or CF_3CH_2OH (cat.), diethyl ether, 15 ˚C.

	Quench	**Catalytic alcohol**	**Highest obtained yield %**
1	EtOH	EtOH	6
2	No	EtOH	20
3	No	CF_3CH_2OH	36
4*	No	CF_3CH_2OH	51

Table 3. Varying conditions for the synthesis of diketone **268** (*mechanically stirred).

Despite the moderate yield, the reaction was easily performed and, after flash chromatography followed by one recrystallisation from diethyl ether and hexane, the diketone **268** could be prepared in multi-gram quantities. The diketone **268** proved to be highly unstable under acid conditions, forming the elimination product **271**. It was also found that the use of chloroform as an NMR solvent resulted in a slow conversion to **271**, possibly due to the trace acidity of the solvent. The use of DMSO as an NMR solvent suppressed the cyclisation. However, it was apparent that the pure compound exists as a 50:50 mixture of the diketone **268** and its enol **268b**. Analysis of **268** by NMR spectroscopy confirmed the structure, with the ^{13}C NMR data indicating the required 18 carbons including 3 carbonyl shifts in the ^{13}C NMR spectrum at 205.3, 194.6 and 193.8 ppm. The ^{1}H NMR spectrum indicated the presence of two OH protons as broad triplets at δ_H 4.44 (0.5H, t, J = 4.5 Hz, OH) and 4.49 (0.5H, t, J = 4.5 Hz, OH) ppm as well as an enol proton present as a broad singlet at δ_H 15.61 (0.5H, b s, OH) ppm with an integral of 0.5. The alkene of the enol was present at δ_H 5.68 (0.5H, s, CH) ppm with the corresponding CH_2 of the keto tautomer appearing as a singlet at δ_H 3.66 (1H, s, CH_2). The structure of **268** was finally confirmed by high resolution mass spectrometry, with a mass of 257.2107 Da being observed for the $[M+H^+]$. This is in close agreement with the required mass of 257.2111 Da.

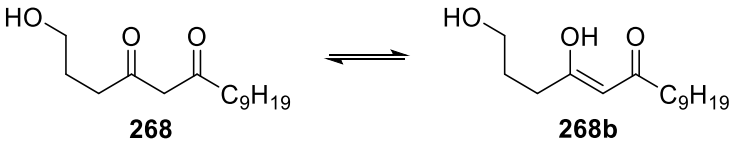

268 **268b**

Figure 40. Keto-enol tautomerism observed in **268**.

With **268** in hand, the next step was the synthesis of the pyrimidine **269** by the addition of guanidine (Scheme 77, Table 4). The first conditions attempted involved heating **268** under reflux with guanidine hydrochloride in absolute ethanol solution. The reaction was observed to gradually turn yellow over a period of 4 hours. On work up, ^{1}H NMR spectroscopic analysis of the reaction indicated that **268** had been completely converted into the previously observed ketone **271** (entry 1). This conversion might be as a result of the slight acidity of guanidine hydrochloride. As a literature[120] report suggested that triethylamine could be added to the reaction leading to weakly basic conditions, the reaction was repeated with one equivalent of triethylamine (entry 2). After being heated under reflux for 12 h, complete consumption of starting material **268** was observed, and product **269** was obtained in an 11 % yield.

It was anticipated that this yield might be improved by replacing the guanidine with free guanidine. Free guanidine can be generated by the treatment of guanidine salts with a stronger base such potassium *t*-butoxide. A possible consideration was that the increased basicity caused by adding potassium *t*-butoxide might promote the formation of the elimination product **271**, and prevent the formation of the desired product **269**. To avoid this, a slight excess (1.1 eqv.) of guanidine hydrochloride was always employed in these reactions. This was treated with one equivalent of potassium *t*-butoxide for 1 h at r.t. to ensure the full consumption of the alkoxide. A solution of 1,3-diketone **268** was then added and the mixture heated under reflux overnight. The reaction gradually turned yellow, which was indicative of the formation of the elimination product **271**. However on work up, the product **269** was isolated in an improved 22 % yield. The reaction was repeated by stirring at r.t. for 12 hours in an attempt to minimise formation of **271**, however the yield was low (18 %) and again considerable formation of **271** was observed (entry 4).

In order to improve the yield, the effect of using other alcohols as the reaction solvent was then explored. The use of *t*-butanol did not improve the overall yield of the reaction, which was conducted at 30 ˚C to ensure that the reaction mixture did not solidify (entry 5). The reaction was next attempted in trifluoroethanol (entry 6) and a small but reproducible improvement in yield was seen, to 25-28 % over 6 separate reactions. However,

elimination product **271** was again formed as a major by-product in up to 52 % yield. The reasons for this improvement in yield are unclear. Further reactions were conducted at r.t. for 48 and 72 h but no appreciable improvement in yield was noted. However, due to the ease of preparation of **268** this yield was considered workable, and on scale up, it was possible to perform this reaction on a 23 mmol (~6 g) scale and to obtain gram quantities of the pyrimidine **269**.

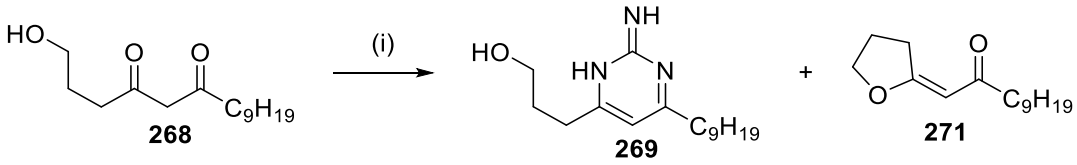

Scheme 77 (i) Base, guanidine HCl, CF_3CH_2OH, r.t.

	Solvent	**Base**	**Temperature**	**Time**	**Yield (266)**
1	Ethanol	none	Reflux	48 h	0%
2	Ethanol	NEt_3	Reflux	12 h	11%
3	Ethanol	KO*t*Bu	Reflux	12 h	22%
4	Ethanol	Ko*t*Bu	r.t.	12 h	18%
5	*t*-butanol	Ko*t*Bu	30 ˚C	12 h	19%
6	trifluoroethanol	Ko*t*Bu	r.t.	12 h	28%

Table 4. Guanylation of **268**.

The structure of **269** was confirmed by the disappearance of the carbonyl peaks in the ^{13}C NMR spectrum. This contained the required 14 carbon signals, including four signals at δ_C 172.8 I. 170.9 (C), 162.7 (C) and 109.7 (CH) ppm, for the pyrimidine ring system. The ^1H NMR spectrum displayed a signal for the pyrimidine CH, which was observed at δ_H 6.38 (s, 1H, CH) ppm, whilst the NH_2 of the pyrimidine was observed at δ_H 5.21 (2H, b s, NH_2) ppm. This, together with signals at δ_H 3.69 (2H, t, J = 6.0 Hz, CH_2), 2.69 (2H, t, J = 8.0 Hz, CH_2), 2.51 (2H, t, J = 8.0 Hz, CH_2), 1.92 (2H, app. *pentet*, J = 7.0 Hz, CH_2), 1.64 (2H, app. *pentet*, J = 7.0 Hz, CH_2), 1.26 (12H, m, 6 x CH_2) and 0.87 (2H, t, J = 8 Hz, CH_3) were confirmation of the structure of **269**, with the singlet at δ_H 5.02 (1H, s, OH) corresponding to the alcohol proton. Final confirmation of the structure was obtained from high resolution

mass spectrometry, giving a mass of 280.2384 Da for $[M+H]$,$^{+}$ which was in good agreement with the expected mass of 280.2383 Da for compound **269**.

The next stage of the synthesis was the formation of the dihydropyrrole ring. As inspiration, the work of Snider was taken,[120] who reported a similar cyclisation in his synthesis of crambine A (**188**) *via* a mesylate intermediate. Thus, the pyrimidine **269** was reacted with methanesulfonyl chloride in the presence of triethylamine to give the crude mesylate **270**. This was taken on to the next step immediately.

Scheme 78. (i) CH_3SO_2Cl, NEt_3, CH_2Cl_2, 0˚C.

A solution of **270** in dichloromethane was heated at reflux with triethylamine for 16 h and, pleasingly, a new product was obtained after purification. NMR spectroscopy signals indicated the presence of the expected product **186**. But astonishingly, it was found that the product isolated still contained a signal corresponding to the methylsufonyl residue. It was thought that this might be the methansulfonic acid salt of the natural product. However, high resolution mass spectrometry demonstrated that the mesyl fragment was part of the structure, as a mass of 362.1872 Da was obtained, corresponding to the $[M+Na]^{+}$ ion of structure **273**. Additionally, the IR spectrum of the product lacked bands corresponding to either an amine or an alcohol function. It was thus speculated that the structure obtained **273**, was the mesylation product of **186**, which was obtained in 11 % yield. In this structure the mesylate group has transferred to the amine function. A possible explanation might be the poor nucleophilicity of the amidine nitrogen in the pyrimidine ring. It is speculated that the NH_2 becomes mesylated on prolonged heating by transfer from another molecule of **270**. This mesylate group helps stabilise the formation of a negative charge by deprotonation at the sulfonamide, and this facilitates cyclisation. Support for this mechanism is that the alcohol **269** was obtained in 15 % yield following flash chromatography of the reaction products.

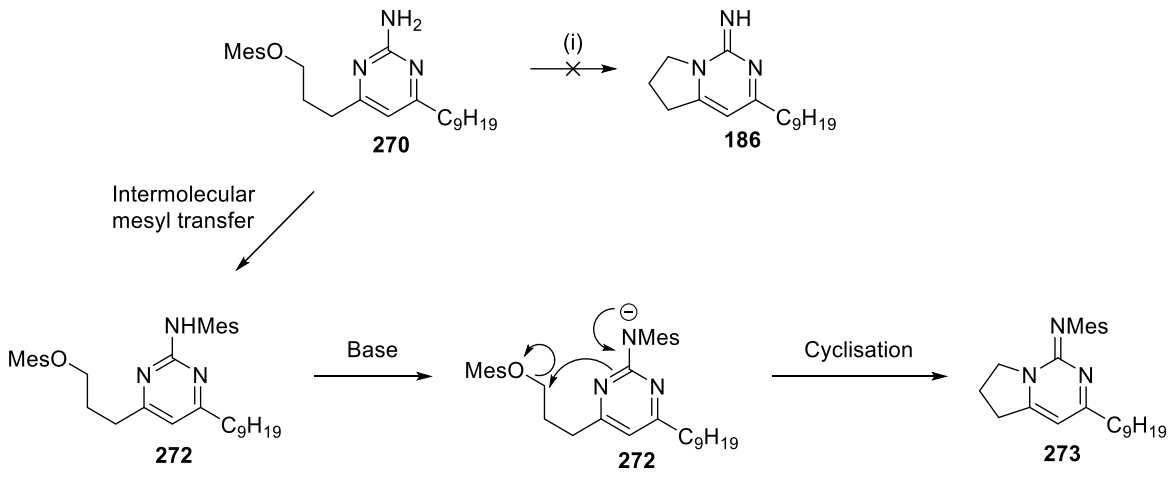

Scheme 79. Proposed mechanism for the formation of **273** (i) NEt_3, CH_2Cl_2, reflux.

A suggested alternative method is the Appel modification of the Mitsunobu reaction using iodine, triphenylphosphine and imidazole. This has been used successfully in the group in other related cyclisations.[107,114,140,141] Thus, **269** was dissolved in dichloromethane and cooled to -18 ˚C. Triphenylphosphine, imidazole and iodine were then added sequentially and the reaction was stirred to r.t. over 6h. After work up and column chromatography the product was treated with 1 M HCl, to give the desired alkaloid **186** in 67 % yield as its hydrochloride salt.

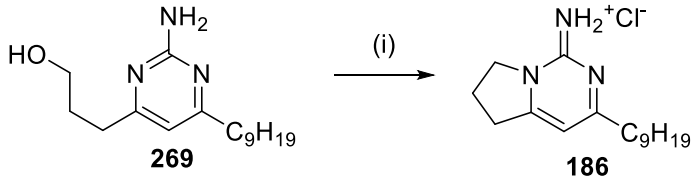

Scheme 80. (i) PPh_3, imidazole, I_2, CH_2Cl_2.

The ^{13}C NMR spectrum of **186** contained the required 14 carbon signals, including four signals at δ_C 179.5 (C). 164.8 (C), 154.9 (C) and 107.0 (CH) ppm for the pyrimidine ring system. The ^1H NMR spectroscopy in DMSO displayed two broad singlets at δ_H 8.99 (1H, s, NH) and 8.33 (1H, s, NH) ppm for the two NH protons, and a signal for the pyrimidine CH was observed at δ_H 7.03 (1H, s, CH) ppm. This together with signals at δ_H 4.14 (2H, t, *J* = 8.0 Hz, CH_2), 3.32 (1H, s, CH), 3.21 (2H, t, *J* = 8.0 Hz, CH_2), 2.69 (2H, t, *J* = 8.0 Hz, CH_2), 2.26 (2H, app. *pentet*, *J* = 8.0 Hz, CH_2), 1.65 (2H, m, CH_2), 1.29 (12H, m, 6 x CH_2) and 0.86 (3H, t, *J* = 8Hz, CH_3) ppm was confirmation of the structure of **186**. Final confirmation of the structure was obtained from high resolution mass spectrometry, which

gave a mass of 262.2271 Da for $[M+H],^{+}$ being in exact agreement with the expected mass of monalidine A (**186**).

5.2.2. Conclusion and biological studies of monalidine A (186)

In conclusion, the metabolite monalidine A (**186**) has been prepared in three steps from cheap, readily available starting materials. The completed synthesis is shown in scheme 81, and it is worth noting that it was achieved without the need for protecting groups. The atom efficiency of the synthesis is good, with all the carbon atoms of the starting materials being found in the product. The overall yield for the synthesis is 9 %. Whilst this is not an overly high yield, the ease of the first 2 steps makes the pathway applicable for the synthesis of gram quantities of the intermediates and indeed the natural metabolite **186**. The final product was indistinguishable from samples of the natural product, and the availability of **186** enables biological studies to be performed. This synthesis was essential to these studies, as only 1.2 mg of natural monalidine was isolated from the sponge *Monanchora arbuscula*, which is insufficient to perform detailed studies.

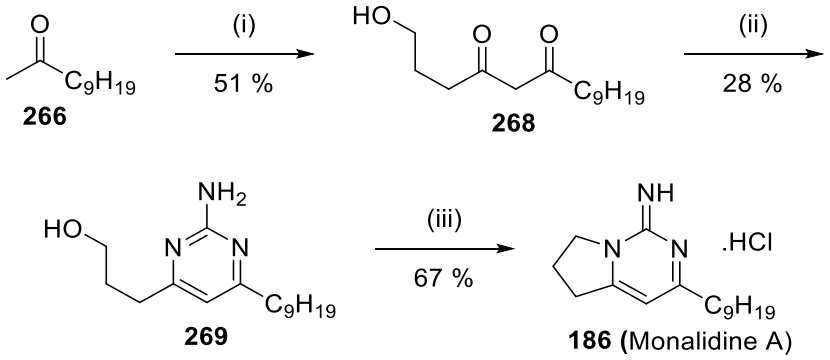

Scheme 81. (i) γ-butyrolactone, NaH, TFE, diethyl ether, r.t.. (ii) *t*-BuOK, guanidine hydrochloride, TFE, r.t.. (iii) PPh_3, imidazole, I_2, CH_2Cl_2, -18 ˚C.

The biological evaluation of synthetic monalidine A (**186**) and the intermediates pyrimidine **269** (noting its close structural similarity to crambine C1 (**1191**)) and crambine C2 (**192**) were performed in the laboratories of R. Berlinck and A. Tempone at the University of Sao Paulo, Brazil. The anti-parasitic activity was also determined against *Trypanosoma cruzi (T. cruzi)*, the parasite responsible for both Chagas disease in South America and sleeping sickness in Africa, and *Leishmania infantum* (*L. infantum*), which is the parasite responsible for visceral leishmaniasis. This latter was studied in both its promastigote and amastigote forms, which relate to the different morphological forms found in the life cycle of the parasite. (Figure 41, table 5)

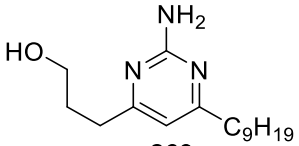

269

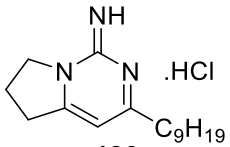

186

Figure 41. Monalidine A **(186)** and the intermediate **269**.

	T. cruzi	*L.infantum* (promastigote)	*L. infantum* (amastigote)	Cytotoxicity
186	8.09	2.45	no activity	26.27[a]
269	8.07	41.68	5.18	8.15[b]
182	ND	16	17	122[a], 241[b]

Table 5. IC_{50} values for monalidine A hydrochloride (**186**) and pyrimidine **269** compared to miltefosine (**182**) (μM). ND = not determined, *a* = monkey kidney LLC Mk2, *b* = NCTC cells.

Both **186** and **269** displayed very similar levels of activity against *T. cruzi*, with IC_{50} value of 8.09 μM and 8.07 μM respectively. In studies with *L. infantum*, monalidine A (**186**) displayed a high activity against the promastigote form of the parasite at a concentration of 2.45 μM, compared to **269** which required a much higher concentration of 41.68 μM. For the parasite in its amastigote form, monalidine A (**186**) displayed no activity, while **269** gave a much higher activity at lower concentrations, with an IC_{50} value of 5.18 μM showing higher activity than the drug miltefosine (**182**), which was used as a standard and gave an IC_{50} concentration of 17 μM. Interestingly, the synthetic monalidine A (**186**) and **269** were much more toxic towards the NCTC and LLC Mk2 (cancerous monkey kidney) mammalian cell lines than the standard miltefosine (**182**), with concentrations of 26.27 μM compared to 122 μM in the case of **186** and 8.15 μM compared to 241 μM in the case of **269**.[116]

It is obvious that the two compounds behave very differently towards *L. infantum*, and possible explanations for these differences is that they may be due to the difference in receptor properties or metabolic differences between the leishamanial promastigote and amastigote forms. The observed difference in activity could also be due to a difference in the lipophilic properties of **186** and **269**. It is also possible that the degree of protonation of the guanidine function in the two molecules might differ in *vivo*, especially as the pyrimidine is aromatic in nature in **269**, whilst it is not in structure **186**.

Overall these results are very promising. Studies are continuing on the synthetic material and there is considerable interest in the compound.

5.3. Approaches to the Synthesis of Arbusculidine A (187)

Attention was next turned to the synthesis of the metabolite arbusculidine A (**187**). As pointed out previously, the related metabolites ptilocaulin (**212**), isoptilocaulin (**215**), netamine E (**218**), 3a-bis-epiptilocaulin (**258**), and mirabilin B (**220**) are similar to arbusculidine A (**187**), only differing in the degree of unsaturated oxidation level of the various rings (Figure 41). A comparison of these metabolites indicates that 3a-bis-epiptilocaulin (**258**) has only one degree of unsaturation in the two 6-membered rings, whilst the metabolites ptilocaulin (**212**), isoptilocaulin (**215**), 7-epineoptilocaulin (**216**) and netamine E (**218**) have two degrees of unsaturation. Before the isolation of arbusculidine A (**187**), the most unsaturated metabolite isolated to date was mirabilin B (**220**) (Figure 42).

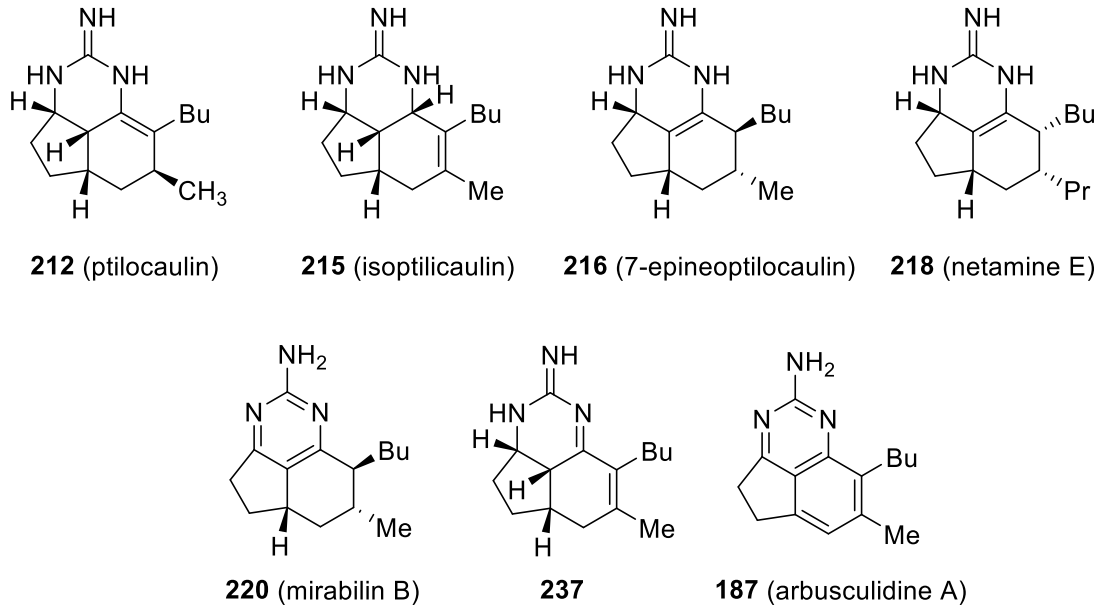

Figure 42. Arbuscilidine A (**187**) and the structurally related ptilocaulin alkaloids.

Snider's biomimetic hypothesis[123] suggests that the more saturated metabolites might have arisen from a common biomimetic precursor **237.** This molecule has three degrees of unsaturation *via* a reductive pathway, with the possibility of rearrangement. It might be speculated that mirabilin B (**220**) has arisen from the aromatisation of a metabolite such as 7-epineoptilocaulin (**216**) by an oxidative process. This would imply that the target molecule **187** might also have arisen from an intermediate such as **237** *via* oxidation (Scheme 82).

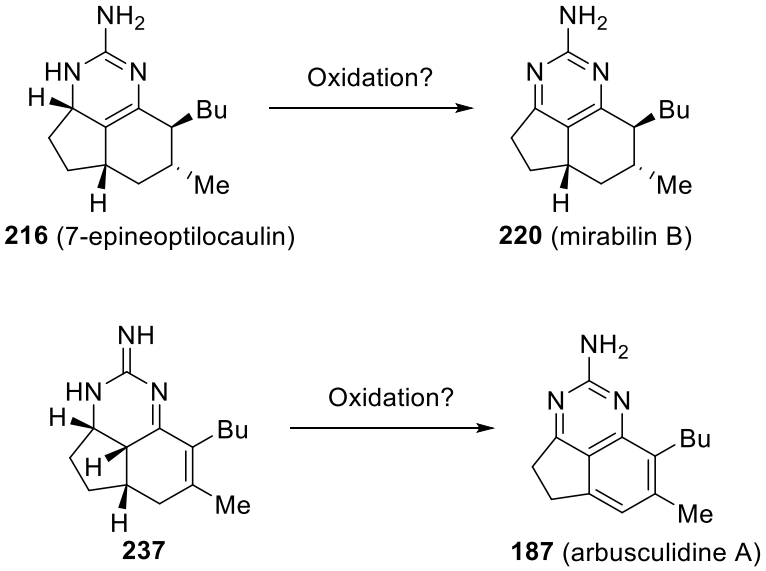

Scheme 82. Proposed biosynthesis of mirabilin B (**220**) and arbusculidine A (**187**).

As previously discussed, in 2008 Snider reported[123] the synthesis of several ptilocaulin metabolites in a biomimetic manner and had as his key intermediates the indenones **249** and **261**. The proposal is that it might be possible to prepare arbusculidine A (**187**) from one of these indenones, *via* the addition of guanidine and the subsequent oxidation of the intermediate addition products such as 7-epineoptilocaulin (**216**) or **237** (Scheme 83).

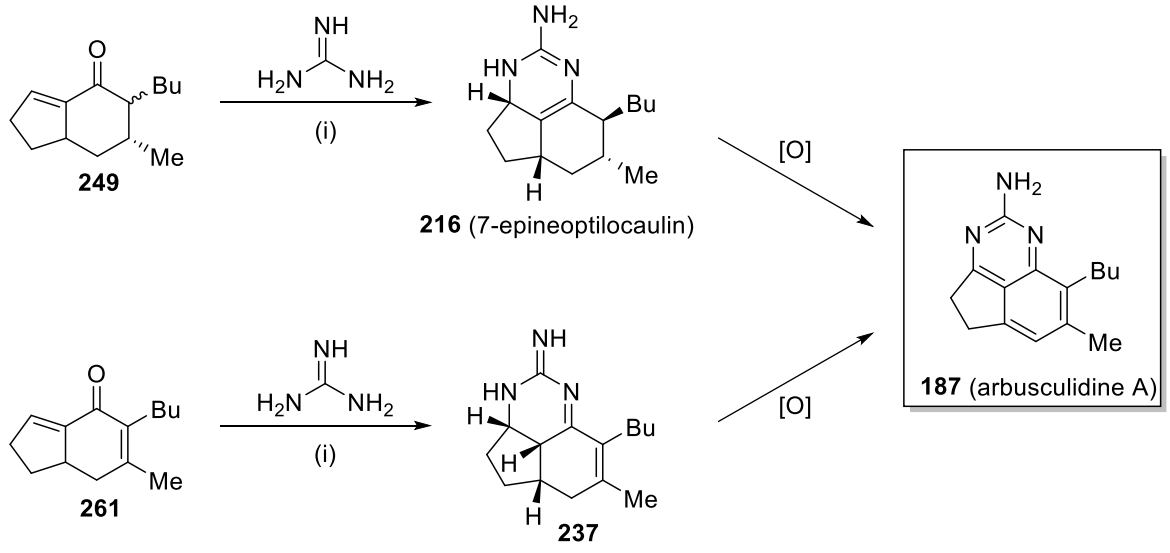

Scheme 83. Proposed synthesis of arbusculidine A: (i) Methanol, 85 ˚C, 24 h (ii) MnO_2 CH_2Cl_2, 55 ˚C, 24 h.

Therefore, a synthesis of the intermediate enone **249** (Scheme 84) was embarked upon. This is prepared by the condensation of the known aldehyde **252** with the β-ketoester

253. Intermediate **253** was prepared by alkylation of the dianion of *tert*-butyl 3-oxobutanoate (**241**) following a literature procedure.[142] Due to availability, iodobutane was utilised as an alkylating agent in place of the bromobutane that was used in the literature preparation. The reaction was carried out on six occasions, each achieving similar yields from 59-65 %, which is comparable to the reported yield of 75 %.[104] The product was then reacted with cucumber aldehyde (**252**) in the presence of potassium *t*-butoxide, to give a crude intermediate as a yellow oil. This oil was then dissolved in toluene, *p*-toluene sulfonic acid was added and the reaction was heated at 80 ˚C overnight to give the cyclohexanone **254** as a racemic mixture. The reaction was performed a total of five times, with yields of 48-61 %. It is speculated that the use of fresh potassium *t*-butoxide would result in yields which are more in line with that of Snider.[123] The ^{1}H NMR spectrum for **253** and **254** was in very close agreement with the literature in both cases (Scheme 85). Enone **254** was then treated with methyl lithium to give an intermediate alcohol, which was subsequently oxidised with PCC without purification to give the cyclohexanone **255** in 52- 56 % yield over 3 attempts.

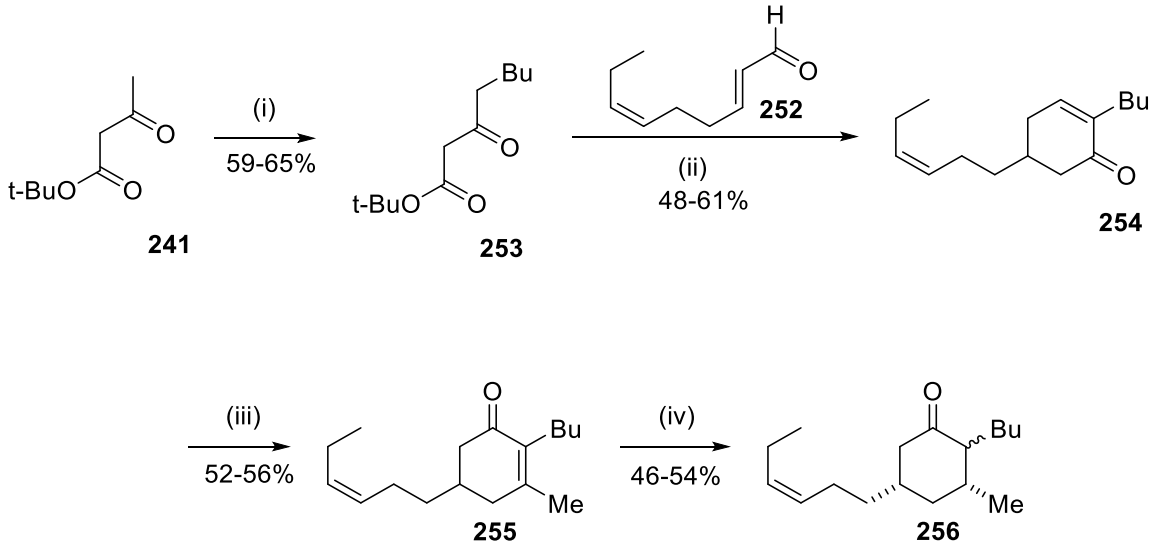

Scheme 84. (i) NaH, *n*-BuLi, then C_4H_9I, THF. (ii) a) *t*-BuOK, then *p*-TsOH, PhMe, 80 ˚C (iii) a) MeLi, Ce(III)Cl_3, THF, -78 ˚C. b) PCC, CH_2Cl_2, r.t.. (iv) Li, *N*-propylamine, ethylenediamine, 0 ˚C, 1.5 h.[123]

For the next step, Snider reports the reduction of the enone double bond using classical Birch reduction conditions.[123] However, liquid ammonia was unavailable and an alternative method was required. In 2000, Garst *et al*. had modified the Birch reduction by substituting liquid ammonia for short chain amines (*N*-propylamine and ethylenediamine), giving results comparable to those obtained when using liquid ammonia but with a much simpler and safer reaction procedure.[105] This reaction was attempted on the cylclohexanone

255, which led smoothly to the formation of **256** as a mixture of isomers in yields of 46-54 % over 4 attempts. Although this is a lower range of yields than the 73 % reported by Snider,[123] it is worth noting that the reaction procedure was much simpler and safer than a conventional Birch reduction.

Ozonolysis was used to convert alkene **256** into aldehyde **257** (Scheme 85) as a 5:1 mixture of isomers in 74 % yield. Aldehyde **257** was then converted into the indenone **249** as a 6:4 mixture of isomers in 74 % yield by heating with 6M HCl in diethyl ether. The ^{1}H and ^{13}C NMR data obtained was in very close agreement with that reported by Snider.[123] Confirmation of structure of **249** was obtained by high resolution mass spectrometry, with a mass of 251.2369 Da being observed for the $[M+H]^{+}$ ion. This is in exact agreement with the required mass (scheme 85). It is worth noting that the relative stereochemistry is not an issue in these reactions, as the planned oxidation of the guanidine intermediates to give arbusculidine A (**187**) will result in a removal of these stereocenters.

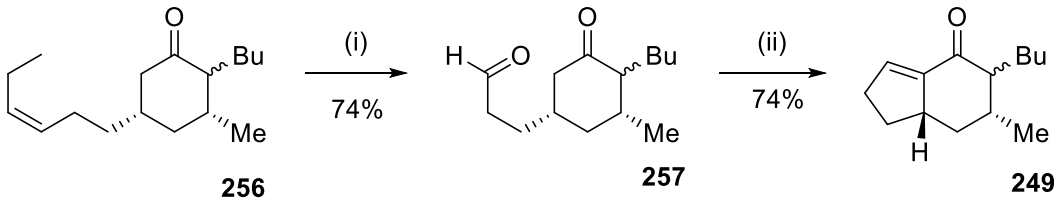

256 **257** **249**

Scheme 85. (i) a) O_3, CH_2Cl_2, -78 ˚C; b) PPh_3. (ii) 6M HCl, DME, 55 ˚C microwave, 10 min.

Indenone **249** was reacted with guanidine in methanol, which was generated by reaction of guanidine hydrochloride with sodium methoxide at r.t. for 30 minutes. This mixture was heated in a sealed tube at 85 ˚C for 24 hrs - conditions which were reported to give 7-epineoptilocaulin (**216**) by Snider.[110]

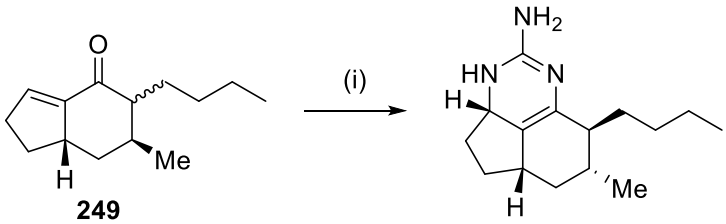

249 **216** (7-epineoptilocaulin)

Scheme 86. (i) Guanidine, MeOH, 85 ˚C, 24 h.

After work up, the product subjected to purification by column chromatography. However, only a complex mixture of products was evident, and not the formation of **216**. The reaction was repeated a further 3 times on the same scale, and the products obtained

were combined to give a sufficient sample for analysis and for subsequent reactions. Analysis of the ^{1}H NMR spectrum of this crude compound gave a complex spectrum. However, analysis of the ^{13}C spectrum gave signals at δ_c 154.7, 126.4, 119.4 ppm, which are indicative of (±)7-epineoptilocaulin (**216**), as well as signals at 157.8/153.6, 126.4/123.2 and 121.2/118.2 ppm, which indicate the presence of either isomeric compounds or oxidised analogues of **216**. Analysis by high resolution mass spectrometry indicated the presence of the desired compound with a m/z found at 248.2122 ($[M+H]^+$), with $C_{15}H_{26}N_3^+$ requiring 248.2121 Da. Other masses at 246.1966 ($[M+H]^+$) corresponded to $C_{15}H_{24}N_3^+$ mirabilin B (**220**), which requires 246.1966 Da, and at 244.1810 ($[M+H]^+$) corresponding to $C_{15}H_{22}N_{3,}^+$ which requires 244.1810 Da, are evident of the oxidised species **274**. A mass at 250.2278 ($[M+H]^+$) corresponds to $C_{15}H_{28}N_{3,}^+$ which requires 225.2278 Daltons, corresponding to the reduced compound **275** (Figure 43).

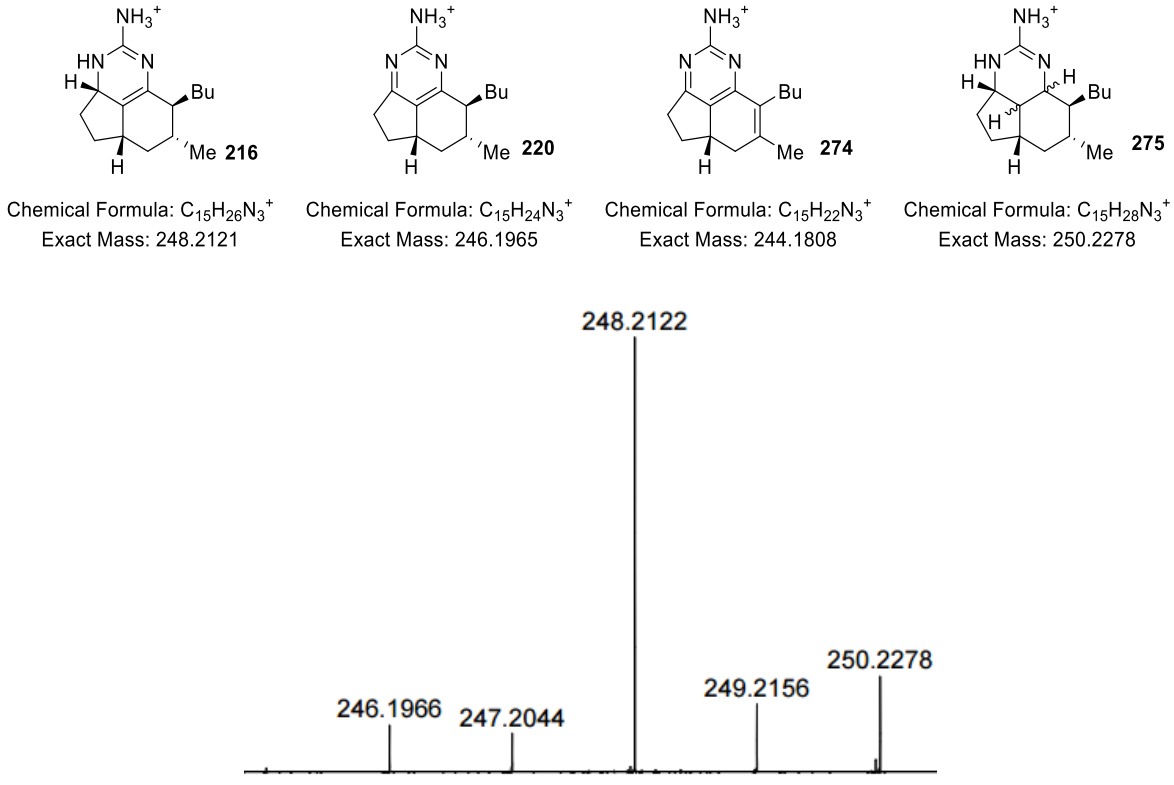

Figure 43. Structures **216**, **2220**, **274** and **275** and the mass spectrum obtained from addition of guanidine to indenone **249**.

Whilst the inability to purify **216** is a problem, the presence of the other isomers in the mixture is not overly worrying, as for the proposed synthesis of arbusculidine A (**187**) oxidative aromatisation of both the A- and C-ring of **216** is required, and the other compounds are intermediates in this process. In Snider's preparation of mirabilin B (**220**), the crude reaction mixture from the preparation of 7-epineoptilocaulin (**216**) was aromatised

in the A-ring by treatment with manganese dioxide in dichloromethane at 55 ˚C for 24 h. It was speculated that an increased reaction time, in addition to the use of an increased amount of oxidant, might allow the further aromatisation of mirabilin B (**220**) to give arbusculidine A (**187**) (Scheme 87).

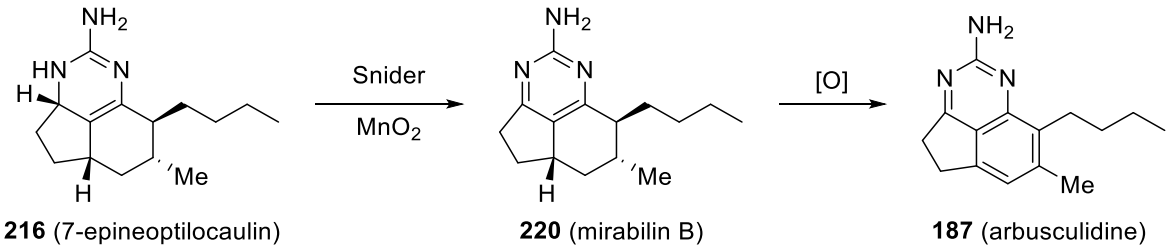

216 (7-epineoptilocaulin) **220** (mirabilin B) **187** (arbusculidine)

Scheme 87. Proposed synthesis of arbusculidine A (**187**).

Several methods are available for the preparation of activated manganese dioxide, and it was decided that the method reported by Carpino[106] in which the manganese dioxide is dispersed upon activated charcoal should be used. This method was reported to give better results in a range of oxidations. Thus, activated carbon was added to an aqueous solution of potassium permanganate, and after 16 h, the solid formed filtered and washed with water to give the manganese dioxide-coated carbon. The activity of the product was tested by oxidising a sample of *N*-propanol in deuterated chloroform, which resulted in the formation of propanal as evidenced by ^{1}H NMR spectroscopy after 1 h. The activity of the reagent was determined by treatment with excess ammonium iron(II) sulfate, followed by back titration of the excess iron(II) with potassium permanganate. From these calculations it was found that 1.0 g of the oxidant contained 2.06 mmol of manganese(II).

Using the method described by Snider, a solution of the crude product **216** in dichloromethane was treated with 10.7 equivalents of manganese dioxide on charcoal, and the mixture was heated in a sealed tube at 55 ˚C for 48 h. This was twice as much oxidising agent and double the reaction time to that reported by Snider. After 48 h the reaction was cooled to r.t. and filtered through a pad of Celite©, washing with copious quantities of methanol. The reaction was carried out on 36.0 mg of the crude product from the previous guanylation (crude 7-epineoptilocaulin (**216**)), but only 7.0 mg of the crude material was obtained after washing. Analysis of this sample by high resolution mass spectrometry interestingly demonstrated that only the reduced compound **275** was present in the crude product, as a mass at m/z 250.2279 (100%, $[M+H]^{+}$) Da was observed. This corresponds closely to the required mass of 250.2278 Da.

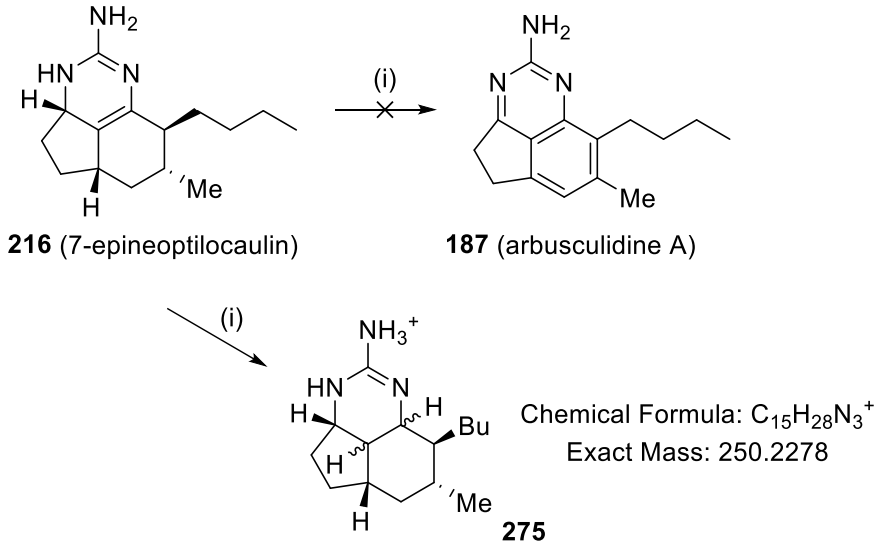

Scheme 88. (i) MnO_2 on carbon, CH_2Cl_2, 55 ˚C, 24 h.

This result suggested that **216** and the part aromatised compounds were undergoing an oxidation reaction, but that the reduced compound **275** was not. In addition, the conditions of the reaction are in some way removing or decomposing the oxidised compounds, or that they were being lost on purification. It was decided that alternative oxidation processes would be investigated, such as the palladium catalysed oxidation of the crude **216** using a method described by Labinger.[145]

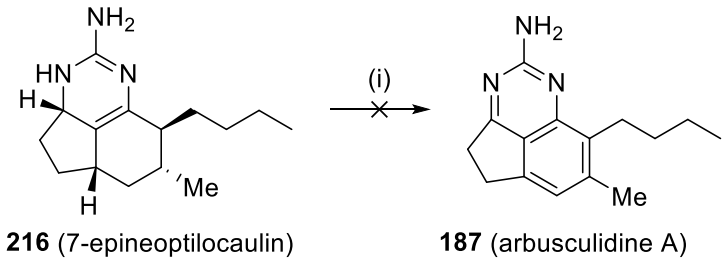

Scheme 89. Attempted oxidation of **216**: (i) $Pd(O_2CCF_3)_2$, O_2, acetone, r.t., 16 h.

Thus, crude **216** was dissolved in acetone with a catalytic quantity of palladium trifluoroacetate. A positive atmosphere of oxygen was maintained using balloons. The balloons were replenished until the consumption of oxygen appeared to cease, indicating that the reaction had finished. After stirring for 16 h, removal of solvent, and analysis by ^1H NMR spectroscopy suggested that no reaction had occurred.

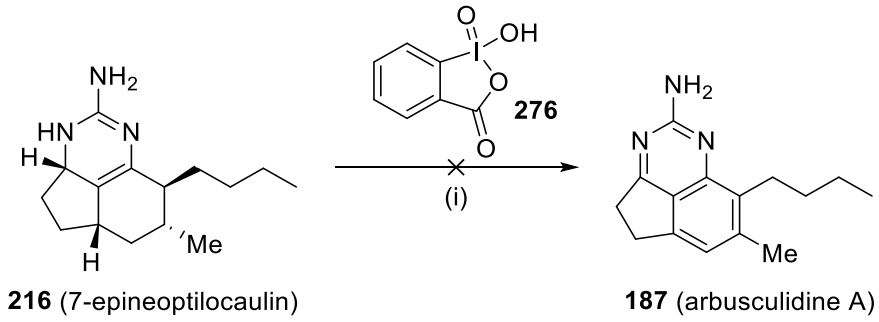

216 (7-epineoptilocaulin) **187** (arbusculidine A)

Scheme 90. Attempted oxidation of **216**: (i) IBX, MeCN, reflux, 48 h.

Finally, the oxidising agent IBX (**276**) was employed. Thus, guanidine **216** was heated under reflux in the absence of light with six equivalents of IBX in anhydrous acetonitrile. On monitoring the reaction by TLC, the rapid production of a new spot, thought to be mirabilin B (**220**), was apparent, and the reaction was continued until this spot disappeared. After aqueous work up, an off-white solid was obtained, which was found to be composed mostly of residual IBX and IBX by-products. Unfortunately, it proved difficult to separate any potential products from this material, and analysis by mass spectrometry indicated that no ions corresponding to arbusculidine A (**187**) were present. However, mass spectrometry did indicated the presence of the starting material at m/z 248.2125 ($[M+H]^+$) with $C_{15}H_{26}N_3^+$ requiring 248.2121 Daltons, as well as masses at 246.1969 ($[M+H]^+$) $C_{15}H_{24}N_3^+$ requiring 246.1966 for mirabilin B (**220**), and 250.2281 ($[M+H]^+$) $C_{15}H_{28}N_3^+$ requiring 250.2278 for (**275**) (Scheme 91).

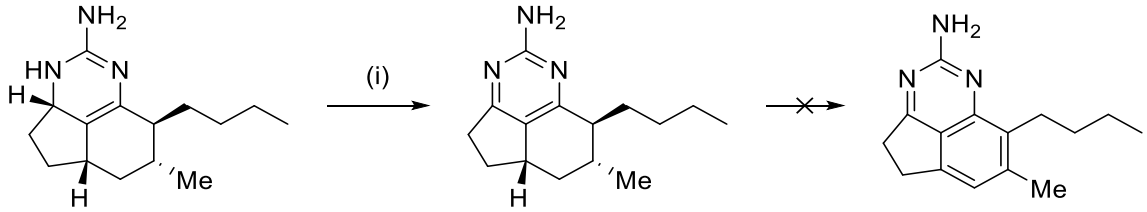

216 (7-epineoptilocaulin) **220** (mirabilin B) **187** (arbusculidine)

Scheme 91. (i) MnO_2, $Pd(OOCCF_3)_2$, IBX.

In conclusion, at this stage of the research the indenone **249** had successfully been prepared and guanylated to form 7-epineoptilocaulin (**216**)**,** which unfortunately was not easily oxidised to arbusculidine A (**187**)**,** and under the conditions employed gave only the previously prepared[110] mirabilin B (**220**). It was thus concluded that either manganese dioxide is not a sufficiently powerful oxidising agent to convert **216** into **187**, or that this transformation is not possible under oxidative conditions. This work might suggest that once

the A-ring is aromatised, the B ring is highly deactivated towards further oxidation, and an alternative route to arbusculidine A (**187**) was required (Scheme 92).

As was noted previously, Snider[85] reported the synthesis of ptilocaulin (**212**) and isoptilocaulin (**215**) *via* the addition of guanidine to the enone **261**, followed by reduction of the proposed intermediate guanidine **237**. If this intermediate could be accessed, then oxidation of this intermedate might be an easier process than the oxidation of the reduced intermediate 7-epineoptilocaulin (**216**) used in the previous oxidations (Scheme 92).

Therefore the double bond in the enone **255** was selectively ozonolysed -78 ˚C in pyridine and dichloromethane, to give the aldehyde **260** in 50 % yield together with 50 % of recovered starting material. The cyclisation of **260** was achieved by microwave-mediated cyclisation, using aqueous 6M HCl in dimethoxyethane. This resulted in a 54 % yield of **261**. The ^{1}H NMR spectrum of **261** was identical to that reported by Snider, and gave key diagnostic signals at δ_H 9.79 (1H, s) for the aldehyde proton and at δ_H 6.66 (1H, d, J = 4.0 Hz, CH) ppm for the enone CH. Next, the reaction was performed as reported by Snider,[123] and the enone **261** was added to a methanolic solution of guanidine. After heating the mixture in a sealed tube at 85 ˚C for 24 h, the solution was evaporated to give a crude sample of the presumed structure **237** as a brown gum (Scheme 92).

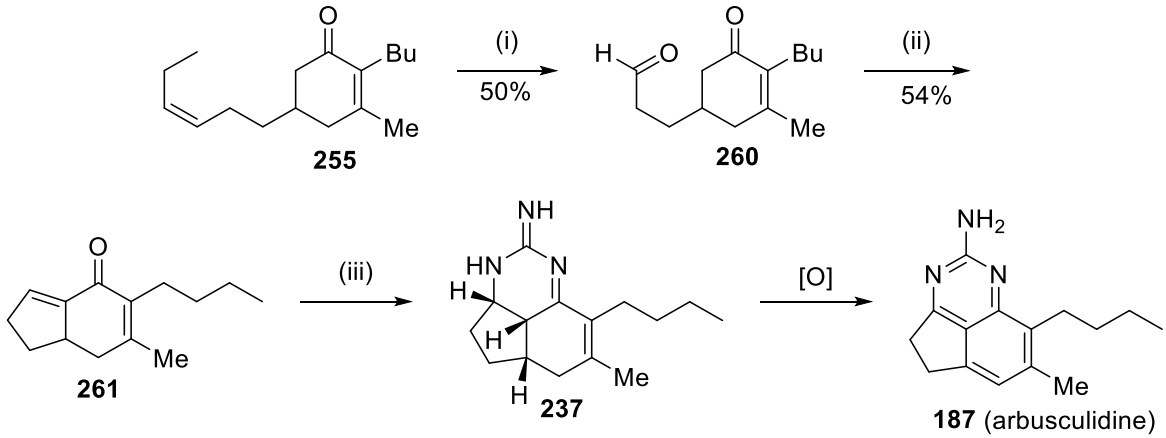

Scheme 92. (i) O_3, CH_2Cl_2, pyridine, PPh_3, -78 ˚C (ii) 6M HCl, 55 ˚C microwave (iii) guanidine, methanol, 85 ˚C, 24 h.

Snider did not isolate **237**, instead reduced it immediately with sodium borohydride to form ptilocaulin (**212**) and isoptilocaulin (**215**).[123] It was desired that its structure was investigated in more detail, so the crude mixture was analysed by high resolution mass spectrometry. It was apparent from this analysis that there were at least three and possibly four structures present in the mass spectrum corresponding to $[M+H]^+$ ions of 242.1653, 244.1809, 246.1966 and 248.2122 Daltons. The mass of the desired product is 246.1965

Daltons and the other three appear to differ by approximately 2 mass units and might suggest that a disproportionation-like process is occurring in the mixture, as was suggested by Snider in his one–pot synthesis of mirabilin B (**220**)[110] (Figure 44).

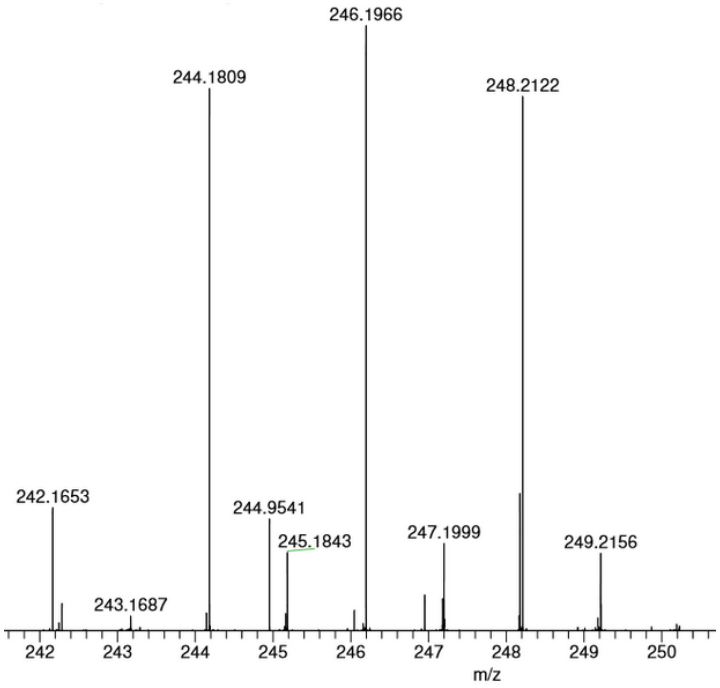

Figure 44. The mass spectrum of the crude product from the preparation of **237**.

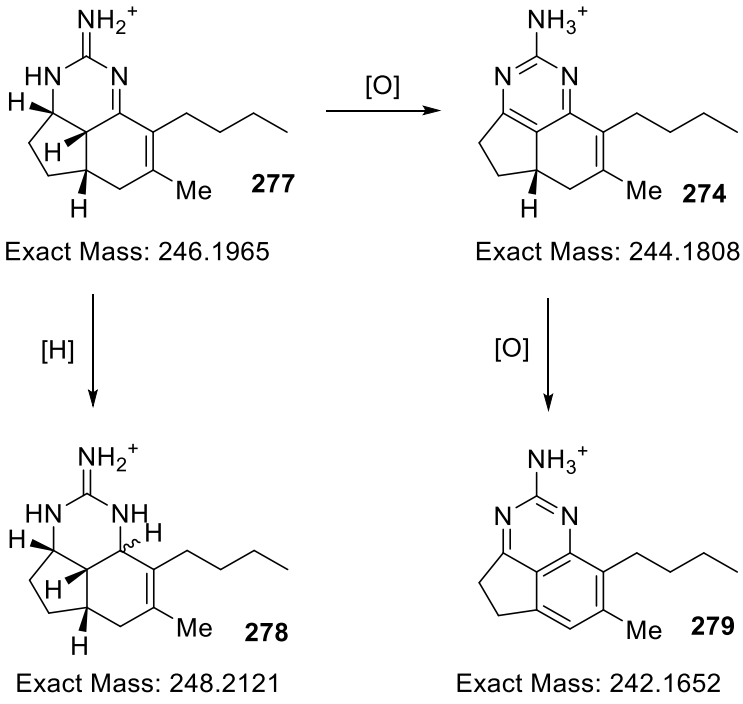

Scheme 93. Proposed structures for the ions observed in the mass spectrum (fig 43).

It is possible to speculate that these masses correspond to the ions **274**, **277**, **278** and **279**. Ion **277** corresponds to the proposed intermediate form Snider's work, which could

disproportionate to the ions **274** and **277**, and further that **274** undergoes oxidative aromatisation to give **279**, which is the protonated form of the desired product arbusculidine A (**187**).

The intensity of the ion corresponding to **187** is very low, but this is persuasive evidence that this is the desired compound and that in nature its formation involves an oxidative process. Indeed, this observation might also suggest that **187** is an artefact from the isolation process from the native sponge due to aerial oxidation.

To determine whether the iminium ion **237** would be oxidised to arbusculidine A (**187**) on exposure to molecular oxygen, the remaining mass spectrum sample was dissolved in methanol before being stirred in the presence of atmospheric oxygen until completely evaporated. This was repeated, and the dissolution- evaporation process repeated once more, the experiment lasting a total of three days. It was hoped that further analysis by mass spectroscopy would show an increase in the peak intensity at 242.1653 Da and a decrease in the intensity of the other three ions. The sample was resubmitted for analysis by mass spectrometry and surprisingly, it was observed that the desired ions between 242 and 248 Daltons were not observed, but there was an intense ion at around 306.2176 Daltons. (Figure 45)

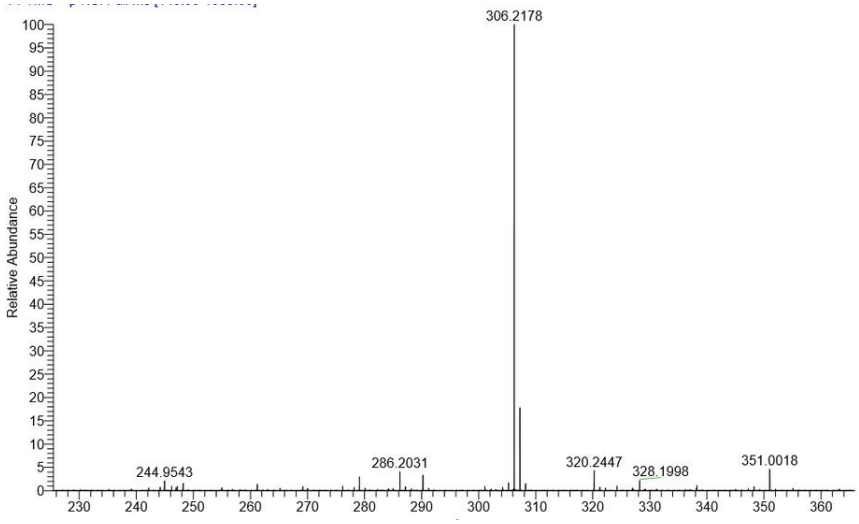

Figure 45. Mass spectrum showing the ion for methanolic addition of arbusculidine A.

This appears to correspond to a structure in which two molecules of methanol have added to arbusculidine A (**188**). It is possible to speculate as to the nature of this $[M+H]^+$ ion, and structures such as **280**-**282** might be suggested, all of which have a mass of 306.2176 (Figure 46).

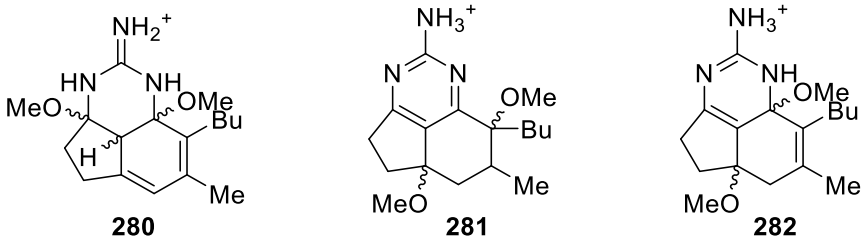

Figure 46. Possible structures corresponding to the exact mass of 306.2176 Daltons.

During preparation for mass spectrometry, the sample had been dissolved in methanol and ammonium acetate was added. Ammonium acetate can act as a proton source under the correct conditions, and it is conceivable that in this case it acted as a catalyst for the addition of two molecules of methanol. Although this is a disappointing result, it does seem to indicate that all of the species which were detected in the previous mass spectrum had possibly oxidised in the air to give arbusculidine A (**187**) or a related intermediate.

It had been speculated that the iminium ion **237** would be highly unstable, and it was desirable to further oxidise it immediately. While waiting to receive the mass spectrometry data for it, the further oxidation of the crude iminium ion **237** was carried out. The oxidation was to be carried out in duplicate in dichloromethane with manganese dioxide in a sealed tube, as described by Snider[123] for the oxidation of 7-epineoptilocaulin (**216**). However, it was found that the crude iminium ion **237** would not dissolve completely in dichloromethane and therefore, three different oxidation reactions were carried out.

Firstly, the crude iminium ion was triturated with dichloromethane and transferred to a Carius tube and oxidised with ten equivalents of manganese dioxide at 55 ˚C for 24 h. Secondly, the remaining undissolved residue was dissolved in methanol and transferred to a Carius tube before removing the methanol under vacuum. Dichloromethane was then added and the oxidation reaction performed using ten equivalents of manganese dioxide at 55 ˚C for 24 h. It was speculated that as the reaction proceeded, the reactants would dissolve. Finally, a sample of crude **237** was dissolved in methanol and transferred to a separate sealed tube, and again the methanol was removed under vacuum before adding dichloromethane and 10 equivalents of manganese dioxide on carbon and heating at 55 ˚C for 24 h. On working up, each reaction was passed through a pad of Celite©, washing with copious quantities of methanol. Evaporation of the solvent yielded a brown gum in each case and a sample of each was submitted for analysis by accurate mass spectrometry. Unfortunately, no ions indicated the formation of **187** or any partially oxidised intermediates of **187**.

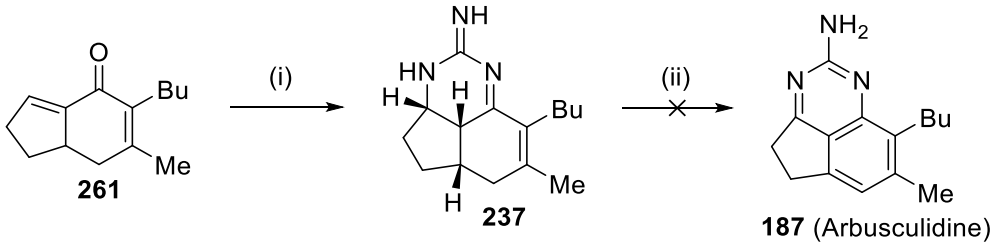

Scheme 94. (i) Guanidine, methanol, 85 ˚C, 24 h. (ii) Activated MnO_2 on carbon, dichloromethane, Carius tube, 55 ˚C for 24 h.

One observation from these reactions was that the mass balance of these reactions was very poor, and considerably less material was recovered from each reaction when compared to the amount originally put into the reaction. For example in one case where 40.0 mg of the indenone **237** was guanylated to give 67.0 mg of **237**, only 10.0 mg of crude product was obtained after the oxidation stage, and it was thus speculated that the activated charcoal used in the oxidation might be retaining much of the aromatised compound. In order to isolate further products, the activated charcoal was washed again but using methanol with a few drops of aqueous 1M HCl added, as it was speculated that as a hydrochloride salt, the product may have less affinity for the activated carbon. The solvent was removed and the residue triturated with dichloromethane to give a further 48.0 mg of crude product. Analysis of this residue by high resolution mass spectrometry did not indicate the presence of **187** or any intermediates relating to **187**. However, the fact that more material was recovered led us to reconsider the oxidation process used.

Activated charcoal is often used as a decolourising agent and to remove trace impurities form organic compounds during recrystallization. It was though possible that a planar aromatic compound such as arbusculidine A (**187**) would show a high affinity to the activated charcoal, which might explain why the desired product was not isolated after washing with dichloromethane or methanol alone.

Following this assumption, a sample of activated manganese dioxide was precipitated from manganese sulfate and potassium permanganate at 60 ˚C under aqueous conditions. The chocolate brown solid was oven dried (120 ˚C) over 2 days then ground to a powder in a pestle and mortar before use.

At this stage two separate reactions were attempted. Firstly the iminium ion **237** was prepared from the indenone **261**. Following guanidine addition, the sample was transferred to a tube where care was taken to thoroughly remove all traces of methanol (under vacuum) before suspending the residue in dichloromethane and adding 6.5 equivalents of activated

manganese dioxide. The reaction was then heated at 55 ˚C for three days, before being filtered and the solvent removed under reduced pressure to give a brown gum (Scheme 95).

A sample was submitted for analysis by mass spectrometry, which revealed that (M+H) ions at 246.1967 and 248.2124 Daltons which were prevalent in the starting material had considerably diminished, and ions at 242.1656 (arbusculidine A (**187**)) and 244.1811 Daltons were present at much higher intensity (Figure 47).

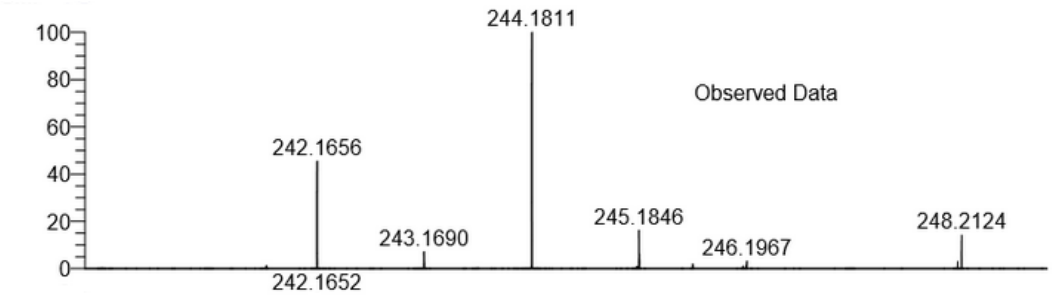

Figure 47. Mass spectrum of the product formed from the oxidation of **237** with activated manganese dioxide.

Attempts were made to purify this mixture by preparative TLC. Unfortunately, no pure compound was obtained from this endeavour and analysis by NMR spectroscopy gave no positive indication for the formation of **187**. Comparisons of the crude samples by NMR spectroscopy in DMSO were attempted but it was apparent that **187** was not present, as considerable contamination was a problem in the reaction.

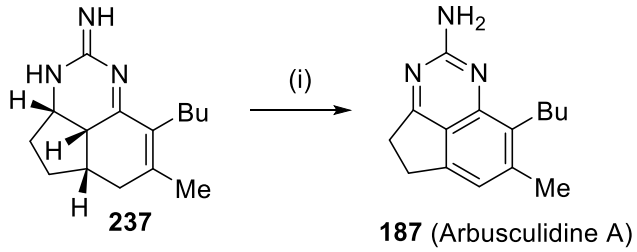

Scheme 95. (i) Activated MnO_2 (6.5 eqv.), dichloromethane, Carius tube, 55 ˚C, 3 days.

In parallel with this experiment, a small sample of the iminium ion **237** was stirred in chloroform in contact with the air until evaporation of the solvent occurred (ca 3 days), at which point further chloroform was added, and this stirring and evaporation repeated a second time. Analysis of the sample by mass spectrometry indicated that a similar transformation of the imine **237**, which gave ions at 246.1967 and 248.2124 Daltons into

ions at 242.1656 (arbusculidine A (**187**)) and 244.1811 Daltons, had occurred. This might suggest that **187** occurs as a consequence of post-isolation oxidation of another related natural product (Scheme 96).

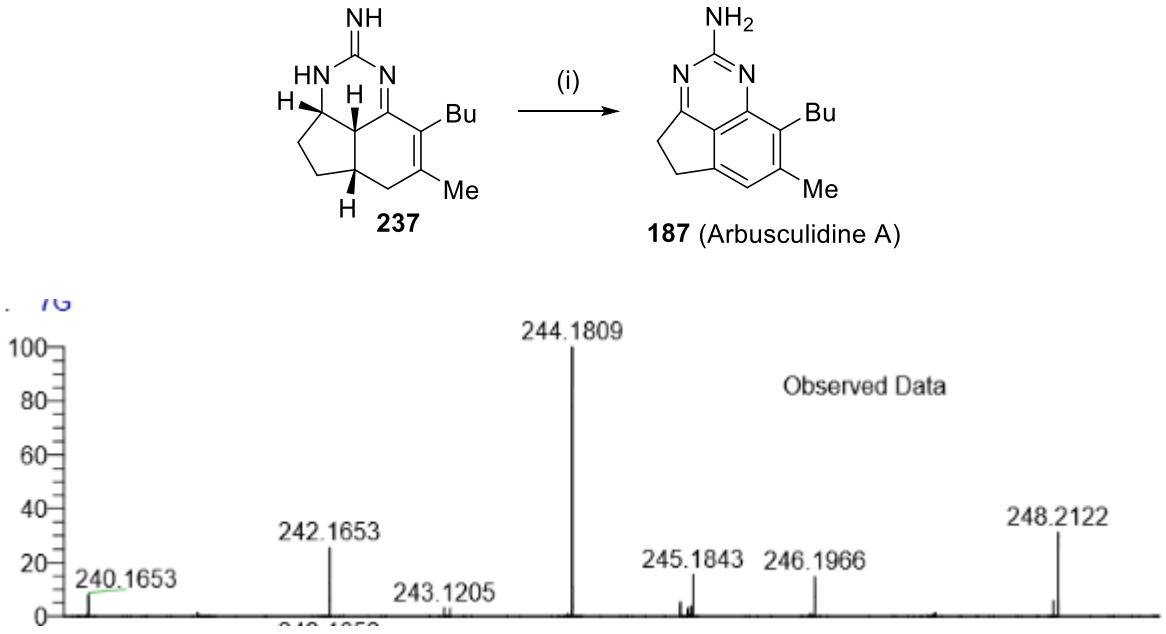

Scheme 96 (i) Air 6 days.

In an attempt to prepare a larger sample of **187** from **237**, the manganese dioxide oxidation reaction was repeated on a larger scale with more equivalents of the oxidising agent and a longer reaction time (7 days). A modified work up was employed, to give a chloroform extract of the oxidation alongside the methanol extract (Scheme 97).

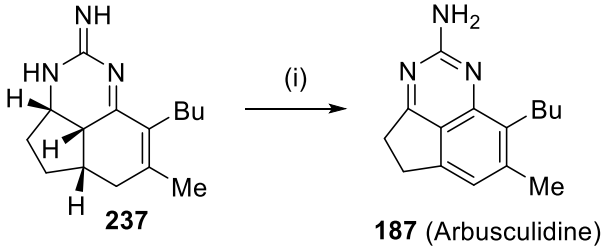

Scheme 97. (i) Activated MnO_2 (8 eqv), dichloromethane, Carius tube, 55 ˚C, 7 days.

Analysis of the chloroform extract by high resolution mass spectrometry indicated a large abundance of the ion at 242.1656 Daltons, corresponding to arbusculidine A (**187**), with small peaks at 244.1812 and 246.1969 Daltons for the intermediate species (Figure 48).

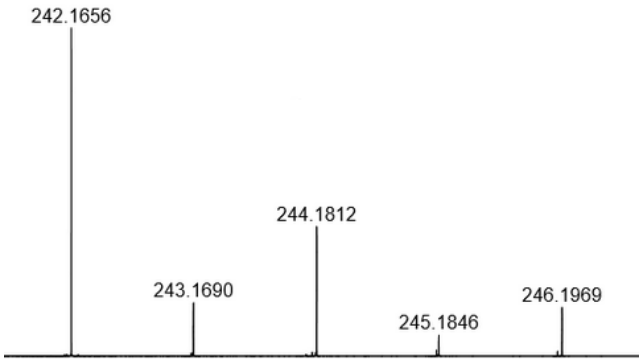

Figure 48. Mass spectrum of the chloroform extracts of the oxidation of imine **237** with MnO_2.

The methanol extract showed considerable amounts of an ion at 242.1654 Daltons, corresponding to arbusculidine A (**187**), with more significant peaks at 244.1812 and 246.1969 Daltons (Figure 49). The presence of these intermediates suggests that the reaction might need further time or more equivalents of oxidant to effect a complete conversion. Additionally, the mixing of the solid oxidant with the reagent in the Carius tube might not be very efficient and this might be reflected in this incomplete oxidation.

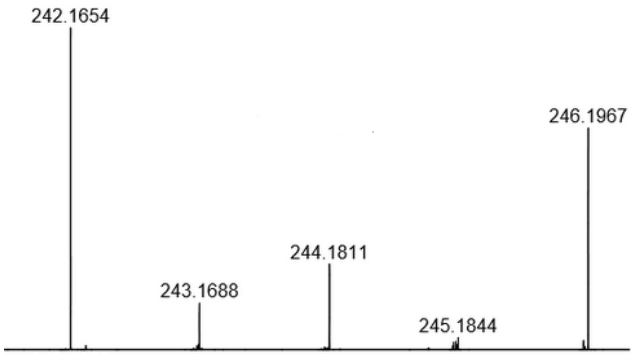

Figure 49. Mass spectrum of the methanol extracts of the oxidation of imine **237** with MnO_2.

The crude products from this reaction are currently undergoing purification using preparative HPLC by the project's collaborator Professor Roberto Berlinck (Sao Paulo, Brazil).

6.0 Conclusions

The bicyclic natural product monalidine A (**187**) was successfully synthesised *via* an efficient procedure, with the novel use of trifluoroethanol negating the need for protecting groups. Biological testing of monalidine A (**187**) showed it to be highly active against *L. infantum amastigotes* (non-infectious form), but no activity was observed against *L. infantum promastigotes* (infectious form). The intermediate **269** showed good activity against *L. infantum promastigotes*, indicating that monalidine A (**186**) shows poor activity due to its relative charge and poor cell uptake.

Extensive research has been conducted towards the synthesis of the tricyclic alkaloid arbusculidine A (**187**), but multiple attempts to synthesize it by oxidising mirabilin B (**220**) failed. The alternative oxidation of the iminium ion **237** with manganese dioxide to give the target compound arbusculidne A (**187**) was attempted with mixed results. Mass spectrometry appeared to give conclusive evidence for the formation of **187** during these reactions, however, NMR spectroscopy evidence was not conclusive. A larger sample of crude **187** has been prepared and is currently being purified and investigated by the project's collaborators in Brazil.

7.0 Experimental

7.1. General experimental synthesis procedures.

Reactions were magnetically stirred and monitored by TLC using Kieselgel 60 F254 silica coated plates, which were visualised using either I_2, phosphomolybdic acid, vanillin reagents or under UV light. General chemicals were obtained from Sigma Aldrich or Alfa Aesar. All anhydrous reactions were carried out in oven dried glassware and under a static argon atmosphere. Anhydrous Et_2O and CH_2Cl_2 were obtained from an Innovative Technology Pure Solv MD-3 solvent purification system. Trifluoroethanol (TFE) was dried over activated molecular sieves (3 Å powder). Flash chromatography was carried out on Davisil® 60A silica gel with the eluting solvent (chloroform, dichloromethane, diethyl ether, ethyl acetate, hexane, methanol, petroleum ether, THF or toluene) stated in each case. ^1H and ^{13}C NMR spectra of reaction products were obtained using a Bruker Ultrashield Plus 400 MHz spectrometer in $CDCl_3$ unless otherwise stated, and are reported as ppm referenced to the solvent internal standard at 7.26 and 77.16 ppm respectively. Infrared spectra were obtained using a Perkin Elmer FTIR spectrometer as either a thin film or as a KBr Disc. Ionisation (CI) and Electrospray Ionisation (ESI) mass spectra were recorded on a Micromass Quattro II spectrometer, and high resolution mass spectra were recorded on either a Finnigan MAT 900 XLT or a Finnigan MAT 95 XP at the EPSRC National Mass Spectrometry Service Centre based in Swansea, UK. All non-aqueous reactions were performed in a static atmosphere of dry argon or nitrogen unless otherwise stated. Microwave reactions were carried out using a CEM Discover SP-D closed vessel microwave reactor.

7.2. Preparative Methods

Preparation of deactivated silica

Silica gel (50 g) was stirred in methanol (100 mL) and triethylamine (10 mL) for 30 minutes before being filtered under vacuum and washing with further methanol. The silica was then air dried before use.

Preparation of activated manganese dioxide on carbon[106]

A solution of potassium permanganate (10.0 g, 63 mmol) in water (125 mL) in a beaker was heated to boiling point before removing from the heat and adding activated carbon (3.12 g) portion wise over 5 minutes, allowing the frothing to subside between additions. The solution was then boiled until the purple colour was discharged. The solution was allowed to stand at r.t. for 10/15 minutes before being filtered on a Buchner funnel and washing the filtrate with water (4 x 25 mL), and allowed to air dry before leaving in an oven at 115 ˚C for 24 h, to give activated manganese dioxide on carbon (7.91 g). The amount of absorbed manganese was calculated by the treatment of 0.50 g of the sample with aqueous ammonium iron(II) sulfate (0.2 M, 25 mL, 5 mmol) and aqueous H_2SO_4 (1 M, 20 mL, 20 mmol), followed by back titration of the excess iron(II) with acidified potassium permanganate (0.008 M) to a persistent pink colour. From these calculations it was found that 22 mL of permanganate solution (0.176 mmol) was required, which equates to 0.88 mmol of excess iron(II). Thus the original permanganate consumed 4.12 mmol of iron (II), equating to 2.06 mmol of MnO_2 per gram.

Reduction of Mn^{4+} $\quad MnO_2 + 2Fe^{2+} + 4H^+ \rightarrow Mn^{2+} + 2Fe^{3+} + H_2O$

Quantification of excess Fe^{2+} $\quad MnO_4^- + 5\ Fe^{2+} + 8H^+ \rightarrow Mn^{2+} + 5\ Fe^{3+} + 4\ H_2O$

Preparation of activated manganese dioxide.

A solution of manganese sulfate monohydrate (25 g) in water (480 mL) was heated to 60 ˚C and added in portion to a heated (60 ˚C) solution of potassium permanganate (17.4 g) in water (330 mL). The suspension formed was stirred at this temperature for 1 h then cooled, filtered and washed with water (100 mL). The solid obtained was dried in an oven at 120 ˚C for 48 h to give activated manganese dioxide (9.0 g) in 70% yield.

Preparation of 6-hydroxy-4,4,5,7,8-pentamethylchroman-2-one (26)[37]

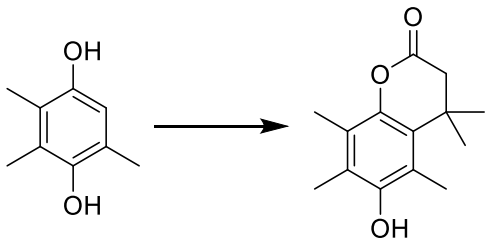

A mixture of 2,3,5-trimethyl-1,4-hydroquinone (**98**) (5.07 g, 33.3 mmol), methyl 3,3-dimethylacrylate (5.0 mL, 41.0 mmol, 1.23 eqv.) was dissolved in methanesulfonic acid (50 mL) and this was heated at 70 ˚C for 3 h. After cooling and stirring at r.t. overnight, the reaction mixture was cautiously added to water (200 mL) and extracted with ethyl acetate (3 x 150 mL). The combined organic layers were washed in turn with water (100 mL), saturated sodium carbonate (100 mL), and brine (100 mL). They were then dried ($MgSO_4$), filtered and the solvent removed under reduced pressure to give a grey/purple solid. The crude product was recrystallized from chloroform/hexane to yield the lactone **26** (6.88 g, 29.4 mmol, 88 % yield) as a white solid. Data was in accordance with the literature.

R_f = 0.39 (50:50 diethyl ether:petroleum ether); $\boldsymbol{\delta_H}$ 4.52 (1H, s, OH), 2.55 (2H, s, CH_2), 2.36 (3H, s, Me), 2.22 (3H, s, Me), 2.18 (3H, s, Me), 1.46 (6H, s, 2 x Me); $\boldsymbol{\delta_C}$ 168.8, 148.8, 143.5, 128.2, 123.4, 121.8, 118.9, 46.1, 35.5, 27.7, 14.4, 12.5, 12.3.

Preparation of 3-methyl-3-(2,4,5-trimethyl-3,6-dioxocyclohexa-1,4-dien-1-yl)butanoic acid 52[37]

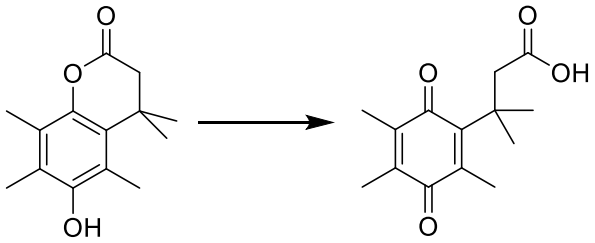

The lactone **26** (6.25 g, 26.68 mmol) was suspended in acetonitrile (15 % aq. v/v, 270 mL), and a solution of NBS (6.41 g, 36.01 mmol, 1.35 eqv.) in acetonitrile (40 % aq. v/v, 120 mL) was added drop wise over 1 h to the suspension. The resulting mixture was stirred for a further 30 min, diluted with water (500 mL) and extracted with dichloromethane (3 x 100 mL). The combined organic layer was washed with water (2 x 100 mL) and brine (100 mL). It was then dried ($MgSO_4$), filtered and the solvent was removed under reduced pressure to give a bright yellow solid. The crude product was re-dissolved in diethyl ether and petroleum ether was added to the cloud point. The solution was then cooled (0 ˚C) overnight. The supernatant liquid was decanted from the crystals formed to give the quinone **52** as a yellow solid (6.60 g, 26.37 mmol, 99 % yield). Data was in accordance with the literature.

R_f = 0.17 (50:50 diethyl ether:petroleum ether); $\boldsymbol{\delta_H}$ 10.06 (1H, b s, OH), 3.02 (2H, s, CH_2), 2.14 (3H, s, Me), 1.95 (3H, s, Me), 1.93 (3H, s, Me), 1.44 (6H, s, 2 x Me); $\boldsymbol{\delta_C}$ 190.8, 187.4, 178.4, 152.0, 143.0, 139.0, 138.4, 47.2, 37.9, 28.8, 14.3, 12.5, 12.1.

Preparation of 2,5-dioxopyrrolidin-1-yl 3-methyl-3-(2,4,5-trimethyl-3,6-dioxocyclohexa-1,4-dien-1-yl)butanoate 52a[37]

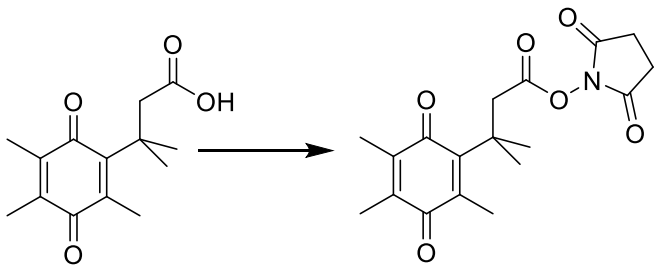

DCC (1.80 g, 8.72 mmol, 1.2 eqv.) was added to a cooled (0 ˚C) solution of quinone **52** (1.80 g, 7.19 mmol, and *N*-hydroxysuccinimide (0.91 g, 7.91 mmol, 1.1 eqv.) in anhydrous THF (60 mL). After stirring for 18 h at r.t., the mixture was filtered to remove DCU and evaporated under reduced pressure. The residue was triturated with ethyl acetate (30 mL) and filtered again. The filtrate was evaporated under reduced pressure to give a yellow solid. This solid was then dissolved in hot ethyl acetate (11 mL) then cooled to 0 ˚C. A crystalline mass formed, and the supernatant solvent was decanted from this, after which it was dried under vacuum to give the crude activated ester **52a** (2.79 g) as a yellow solid, which was used without further purification.

R_f = 0.09 (25:75 EtOAc:hexane), $\boldsymbol{\delta_H}$ 3.22 (2H, s, CH_2); 2.71 (4H, s, 2 x CH_2), 2.11 (3H, s, Me), 1.96 (6H, s, 2 x Me), 1.46 (6H, s, 2 x Me); $\boldsymbol{\delta_C}$ 190.4, 187.5, 169.0, 167.8, 150.1, 143.0, 140.6, 139.0, 44.3, 39.0, 29.3, 25.7, 14.4, 12.7, 12.4.

Preparation of *N,N*'-bis(2-Chloroethyl)benzene-1,4-diamine (70)[37]

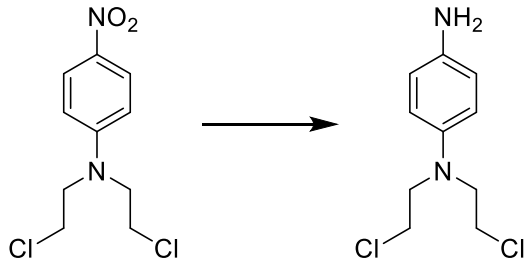

Pd/C (5 %, 0.40 g) was added to a solution of *N,N-bis*(2-chloroethyl)-4-nitroaniline (**124**) (0.40 g, 1.52 mmol) dissolved in EtOH (35 mL), and this mixture was stirred under an atmosphere of hydrogen gas (balloons) for 17 h. After filtration through a Celite© pad, which was washed with a 2:1 mixture of EtOAc and hexane (ca 100 mL), the red/brown filtrate was concentrated *in vacuo* to give a brown solid (0.99 g). The crude product was then adsorbed onto silica and purified by flash chromatography (50:50 EtOAc:hexane) to give **70** (0.24 g, 1.03 mmol, 68 % yield) as a brown solid. The data was in agreement with the literature.

R_f = 0.16 (33:67 EtOAc:hexane); $\boldsymbol{\delta_H}$ 7.02 (2H, b s, NH_2), 6.79 (2H, d, *J* = 3.6 Hz, 2 x CH), 6.70 (2H, d, *J* = 3.6 Hz, 2 x CH), 3.58-3.70 (8H, m, 4 x CH_2); $\boldsymbol{\delta_C}$ 135.7, 126.0, 116.3, 114.0, 54.1, 14.8.

Preparation of 3-amino-1,2,4-benzotriazine-1-oxide (77) [81]

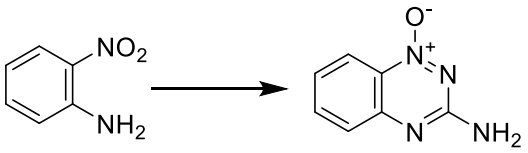

*From 2-nitroaniline (**134**):* 2-Nitroaniline (5.00 g, 36.2 mmol) and cyanamide (7.60 g, 181 mmol, 5 eqv.) were heated at 100 ˚C with stirring until a deep red melt formed. The reaction was then cooled to 40 ˚C, and concentrated hydrochloric acid (15 mL) was cautiously added in a drop wise fashion. The resulting exothermic reaction was allowed to subside, and this was followed by heating at 100 ˚C for 2 hrs. The reaction was then allowed to cool to 40 ˚C, and NaOH solution (50 mL, 16 M) was added cautiously in a drop wise fashion, before heating the now bright orange solution at 100 ˚C for 2 hrs. The reaction was then cooled to room temperature and water (50 mL) was added and the mixture was stirred for 30 minutes. The yellow suspension was then filtered and washed with water (10 mL) followed by diethyl ether (2 x 5 mL), collected and dried in a vacuum desiccator over P_2O_5. The product **75** (5.05 g, 31.17 mmol, 86 % yield) was obtained as a bright yellow solid and was used without further purification. Data was in agreement with the literature.

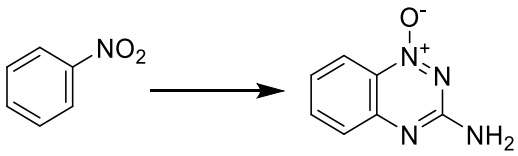

*From nitrobenzene (**139**):* Potassium *t*-butoxide (6.52 g, 58.23 mmol, 8.3 eqv.) was stirred in anhydrous THF (30 mL) under a positive argon atmosphere at 25 ˚C for 30 minutes. Guanidine hydrochloride (4.23 g, 13.70 mmol, 2.0 eqv.) was then added, followed by nitrobenzene (1 g, 6.85 mmol) in anhydrous THF (10 mL), and the suspension formed was stirred at 65 ˚C overnight. The progress of the reaction was monitored by TLC and once the starting material had disappeared, water (1.2 mL) was added. After stirring for 15 mins, the reaction was dried ($MgSO_4$) and filtered, washing the filter pad with copious quantities of ethyl acetate. Evaporation of the filtrate gave a brown/black residue which was purified by column chromatography (25-40 THF:petroleum ether in 5 % increments). This gave **77** as a bright yellow solid (0.53 g, 3.3 mmol, 48 % yield).

R_f = 0.60 (100 % ethyl acetate); $\boldsymbol{\delta_H}$ (DMSO) 8.12 (1H, dd, *J* = 0.9, 8.6 Hz, CH), 7.78 (1H, ddd, *J* = 1.4, 7.0, 8.3 Hz), 7.53 (1H, dd, *J* = 0.8, 8.3 Hz), 7.30-7.36 (3H, m, CH, NH_2); $\boldsymbol{\delta_C}$ 160.3, 148.8, 135.8, 129.9, 125.9, 124.7, 119.9.

Preparation of 3,6-Dimethoxy-1,2,4-trimethylcyclohexa-1,4-diene (99)[37]

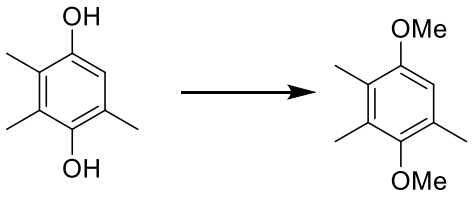

2,3,5-Trimethyl-1,4-hydroquinone (10.02 g, 65.83 mmol) was dissolved in methyl ethyl ketone (150 mL), and potassium carbonate (45.0 g, 325.6 mmol, 4 eqv.) was added. The mixture was stirred at r.t. for 30 minutes and iodomethane (16.2 mL, 260.67 mmol, 4 eqv.) was added. The mixture was stirred for 16 h at 65 ˚C. The reaction mixture was then cooled to r.t. and the solvent was removed under reduced pressure. The solid residue was triturated with diethyl ether (2 x 100 mL). The filtered triturates were evaporated under reduced pressure to give a brown oil, which was purified by column chromatography (5:95 diethyl ether:hexane) to give **99** as a colourless oil (7.70 g, 42.79 mmol, 65 % yield). Data was in agreement with the literature.

R_f = 0.33 (5:95 diethyl ether:hexane); δ_H 6.53 (1H, s, CH), 3.78 (3H, s, Me), 3.65 (3H, s, Me), 2.28 (3H, s, Me) 2.20 (3H, s, Me); 2.11 (3H, s, Me).

Preparation of 3,3,6,6-tetramethoxy-1,2,4-trimethylcyclohexa-1,4-diene (100)[37]

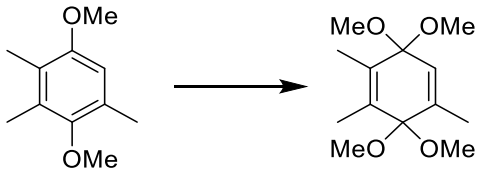

1,4-Dimethoxy-2,3,5-trimethyl-benzene (**99**) (7.35 g, 40.78 mmol) was dissolved in cooled (5 ˚C) methanolic potassium hydroxide (2 % (w/v), 250 mL) in an electrolysis cell (See appendix p191) , and a current of 1.0 Amp was passed through the solution for 3.5 h. The solvent was then removed *in vacuo* to yield a brown solid which was dissolved in water (200 mL), and the mixture was extracted with ether (3 x 100 mL). The combined organic layers were washed with brine (2 x 100 mL), dried ($MgSO_4$), filtered, and the solvent was removed under reduced pressure to give **100** (8.60 g, 35.48 mmol, 87 % yield) as a pale yellow solid, which was used without further purification. Data was in agreement with the literature.

R_f = 0.21 (40:60 diethyl ether:hexane); $\boldsymbol{\delta_H}$ 6.02 (1H, b q, *J* = 1.4 Hz, CH), 3.19 (6H, s, 2 x Me), 2.98 (6H, s, 2 x Me), 1.77 (3H, d, *J* = 1.4 Hz, Me), 1.75 (3H, d, *J* = 0.7 Hz, Me), 1.68 (3H, d, *J* = 0.7 Hz, Me).

Preparation of 4,4-dimethoxy-2,3,5-trimethylcyclohexa-2,5-dien-1-one (101)[37]

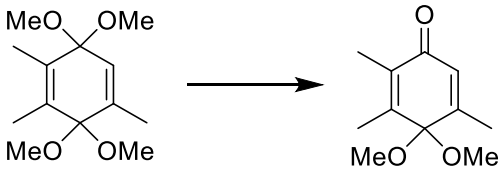

A solution of 3,3,6,6-tetramethoxy-1,2,4-trimethyl-cyclohexa-1,4-diene (**100**) (10.94 g, 45.15 mmol) in acetone (50 mL) was cooled (0 ˚C) and stirred vigorously, whereupon a cooled (ca 5 ˚C) acetic acid solution (2 % v/v, 55 mL) was added drop wise over 10 min. The resulting mixture was stirred at 0 ˚C for 25 min, then at r.t. for 3 h. The mixture was poured into sodium hydrogen carbonate solution (5 %, 260 mL) and then extracted with diethyl ether (4 x 100 mL). The combined extracts were washed with water (2 x 100 mL) and brine (100 mL), dried ($MgSO_4$), filtered and evaporated under reduced pressure to give **101** (8.06 g, 41.09 mmol, 91 % yield) as a yellow solid which was used without further purification. Data was in agreement with the literature.

R_f = 0.21 (40:60 diethyl ether:hexane); δ_H 6.33 (1H, q, *J* = 1.4 Hz, CH), 3.00 (6H, s, 2 x Me), 1.92 (3H, b s, Me), 1.90 (3H, d, *J* = 1.4 Hz, Me), 1.89 (3H, b s, Me).

Preparation of 2,3,5-trimethyl-3'*H*-spiro[cyclohexane-1,1'-isobenzofuran]-2,5-diene-3',4-dione (103)[37]

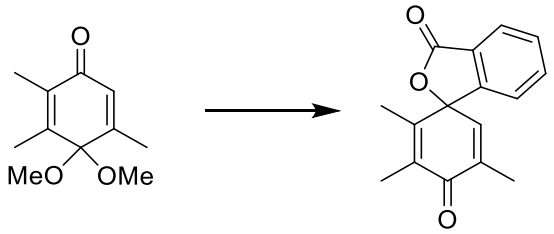

A solution of *n*-butyllithium (12.6 mL, 2.2 M, 27.63 mmol, 2 eqv.) was added drop wise to a cooled (-78 ˚C) solution of *N*-phenylbenzamide (**102**) (2.73 g, 13.82 mmol) in THF (33 mL), and the resulting mixture was stirred at -78 ˚C for 30 min and then at 0 ˚C for 1 h. This solution was then re-cooled (-78 ˚C) and a solution of monoketal **101** (2.92 g, 14.86 mmol, 1.08 eqv.) in THF (10 mL) was added drop wise. The resulting bright green solution was stirred for 4h then allowed to warm to r.t. overnight. The reaction mixture was diluted with diethyl ether (100 mL) and vigorously washed with 3 M hydrochloric acid (3 x 100 mL) and separated. The combined aqueous layers were further extracted with diethyl ether (3 x 50 mL), and the combined organic layers were then washed with brine (100 mL), dried ($MgSO_4$), filtered and evaporated under reduced pressure to give a dark brown solid. This solid was recrystallized by dissolving in hot diethyl ether and diluting this with methanol, to give on standing the spirolactone **103** (2.10 g, 8.27 mmol, 60 % yield) as white crystals after filtration. ^{1}H NMR data were in agreement with the literature.

δ_H 7.97 (1H, d, J = 7.6 Hz, CH), 7.66 (1H, ddd, J = 1.0, 7.4, 7.6 Hz, CH), 7.58 (1H, ddd, J = 0.8, 7.4, 7.7 Hz, CH), 7.15 (1H, d, J = 7.7 Hz, CH), 6.35 (1H, q, J = 1.4 Hz Me), 1.98 (3H, q, 0.7 Hz, Me), 1.96 (3H, d, 1.4 Hz, Me), 1.55 (3H, q, 0.7 Hz, Me).

Preparation of 2-hydroxy-1,3,4-trimethyl-6H-benzo[c]chromen-6-one (104)[37]

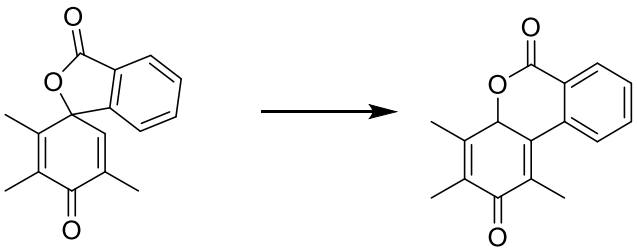

A mixture of the spirolactone **103** (0.50 g, 1.97 mmol), trifluoroacetic acid (5 mL), trifluoroacetic anhydride (10 mL) and concentrated sulfuric acid (10 drops) was heated at reflux for 7 h. The solvent was removed under reduced pressure and the residue was dissolved in methanol (25 mL), before being partitioned between dichloromethane (100 mL) and water (200 mL). The layers were separated and the aqueous phase further extracted with dichloromethane (3 x 50 mL). The combined organic extracts were then dried ($MgSO_4$) and the solvent was removed under reduced pressure to give a pale yellow solid. The crude product was recrystallized from dichloromethane/hexane to give lactone **104** (0.50 g, 1.95 mmol, 99 % yield) as white crystals. Data was in agreement with the literature.

R_f = 0.21 (dichloromethane); **Mp**. 198-199 ˚C (lit.[37] 200-201 ˚C); **δ_H** 8.46 (1H, dd, *J* = 1.5, 7.9 Hz, CH), 8.26 (1H, b d, *J* = 8.3 Hz, CH), 7.78 (1H, dt, *J* = 1.5, 8.2, 8.3 Hz, CH), 7.55 (1H, b dd, *J* = 7.9, 8.2 Hz, CH), 4.75 (1H, b s, OH), 2.72 (3H, s, Me), 2.43 (3H, s, Me), 2.32 (3H, s, Me); **δ_C** 161.7, 148.9, 144.4, 136.4, 133.7, 130.5, 127.6, 126.5, 125.3, 123.5, 122.2, 117.4, 116.0, 16.2, 12.9, 12.4.

Preparation of 3',4',6'-trimethyl-2',5'-dioxo-2',5'-dihydro-[1,1'-biphenyl]-2-carboxylic acid (105)[37]

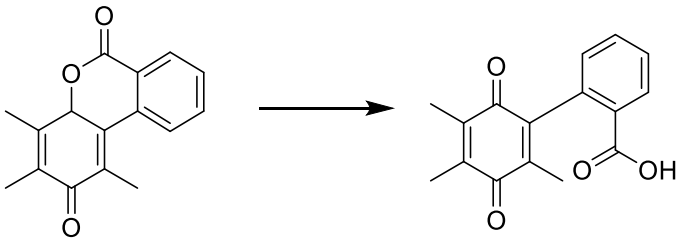

Lactone **104** (0.82 g, 3.22 mmol) was suspended in a water/acetonitrile mixture (15 %: v/v, 40 mL), and a solution of NBS (0.78 g, 4.38 mmol, 1.36 eqv.) in water/acetonitrile (40 %: v/v, 12 mL) was added drop wise over 1h. The resulting mixture was stirred for a further 30 min, then diluted with water (120 mL) and extracted with dichloromethane (3 x 50 mL). The combined organic layers were washed with water (2 x 50 mL) and brine (50 mL), then dried ($MgSO_4$) and evaporated under reduced pressure to give a crude yellow oil. The crude product was purified by column chromatography (dichloromethane then 20:80 EtOAc:petroleum ether) to give **105** (0.70 g, 2.61 mmol, 81 % yield) as a waxy yellow solid. Data was in agreement to that reported previously.[1]

R_f = 0.59 (5:95 MeOH:EtOAc); **Mp**. 154-156 ˚C (lit.[37] 155-157 ˚C); $\boldsymbol{\delta_H}$ 9.50 (1H, s, OH), 8.16 (1H, d, *J* = 7.6 Hz CH), 7.61 (1H, t, *J* = 7.6 Hz, CH), 7.48 (1H, t, *J* = 7.6 Hz), 7.14 (1H, d, *J* = 7.6 Hz), 2.08 (3H, s, Me), 2.01 (3H, s, Me), 1.82 (3H, s, Me); $\boldsymbol{\delta_C}$ 188.0, 186.4, 170.9, 145.1, 141.0, 140.9, 138.8, 136.4, 133.4, 131.6, 130.5, 128.8, 128.6, 13.8, 12.6, 12.5.

Preparation of *N*-(4-(bis(2-chloroethyl)amino)phenyl)-3',4',6'-trimethyl-2',5'-dioxo-2',5'-dihydro-[1,1'-biphenyl]-2-carboxamide (116)

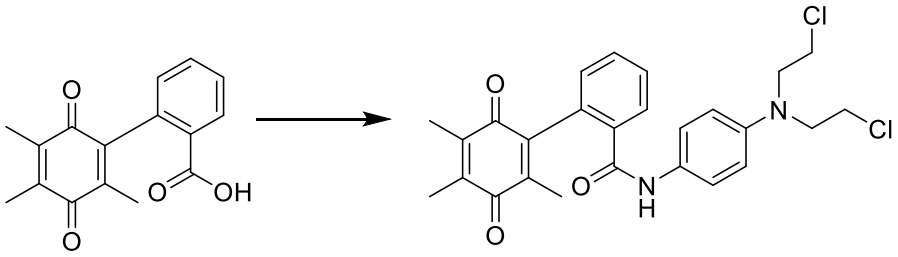

Carboxylic acid **105** (51.0 mg, 0.19 mmol), EDC (35.7 mg, 0.23 mmol, 1.2 eqv.) and HOBT (30.8 mg, 0.23 mmol, 1.2 eqv.) were dissolved in THF (5 mL) and stirred for 2 h. A solution of the mustard **99** (53.7 mg, 0.23 mmol, 1.2. eqv.) dissolved in THF (2 mL) was then added, and the mixture was stirred at r.t. for 48 h. After completion of the reaction (TLC), the product was diluted with EtOAc (50 mL), and the mixture was washed with water (3 x 100 mL), dried ($MgSO_4$) and evaporated under reduced pressure to give the crude product as a brown gum. This was purified *via* flash chromatography (1:5 EtOAc in petroleum ether) to give **116** as a brown gum (30.0 mg, 0.062 mmol, 33 % yield).

R_f = 0.22 (20:80 EtOAc:petroleum ether); δ_H ($CDCl_3$) 7.70 (1H, b d, *J* = 7.7 Hz, CH), 7.47-7.56 (2H, m, 2 x CH, NH), 7.32 (2H, d, *J* = 8.6 Hz, 2 x CH), 7.16 (1H, dd, *J* = 1.2, 7.6 Hz, CH), 6.67 (2H, d, *J* = 8.6 Hz, CH), 3.70 (4H, t, *J* = 6.5 Hz, 2 x CH_2), 3.61 (4H, t, *J* = 6.5 Hz, 2 x CH_2), 2.05 (3H, q , *J* = 0.7 Hz, CH_3), 1.99 (3H, b q , *J* = 0.7 Hz, CH_3), 1.90 (3H, s, CH_3); δ_C 188.4, 187.8, 187.1, 143.8, 141.4, 141.2, 140.4, 133.9, 133.3, 130.9, 130.6, 130.5, 127.9, 127.8, 127.1, 126.7, 122.7, 55.1, 39.5, 14.2, 12.7, 12.6; **LRCIMS** *m*/*z* 485.1 (100 %, $[M+H]^+$), 487.1 (65 %) 489.1 (10 %); **HRCIMS** *m*/*z* found 485.1387 ($[M+H]^+$), $C_{26}H_{27}{}^{35}Cl_2N_2O_3$ requires 485.1399.

Attempted coupling of quinone 52a with Tirapazamine (38), 77, 147 and 161

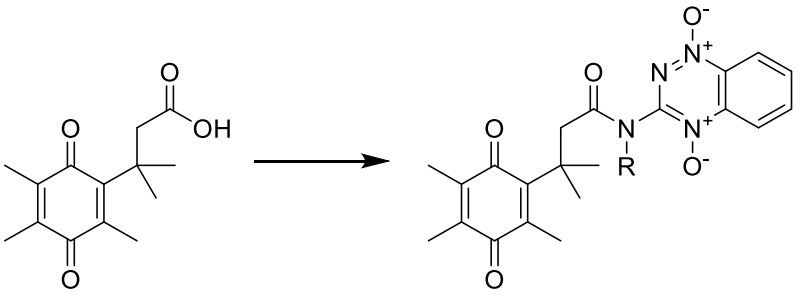

*i) From the activated ester **52a**:* Tirapazamine **38** (102.0 mg, 0.58 mmol. 1.5 eqv.) was suspended in acetonitrile (10 mL), and the activated ester **52a** was added after dissolving in anhydrous acetonitrile (5 mL). The reaction mixture was stirred at r.t. for 48 h and monitored by TLC with 100 % ethyl acetate. Once the starting material **52a** had been fully consumed, the solvent was removed by rotary evaporation. Analysis by NMR spectroscopy and TLC suggested the presence of only tirapazamine (**38**) and the quinone acid **52**. This reaction was repeated at 40 ˚C and 60 ˚C with similar results.

An identical series of reaction were performed on the same scale using 3-amino-1,2,4-benzotriazine-1-oxide (**77**), *N*-octylbenzo[1,2,4]triazin-3-amine (**147**) and 3-(heptylamino)benzo[1,2,4]triazine 1-oxide (**161**) at r.t., 40 ˚C and 60 ˚C, with only the recovery of starting materials being observed.

(ii) Using HOBT activation: Quinone **52** (100.0 mg, 0.40 mmol), was dissolved in anhydrous acetonitrile (10 mL). DCC (69.0 mg, 0.33 mmol, 1.2 eqv.) was then added followed by HOBT (80.0 mg, 0.52 mmol, 1.3 eqv.). The reaction was stirred at r.t. for 1 hour whereupon a solution of tirapazamine (**38**) (102.0 mg, 0.58 mmol, 1.5 eqv.) in acetonitrile (15 mL) was added. The reaction was stirred at r.t. for 48 h, and then evaporated under reduced pressure. After this, ethyl acetate (10 mL) was added and the mixture was cooled (0 ˚C) with stirring. After filtering through a cotton wool plug to remove undissolved DCU, the filtrate was evaporated, and this procedure was repeated twice more with ethyl acetate (5 mL) to give a crude gum (115.6 mg). Analysis of the product and the precipitated DCU residues by NMR spectroscopy and TLC suggested only the presence of tirapazamine (**38**) and the quinone acid **52**.

An identical series of reaction were performed on the same scale using 3-amino-1,2,4-benzotriazine-1-oxide (**77**), *N*-octylbenzo[1,2,4]triazin-3-amine (**147**) and 3-(heptylamino)benzo[1,2,4]triazine 1-oxide (**161**) at r.t., 40 ˚C and 60 ˚C, with only the recovery of starting materials being observed.

iii) Via an acid chloride: Quinone acid **52** (100.0 mg, 0.40 mmol) was dissolved in thionyl chloride (3 mL) and heated under reflux for 30 minutes. Excess thionyl chloride was removed under reduced pressure, and a solution of tirapazamine (**38**) (102.0 mg, 0.58 mmol, 1.5 eqv.) in anhydrous pyridine (20 mL) was added. The reaction was stirred at r.t for 4 hrs, and the solvent was removed under reduced pressure to give a brown semi-solid. Analysis by NMR spectroscopy showed the resulting product to be unchanged tirapazamine and quinone acid **52**.

iv) Via a mixed anhydride: Quinone **52** (100.0 mg, 0.40 mmol) was dissolved in THF (10 mL) and cooled (-5 ˚C), whereupon a solution of isopropylchloroformate (1 M, 0.4 mL, 0.40 mmol, 1.0 eqv.) in toluene was added. Triethylamine (0.055 mL, 0.40 mmol, 1.0 eqv.) was then added and the reaction stirred at -5 °C for 30 minutes. A solution of tirapazamine (102.0 mg, 0.58 mmol, 1.5 eqv.) dissolved in acetonitrile (10 mL) was then added, and after stirring to r.t. over 24 hrs, the solvent was evaporated under reduced pressure. Analysis by NMR spectroscopy and TLC suggested the presence of only tirapazamine (**38**) and the quinone acid **52**.

An identical series of reactions were performed on the same scale using 3-amino-1,2,4-benzotriazine-1-oxide (**77**), *N*-octylbenzo[1,2,4]triazin-3-amine (**147**), and 3-heptylamino)benzo[1,2,4]triazine 1-oxide (**161**) at r.t., 40 ˚C and 60 ˚C with only the recovery of starting materials being observed.

Preparation of 2,2'-((4-nitrophenyl)azanediyl)bis(ethan-1-ol) (123)[82]

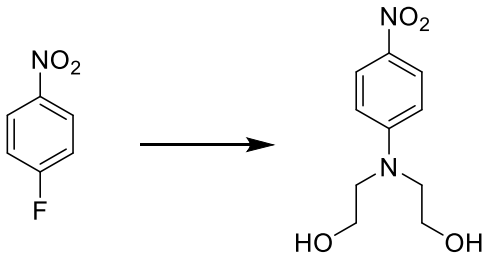

A mixture of 1-fluoro-4-nitrobenzene (8.8 mL, 11.69 g, 82.9 mmol) and 2,2-iminoethanol (8.0 mL, 8.76 g, 83.5 mmol, 1.1 eqv.) were heated (130 ºC) in a sealed tube for 19 h. After cooling to r.t., NaOH solution (aq, 0.6 % w/v, 50 mL) was added and the suspension formed was heated to 60 ºC for 30 min. It was then filtered and the solid obtained was air dried. The residue was recrystallised from EtOAc to give the product **123** (13.68 g, 73% yield) as yellow crystals. Data was in accordance with the literature.[91]

R_f = 0.69 (50:50 MeOH:EtOAc); **Mp**. 101-103°C (lit.[91] 100-102 ˚C); **δ_H** 8.11 (2H, d, *J* = 8.2 Hz, 2 x CH), 6.67 (2H, d, *J* = 8.2 Hz, 2 x CH), 3.95 (4H, t, *J* = 5.0 Hz, 2 x CH_2) 3.73 (4H, t, *J* = 5.0 Hz, 2 x CH_2), 2.82 (2H, b s, 2 x OH); **δ_C** 152.7, 137.5, 126.3, 111.3, 60.5, 55.2.

Preparation of *N,N*-bis(2-chloroethyl)-4-nitroaniline (124)[37,91]

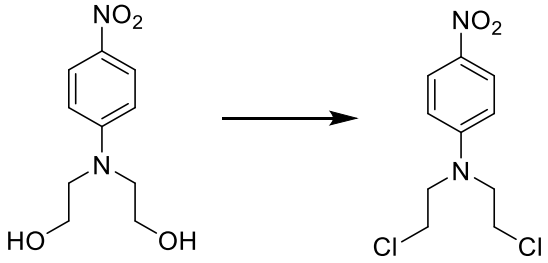

*From **123***: Diol **123** (0.80 g, 3.53 mmol) was suspended in anhydrous dichloromethane (8 mL) and pyridine (1 mL, 12.36 mmol), and the mixture was cooled to 0 ˚C. Thionyl chloride (1.2 mL, 16.45, 4.7 eqv.) was added slowly, and the mixture was heated under reflux for 7 h. After cooling to r.t., the mixture was then extracted with dichloromethane (2 x 100 mL), the organic layer was washed with water (2 x 100 mL), dried and filtered, and the solvent was removed under reduced pressure to give a yellow solid. The crude product was then purified *via* flash chromatography (20:80 EtOAc:petroleum ether) to give the target compound as a yellow crystalline solid (0.74 g, 2.83 mmol, 80 % yield), which was contaminated with ca. 10 % of an inseparable impurity.

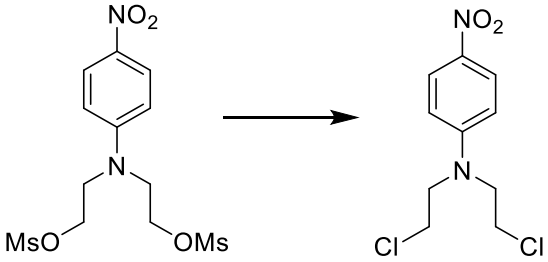

*From **127:*** Mesylate **127** (2.13 g, 6.01 mmol) and sodium chloride (1.15 g, 19.68 mmol, 3.3 eqv,) were dissolved in anhydrous DMF (10 mL) and heated at 160 ˚C for 15 minutes. The reaction was then cooled to r.t. and stirred overnight. The solvent was removed under reduced pressure (toluene azeotrope) and the residue dissolved in ethyl acetate (100 mL) and washed with water (500 mL) followed by brine (300 mL). After drying ($MgSO_4$), filtration and evaporation under reduced pressure gave a crude brown solid, which was purified by flash chromatography (20:80 EtOAc:hexane) to give the product as yellow crystals (0.77 g, 2.93 mmol, 49 % yield). Data were in agreement with the literature.[91]

R_f = 0.15 (10:90 EtOAc:petroleum ether), 88-91°C (lit.[91] 92-93 °C), $\boldsymbol{\delta_H}$ 8.14 (2H, d, *J* = 9.1 Hz, 2 x CH), 6.68 (2H, d, *J* = 9.1 Hz, 2 x CH), 3.87 (4H, t, *J* = 6.8 Hz, 2 x CH_2), 3.69 (4H, t, *J* = 6.8 Hz, 2 x CH_2); $\boldsymbol{\delta_C}$ 151.3, 138.6, 126.6, 110.9, 53.5, 40.0

Preparation of ((4-Nitrophenyl)azanediyl)bis(methylene) dimethanesulfonate (127)[91]

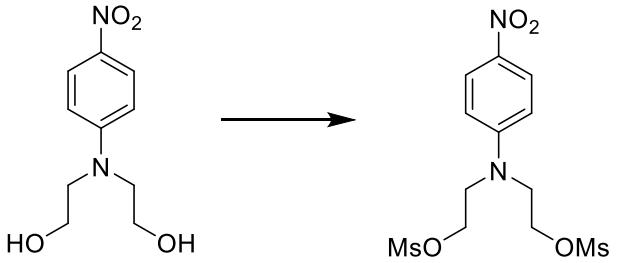

Diol **123** (2.00 g, 8.8 mmol) was suspended in EtOAc (30 mL) and the mixture was gently heated until full dissolution occurred. $MeSO_2Cl$ (1.9 mL, 2.87 g, 25.2 mmol, 2.9 eqv.) was then added drop wise over 10 minutes, followed by the drop wise addition of triethylamine (3.9 mL, 2.84g, 28.16 mmol, 3.2 eqv.). After 5 minutes, the reaction mixture was filtered, the filter pad washed with acetone (ca. 50 mL) and the combined filtrate and acetone washings evaporated under reduced pressure to give an orange residue. Recrystallisation from ethanol/EtOAc gave **127** (2.13 g, 6.01 mmol, 68 % yield) as yellow/orange crystals. Data was in accordance with the literature.[91]

Mp. 90-93 °C (lit.[91] 94-95 ˚C); **δ_H** 8.17 (2H, d, *J* = 9.4 Hz, 2 x CH), 6.72 (2H, d, *J* = 9.4 Hz, 2 x CH), 4.42 (4H, t, *J* = 5.7 Hz, 2 x CH_2), 3.91 (4H, t, *J* = 5.7 Hz, 2 x CH_2), 3.02 (6H, s, 2 x Me); **δ_C** 168.6, 151.5, 126.6, 111.2, 65.6, 51.0, 37.9.

Preparation of 3-(octylamino)benzo[1,2,4]triazine 1-oxide (147)

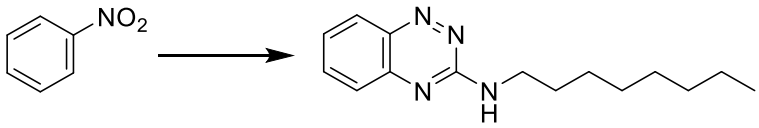

Potassium *t*-butoxide (2.72 g, 24.33 mmol, 8.3 eqv.) was stirred in anhydrous THF (20 mL) under a positive argon atmosphere at 25 ˚C for 30 minutes. Octyl guanidine hemisulfate (1.29 g, 5.86 mmol, 2 eqv.) was then added, followed by nitrobenzene (0.36 mL, 2.93 mmol) in anhydrous THF (5 mL). The resulting suspension was stirred at 65 ˚C for 20 h and monitored by TLC (50:50 EtOAc:petroleum ether) until the nitrobenzene had been consumed. The reaction was cooled to r.t. and water (10 mL) was added before stirring for 15 minutes. The aqueous reaction mixture was extracted with chloroform (4 x 50 mL), and the combined organic extracts were dried ($MgSO_4$) and filtered, and the solvent was removed by rotary evaporation to give a brown/black residue. This was purified by column chromatography (30:70 diethyl ether:petroleum ether) to give the product as a bright yellow solid (321 mg, 1.2 mmol, 30 % yield) which was of ca 90-95% purity.

R_f = 0.30 (30:70 diethyl ether:petroleum ether); **Mp**. 66-69 ˚C; **δ_H** 8.22 (1H, b d, *J* = 8.2 Hz, CH), 7.77 (1H, ddd, *J* = 1.4, 7.0, 8.4 Hz, CH), 7.61 (1H, b d, J = 8.4 Hz, CH), 7.41 (1H, ddd, *J* = 1.0, 7.0, 8.2 Hz), 6.18 (1H, b s, NH), 3.58 (2H, b s, CH_2), 1.72 (2H, *apparent pentet*, *J* = 7.3 Hz, CH_2), 1.20-1.48 (12H, m, 6 x CH_2), 0.88 (3H, t, *J* = 6.7 Hz, CH_3); **δ_C** 14.2, 22.8, 27.1, 29.4, 29.4, 29.8, 31.9, 41.5, 125.2, 125.6, 128.9, 139.1, 130.1 (2 x C), 136.1; **ν_{max} (film)** 3249, 3061, 2954, 2924, 2852, 2223, 1674, 1586, 1563, 1499, 1466, 1487, 1446, 1377, 1235, 758, 718, 693 cm^{-1}; **LRCIMS** *m*/*z* 259.2 (100%); **HRCIMS** *m*/*z* found 259.1917 ($[M+H]^+$), $C_{15}H_{23}N_4$ required 259.1923.

Preparation of 1-(3-hydroxypropyl)guanidine hydrochloride (149)[84]

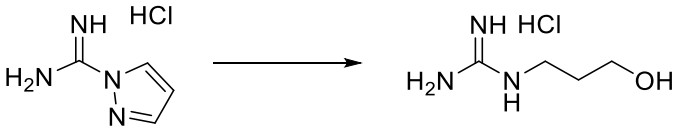

1*H*-Pyrazole-1-carboxamidine hydrochloride (5 g, 34.2 mmol) was stirred in anhydrous DMF together with 3-amino-1-propanol (2.87 mL, 37.62 mmol, 1.10 eqv.) and DIPEA (5.25 mL, 37.6 mmol, 1.10 eqv.) for 16 h. The reaction was checked for completion by TLC (1% methanol in chloroform), after which anhydrous diethyl ether (300 mL) was added, precipitating a yellow oil. The cloudy diethyl ether layer was then carefully decanted from the yellow oil before adding a further portion of anhydrous diethyl ether (300 mL) and stirring with an overhead stirrer overnight. The diethyl ether layer was again decanted from the yellow oil, and any residual ether was removed under vacuum, before checking for residual DMF by using NMR spectroscopy. Fresh anhydrous diethyl ether (300 mL) was added and the mixture was stirred overnight. The solvent was decanted and pure product was obtained as a brown/yellow oil (4.80 g, 31.37 mmol, 91 % yield) after the removal of residual traces of solvent by rotary evaporation.

δ_H (CD_3OD) 3.61 (2H, t, *J* = 6.0 Hz, CH_2), 3.26 (2H, t, *J* = 6.7 Hz, CH_2), 1.75 (2H, apparent *pentet*, *J* = 6.3 Hz); **δ_C** (CD_3OD) 158.9, 59.7, 39.7, 32.4; **LRCIMS** *m*/*z* 118 (100 %, $([M+H]^+)$); **HRCIMS** *m*/*z* found 118.0975 ($[M+H]^+$), $C_4H_{11}N_3O$ requires 118.0975.

Attempted preparation of 3-(benzo[e][1,2,4]triazin-3-ylamino)propan-1-ol (150)

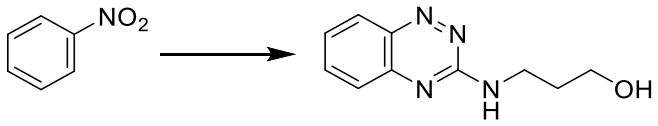

Potassium *t*-butoxide (10.45 g, 93 mmol, 9.3 eqv.) was added to THF (40 mL) and the mixture was stirred to ensure dissolution. At this point, the solution was transferred *via* cannula to a flask containing 1-(3-hydroxypropyl)guanidine hydrochloride (**149**) (3.06 g, 20.0 mmol, 2.0 eqv.), and the mixture was stirred for 5 mins. Nitrobenzene (1.00 g, 10.0 mmol) dissolved in THF (10 mL) was added, and the solution (which darkened considerably within 1 min) was heated at 65 ˚C for 20 h. The progress of the reaction was monitored by TLC (20:80 THF:petroleum ether), and once the nitrobenzene had been consumed, the reaction was cooled to r.t. and quenched with water (2 mL). The reaction mixture was then dried ($MgSO_4$) and filtered. Removal of the solvent gave a brown oil. Attempts at purification by column chromatography (20-100% EtOAc:petroleum ether) proved unsuccessful and no product was isolated.

Preparation of 3-((*tert*-butyldimethylsilyl)oxy)propan-1-amine (156)

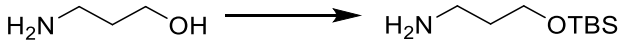

Imidazole (0.65 g, 8.89 mmol, 1.3 eqv.) was added in portions to a stirred solution of 3-amino-1-propanol (1.0 g, 6.84 mmol) and TBSCl (1.34 g, 8.89 mmol, 1.3 eqv.) dissolved in dichloromethane (10 mL). After 16 h, water (15 mL) was added and the mixture separated and the organic phase was washed with water (3 x 5 mL) followed by brine (10 mL). The organic phase was dried ($MgSO_4$), filtered the solvent removed by rotary evaporation to give a light yellow oil (1.33 g, 5.12 mmol, 75 % yield), which was used without further purification.

δ_H 3.70 (2H, t, *J* = 6.1 Hz, CH_2), 2.80 (2H, t, *J* = 6.8 Hz, CH_2), 1.66 (2H, app *pentet*, *J* = 6.5 Hz, CH_2), 1.46 (2H, b s, NH_2), 0.89 (9H, s, 3 x Me), 0.05 (6H, s, 2 x Me); **δ_C** 61.6, 39.4, 36.3, 25.9, 18.3, -5.4.

Preparation of 3-(heptylamino)benz(1,2,4)triazine 1-oxide (161)

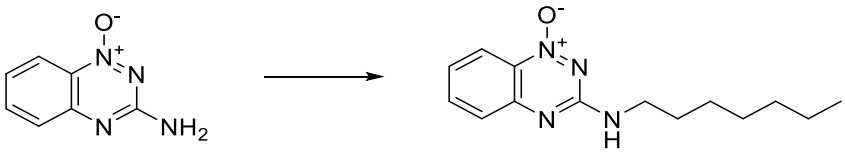

Potassium carbonate (140 mg, 1.01 mmol, 1.5 eqv.) was added to a suspension of 3-amino-1,2,4-benzotriazine-1-oxide (**77**) (100 mg, 0.62 mmol) in anhydrous DMF (15 mL) containing powdered molecular sieves (3 Å, ca. 0.2 g). 1-Iodoheptane (224 mg, 0.99 mmol, 1.5 eqv.) was added, and the reaction was heated at 120 °C for 20 h. The solution changed from yellow to orange in colour, and the reaction was checked for completion by TLC before cooling and filtering the product. The solvent was then removed by co-evaporation with toluene, until a solid residue formed. This crude material was purified by column chromatography (25:75 diethyl ether:petroleum ether), to give the product as a bright yellow solid (41.0 mg, 0.16 mmol, 25 % yield).

This reaction was repeated on nine occasions

i) Using **77** (536 mg, 3.3 mmol) in acetonitrile (40 mL) with 1-iodoheptane (1.12 g, 4.96 mmol, 1.5 eqv.) and potassium carbonate (0.7 g, 4.96 mmol, 1.5 eqv.), with heating under reflux for 24 h to give **161** (18.6 mg, 0.072 mmol, 2 % yield).

ii) Using **77** (108 mg, 0.67 mmol) in acetonitrile (10 mL) with 1-iodoheptane (224 mg, 1.01 mmol, 1.5 eqv.) and potassium carbonate (140 mg, 1.01 mmol, 1.5 eqv.), heating under reflux for 7 d to give **161** (5.23 mg, 0.02 mmol, 3 % yield)

iii) **77** (108 mg, 0.67 mmol) in acetonitrile (10 mL) with 1-iodoheptane (224 mg, 1.01 mmol, 1.5 eqv.) and potassium carbonate (140 mg, 1.01 mmol, 1.5 eqv.), heating at 130 ˚C in a sealed tube for 20 hours to give **161** (19.8 mg, 0.08 mmol, 11 % yield).

iv), **77** (100 mg, 0.62 mmol) in anhydrous DMF (13 mL) with 1-iodoheptane (224 mg, 1.01 mmol, 1.5 eqv.) and potassium carbonate (140 mg, 1.01 mmol, 1.5 eqv.), heating at 135 ˚C to give **161** (48.4 mg, 0.19 mmol, 30 % yield), which eluted with an inseparable impurity.

iv) **77** (100 mg, 0.62 mmol) in anhydrous DMF (13 mL) with 1-iodoheptane (224 mg, 1.01 mmol, 1.5 eqv.) and potassium carbonate (140 mg, 1.01 mmol, 1.5 eqv.), heating at 125 ˚C to give **161** (38.7 mg, 0.15 mmol, 24 % yield), which eluted with an inseparable impurity.

v) Using **77** (100 mg, 0.62 mmol) in anhydrous DMF (13 mL) with 1-iodoheptane (224 mg, 1.01 mmol, 1.5 eqv.) and potassium carbonate (85.6 mg, 0.62 mmol, 1.0 eqv.), heating at 120 ˚C to give **161** (40.3 mg, 0.16 mmol, 25 % yield).

vi) Using **77** (100 mg, 0.62 mmol) in anhydrous DMF (13 mL) with 1-iodoheptane (224 mg, 1.01 mmol, 1.5 eqv.) and potassium carbonate (42.8 mg, 0.31 mmol, 0.5 eqv.), heating at 120 ˚C to give **161** (14.5 mg, 0.06 mmol, 9 % yield)

vii) Using **77** (100 mg, 0.62 mmol) in anhydrous DMF (13 mL) with 1-iodoheptane (168 mg, 0.74 mmol, 1.2 eqv.) and potassium carbonate (140 mg, 1.01 mmol, 1.5 eqv.), heating at 120 ˚C to give **161** (35.5 mg, 0.14 mmol, 22 % yield)

viii) Using **77** (100 mg, 0.62 mmol) in anhydrous DMF (13 mL) with 1-iodoheptane (140 mg, 0.62 mmol, 1.0 eqv.) and potassium carbonate (140 mg, 1.01 mmol, 1.5 eqv.), heating at 120 ˚C to give **161** (29.0 mg, 0.11 mmol, 18 % yield)

ix) Using **77** (100 mg, 0.62 mmol) in anhydrous dioxane (20 mL) with 1-iodoheptane (224 mg, 1.01 mmol, 1.5 eqv.) and potassium carbonate (140 mg, 1.01 mmol, 1.5 eqv.), heat under reflux for 4 days. **161** was not isolated.

R_f = 0.29 (30:70 diethyl ether:petroleum ether); **Mp**. 130-132 ˚C; **δ_H** 8.25 (1H, dd, *J* = 0.6, 8.3 Hz, CH), 7.61 (1H, ddd, J = 1.1, 7.2, 8.3 Hz, CH), 7.51 (1H, b d, J = 8.3 Hz, CH), 7.20 (1H, ddd, 1.1, 7.2, 8.3 Hz, CH), 5.31 (1H, b s, NH), 3.44 (2H, apparent q, *J* = 6.9 Hz, CH_2), 1.59 (2H, apparent *pentet*, *J* = 7.2 Hz, CH_2), 1.15-1.36 (8H, m, 4 x CH_2), 0.81 (3H, t, 6.6 Hz, Me); **δ_C** 158.9, 148.6, 135.5, 130.8, 129.8, 126.3, 124.8, 120.4, 41.4, 29.3, 28.9, 26.8, 22.6, 14.0; **ν_{max} (film)** 3294, 2952, 2850, 1732, 1586, 1570, 1494, 1418, 759, 673, 647 cm^{-1}; **LRCIMS** *m*/*z* 261.17 (100 %, ($[M+H]^+$)), 283.2 (50 %, ($[M+Na]^+$)), 543.3 (55 %, ($[2M+Na]^+$); **HRCIMS** *m*/*z* found 261.1711 ($[M+H]^+$) $C_{14}H_{21}O_1N_4$ required 261.1710; for X-ray structure see appendix.

Attempted preparation of 3-((9-hydroxynonyl)amino)-1,4-benzo[1,2,4]triazin-1-olate (163).

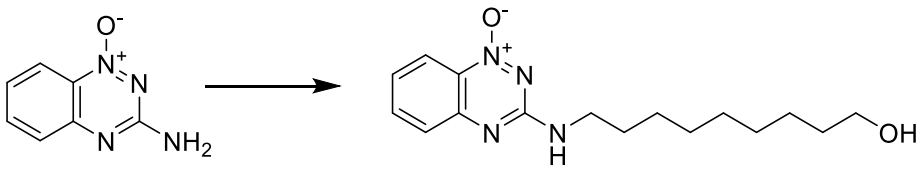

Potassium carbonate (140.0 mg, 1.01 mmol, 1.5 eqv.) was added to a suspension of 3-amino-1,2,4-benzotriazine-1-oxide **77** (100.0 mg, 0.62 mmol) in anhydrous DMF (15 mL) containing potassium iodide (10.0 mg, 0.06 mmol, 0.1 eqv.) and powdered molecular sieves (3 Å, ca 0.2 g). 9-Brononon-1-ol (221.0 mg, 0.99 mmol, 1.5 eqv.) was then added and the reaction was heated at 120 °C for 92 h. Analysis by NMR spectroscopy indicated that no reaction had occurred, as the major product recovered was **77**. A repeat of this reaction with fresh potassium iodide was also unsuccessful.

Preparation of 10-bromodecan-1-ol (165)[87]

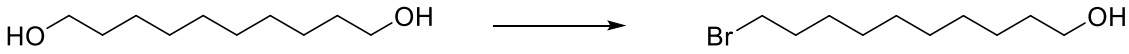

Decane-1,10-diol (5.0 g, 33.8 mmol) was dissolved in toluene (90 mL), and HBr (48 % aqueous, 3.88 mL, 34.17 mmol, 1.01 eqv.) was added. The mixture was heated under reflux overnight. After cooling to r.t., the organic layer was separated. The organic extract was dried ($MgSO_4$), filtered and the solvent was removed under reduced pressure to give the crude product as a yellow oil. Purification by column chromatography (50:50 diethyl ether:hexane) gave the product as a pale yellow oil (2.55 g, 10.75 mmol, 32 % yield). Data was in agreement with the literature.

R_f = 0.33 (15:85 EtOAc:petroleum ether) $\boldsymbol{\delta_H}$ 3.64 (2H, t, *J* = 6.6 Hz, CH_2), 3.41 (2H, t, *J* = 6.9 Hz, CH_2), 1.81 (2H, apparent *pentet*, *J* = 7.2 Hz, CH_2), 1.57 (2H, apparent *pentet*, *J* = 7.0 Hz, CH_2), 1.45 -1.24 (13H, m, 7 x CH_2, OH), $\boldsymbol{\delta_C}$, 63.1, 34.1, 32.8, 32.8, 29.5, 29.4 (2 x CH_2), 28.7, 28.2, 25.7.

Preparation of (10-bromodecyl)oxy)methyl)benzene (166)[146]

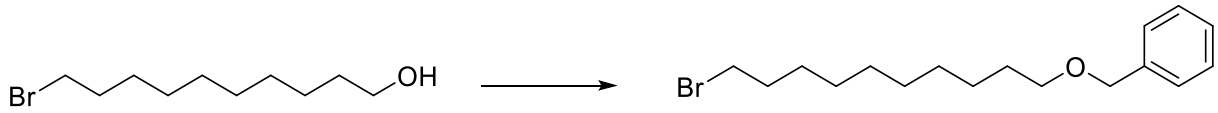

10-Bromodecan-1-ol (1.00 g, 3.94 mmol) was added to a cooled (0 °C) suspension of sodium hydride (60% in oil, 0.23 g, 9.45 mmol, 1.8 eqv.) in THF (20 mL), and the mixture was stirred for 1 h. Benzyl bromide (1.47 mL, 2.12 g, 3.98 mmol, 1.01 eqv.) was added, and the creamy white suspension was heated under reflux for 16 h. The reaction was cooled to 0 °C before carefully adding saturated ammonium chloride solution (30 mL). The reaction mixture was then extracted with diethyl ether (3 x 50 mL), and the combined organic extracts were washed with brine (100 mL) then dried ($MgSO_4$), and the solvent was removed under reduced pressure, to give a crude yellow oil. This was purified by column chromatography (40:60 dichloromethane:hexane) to give the product as a colourless oil (0.66 g, 2.01 mmol, 51 % yield). Data was in agreement with the literature.

δ_H 7.37-7.27 (5H, m, 5 x CH), 4.50 (2H, s, CH_2), 3.46 (2H, t, *J* = 6.6 Hz, CH_2), 3.40 (2H, t, *J* = 6.9 Hz, CH_2), 1.85 (2H, apparent *pentet*, *J* = 7.2 Hz, CH_2), 1.66-1.58 (2H, m, CH_2), 1.43-1.28 (12H, m, 6 x CH_2); **δ_C** 138.9, 128.5, 127.8, 127.6, 73.0, 70.6, 34.2, 33.0, 29.9, 29.6, 29.6, 29.5, 28.9, 28.3, 26.3.

Preparation of 3-((10-(benzyloxy)decyl)amino)benzo[1,2,4]triazine 1-oxide (167)

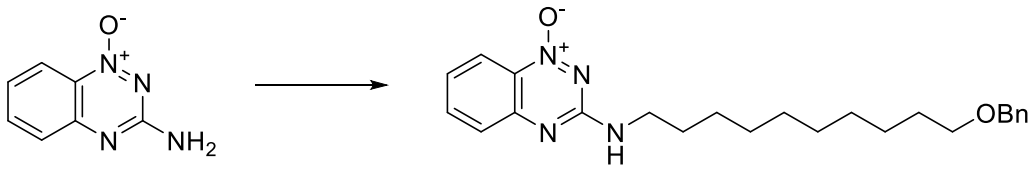

Potassium carbonate (279.0 mg, 2.02 mmol, 1.5 eqv.) was added to a solution of 3-amino-1,2,4-benzotriazine-1-oxide (**77**) (218.0 mg, 1.35 mmol) in anhydrous DMF (15 mL) containing powdered molecular sieves (3 Å, ca 0.2 g) and potassium iodide (30 mg, 0.18 mmol, 0.1 eqv.) Bromide **166** (660.0 mg, 2.02 mmol, 1.5 eqv.) was then added, and the reaction was heated at 120 °C for 20 h. The resulting solution, which changed from yellow to orange in colour, was cooled and filtered, and the solvent was then removed by co-evaporation with toluene to give a crude solid residue. This was purified by column chromatography (40:60 diethyl ether:petroleum ether) to give the product as a bright yellow solid (334 mg, 0.81 mmol, 60 % yield), which was contaminated with impurities.

R_f = 0.29 (40:60 diethyl ether:petroleum ether); **Mp**. 60-63 ˚C; **δ_H** 8.26 (1H, dd, J = 1.1, 8.7 Hz, CH), 7.69 (1H, ddd, J = 1.4, 6.9, 8.5 Hz, CH) 7.59 (1H, b d, J = 8.4 Hz, CH), 7.32-7.35 (5H, m, Ph) 7.25-7.30 (1H, m, CH), 5.19 (1H, b s, NH), 4.50, (2H, s, CH_2), 3.50 (2H, app q, J = 7.0 Hz, CH_2), 3.46 (2H, t, J = 6.6 Hz, CH_2), 1.51-1.75 (4H, m, 2 x CH_2), 1.18-1.41 (12H, m, 6 x CH_2); **δ_C** 159.0, 139.0, 135.8, 129.1, 129.0 128.6, 128.2, 127.9, 127.8, 127.8, ,125.15, 125.1, 120.8, 73.2, 70.8, 30.1, 30.0, 29.8, 29.8, 29.7, 29.7, 29.6, 27.1, 26.5; **ν_{max} (film)** 3307, 2921, 2851, 1716, 1569, 1494, 1464, 1416, 1358, 1274, 1113, 760, 713, 693 cm^{-1}; **LRCIMS** *m/z* 409.3 (100%, ($[M+H]^+$)), 431.2 (75%, ($[M+Na]^+$); **HRCIMS** *m/z* found 409.2598 ($[M+H]^+$) $C_{24}H_{33}N_4O_2$ requires 409.2598.

Attempted Preparation of 3-((10-hydroxydecyl)amino)-1,4-benzo[e][1,2,4]triazin-1-olate (168).

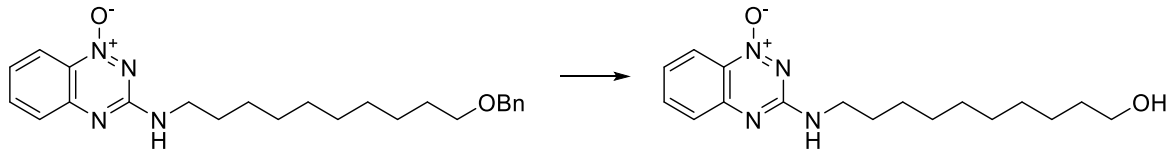

*i) Via hydrogenation of **167***: Palladium on charcoal (5 %, 330.0 mg) was added to 3-((10-(Benzyloxy)decyl)amino)benzo[1,2,4]triazine-1-oxide (**167**) (330.0 mg, 0.81 mmol) dissolved in ethanol (5 mL), and the mixture was stirred under a hydrogen atmosphere. After 30 hrs, TLC (EtOAc) indicated the disappearance of the starting material, and the mixture was filtered through a Celite© pad and evaporated to give a brown gum. This was purified by column chromatography (20-50 % EtOAc: Hexane) to give 3-amino-1,2,4-benzotriazine-1-oxide (**77**) (111 mg, 85 % yield).

*ii) Via HBr mediated debenzylation of **167:*** HBr (33 % in acetic acid, 10 mL) was added to 3-((10-(benzyloxy)decyl)amino)benzo[1,2,4]triazine 1-oxide **167** (169.0 mg, 0.41 mmol), and the mixture was stirred at r.t. for 2 hours, at which point the reaction mixture had turned orange. The reaction mixture was poured into water (50 mL) and extracted with dichloromethane (3 x 100 mL). The organic extracts were then collected, washed with brine (50 mL), dried ($MgSO_4$), filtered and the solvent was removed under reduced pressure to give the crude product (213.0 mg). Analysis by TLC and NMR spectroscopy indicated only the presence of the starting material **167**.

Preparation of 3-(((4-hydroxybutoxy)methyl)amino)benzo[1,2,4]triazine 1-oxide (171)

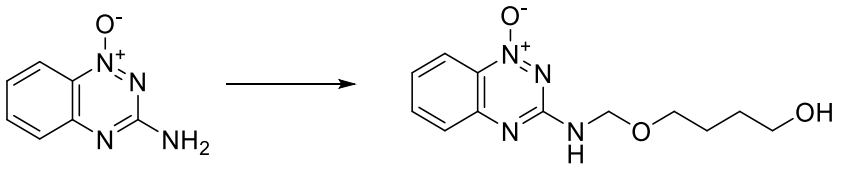

3-Amino-1,2,4-benzotriazine-1-oxide (**77**) (178 mg, 1.10 mmol) and paraformaldehyde (141 mg, 4.7 mmol, 4.2 eqv.) were suspended in butane-1,4-diol (10 mL, 10.2 g, 112.0, 103 eqv.) with gentle warming (~25 ˚C) to keep the mixture fluid. A catalytic quantity of glacial acetic acid (5-10 drops) was added, and the resulting suspension was heated (80 ˚C) for 5 h, by which point all the solid components had dissolved to give a yellow solution. This was cooled to r.t. and poured into water (100 mL) before extracting with chloroform (3 x 100 mL). The combined organic extracts were dried ($MgSO_4$) and the solvent was removed under reduced pressure to give a viscous yellow oil. This crude product was dissolved in a minimum (>5 mL) of chloroform, and diethyl ether was added until the solution clouded, at which point the solution was placed in a freezer for 3 hours. This precipitated a crude yellow solid, which was purified by flash chromatography (60:40 EtOAc:hexane) to give the product as a bright yellow solid (160 mg, 0.60 mmol, 55 % yield).

R_f = 0.31 (60:40 EtOAc:Hexane); **Mp**. 161-165 ˚C; **δ_H** 8.28 (1H, b d, *J* = 8.5 Hz, CH), 7.75 (1H, b t, *J* = 8.1 Hz, CH), 7.68 (1H, b d, *J* = 8.4 Hz, CH), 7.37 (1H, b t, *J* = 7.2 Hz, CH), 6.18 (1H, b t, *J* = 7.2 Hz, NH), 5.07 (2H, d, *J* = 7.2 Hz, CH_2), 3.67 (4H, b t, *J* = 6.0 Hz, 2 x CH_2), 1.93 (1H, b s, OH), 1.75-1.62 (4H, m, 2 x CH_2*);* ***δ_C*** 158.9, 148.8, 136.1, 136.0, 135.9, 126.1, 120.7, 72.5, 68.4, 63.1, 30.0, 26.6*;* **ν_{max} (film)** 3432, 3295, 2923, 2853, 1561, 1459, 1419, 1327, 1328, 919 cm^{-1}; **LRCIMS** *m/z* 287.1 (100 %, ($[M+Na]^+$)), 461.2 (30 %), 551.2 (40 %, ($[2M+Na]^+$)); **HRCIMS** *m/z* found 287.1109 ($[M+Na]^+$), $C_{12}H_{16}N_4O_3Na$ requires 287.1109.

Preparation of 3-(((4-((3-methyl-3-(2,4,5-trimethyl-3,6-dioxocyclohexa-1,4-dien-1-yl)butanoyl)oxy)butoxy)methyl)amino)benzo[e][1,2,4]triazine 1-oxide (172)

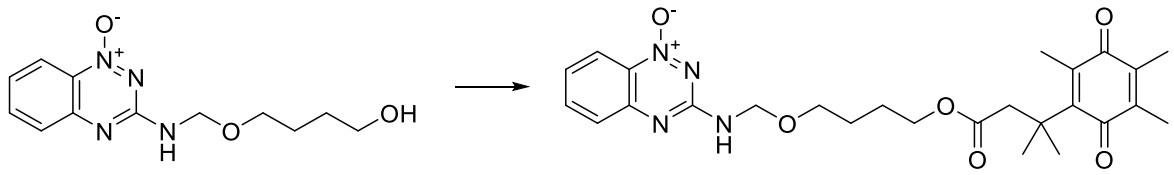

Quinone acid **52** (600 mg, 2.40 mmol, 2 eq.) was stirred with DCC (247.6 mg, 1.20 mmol, 1 eqv.) and DMAP (1.47 g, 12 mmol, 10 eqv.) in THF (30 mL) for 45 minutes. Triazine **171** (317 mg, 1.20 mmol) was then added, and the mixture was stirred for 48 h. On completion (TLC), the reaction mixture was filtered and the solvent was removed under reduced pressure. The crude residue was then dissolved in a minimum volume of EtOAc, cooled (0 ˚C) and filtered to remove precipitated DCU. This process was repeated twice more, and after evaporation of the remaining solvent, the crude product was purified by flash chromatography on triethylamine-deactivated silica (40:60 diethyl ether:hexane). This gave **172** as an unstable bright yellow oil (232 mg, 0.47 mmol, 39 % yield), which was contaminated with DCCU.

R_f = 0.32 (40:60 diethyl ether:hexane); $\boldsymbol{\delta_H}$ (DMSO) 8.27 (1H, dd, *J* = 0.7, 8.6 Hz, CH), 7.86 (1H, dt, *J* = 1.2, 7.1 Hz, CH), 7.68 (1H, b d, *J* = 9.6 Hz, CH), 7.47 (1H, dt, *J* = 1.0, 7.3 Hz, CH), 7.03 (1H, b t, NH), 5.01 (2H, b d, *J* = 7.0 Hz, CH_2), 4.01 (2H, t, *J* = 6.0 Hz, CH_2), 3.61 (2H, t, 5.9 Hz, CH_2) 2.95 (2H, s, CH_2), 2.15 (3H, s, Me), 1.99 (3H, s, Me), 1.98 (3H, s, Me), 1.68-1.62 (4H, m, 2 x CH_2), 1.46 (6H. s, 2 x Me); $\boldsymbol{\nu_{max}}$ **(film)** 3329, 2958, 2872, 1793, 1714, 1242 cm^{-1}; **LRCIMS** *m*/*z* 497.2 (100 %, ($[M+H]^+$)); **HRCIMS** *m*/*z* found 497.2388 ($[M+H]^+$), for $C_{26}H_{33}N_4O_6$ requires 497.2395.

Preparation of 3-(((4-(propionyloxy)butoxy)methyl)amino)benzo[1,2,4]triazine 1-oxide (173)

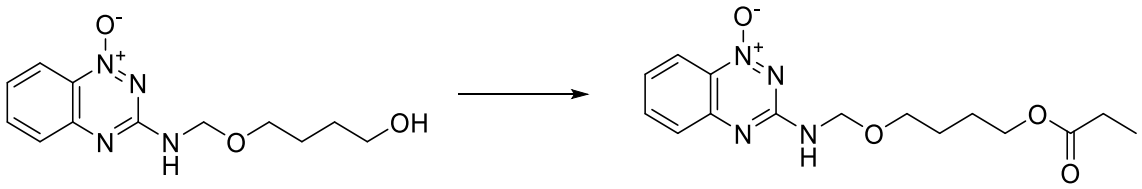

Propionic acid (29.0 mg, 0.38 mmol, 2.0 eq.) was stirred with DCC (37.0 mg, 0.18 mmol, 1.0 eqv.) and DMAP (220.0 mg, 1.8 mmol, 10 eqv.) in anhydrous THF (10 mL) under a positive argon atmosphere for 30 minutes. Triazine **171** (50.0 mg, 0.18 mmol) was then added, and the reaction mixture was stirred for 48 hours and monitored by TLC (60:40 EtOAc:hexane, starting material R_f = 0.31). On completion, the mixture was filtered through a sinter, then poured into water (100 mL). The aqueous mixture was then extracted with diethyl ether (3 x 20 mL), and the organic extracts were dried, filtered, and the solvent was removed by rotary evaporation. The crude product was then purified by column chromatography (30:70 EtOAc:hexane) to give the product as a bright yellow oil which solidified on standing (35.0 mg, 0.11 mmol, 60 % yield).

R_f = 0.33 (30:70 EtOAc:hexane); **Mp**. 75-78 ˚C; **δ_H** (CD_3CN) 8.21 (1H, dd, *J* = 1.2, 8.6, Hz, CH), 7.79 (1H, ddd, *J* = 1.2, 7.0, 8.4 Hz, CH), 7.62 (1H, b d, *J* = 8.4 Hz, CH), 7.40 (1H, ddd, *J* = 1.2, 7.0, 8.6 Hz, CH), 6.84 (1H, t, NH), 4.86 (2H, d, *J* = 7.1 Hz, CH_2), 4.02 (2H, t, *J* = 6.4 Hz, CH_2), 3.56 (2H, t, 6.0 Hz, CH_2) 2.19 (2H, q, 7.5 Hz, CH_2), 1.67-1.55 (4H, m, 2 x CH_2), 1.03 (3H, t, *J* = 7.5 Hz, Me); **δ_C** (CD_3CN) 175.1, 160.0, 149.4, 136.7, 132.4, 127.5, 126.5, 120.9, 72.5, 68.2, 64.7, 28.0, 26.9, 26.3, 9.4; **ν_{max} (film)** 3307, 3092, 3072, 2977, 2925, 2872, 1728, 1567, 1558, 1497, 1417, 1361, 1328, 1201, 1120, 1112, 1080, 764, 675, 653 cm^{-1}; **LRCIMS** m/z 175.1 (100 %), 321.2 (55 %, $[M+H]^+$), 343.1 (90 %, $[M+Na]^+$); **HRCIMS** m/z found 321.1561 ($[M+H]^+$), $C_{15}H_{21}N_4O_4$ requires 321.1557.

Preparation of 3-((((5-hydroxypentyl)oxy)methyl)amino)benzo[1,2,4]triazine 1-oxide (175)

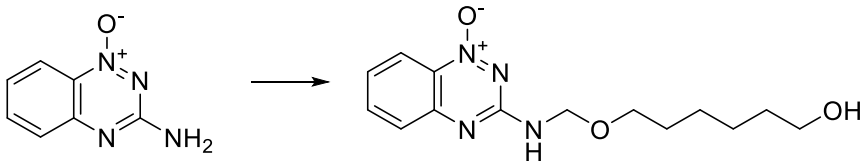

A mixture of 3-amino-1,2,4-benzotriazine-1-oxide (**77**) (500 mg, 3.09 mmol), paraformaldehyde (435 mg, 14.5 mmol, 4.7 eqv), and hexane-1,6-diol (16.0 g, 135.4 mmol, 44.0 eqv) was heated with stirring at 60 ˚C until the diol melted and a yellow suspension formed. A catalytic amount of glacial acetic acid (5-10 drops) was then added, and the mixture was heated (85 ˚C) for 16 h. The resulting yellow solution was poured into water (150 mL) and extracted with chloroform (4 x 50 mL). The combined organic extracts were dried ($MgSO_4$) and the solvent was removed under reduced pressure to give a viscous yellow oil. This was purified by repeated column chromatography (20:80 EtOAc:hexane), to give **175** as a bright yellow solid (138 mg, 0.47 mmol, 15 % yield) which contained trace amounts (ca. 5-10%) of hexane-1,6-diol.

R_f = 0.29 (20:80 EtOAc:hexane); **Mp**. 76-78 ˚C; **δ_H** 8.23 (1H, b d, *J* = 8.0 Hz, CH), 7.70 (1H, ddd, *J* = 1.2, 7.2, 8.0 Hz, CH), 7.64 (1H, b d, 8.1 Hz, CH), 7.32 (1H, ddd, *J* = 1.2, 7.1, 8.3 Hz, CH), 6.68 (1H, b t, *J* = 7.1 Hz, NH), 5.04 (2H, d, *J* = 7.1 Hz, CH_2), 3.62-3.50 (4H, m, 2 x CH_2), 2.07 (1H, b s, OH), 1.61-1.47 (4H, m, 2 x CH_2), 1.40-1.24 (4H, m, 2 x CH_2); **δ_C** 158.8, 148.7, 135.8, 127.1, 126.0, 120.5, 72.4, 68.5, 63.1, 32.8, 29.7, 26.0, 25.7, 1 x quaternary not observed; **ν_{max} (film)** 3308, 2931, 2859, 1722, 1560, 1495, 1418, 1356, 1319, 1241, 1069, 760 cm^{-1}; **LRCIMS** *m*/*z* 175.1 (100 %), 293.2 (75 %, ($[M+H]^+$)); **HRCIMS** *m*/*z* found 293.1611 ($[M+H]^+$), $C_{14}H_{21}N_4O_3$ requires 293.1608.

Preparation of 3-((((6-((3-methyl-3-(2,4,5-trimethyl-3,6-dioxocyclohexa-1,4-dien-1-yl)butanoyl)oxy)hexyl)oxy)methyl)amino)benzo[e][1,2,4]triazine 1-oxide (176)

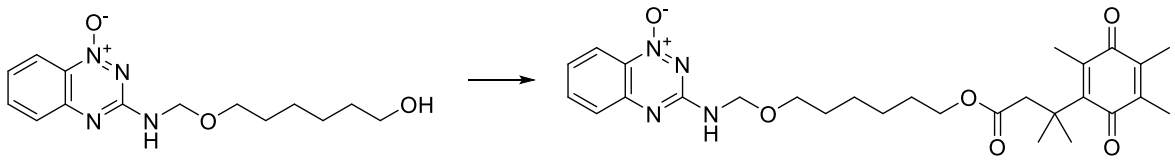

Quinone acid **52** (112.5 mg, 0.45 mmol, 2 eq.) was stirred with DCC (45.9 mg, 0.22 mmol, 1.0 eqv.) and DMAP (268.4 g, 2.2 mmol, 10 eqv.) in THF (10 mL) under a positive argon atmosphere for 45 minutes. Triazine **175** (112.5 mg, 0.45 mmol, 2.0 eqv.) was then added and the reaction mixture stirred for 48 hours. On completion (TLC), the reaction mixture was filtered and the solvent was removed under reduced pressure. The crude reaction residue was then dissolved in a minimum volume of EtOAc, cooled (0 ˚C) and filtered to remove precipitated DCU. This process was repeated twice more. After evaporation of the solvent, the crude product was then purified by flash chromatography on triethylamine-deactivated silica (40:60 diethyl ether:hexane) to give the product as an unstable yellow oil (64.0 mg, 0.12 mmol, 27 % yield), which was contaminated with DCU.

R_f = 0.35 (40:60 diethyl ether:hexane); **δ_H** 8.18 (1H, dd, *J* = 1.4, 8.5 Hz, CH), 7.77 (1H, ddd, *J* = 1.4, 7.0, 8.5 Hz, CH), 7.59 (1H, b d, *J* = 8.5 Hz, CH), 7.38 (1H, ddd, *J* = 1.1, 7.0, 8.5 Hz, CH), 6.89 (1H, b t, *J* = 7.0 Hz, 1H, NH), 4.90 (2H, d, *J* = 7.0 Hz, CH_2), 3.88 (2H, t, *J* = 6.5 Hz, CH_2), 3.50 (2H, t, *J* = 6.6 Hz, CH_2), 2.86 (2H, s, CH_2), 2.07 (3H, s, Me), 1.89 (3H, s, 2 x Me), 1.40-1.55 (4H, m, 2 x CH_2) 1.38 (6H, s, 2 x Me), 1.18-1.30 (4H, m, 2 x CH_2); **δ_C** 191.7, 188.2, 173.2, 160.0, 153.6, 149.4, 143.9, 139.6, 139.6, 139.1, 136.7, 127.5, 126.6, 121.0, 72.6, 68.6, 65.0, 48.4, 39.0, 30.3, 29.3, 29.1, 29.0, 26.5, 26.4, 14.5, 12.8, 12.2; **ν_{max} (film)** 3369, 2935, 1794, 1717, 1555, 1493, 1464, 1419, 1358, 1240, 766 cm^{-1}; Mass data not obtained due to instability.

Preparation of 3-((butoxymethyl)amino)benzo[1,2,4]triazine-1,4-dioxide (177)

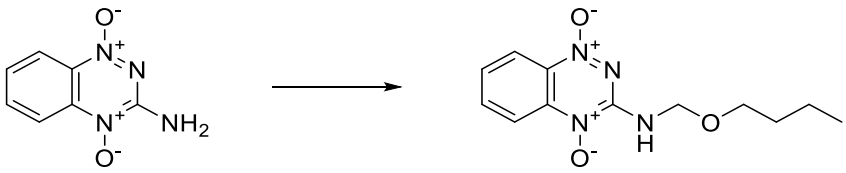

Tirapazamine (**38**) (100.0 mg, 0.56 mmol) and paraformaldehyde (71.0 mg, 2.4 mmol, 4.2 eqv.) were suspended in *n*-butanol (5 mL). Glacial acetic acid (1 mL) was then added and the suspension was heated at 80 ˚C for 5 h, by which point all the solid components had dissolved to give a red solution. After cooling to r.t., the reaction mixture was poured into water (100 mL), extracted with chloroform (3 x 100 mL) and the organic extracts dried ($MgSO_4$). The solvent was removed by rotary evaporation to give a crude red solid. Purification by flash chromatography (75:25 EtOAc;dichloromethane) gave the product as a bright red solid (93.0 mg, 0.35 mmol) in 63 % yield. Data was in accordance with the literature.[89]

R_f = 0.21 (50:50 EtOAc:dichloromethane); **Mp**. 154-156 ˚C (lit.[89] 158-160 ˚C); $\boldsymbol{\delta_H}$ 8.36 (2H, m, 2 x CH), 7.91 (1H, t, *J* = 7.2 Hz, CH), 7.72 (1H, b s, CH), 7.58 (1H, t, *J* = 8.0 Hz, CH), 5.10 (2H, d, *J* = 5.6 Hz, CH_2), 3.58 (2H, t, *J* = 6.6 Hz, CH_2), 1.57 (2H, m, CH_2), 1.36 (2H, m, CH_2), 0.90 (3H, t, *J* = 7.4 Hz, CH_3); $\boldsymbol{\delta_C}$ 149.8, 138.4, 135.9, 131.3, 127.9, 121.7, 117.8, 72.0, 68.7, 31.6, 19.3, 13.9; **LRCIMS** *m*/*z* 191 (90 %), 265.1 (100 %, $[M+H]^+$), 287.1 (65 %, $[M+Na]^+$), 529.3 (30 %, $[2M+H]^+$), 551.2 (40 %, $[2M+Na]^+$); **HRCIMS** *m*/*z* found 265.1297, ($[M+H]^+$), $C_{12}H_{17}N_4O_3$ requires 265.1295.

Preparation of monalidine A hydrochloride (186)[116]

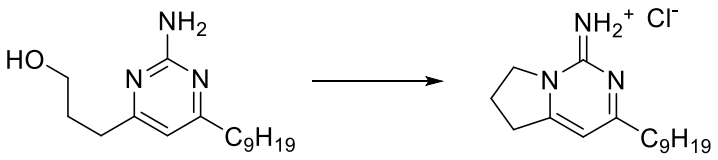

A solution of **269** (905.0 mg, 3.24 mmol) in anhydrous dichloromethane (80 mL) was cooled to -18˚C, and triphenylphosphine (1.96 g, 7.47 mmol, 2.31 eqv.), imidazole (823.0 mg, 12.09 mmol, 3.73 eqv.) and iodine (820.0 mg, 3.23 mmol, 1.00 eqv.) were added sequentially. The reaction was stirred to r.t over 6 h. On completion, flash silica (7.0 g) was added and the solvent was removed under reduced pressure to give a free flowing solid, which was loaded onto a flash column. The column was eluted with ethyl acetate until the triphenylphosphine oxide by-product had been eluted, and then with 15:85 MeOH:EtOAc. The product-containing fractions were evaporated, dissolved in chloroform (50 mL) and washed with aqueous HCl (1M, 2 x 10 mL), and the organic phase was dried ($MgSO_4$). The solvent was then removed to give **186** (652 mg, 2.18 mmol, 68 % yield) as an amorphous yellow gum.

R_f = 0.33 (15:85 MeOH:chloroform); **δ_H** (DMSO-d_6) δ 8.96 (1H, s, NH), 8.45 (1H, s, NH), 7.03 (1H, s, CH), 4.16 (2H, t, J = 7.5 Hz, CH_2), 3.21 (2H, t, J = 7.9 Hz, CH_2), 2.67 (2H, t, J = 7.1 Hz, CH_2), 2.26 (2H, *apparent pentet*, J = 7.7 Hz, CH_2), 1.63 (2H, *apparent pentet*, J = 7.3 Hz, CH_2), 1.15-1.36 (12H, m, 6 x CH_2), 0.84 (3H, t, J = 6.8 Hz, CH_3); **δ_C** (DMSO-d_6) δ 179.5, 164.8, 154.9, 107.0, 80.1, 59.6, 38.3, 32.2, 32,1, 29.8, 29.7, 29.4, 28.5, 23.0, 20.9, 14.9; **ν_{max} (film)** 3469 (NH), 3402 (NH) and 3307 (NH), 2957 (CH), 2730 (aromatic CH), 1662, 1579 cm^{-1}; **LRCIMS** *m*/*z* 262.2 (100 %, $[M+H]^+$); **HRCIMS** *m*/*z* found 262.2271 ($[M+H]^+$), $C_{16}H_{28}N_3$ requires 262.2278.

Attempted synthesis of arbusculidine A (187)

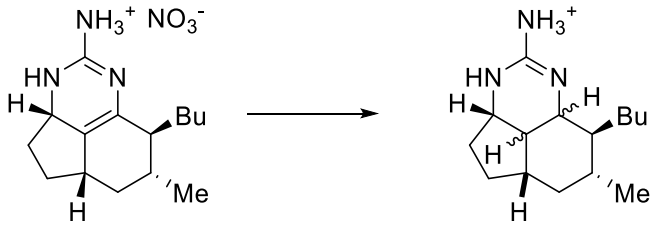

*Attempted synthesis from ±7-epineoptilocaulin nitrate (**216**) with manganese dioxide on charcoal: preparation of **187**.* Crude **216** (36.0 mg, ca. 0.144 mmol) was dissolved in anhydrous dichloromethane (5 mL) and placed in a Carius tube. Activated manganese dioxide on charcoal (750 mg, 1.55 mmol, 10.7 eqv.) was then added, and the tube was sealed and heated (55 ˚C) with stirring for 48 h. The reaction was cooled and then filtered through a pad of Celite©, and the solvent was removed under reduced pressure to give a brown semi-solid (7.0 mg), which from mass spectrometry appeared to be the reduced compound **275** (For a full discussion of MS data please see the discussion section (page 105). **HRMS** m/z 250.2279 (100%, $[M+H]^+$), $C_{15}H_{28}N_3^+$ requires 250.2278.

Attempted synthesis with palladium trifluoroacetate and molecular oxygen: Crude **216** (92.0 mg, 0.3 mmol) was dissolved in acetone (5 mL) and palladium trifluoroacetate (5 mg, 0.015 mmol, 0.05 eqv.) was added. The reaction mixture was degassed under vacuum/N_2 over three cycles. On the final cycle oxygen gas was added and the mixture was stirred for 16 hrs. Evaporation gave a crude product (124.0 mg) as an orange gum. Analysis by NMR spectroscopy indicated largely unchanged starting material.

Attempted oxidation using IBX: Crude **216** (10.0 mg, 0.032 mmol) was dissolved in anhydrous acetonitrile (2 mL) under an argon atmosphere. IBX (44.1 mg, 0.194 mmol, 6.0 eqv.) was then added and the reaction was stirred in the dark at r.t. for 20 h. The reaction was then heated under reflux for a further 20 h. The reaction mixture was filtered and diluted with dichloromethane (50 mL), after which it was washed with water (2 x 20 mL) and saturated sodium carbonate solution (20 mL). The combined aqueous fractions were then back extracted with dichloromethane (3 x 20 mL), and the combined organic fractions were dried ($MgSO_4$) and the solvent was removed under reduced pressure to give a brown semi-solid (70 mg). Attempted purification by precipitation/filtration in chloroform was unsuccessful. Analysis by high resolution mass spectrometry indicated the presence of the starting material at m/z 248.2125 ($[M+H]^+$) with $C_{15}H_{26}N_3^+$ requiring 248.2121 Daltons as well as other masses at 246.1969 ($[M+H]^+$) $C_{15}H_{24}N_3^+$ requiring 246.1966 for mirabilin B

220 and 250.2281 ($[M+H]^+$) $C_{15}H_{28}N_3^+$ requiring 250.2278 for **275**. (For a full discussion of MS date please see the discussion section (page 106)).

Putative synthesis of arbusculidine A (187) from imine 237.

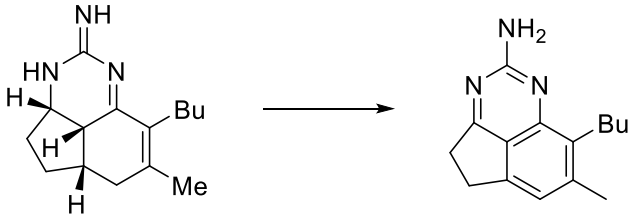

i) With 6 eqv. activated MnO_2: A solution of crude imine **237** (61.0 mg, 0.30 mmol) dissolved in methanol was transferred to a Carius tube and the methanol was removed under vacuum. Once evaporated to dryness, dichloromethane (5 mL) was added together with activated manganese dioxide (170.0 mg, 1.02 mmol, 6.5 eqv.), and the tube was sealed and heated (55 ˚C) for 4 days. After cooling, the mixture was filtered through Celite©, washed with chloroform and the solvent was removed to give a brown gum (23.8 mg). Attempts at purification by silica gel chromatography were unsuccessful, leading to a complex mixture of products.

HRCIMS *m/z* for **187**, found 242.1656 ($[M+H]^+$), $C_{16}H_{28}N_3^+$ equires 242.1652. Other ions were present at 244.1811 (**277**), 246.1967 (**278**) and 248.2124 (**279**) Daltons. (For a full discussion of MS date please see the discussion section).

ii) With 8 eqv. activated MnO_2: A solution of crude imine **237** (385.0, 1.10 mmol) dissolved in methanol was transferred to a Carius tube and the methanol was removed under vacuum. Once evaporated to dryness, dichloromethane (6 mL) was added together with activated manganese dioxide (765.6 mg, 8.80 mmol, 8 eqv.) and the tube was sealed and heated (55 ˚C) for 7 days. After cooling, the mixture was filtered through Celite©, washed with chloroform and the solvent was removed to give a crude sample of **187** as a brown gum (319.4 mg). Washing of the Celite© with methanol gave a further sample (1.230 g) which also contained **187**. These samples await purification.

HRCIMS *m/z* found 242.1656 ($[M+H]^+$), $C_{16}H_{28}N_3^+$ requires 242.1652. Other ions were present at 244.1811 (**277**), 246.1967 (**278**) and 248.2124 (**279**) Daltons. (For a full discussion of MS date please see the discussion section).

Preparation of (±)-epineoptilocaulin nitrate (216)[123]

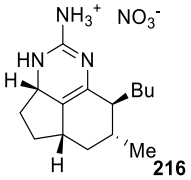

216

Chemical Formula: $C_{15}H_{26}N_3^+$
Exact Mass: 248.2121

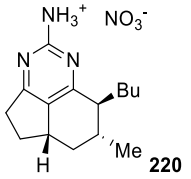

220

Chemical Formula: $C_{15}H_{24}N_3^+$
Exact Mass: 246.1965

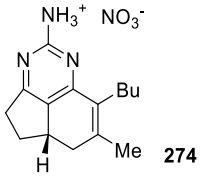

274

Chemical Formula: $C_{15}H_{22}N_3^+$
Exact Mass: 244.18

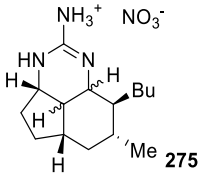

275

Chemical Formula: $C_{15}H_{28}N_3^+$
Exact Mass: 250.2278

A 0.18 M solution of guanidine in methanol was prepared by adding guanidine hydrochloride (86.0 mg, 0.90 mmol) to a solution of sodium methoxide (which was prepared by adding sodium (21 mg, 0.90 mmol) to anhydrous methanol (5.0 mL) under nitrogen). Guanidine in methanol (0.18 M, 2.5 mL, 0.45 mmol) was transferred to a re-sealable tube containing the indenone **249** (41.0 mg, 0.20 mmol) in anhydrous methanol (2.5 mL) under nitrogen. The tube was then flushed with nitrogen, sealed and heated at 85 ˚C for 24 h. The mixture was then cooled to r.t. and quenched with nitric acid HNO_3 (1%, w/v, 3.0 mL) and diluted with chloroform (20 mL). The organic layer was separated and the aqueous layer was extracted with chloroform (2 x 30 mL) to give an oil (63.6 mg). Attempted purification *via* flash chromatography (3-5% MeOH in $CHCl_3$) gave a complex mixture of products. The reaction was repeated a further 3 times at the same scale and the products obtained were combined to give 103.0 mg of crude material, which was used in the further reactions. Although analysis of the ^{1}H NMR spectrum gave a complex spectrum, analysis of the ^{13}C spectrum gave signals as δ_c 154.7, 126.4, 119.4 ppm, which are indicative of (±)7-epineoptilocaulin nitrate **216**, as well as signals at 157.8/153.6, 126.4/123.2 and 121.2/118.2 ppm, which indicate the presence of either isomeric compounds or oxidised analogues of **216**. Analysis by high resolution mass spectrometry indicated the presence of the desired compound with a m/z found at 248.2122 ($[M+H]^+$) with $C_{15}H_{26}N_3^+$ requiring 248.2121 Daltons. Other masses at 246.1966 ($[M+H]^+$) corresponding to $C_{15}H_{24}N_3$ requiring 246.1966 Daltons and at 244.1810 ($[M+H]^+$) corresponding to with $C_{15}H_{22}N_3$ requiring 244.1810 Daltons are evident of the oxidised species mirabilin B (**220**) and **274**. A mass at 250.2278 ($[M+H]^+$) corresponding to $C_{15}H_{28}N_3$ requiring 250.2278 Daltons corresponds to the reduced compound **275**. (For a full discussion of MS date please see the discussion section).

Preparation of intermediate imine 237

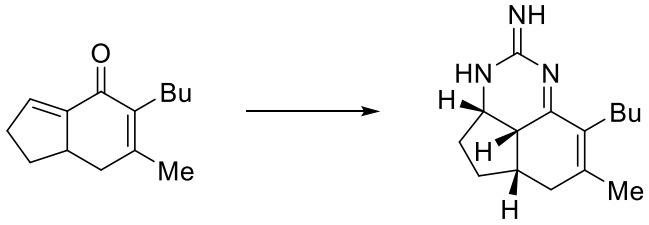

Small scale: A 0.36 M solution of guanidine in MeOH was prepared by adding guanidinium hydrochloride (170.0 mg, 1.8 mmol) to a solution of NaOMe in MeOH (prepared by reacting Na (42 mg, 1.8 mmol) with anhydrous MeOH (5.0 mL)). A portion of this solution of guanidine in MeOH (0.36 M, 0.84 mL, 0.30 mmol) was transferred to a Carius tube containing indenone **261** (35.0 mg, 0.17 mmol) dissolved in methanol (2.5 mL). The tube was sealed and heated (85 °C) for 24 hrs after which the mixture was cooled and the solvent was removed under reduced pressure to give crude **237** as a sticky brown oil (61.0 mg), which was used in the following step without further purification. Analysis by MS indicated the formation of 4 species at m/z 242.1653 ($[M+H]^+$) with $C_{15}H_{20}N_3^+$ requiring 242.1652 **187** (arbusculadine A), m/z 244.1809 ($[M+H]^+$) with $C_{15}H_{22}N_3^+$ requiring 244.1808 **277**, m/z 246.1966 ($[M+H]^+$) with $C_{15}H_{24}N_3^+$ requiring 246.1965 **278**, m/z 248.2122 ($[M+H]^+$) with $C_{15}H_{26}N_3^+$ requiring 248.2121 **279**. (For a full discussion of MS date please see the discussion section).

Large Scale: A 2.30 M solution of guanidine in MeOH was prepared by adding guanidinium hydrochloride (1.10 g, 11.5 mmol) to a solution of NaOMe in MeOH (prepared by reacting Na (271.2 mg, 11.8 mmol) with anhydrous MeOH (5.0 mL)). A portion of this solution of guanidine in MeOH (2.30 M, 0.84 mL, 1.93 mmol) was transferred to a Carius tube containing indenone **261** (226.0 mg, 1.11 mmol) dissolved in methanol (2.5 mL). The tube was sealed and heated (85 °C) for 24 hrs after which the mixture was cooled and the solvent was removed under reduced pressure to give crude **237** as a sticky brown oil (385.0 mg) which was used in the following step without further purification. Analysis by MS gave a near identical spectrum to the small scale reaction. (For a full discussion of MS date please see the discussion section).

Preparation of 5-butyl-6-methyl-1,2,5,6,7,7-hexahydro-4H-inden-4-one (249)[123]

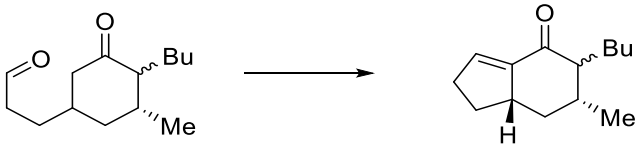

3-(4-Butyl-3-methyl-5-oxocyclohexyl) propanal (**257**) (1.19 g, 5.3 mmol) was dissolved in DME (13 mL) in a microwave reaction vial and then aqueous HCl (6M, 2.16 mL) was added. The mixture was then irradiated in a microwave reaction at 55 ˚C for 10 minutes. After cooling to r.t., the reaction mixture was poured into $NaHCO_3$ solution (aqueous 5 %, 52 mL) and extracted with diethyl ether (300 mL). The organic phase was washed with brine (250 mL), dried ($MgSO_4$) and the solvent removed under reduced pressure to give a crude yellow oil. The crude product was purified by flash chromatography (10:90 EtOAc:hexane) to give **249** as a colourless oil (807 mg, 3.9 mmol, 74 % yield) as a 3:2 mixture of isomers. ^{1}H data was in agreement with the literature.

R_f 0.28 (10:90 EtOAc:petroleum ether); **δ_H** 6.49 (1H, *apparent quartet*, *J* = 2,7 Hz, CH), 2.84-2.97 (2H, m, 2 x CH), 2.31-2.45 (1H, m, CH), 2.09-2.30 (2H, m, 2 x CH), 1.79-2.08 (4H, m, 2 x CH_2), 1.42-1.75 (3H, m, CH, CH_2), 1.16-1.38 (3H, m, CH, CH_2), 0.97 (3H, d, *J* = 6.8 Hz, Me; minor isomer at 0.95, d, *J* = 6.8 Hz, Me), 0.89 (3H, t, *J* = 7.0 Hz, Me; minor isomer 0.87, t, J = 7.0 Hz).

Preparation of *tert*-Butyl 3-oxooctanoate (253)[142]

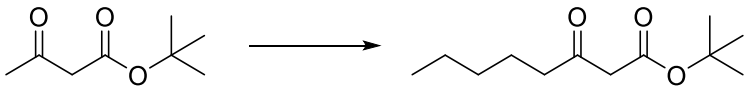

Sodium hydride (60 % dispersion in mineral oil, 1.53 g, 38.4 mmol, 1.2 eqv.) was suspended in anhydrous THF (200 mL) and cooled (0 ˚C). To this mixture, *t*-butyl 3-oxobutanoate (5.24 mL, 5.08 g, 32.0 mmol) was added drop wise and the reaction mixture stirred at 0 ˚C for 10 minutes. A solution of *n*-BuLi (2.5 M in hexane, 14.08 mL, 35.2 mmol, 1.1 eqv.) was then added drop wise to the reaction mixture, which was stirred at 0 ˚C for 30 minutes. Then 1-iodobutane (4.7 mL, 7.66 g, 41.6 mmol, 1.3 eqv.) was added and the reaction mixture was warmed to r.t. over 6 h. After cooling (0 ˚C), ammonium chloride solution (saturated, 200 mL) was added carefully. The reaction mixture was then extracted with diethyl ether (3 x 200 mL), and the combined organic extracts dried ($MgSO_4$) and the solvent was removed under reduced pressure to give the crude product as a yellow oil. Purification by column chromatography (10:90 EtOAc:hexane) gave **253** as a colourless oil (4.48 g**,** 21 mmol, 65 % yield). Data were in agreement with the literature.

δ_H 3.33 (2H, s, CH_2), 2.51 (2H, *t*, *J* = 7.4 Hz, CH_2), 1.11-1.63 (2H, m, CH_2), 1.47 (9H, s, 3 x Me), 1.21-1.36 (4H, m, 2 x CH_2), 0.89 (3H, t, *J* = 7.0 Hz, Me); **δ_C** 203.7, 166.7, 82.0, 50.8, 43.0, 31.4, 28.1, 23.3, 22.6, 14.0.

Preparation of (*Z*)-2-butyl-5-(hex-3-en-1-yl)cyclohex-2-en-1-one (254)[123]

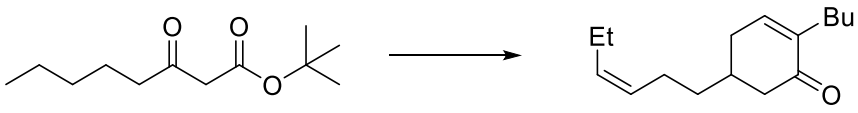

Potassium *t*-butoxide (100.0 mg, 0.89 mmol, 0.05 eqv.) was added to a cooled (0 ˚C) stirred solution of *t*-butyl 3-oxooctanoate (3.77 g, 17.59 mmol) and (*E*,*Z*)-2,6-nonadienal (2.57 g, 18.59 mmol, 1.0 eqv.) in anhydrous *t*-butanol (20 mL). The reaction mixture was stirred for 30 min before adding further potassium *t*-butoxide (400.0 mg, 3.57 mmol, 0.2 eqv.) and heating the mixture at reflux overnight. The reaction mixture was cooled and quenched with aqueous HCl (1 M, 15 mL), then diluted with ether (100 mL) and separated. The organic phase was washed with brine (30 mL), and dried ($MgSO_4$) and the solvent was removed under reduced pressure to give the crude intermediate *t*-butyl 3-butyl-6-(3-(*Z*)-hexenyl)-2-oxocyclohex-3-ene-1-carboxylate as a yellow oil. This ester was dissolved in toluene (40 mL), and *p*-toluenesulfonic acid (685 mg, 3.61 mmol, 0.2 eqv.) was added. The mixture was heated at 80 ˚C overnight. After cooling to r.t., EtOAc (60 mL) was added and the reaction mixture was washed in turn with $NaHCO_3$ (saturated, 20 mL), HCl (1M, aqueous, 15 mL) and brine (15 mL), and then dried ($MgSO_4$). After filtration and evaporation, the crude yellow oil (2.27 g) was purified by flash chromatography (gradient elution, 1:99-2:98 EtOAc:hexane), giving **254** (1.97 g, 8.4 mmol, 48 % yield). Data were in agreement with the literature.

R_f = 0.22 (5:95, EtOAc:petroleum ether); **δ_H** 6.66-6.69 (1H, m, CH), 5.27-5.44 (2H, m, 2 x CH), 2.39-2.61 (2H, m, 2 x CH), 2.15-2.22 (2H, m, CH_2), 1.99-2.14 (7H, m, 3 x CH_2, CH), 1.26-1.46 (6H, m, 3 x CH_2), 0.98 (3H, t, *J* = 7.5 Hz, Me), 0.91 (3H, t, *J* = 7.1 Hz, Me); **δ_C** 199.9, 144.1, 140.0, 132.4, 128.4, 45.0, 35.9, 35.2, 32.7, 30.9, 29.2, 24.2, 22.6, 20.7, 14.5, 14.1.

Preparation of (Z)-2-butyl-5-(hex-3-en-1-yl)-3-methylcyclohex-2-en-1-one (255)[123]

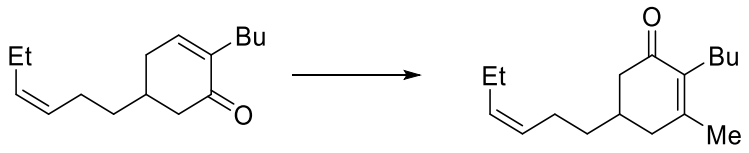

Anhydrous cerium(III) chloride (10 g, 41 mmol, 4.8 eqv.) was stirred in THF (100 mL) for 4 hours under a positive argon atmosphere. The reaction mixture was cooled (-78 ˚C) and a solution of MeLi (1.6 M in diethyl ether, 25.6 mL, 41.0 mmol, 4.3 eqv.) was added drop wise to the suspension. The mixture was stirred for 1.5 h. Ketone **254** (1.97 g, 8.39 mmol) dissolved in THF (5 mL) was then added over 5 min and the reaction mixture was stirred for 45 minutes. Acetic acid (aqueous 10%, 50 mL) was added and the mixture was warmed to r.t and diluted with diethyl ether (200 mL). The organic layer was separated and washed sequentially with brine (70 mL), saturated $NaHCO_3$ solution (50 mL) and further brine (70 mL), and then dried ($MgSO_4$). The solvent was removed under reduced pressure to give crude 2-butyl-5-(3*Z*-hexenyl)-1-methylcyclohex-2-en-1-ol as a yellow oil. This alcohol was dissolved in dichloromethane (100 mL). NaOAc (0.35 g, 4.23 mmol, 0.5 eqv.) and PCC (3.63 g, 16.9 mmol, 2 eqv.) were added, and the mixture was stirred at r.t. for 4 h. The reaction mixture was poured directly onto a flash column and was eluted with 50:50 dichloromethane:hexane to give **255** as a yellow oil (1.13 g, 4.70 mmol, 56 % yield). Data was in agreement with the literature.

δ_H 5.35-5.41 (1H, m, CH), 5.25-5.32 (1H, m, CH), 2.50 (1H, dd, *J* = 1.6, 11.8 Hz CH), 2.23-2.37 (3H, m, CH, CH_2), 1.99-2.13 (7H, m, CH, 3 x CH_2), 1.93 (3H, s, Me), 1.34-1.44 (2H, m, CH_2), 1.21-1.33 (4H, m, 2 x CH_2), 0.96 (3H, t, *J* = 7.5 Hz, Me), 0.89 (3H, t, *J* = 7.1 Hz, Me).

Preparation of 2-butyl-5-(hex-3-en-1-yl)-3-methylcyclohexan-1-one (256)[123]

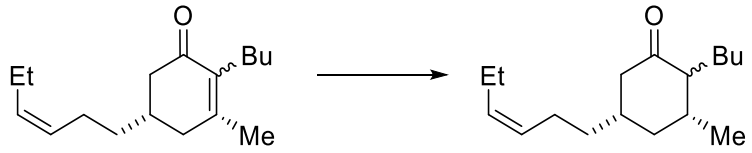

Lithium metal (70 mg, 10.06 mmol, 2.2 eqv.) was added to a cooled (0 ˚C) solution of 2-butyl-5-(hex-3-en-1-yl)-3-methylcyclohex-2-en-1-one (**255**) (1.13 g, 4.57 mmol) in *N*-propylamine (5 mL) and ethylene diamine (0.55 mL, 603 mg, 10.06 mmol, 2.2 eqv.). The reaction mixture was stirred to r.t. over 1.5 h, at which point all the lithium had dissolved and the blue colour had dissipated. The mixture was diluted with water (25 mL) and the aqueous portion was extracted with diethyl ether (3 x 20 mL). The combined organic extracts were then washed with brine (30 mL) and the organic phase dried ($MgSO_4$). The solvent was removed under reduced pressure to give a colourless oil. The crude product was purified by flash chromatography (1:99-2:98, EtOAc:hexane) to give **256** as a colourless oil (618.0 mg, 2.47 mmol, 54 %). Data was in agreement with the literature

R_f = 0.34 (5:95, EtOAc:petroleum ether) **δ_H** 5.33-5.41 (1H, m, CH), 5.23-5.31 (1H, m, CH), 2.40 (1H, ddd, *J* = 2.3, 4.8, 11.7 Hz, CH), 1.83-2.07 (7H, m, 3 x CH_2, CH), 1.11-1.80 (11H, m, 5 x CH_2, CH), 1.06 (3H, d, *J* = 6.4 Hz, Me), 0.96 (3H, t, *J* = 7.6 Hz, Me), 0.89 (3H, t, *J* = 7.1 Hz, CH_2); **LRCIMS** *m/z* 251.2 (100 %, $[M+H]^+$), 501.5 (50 %, $[2M+H]^+$); **HRCIMS** *m/z* found 251.2369 ($[M+H]^+$), $C_{17}H_{31}O$ requires 251.2369.

Preparation of 3-(4-butyl-3-methyl-5-oxocyclohexyl)propanal (257)[123]

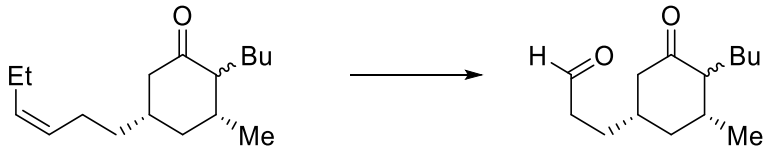

2-Butyl-5-(hex-3-en-1-yl)-3-methylcyclohexan-1-one (**256**) (1.76 g, 7.12 mmol) was dissolved in dichloromethane (100 mL) and cooled (-78˚C), whereupon ozone was bubbled through the solution with stirring until the solution remained light blue. Triphenylphosphine (2.8 g, 10.68 mmol, 1.5 eqv.) was then added and the colourless solution was stirred to r.t. overnight. The solvent was evaporated at below 20 ˚C to give a crude semi-solid residue, which was purified by flash chromatography on triethylamine deactivated silica gel (10:90 EtOAc:hexane) to give **257** (1.19 g, 5.3 mmol, 74 % yield) as a colourless oil in a 5:1 mixture of isomers. Data were in good agreement with the literature.

δ_H 9.78 (1H, t, *J* = 1.4 Hz, CH), 2.47 (2H, dt, *J* = 1.4, 7.4 Hz, CH_2), 2.39 (1H, ddd, *J* = 2.4, 3.4, 12.8 Hz, CH), 1.99 (1H, dt, J = 0.8, 12.7 Hz), 1.83-1.94 (2H, m, 2 x CH), 1.10-1.94 (11 H, m, 5 x CH_2, CH), 1.06 (3H, d, *J* = 6.4 Hz, Me, minor isomer 0.99, d, *J* = 6.7 Hz), 0.88 (3H, t, *J* = 7.0 Hz, Me); **δ_C** 211.0, 201.9, 56.8, 48.3, 41.5, 41.3, 38.0, 37.5, 29.7, 29.0, 25.4, 23.3, 20.9, 14.2.

Preparation of 3-(4-Butyl-3-methyl-5-oxocyclohex-3-en-1-yl)propanal (260)

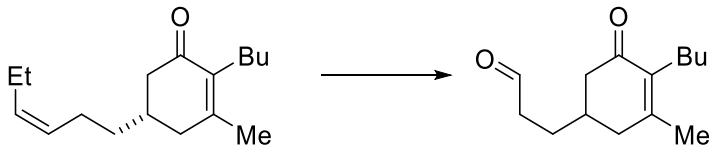

(*Z*)-2-Butyl-5-(hex-3-en-1-yl)-3-methylcyclohex-2-en-1-one (**255**) (790.0 mg, 3.15 mmol) was dissolved in dichloromethane (85 mL) and pyridine (0.85 mL). The solution was cooled (-78 ˚C) and ozone was bubbled for 30 second intervals. After each, the progress of the reaction was monitored by TLC. Once the spot corresponding to **255** appeared to have disappeared, the reaction was quenched with triphenylphosphine (1.24 g, 4.72 mmol, 1.5 eqv.) and the product was stored in a freezer overnight. The solvent was then evaporated under reduced pressure, and the crude residue was purified by flash chromatography on triethylamine -deactivated silica (10:90 EtOAc:hexane), to give **260** as a colourless oil (347.0 mg, 1.56 mmol, 50 % yield), together with recovered **255** (297.0 mg, 1.18 mmol, 38 % yield). Data was in agreement with the literature.

δ_H 9.79 (1H, s), 2.42-2.51 (3H, m, CH_2, CH), 2.22-2.42 (3H, m, CH, CH_2), 1.99-2.17 (3H, m, CH_2, CH), 1.93 (3H, s, Me), 1.59-1.77 (2H, m, CH_2), 1.21-1.33 (4H, m, 2 x CH_2), 0.89 (3H, t, *J* = 7.1 Hz, Me).

Preparation of 5-Butyl-6-methyl-1,2,7,7a-tetrahydro-4H-inden-4-one (257)[123]

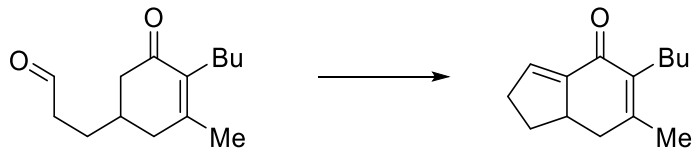

Aldehyde **260** (347 mg, 1.56 mmol) was dissolved in DME (13 mL) in a microwave reaction vial together with aqueous HCl (6 M, 2.16 mL), and the mixture was irradiated in a microwave reactor at 55 ˚C for 10 minutes. After cooling to r.t., the reaction mixture was poured into $NaHCO_3$ solution (aqueous 5 %, 30 mL) and extracted with diethyl ether (200 mL). The organic phase was washed with brine (200 mL), dried ($MgSO_4$) and the solvent removed under reduced pressure to give a crude yellow oil. Purification by flash chromatography on silica gel (10:90 EtOAc:hexane) gave **261** (172 mg, 0.84 mmol, 54 % yield) as an unstable colourless oil. Data was in agreement with the literature.

R_f 0.36 (10:90, EtOAc:petroleum ether); **δ_H** 6.66 (1H, broad apparent q, *J* = 2.6 Hz, CH), 3.00-3.15 (1H, m, CH), 2.14-2.56 (7H, m, 3 x CH_2, CH), 1.96 (3H, s, Me), 1.50-1.60 (1H, m, CH), 1.20-1.36 (4H, m, 2 x CH_2), 0.90 (3H, t, *J* =7.0 Hz, Me); **δ_C** 186.3, 154.1, 142.6, 137.6, 136.5, 42.3, 40.9, 32.4, 32.3, 31.4, 25.3, 23.0, 21.9, 14.2.

Preparation of 1-hydroxypentadecane-4,6-dione (263)

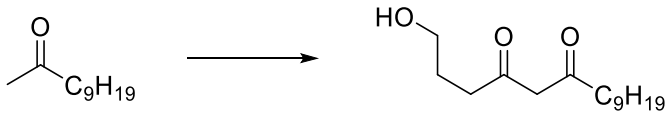

i) *Using ethanol with an ethanolic quench*: Anhydrous ethanol (1.0 mL) was added to a magnetically stirred suspension of sodium hydride (60% dispersion in mineral oil, 4.8 g, 120.0 mmol, 2.40 eqv.) in diethyl ether (200 mL). The resulting suspension was cooled (5 ˚C) and γ-butyrolactone (4.5 g, 4.0 mL, 52.3 mmol, 1.05 eqv.) was added drop wise. The mixture was stirred for 30 minutes. 2-Undecanone (8.5 g, 49.9 mmol) was then added drop wise and stirring continued at r.t. for 48 hours. After complete consumption of undecanone (TLC, R_f = 0.74, 50:50 diethyl ether:petroleum ether), the mixture was cooled (0 ˚C) and the remaining unreacted sodium hydride was destroyed by the cautious addition of ethanol (30 mL) followed by ammonium sulfate solution (aqueous, 10 %, 300 mL). If necessary, the pH of the aqueous layer was adjusted to pH = 6 by the addition of further ammonium sulfate solution, and the organic phase was separated. The aqueous layer was extracted with diethyl ether (3 x 150 mL) and the combined organic extracts were dried ($MgSO_4$). The solvent was removed under reduced pressure to give the crude product as a yellow oil. Purification by silica gel chromatography (75:25 diethyl ether:petroleum ether) gave a waxy solid which was recrystallized (diethyl ether/hexane) to give **268** (0.766 g, 2.99 mmol) in 6 % yield as pale yellow needles.

ii) *Using ethanol with an aqueous quench*: Anhydrous ethanol (1.0 mL) was added to a magnetically stirred suspension of sodium hydride (60% dispersion in mineral oil, 4.8 g, 120.0 mmol, 2.40 eqv.) in diethyl ether (150 mL). The resulting suspension was cooled (5 ˚C) and γ-butyrolactone (4.5 g, 4.0 mL, 52.3 mmol, 1.05 eqv.) was added drop wise. The mixture was stirred for 30 minutes. 2-Undecanone (8.5 g, 49.9 mmol) was then added drop wise and stirring continued at r.t. for 48 hours. After the complete consumption of undecanone (TLC, R_f = 0.74, 50:50 diethyl ether:petroleum ether), the mixture was cooled (0 ˚C) and the remaining unreacted sodium hydride was destroyed by the cautious addition of ammonium sulfate solution (aqueous, 10 %, 300 mL). If necessary, the pH of the aqueous layer was adjusted to pH = 6 by the addition of further ammonium sulfate solution, and the organic phase was separated. Work up as detailed in i) gave **268** (2.55 g, 9.98 mmol, 20 % yield) as pale yellow needles.

Using trifluoroethanol and an aqueous quench: Anhydrous trifluoroethanol (1.0 mL) was added to a stirred suspension of sodium hydride (60% dispersion in mineral oil, 4.8 g, 120.0 mmol, 2.40 eqv.) in anhydrous diethyl ether (200 mL), taking care to vent the pressure as necessary. The resulting suspension was cooled (5 ˚C) and γ-butyrolactone (4.5 g, 4 mL, 52.3 mmol, 1.05 eqv.) was added drop wise. The mixture was stirred for 30 minutes. 2-Undecanone (8.5 g, 49.9 mmol) was then added dropwise and stirring continued at r.t. for 48 h. After the complete consumption of undecanone (TLC, R_f = 0.74, 50:50 diethyl ether:petroleum ether), the mixture was cooled (0˚C) and ammonium sulfate solution (aqueous, 10 %, 300 mL) was cautiously added. If necessary, the pH of the aqueous layer was adjusted to pH = 6 by the addition of further ammonium sulfate solution, and the organic phase was separated. The aqueous layer was extracted with diethyl ether (3 x 150 mL) and the combined organic extracts were dried ($MgSO_4$) and the solvent removed under reduced pressure to give the crude product as a yellow oil. Purification by silica gel chromatography (75:25 diethyl ether:petroleum ether) gave a waxy solid which was recrystallized (diethyl ether/hexane) to give **268** (4.29 g, 16.7 mmol, 34 % yield) as pale yellow needles. This reaction was repeated on the same scale and gave **268** (4.60 g, 17.9 mmol, 36 % yield) as pale yellow needles.

R_f = 0.33 = (75:25 diethyl ether:petroleum ether); **Mp**. 56-57 ºC; **δ_H** (DMSO-d_6) *1:1 mixture of keto/enol forms:* 15.61 (0.5H, s, OH *enol*), 5.68 (0.5H, s, CH *enol*), 4.49 (0.5H, t, *J* = 4.5 Hz, OH), 4.44 (0.5H, t, *J* = 4.5 Hz, OH), 3.66 (1H, s, 0.5 CH_2 *keto*), 3.33-3.42 (2H, m, CH_2), 2.47 (2H, *apparent pentet*, *J* = 7.5, CH_2), 2.32 (1H, t, *J* = 7.4, Hz, 0.5 CH_2), 2.27 (1H, t, *J* = 7.4, Hz, 0.5 CH_2), 1.66 (1H, tt, *J* = 6.4, 7.2 Hz, 0.5 CH_2), 1.59 (1H, *apparent pentet*, *J* = 6.9 Hz, 0.5 CH_2), 1.51 (1H, *apparent pentet*, *J* = 7.2 Hz, 0.5 CH_2), 1.43 (1H, *apparent pentet*, *J* = 7.1 Hz, 0.5 CH_2), 1.17-1.31 (12H, m, 6 x CH_2), 0.85 (t, *J* = 7.0 Hz, 3H, CH_3); **δ_C** *1:1 mixture of keto/enol forms* δ 205.3, 194.6, 193.8, 99.2, 60.0, 59.9, 56.3, 31.3, 31.3, 28.9, 28.8, 28.7, 28.7, 28.6, 28.6, 28.4, 22.1, 13.9; **ν_{max} (KBr)** 3278, 2954, 2932, 2919, 2873, 2849, 1638, 1598 cm^{-1}; **LRCIMS** *m*/*z* 257.2 (23 %, $[M+H]^+$), 239.2 (100 %, $[M+H-H_2O]^+$); **HRCIMS** *m*/*z* found 257.2107 ($[M+H]^+$), $C_{15}H_{29}O_3$ requires 257.2111.

Preparation of 3-(2-amino-6-nonylpyrimidin-4-yl)propan-1-ol (269)

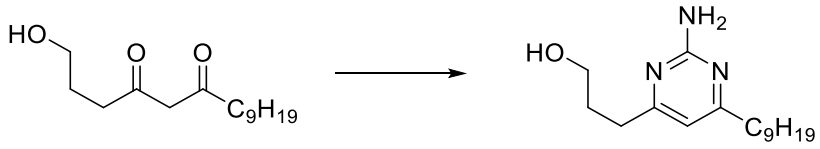

i) Using trifluoroethanol: Guanidine hydrochloride (1.27 g, 13.29 mmol, 1.02 eqv.) was added to a solution of potassium *t*-butoxide (1.47 g, 13.10 mmol, 1.01 eqv.) in anhydrous trifluroethanol (10 mL). The resulting suspension was stirred at r.t. for 30 minutes. Diketone **268** (3.33 g, 13.01 mmol) was then added and stirring continued at r.t. for 48 h. After the complete consumption of 1-hydroxypentadecane-4,6-dione (TLC, R_f = 0.33, 75:25 diethyl ether:petroleum ether), the solvent was removed under reduced pressure to give the crude product as a yellow solid. Purification by silica gel chromatography (10:90 MeOH:EtOAc) gave **269** (905.0 mg, 3.24 mmol, 25 % yield) as an amorphous white solid. This reaction was repeated on an identical scale to give **269** (1.0163 g, 3.64 mmol, 28 % yield).

The process was repeated under different conditions as follows.

ii) Using guanidine hydrochloride: Diketone **268** (287.0 mg, 1.12 mmol) was heated at reflux with guanidine hydrochloride (128.0 mg, 1.35 mmol, 1.20 eqv.) in absolute ethanol (5 mL) for 48 h. From analysis of the ^{1}H NMR spectrum of the crude product, only the formation of the elimination product **271** was apparent.

iii) Using guanidine hydrochloride and triethylamine: Diketone **268** (529.0 mg, 1.95 mmol) was heated at reflux with guanidine hydrochloride (236.0 mg, 2.34 mmol, 1.2 eqv.) in absolute ethanol (5 mL) with triethylamine (0.54 mL, 3.9 mmol, 2 eqv. for 48 h to give **269** (60.0 mg, 0.21 mmol, 11 % yield).

iv) In ethanol: Potassium *t*-butoxide (0.22 g, 1.97 mmol, 1.01 eqv.) was suspended in absolute ethanol (10 mL) and guanidine hydrochloride (0.19 g, 1.97 mmol, 1.01 eqv.) was added. The suspension was stirred at r.t. for 2 hrs. Diketone **268** (500.0 mg, 1.90 mmol) was then added and the mixture was stirred at r.t. for 12 hrs to give **269** (95.4 mg, 0.34 mmol, 18 % yield).

v) In ethanol under reflux: Potassium *t*-butoxide (0.22 g, 1.97 mmol, 1.01 eqv.) was suspended in absolute ethanol (10 mL) and guanidine hydrochloride (0.19 g, 1.97 mmol, 1.01 eqv.) was added. The suspension was stirred at r.t. for 2 hours. Diketone **268** (500 mg,

1.90 mmol) was then added and the mixture was heated at reflux for 12 h to give **269** (116.6 mg, 0.42 mmol, 22 % yield).

R_f = 0.33 (10:90 MeOH:$CHCl_3$); **Mp**. 56-58 °C; **δ_H** 6.38 (1H, s, CH), 5.21 (2H, s, NH_2), 3.68 (2H, t, *J* = 5.9 Hz, CH_2), 2.68 (2H, t, *J* = 7.0 Hz, CH_2), 2.50 (2H, t, *J* = 7.7 Hz, CH_2), 1.91 (2H, *apparent pentet*, *J* = 6.9 Hz, CH_2), 1.63 (2H, *apparent b pentet*, *J* = 7.4 Hz, CH_2), 1.26 (12H, m, 6 x CH_2), 0.86 (2H, t, *J* = 6.8 Hz, CH_3); **δ_C** 172.8, 170.9, 162.7, 109.7, 62.3, 38.0, 34.7, 32.1, 31.1, 29.7, 29.7, 29.5, 29.1, 22.9, 14.3, one quaternary not observed; **ν_{max} (film)** 3470, 3445, 3321, 3174, 2955, 2926, 2919, 2849, 1653, 1639, 1589, 1562 cm^{-1}; **LRCIMS** *m*/*z* 280.2 (100 %, $([M+H]^+)$, 302.2 (10 %, $[M+Na]^+$); **HRCIMS** *m*/*z* found 280.2384 ($[M+H]^+$), $C_{16}H_{30}O_1N_3$ requires 280.2383.

Preparation of 3-(2-imino-6-nonyl-2,3-dihydropyrimidin-4-yl)propyl methanesulfonate (270) and *(*Z)-N-(3-nonyl-6,7-dihydropyrrolo[1,2-c]pyrimidin-1(5H)-ylidene)methanesulfonamide (273).

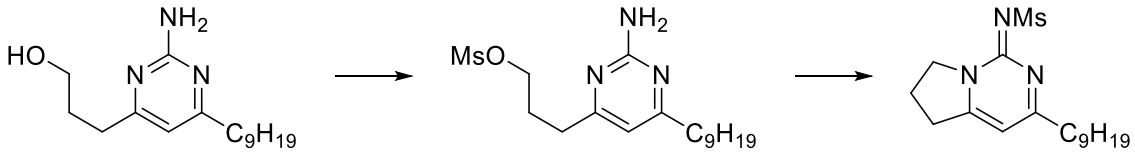

Triethylamine (0.13 mL, 94.0 mg, 0.93 mmol, 3.0 eqv.) was added to a stirred solution of 3-(2-imino-6-nonyl-2,3-dihydropyrimidin-4-yl)propan-1-ol (**269**) (85.3 mg, 0.31 mmol) dissolved in dichloromethane (5 mL), whereupon methanesulfonyl chloride (23.0 μL mL, 0.34 mmol, 1.1 eqv.) was added. After 1 h the reaction was poured through a short (1 cm) pad of silica, which was then eluted with an EtOAc/MeOH mixture (20:1 ca 100 mL). Evaporation of the filtrate under reduced pressure gave **270** as a crude brown semi-solid (31.4 mg) which was used without further purification. The crude **270** (31.4 mg, 0.087 mmol) was dissolved in anhydrous dichloromethane (2 mL) with triethylamine (0.025 mL, 0.18 mmol, 2.0 eqv.), The reaction mixture was then heated in a sealed tube overnight at 80 ˚C. When the reaction was complete, it was cooled to r.t. and the solvent was removed under reduced pressure to give a brown gum. Purification by flash chromatography (10:90 MeOH:EtOAc) gave **273** (11.2 mg, 0.033 mmol, 11 % yield) as a gum, as well as 15 % of recovered starting material **269** (12.6 mg, 0.045 mmol).

R_f = 0.28 (10:90 MeOH:EtOAc); δ_H 6.44 (1H, s), 4.23 (2H, t, *J* = 7.5 Hz), 3.24 (3H, s, Me), 3.15 (2H, t, *J* = 7.7 Hz), 2.70 (2H, t, *J* = 7.7 Hz), 2.26 (2H, *apparent pentet*, *J* = 7.6 Hz, CH_2), 1.72 (2H, *apparent pentet*, *J* = 5.6 Hz, CH_2), 1.13-1.40 (12 H, m, 6 x CH_2), 0.88 (3H, t, *J* = 7.0 Hz); δ_C 178.6, 165.6, 154.2, 103.7, 51.7, 38.9, 32.1, 32.0, 39.8, 29.8, 29.6, 29.5, 29.4, 28.1, 22.8, 20.3, 14.2; **LRCIMS** *m*/*z* 362.2 (100 %, $[M+Na]^+$), 701.4 (15 %, $[2M+Na]^+$); **HRCIMS** *m*/*z* found 362.1872 ($[M+Na]^+$), $C_{17}H_{29}O_2N_3SNa$ requires 362.1873.

8.0 References

1 World Health Organisation, Cancer Factsheet no. 297, 2015.

2 N. J. Harper, *J.Med. Pharm. Chem* 1959, **1**, 467-500.

3 A. Albert, *Nature*, 1958, 421-423.4

4 J. B. Zawilska, J. Wojcieszak and A. B. Olejniczak, *Pharmacol. Reports*, 2013, **65**, 1–14.

5 Y. Shi, S. A. Liu, D. J. Kerwood, J. Goodisman and J. C. Dabrowiak, *J. Inorg. Biochem.*, 2012, **107**, 6–14.

6 B. Testa, *Curr. Opin. Chem. Biol.*, 2009, **13**, 338–344.

7 K. M. Huttunen, H. Raunio and J. Rautio, *Pharmacol. Rev.*, 2011, **63**, 750–771.

8 R. Mahato, W. Tai and K. Cheng, *Adv. Drug Deliv. Rev.*, 2011, **63**, 659–670.

9 M. Miwa, M. Ura, M. Nishida, N. Sawada, T. Ishikawa, K. Mori, N. Shimma, I. Umeda and H. Ishitsuka, *Eur. J. Cancer*, 1998, **34**, 1274–1281.

10 M. F. Belcourt, W. F. Hodnick and S. Rockwellt, 1996, **93**, 456–460.

11 W. A. Denny, *Eur. J. Med. Chem.*, 2001, **36**, 577–595.

12 E. Hatzigrigoriou, M. V. Papadopoulou, D. Shields and W. D. Bloomer, *Oncol. Res.*, 1993, **5**, 29–36.

13 M. Tomasz and Y. Palom, *Pharmacol. Ther.*, 1997, **76**, 73–87.

14 M. F. Belcourt, W. F. Hodnick, S. Rockwell and a. C. Sartorelli, *J. Biol. Chem.*, 1998, **273**, 8875–8881.

15 C. Lee, P. Pfeifer and N. W. Gibson, *Biochemistry*, 1994, **33**, 6024–6030.

16 J. Cummings, V. J. Sapnswick, J. Gardiner, A. Ritchie and J. F. Smyth, *Biochem. Pharmacol.*, 1998, **55**, 253–260.

17 H. L. McLeod, M. A. Graham, S. Aamdal, A. Setanoians, Y. Groot and B. Lund, *Eur. J. Cancer*, 1996, **32A**, 1518–1522.

18 P. Wardman, *Curr. Med. Chem.*, 2001, **8**, 739–761.

19 M. Jaffar, A. V. Patterson and N. J. Howe, in *Proceedings of the Br. Pharm. Soc. Conference, Birmingham*, 2000.

20 A. Passioukov, K. Van, A. Fernandez, J. Abarca-quinones, R. Baurain, T. J. Lobl, C. Oliyai, D. Shochat and V. Dubois, *Cancer Research*, 2001, **61** 2843–2846.

21 W. A. Denny, *The Lancet Oncol.*, 2000, **1**, 25–29.

22 M. P. Hay, G. J. Atwell, W. R. Wilson, S. M. Pullen and W. A. Denny, *J. Med. Chem.*,2003, **46**, 2456–2466.

23 B. Palcic, B. Faddagon and L.D. Skarsgard, *Radiation Research*, 2014, **100**, 340–347

24 A. V Patterson, H. M. Barham, E. C. Chinjel, G. E. Adams, A. L. Harrs and I. J. Stratford, *British Journal of Cancer*, 1995, **72**, 1144-1150.

25 A. Christofferson and J. Wilkie, *Biochem. Soc. Trans.*, 2009, **37**, 413–418.

26 L. H. Patterson and S. R. Mckeown, *British Journal of Cancer,* 2000, **83**, 1589–1593.

27 S. M. Bailey, F. Friedlos, J. A. Hartley, R. J. Knoxt, A. D. Lewis and P. Workman, *British Journal of Cancer,* 1997, **76**, 1596–1603.

28 S. M. Raleigh, E. Wanogho, M. D. Burke, S. R. McKeown and L.H. Patterson, *Int. J. Radiation Oncology. Phys.,* 1998, **42**, 763–767.

29 R. Gallagher, C. M. Hughes, M. M. Murray, O. P. Friery, L. H. Patterson, D. G. Hirst and S. R. Mckeown, *British Journal of Cancer*, 2001, **84**, 625–629.

30 William R. Wilson, Pierre Van Zijl, William A. Denny, *Int. J. Radiat. Oncol. Biol. Phys.*, 1992, **22**, 693–696.

31 D. W. A. Lee H., Wilson W.R., Ferry D.M., van Zijl P., Pullen S.M., *J, Med. Chem.*, 1996, **39**, 2508–2517.

32 H. H. Lee, W. R. Wilson, D. M. Ferry, P. Van Zijl, S. M. Pullen and W. A. Denny, *J. Med. Chem.,* 1996, **39**, 2508–2517.

33 D. W. A. Lee H.H., wilson W.R., *Anti-Cancer Drug Des.*, 1999, **14**, 487–497.

34 J. M. Brown, *Cancer Research,* 1999, **59**, 5863–5870.

35 M. Ángel, M. José, F. J. Martínez-crespo, Y. Sainz, M. Elena, A. López, D. Ceráin and A. Monge, *J. Med. Chem,* 2000, **35**, 21–3036 Patterson A.V., Saunders M.P.. Chinje E.C., Patterson L.H., Stratford I.J., *Anti-Cancer Drug Des.*, 1998, **13**, 541–573.

36 A.V. Patterson, M. P. Saunders, E. C. Chinje,, L.H. Patterson, I. J. Stratford, *Anti-Cancer Drug Des.*, 1998, **13**, 541–573.

37 C. M. Martin, PhD Thesis, Bangor University, 2012.

38 S. Milstien and L. A. Cohen, *J. Am. Chem. Soc.,* 1972, **94**, 9158.

39 C. M. N. Levine and R. T. Raines, *Chem. Sci*, 2012, **3,** 2412–2420.

40 R. M. Beesley, C. K. Ingold and J. F. Thorpe, *J. Chem. Soc. Trans*, 1915, **107**, 1080.

41 M. Volpato, N. Abou-Zeid, R. W. Tanner, L. T. Glassbrook, J. Taylor, I. Stratford, P. M. Loadman, M. Jaffar and R. M. Phillips, *Mol. Cancer Ther.*, 2007, **6**, 3122–30.

42 K. Achilles, *Arch. Pharm. Pharm. Med. Chem.*, 2001, **334**, 209–215.

43 D. Shan, M. G. Nicolaou, R. T. Borchardt and B. Wang, *J. Pharm. Sci.*, 1997, **86**, 765–767.

44 M. N. Levine, L. D. Lavis and R. T. Raines, *Molecules*, 2008, **13**, 204-207

45 A. Gilman and F. S. Philips, *Science*, 1946, **103**, 409–416.

46 W. B. Mattes, C. Lee, J. Laval and T. R. O. Connor, *Carcinogenesis,* 1996, **17**, 643–648.

47 a Masta, P. J. Gray and D. R. Phillips, *Nucleic Acids Res.*, 1994, **22**, 3880–3886.

48 S. M. Rink, M. S. Solomon, M. J. Taylor, S. B. Rajur, L. W. Mclaughlin and P. B. Hopkins, *J. Am. Chem. Soc.,* 1993, **115**, 2551–2557.

49 B. D. Palmer, W. R. Wilson, S. Cliffe and W. A. Denny, *J. Med. Chem.*, 1992, **35**, 3214–3222.

50 N. Kapuriya, R. Kakadiya, H. Dong, A. Kumar, P.-C. Lee, X. Zhang, T.-C. Chou, T.-C. Lee, C.-H. Chen, K. Lam, B. Marvania, A. Shah and T.-L. Su, *Bioorg. Med. Chem.*, 2011, **19**, 471–485.

51 K. R. Rai, B. L. Peterson, F. R. Appelbaun, J. Kolitz, L. Elias, L. Shepard, J. Hines, G. A. Threatte, R. A. Larson, B .D. Cheson and C. A. Schiffer, *N. Engl. J. Med.*, 2000, 1750–1757

52 J. a Moscow, C. a Swanson and K. H. Cowan, *Br. J. Cancer*, 1993, **68**, 732–737.

53 J. Rothbarth, R. E. M. Tollenaar, J. H. M. Schellens, J. W. R. Nortier, L. J. S. Kool, P. J. K. Kuppen, G. J. Mulder and C. J. H. Van De Velde, *Eur. J. Cancer*, 2004, **40**, 1812–1824.

54 N. Kapuriya, K. Kapuriya, H. Dong, X. Zhang, T.-C. Chou, Y.-T. Chen, T.-C. Lee, W.-C. Lee, T.-H. Tsai, Y. Naliapara and T.-L. Su, *Bioorg. Med. Chem.*, 2009, **17**, 1264–75.

55 N. Kapuriya, K. Kapuriya, X. Zhang, T. C. Chou, R. Kakadiya, Y. T. Wu, T. H. Tsai, Y. T. Chen, T. C. Lee, A. Shah, Y. Naliapara and T. L. Su, *Bioorganic Med. Chem.*, 2008, **16**, 5413–5423.

56 T. a Gourdie, K. K. Valu, G. L. Gravatt, T. J. Boritzki, B. C. Baguley, L. P. Wakelin, W. R. Wilson, P. D. Woodgate and W. A. Denny, *J. Med. Chem.*, 1990, **33**, 1177–1186.

57 T. L. Su, Y. W. Lin, T. C. Chou, X. Zhang, V. A. Bacherikov, C. H. Chen, L. F. Liu and T. J. Tsai, *J. Med. Chem.*, 2006, **49**, 3710–3718.

58 V. A. Bacherikov, T. C. Chou, H. J. Dong, C. H. Chen, Y. W. Lin, T. J. Tsai and T. L. Su, *Bioorganic Med. Chem. Lett.*, 2004, **14**, 4719–4722.

59 G. L. Gravatt, B. C. Baguley, W. R. Wilson and W. A. Denny, *J. Med. Chem.*, 1991, **34**, 1552–1560.

60 M. G. Ferlin, L. D. Via and O. M. Gia, *Bioorganic Med. Chem.*, 2004, **12**, 771–777.

61 R. Kakadiya, H. Dong, A. Kumar, D. Narsinh, X. Zhang, T. C. Chou, T. C. Lee, A. Shah and T. L. Su, *Bioorganic Med. Chem.*, 2010, **18**, 2285–2299.

62 N. H. Greig, S. Genka, E. M. Daly, D. J. Sweeney and S. I. Rapoport, *Cancer Chemother. Pharmacol.*, 1990, **25**, 311–319.

63 M. Wickström, J. I. Johnsen, F. Ponthan, L. Segerström, B. Sveinbjörnsson, M. Lindskog, H. Lövborg, K. Viktorsson, R. Lewensohn, P. Kogner, R. Larsson and J. Gullbo, *Mol. Cancer Ther.*, 2007, **6**, 2409–17.

64 S. Mittal, X. Song, B. S. Vig and G. L. Amidon, *Pharm. Res.*, 2007, **24**, 1290–8.

65 S. Mittal, Y. Tsume, C. P. Landowski, K.-D. Lee, J. M. Hilfinger and G. L. Amidon, *Eur. J. Pharm. Biopharm.*, 2007, **67**, 752–8.

66 P. J. Pedersen, M. S. Christensen, T. Ruysschaert, L. Linderoth, T. L. Andresen, F. Melander, O. G. Mouritsen, R. Madsen and M. H. Clausen, 2009, **52**, 3408–3415.

67 L. Gharat, R. Taneja, N. Weerapreeyakul, B. Rege, J. Polli and P. J. Chikhale, *Int. J. Pharm.*, 2001, **219**, 1–10.

68 N. Weerapreeyakul, R. G. Hollenbeck and P. J. Chikhale, *Bioorg. Med.*, 2000, **10**, 2391–2395.

69 R. A. Abramovitch and K. Schofield, *J. Chem.Soc.*, 1955, 2326–2336.

70 R. F. Robbins and K. Schofiled, *J. Chem. Soc.*, 1957, 3186–3194

71 D. J. Lee, A. Trotti, S. Spencer, R. Rostock, C. Fisher, R. V. Roemeling, E. Harvey and E. Groves, *Int. J. Radiation Oncology Biol. Phys.*,1998, **42**, 811–815.

72 M. V. Papadopoulou, W. D. Bloomer, A. P. Taylor, M. Hernandez, D. Rosalyn, M. G. Hollingshead and D. Blumenthal, *Radiation Research Society*, 2007, **1**, 65–71.

73 M. P. Hay, K. O. Hicks, K. Pchalek, H. H. Lee, A. Blaser, F. B. Pruijn, R. F. Anderson, S. S. Shinde, W. R. Wilson and W. A. Denny, *J. Med. Chem.*, 2008, **21**, 6853–6865.

74 M. P. Hay, K. O. Hicks, F. B. Pruijn, K. Pchalek, B. G. Siim, W. R. Wilson and W. A. Denny, *J. Med. Chem.*, 2007, **50**, 6392–6404.

75 M. P. Hay, S. A. Gamage, M. S. Kovacs, F. B. Pruijn, R. F. Anderson, A. V Patterson, W. R. Wilson, J. M. Brown and W. A. Denny, 2003, **46**, 169–182.

76 K. O. Hicks, B. G. Siim, J. K. Jaiswal, F. B. Pruijn, M. Annie, R. Patel, A. Hogg, H. D. S. Liyanage, M. J. Dorie, J. Martin, W. A. Denny, M. P. Hay and W. R. Wilson, 2012, **16**, 4946–4957.

77 F. W. Hunter, J. Wang, R. Patel, H.-L. Hsu, A. J. R. Hickey, M. P. Hay and W. R. Wilson, *Biochem. Pharmacol.*, 2012, **83**, 574–585.

78 S. W. Lin, Q. Sun, Z. M. Ge, X. Wang, J. Ye and R. T. Li, *Bioorganic Med. Chem. Lett.*, 2011, **21**, 940–943.

79 R. D. Rohde, H. D. Agnew, W. Yeo, R. C. Bailey and J. R. Heath, *J. Am. Chem. Soc.*, 2006, **128**, 9518–9525.

80 M. Boyd, M. P. Hay and P. D. W. Boyd, *Magn. Reson. Chem.*, 2006, **44**, 948–954.

81 T. Fuchs, G. Chowdhury, C. L. Barnes and K. S. Gates, *J. Ortd. Chem.*, 2001, **66**, 107–114.

82 G. A. Zhumabaeva, S. K. Kotovskaya, N. M. Perova, V. N. Charushin and O. N. Chupakhin, *Russ. Chem. Bull.*, 2006, **55**, 1243–1247.

83 J. Jiu and G. P. Mueller, 1959, **24**, 813-818.

84 P. Nowak, D. C. Cole, A. Aulabaugh, J. Bard, R. Chopra, R. Cowling, K. Y. Fan, B. Hu, S. Jacobsen, M. Jani, G. Jin, M. C. Lo, M. S. Malamas, E. S. Manas, R. Narasimhan, P. Reinhart, A. J. Robichaud, J. R. Stock, J. Subrath, K. Svenson, J. Turner, E. Wagner, P. Zhou and J. W. Ellingboe, *Bioorganic Med. Chem. Lett.*, 2010, **20**, 632–635.

85 C. A. Mills, D. M. Taylor, P. J. Murphy, C. Dalton, G. W. Jones, L. M. Hall and a. V. Hughes, *Synth. Met.*, 1999, **102**, 1000–1001.

86 E. Novellino, E. Abignente, B. Cosimelli, G. Greco, M. Iadanza, S. Laneri, A. Lavecchia, M. G. Rimoli, D. Tuscano, L. Trincavelli and C. Martini, *J. Med. Chem.*, 2002, **45**, 5030–5036.

87 E. H. Huws. PhD Thesis, University of Wales Bangor, 2012.

88 P. Leighton and J. K. M. Sanders, *J. Chem. Soc.*, 1987, 2385-2393.

89 Q. Xia, L. Zhang, J. Zhang, R. Sheng, B. Yang, Q. He and Y. Hu, *Eur. J. Med.*

Chem., 2011, **46**, 919–26.

90 R. C. Weast, *CRC Handbook of Chemistry and Physics (62nd ed.)*, CRC Press, 1981.

91 B. D. Palmer, W. R. Wilson, S. M. Pullen and W. A. Denny, *J. Med. Chem.*, 1990, **33**, 112–121.

92 World Health Organisation, Leishmaniasis Factsheet no. 375, 2014.

93 M. P. Barrett and S. L. Croft, *Br. Med. Bull.*, 2012, **104**, 175–96.

94 G. C. Harbour, A. A. Tymiak and K. L. Rinehart, *J. Am. Chem. Soc.*, 1981, **103**, 5604-5606.

95 R. Montaser and H. Luesch, *Future Med. Chem.*, 2011, **3**, 1475–89.

96 D. Khanna, G. Sethi, K. S. Ahn, M. K. Pandey, A. B. Kunnumakkara, B. Sung, A. Aggarwal and B. B. Aggarwal, *Curr. Opin. Pharmacol.*, 2007, **7**, 344–351.

97 J. R. Hanson, *Natural Products: The Secondary Metabolite*, Royal Society of Chemistry, 2003.

98 D. A. Dias, S. Urban and U. Roessner, *Metabolites*, 2012, **2**, 303–36.

99 G. T. Carter, *Nat. Prod. Rep.*, 2011, **28**, 1783–9.

100 A. Martins, H. Vieira, H. Gaspar and S. Santos, *Mar. Drugs*, 2014, **12**, 1066–101.

101 W. H. Gerdwick, B. S. Moore, *Chem. Biol.*, 2013, **19**, 85–98.

102 M. Schumacher, M. Kelkel, M. Dicato and M. Diederich, *Biotechnol. Adv.*, 2011, **29**, 531–47.

103 B. B. Mishra and V. K. Tiwari, *Eur. J. Med. Chem.*, 2011, **46**, 4769–807.

104 S. Sudek, N. B. Lopanik, L. E. Waggoner, M. Hildebrand, C. Anderson, H. Liu, A. Patel, D. H. Sherman and M. G. Haygood, *J. Nat. Prod.*, 2007, **70**, 67–74.

105 A. Martins, T. Tenreiro, G. Andrade, M. Gadanho, S. Chaves, M. Abrantes, P. Calado, R. Tenreiro and H. Vieira, *Mar. Drugs*, 2013, **11**, 1506–23.

106 J. Berdy, *J. Antibiot.*, 2005, **58**, 1–26.

107 D. M. Evans,PhD Thesis, Bangor University, 2012.

108 P. J. Murphy, L. Williams, M. B. Hursthouse and K. M. A. Malik, *J. Chem. Soc. Chem. Commun.*, 1994, 119–120.

109 P. J. Murphy and H. L. Williams, *J. Chem. Soc. Chem. Commun.*, 1994, 819–820.

110 G. P. Black, P. J. Murphy, N. D. A. Walshe and D. E. Hibbs, *Tetrahedron Lett.*, 1996, **37**, 6943–6946.

111 P. J. Murphy, H. L. Williams, D. E. Hibbs, M. B. Hursthouse and K. M. A. Malik, *Tetrahedron Lett.*, 1996, **52**, 8315–8332.

112 G. P. Black, P. J. Murphy and N. D. A. Walshe, *Tetrahedron*, 1998, **54**, 9481–9488.

113 R. G. S. Berlinck, A. C. B. Burtoloso, A. E. Trindade-Silva, S. Romminger, R. P. Morais, K. Bandeira and C. M. Mizuno, *Nat. Prod. Rep.*, 2010, **27**, 1871–907.

114 D. M. Evans and P. J. Murphy, *Alkaloids. Chem. Biol.*, 2011, **70**, 1–77.

115 E. L. Bennett, G. P. Black, P. Browne, A. Hizi, M. Jaffar, J. P. Leyland, C. Martin, I. Oz-Gleenberg, P. J. Murphy, T. D. Roberts, A. J. Thornhill and S. a. Vale, *Tetrahedron*, 2013, **69**, 3061–3066.

116 M. F. C. Santos, P. M. Harper, D. E. Williams, J. T. Mesquita, É. G. Pinto, T. A. da.

Costa-Silva, E. Hajdu, A. G. Ferreira, R. A. Santos, P. J. Murphy, R. J. Andersen, A. G. Tempone and R. G. S. Berlinck, *J. Nat. Prod.*, 2015, **78**, 1101-1112.

117 R. G. Berlinck, J. C. Braekman and D. Daloze, *J. Nat. Prod.*, 1992, **55**, 528–532.

118 R. G. S. Berlinck, J. C. Braekman, D. Daloze, K. Hallenga and R. Ottinger, *Tetrahedron Lett.*, 1990, **31**, 6531–6534.

119 R. G. S. Berlinck and M. H. Kossuga, *Nat. Prod. Rep.*, 2005, **22**, 516–550.

120 B. B. Snider and Z. Shi, *J. Org. Chem.* 1993, **58**, 3828–3839.

121 J. A. C. Soc, K. L. Rinehart, P. D. Shaw, L. H. Li and S. L. Kuentzel, *J. Am. Chem. Soc.*, 1981, **104**, 5604–5606.

122 A. D. Patil, N. V. Kumar, W. C. Kokke, M. F. Bean, A. J. Freyer, C. De Brosse, S. Mai, A. Truneh, D. J. Faulkner, B. Carte, A. L. Breen, R. P. Hertzberg, R. K. Johnson, J. W. Westley and B. C. M. Potts, 1995, **60**, 1182–1188.

123 M. Yu, S. S. Pochapsky and B. B. Snider, *J. Org. Chem.*, 2008, **73**, 9065–74.

124 R. Tavares, D. Daloze and E. Hajdu, *J. Nat. Prod.*, 1995, **58**, 1139–1142.

125 A. D. Patil, A. J. Freyer, P. Offen, M. F. Bean and R. K. Johnson, *J. Nat. Prod.*, 1997, **60**, 704–707.

126 R. J. Capon, M. Miller and F. Rooney, *J. Nat. Prod.*, 2001, **64**, 643–644.

127 H. Hua, J. Peng, F. R. Fronczek, M. Kelly and M. T. Hamann, *Bioorg. Med. Chem.*, 2004, **12**, 6461–4.

128 H. Sorek, A. Rudi, S. Gueta, F. Reyes, M. J. Martin, M. Aknin, E. Gaydou, J. Vacelet and Y. Kashman, *Tetrahedron*, 2006, **62**, 8838–8843.

129 P. M. Brown, N. Käppel, P. J. Murphy, S. J. Coles and M. B. Hursthouse, *Tetrahedron*, 2007, **63**, 1100–1106.

130 J. G. Urones, N. M. Garrido, D. Díez, M. El Hammoumi, S. H. Dominguez, J. A. Casaseca, G. Davies and A. D. Smith, *Org. Biomol. Chem.*, 2004, **2**, 364-372.

131 B. B. Snider and W. C. Faith, *Tetrahedron Lett.*, 1983, **24**, 861–864.

132 K. Schellhaas, H. Schmalz and J. W. Bats, *Chem. Eur. J.*, 1998, **4**, 57–65.

133 T. Uyehara, Y. Kabasawa, J. Yamada and T. Kato, *J. Chem.Soc., Chem. Commun.*, 1986, 539–540.

134 Y. Kabawawa, T. Kato and Y. Yamamoto, *J. Am. Chem. Soc.*, 1988, **53**, 3669–3673.

135 M. Asaoka, M. Sakurai and H. Takei, *Tetrahedron Lett.*, 1990, **31**, 4759–4760.

136 J. Cossy and S. BouzBouz, *Tetrahedron Lett.*, 1996, **37**, 5091–5094.

137 H. G. Schmalz and K. Schellhaas, *Agnew. Chem. Int. Ed. Engl.*, 1996, **35**, 2146-2148.

138 H. House, R. W. Giese, K. Kronberger, J. P. Kaplan and J. F. Simeone, *J. Am. Chem. Soc.*, 1970, **72**, 2800–2810.

139 M. R. Detty, *J. Org. Chem.*, 1979, **44**, 3–7.

140 Z. Al Shuhaib, D. H. Davies, M. Dennis, D. M. Evans, M. D. Fletcher, H. Franken, P. Hancock, J. Hollinshead, I. Jones, K. Kähm, P. J. Murphy, R. Nash, D. Potter and R. Rowles, *Tetrahedron*, 2014, **70**, 4412–4419.

141 D. M. Evans and P. J. Murphy, *Chem. Commun.*, 2011, **47**, 3225–3226.

142 T. Shono and N. Kise, *Tetrahedron Lett.*, 1990, **31**, 1303–1306.

143 M. Garst, L. Dolby, S. Esfandiari, N. Fedoruk, N. Chamberlain and A. Avey, *J. Org. Chem.*, 2000, **65**, 7098–104.

144 I. M. Goldman, *J. Org. Chem.*, 1979, **34**, 1969–1970.

145 J. E. Bercaw, N. Hazari and J. A. Labinger, *J. Org. Chem.*, 2008, **73**, 8654–8657.

146 M. Hanbali, M. Vela-Ruiz, D. Bagnard and B. Luu, *Bioorg. Med. Chem. Lett.*, 2006, **16**, 2637–40.

9.0 Appendices

X-ray data for compound 161.

Table 6. Crystal data and structure refinement details.

Identification code	**2013ncs0205ba**	
Empirical formula	$C_{14}H_{20}N_4O_1$	
Formula weight	260.34	
Temperature	100(2) K	
Wavelength	0.71075 Å	
Crystal system	Monoclinic	
Space group	*P*121/*c*1	
Unit cell dimensions	a = **15.698(9) Å**	α = **90°**
	b = **5.232(3) Å**	β = **112.188(7)°**
	c = **18.133(11) Å**	γ = **90°**
Volume	1379.0(14) $Å^3$	
Z	4	
Density (calculated)	1.254 Mg / m^3	
Absorption coefficient	0.082 mm^{-1}	
F(000)	560	
Crystal	Block; Yellow	
Crystal size	0.06 × 0.03 × 0.02 mm^3	
θ range for data collection	2.298 – 27.474°	
Index ranges	$-20 \le h \le 20$, $-6 \le k \le 6$, $-23 \le l \le 23$	
Reflections collected	9423	
Independent reflections	3143 [R_{int} = 0.1676]	

Completeness to θ = 25.242°	99.9 %
Absorption correction	Semi−empirical from equivalents
Max. and min. transmission	1.000 and 0.325
Refinement method	Full-matrix least-squares on F^2
Data / restraints / parameters	3143 / 1 / 176
Goodness-of-fit on F^2	0.903
Final *R* indices [$F^2 > 2\sigma(F^2)$]	*R1* = 0.0687, *wR2* = 0.1127
R indices (all data)	*R1* = 0.2025, *wR2* = 0.1529
Extinction coefficient	n/a
Largest diff. peak and hole	0.251 and −0.244 e Å^{-3}

Diffractometer: *Rigaku AFC12* goniometer equipped with an enhanced sensitivity (HG) *Saturn724+* detector mounted at the window of an *FR-E+ SuperBright* molybdenum rotating anode generator with VHF *Varimax* optics (70µm focus). **Cell determination and data collection**: *CrystalClear-SM Expert 3.1 b27 (Rigaku, 2013).* **Data reduction, cell refinement and absorption correction**: *CrystalClear-SM Expert 2.1 b29 (Rigaku, 2013).* **Structure solution**: *SUPERFLIP* (Palatinus, L. & Chapuis, G. (2007). J. Appl. Cryst. 40, 786-790). **Structure refinement**: *SHELXL-2013* (Sheldrick, G.M. (2008). Acta Cryst. A64, 112-122). **Graphics:** *OLEX2* (Dolomanov, O. V., Bourhis, L. J., Gildea, R. J., Howard, J. A. K. & Puschmann, H. (2009). J. Appl. Cryst. 42, 339-341).

Table 7. Bond lengths [Å] and angles [°].

O1–N2	1.251(3)
N1–C1	1.312(3)
N1–C2	1.370(4)
N2–N3	1.312(3)
N2–C7	1.410(4)
N3–C1	1.383(4)
N4–H4	0.881(2)
N4–C1	1.349(4)
N4–C8	1.458(4)
C2–C3	1.406(4)
C2–C7	1.403(4)
C3–H3	0.9500
C3–C4	1.363(4)
C4–H4A	0.9500
C4–C5	1.402(4)
C5–H5	0.9500
C5–C6	1.361(4)
C6–H6	0.9500
C6–C7	1.400(4)
C8–H8A	0.9900
C8–H8B	0.9900
C8–C9	1.504(4)
C9–H9A	0.9900
C9–H9B	0.9900
C9–C10	1.531(4)

C10–H10A	0.9900
C10–H10B	0.9900
C10–C11	1.513(4)
C11–H11A	0.9900
C11–H11B	0.9900
C11–C12	1.519(4)
C12–H12A	0.9900
C12–H12B	0.9900
C12–C13	1.504(4)
C13–H13A	0.9900
C13–H13B	0.9900
C13–C14	1.524(4)
C14–H14A	0.9800
C14–H14B	0.9800
C14–H14C	0.9800

C1–N1–C2	114.2(3)
O1–N2–N3	118.0(3)
O1–N2–C7	119.7(3)
N3–N2–C7	122.3(3)
N2–N3–C1	116.2(3)
C1–N4–H4	124(2)
C1–N4–C8	124.4(3)
C8–N4–H4	111(2)
N1–C1–N3	128.1(3)
N1–C1–N4	121.0(3)
N4–C1–N3	110.9(3)

N1–C2–C3	120.3(3)
N1–C2–C7	123.2(3)
C7–C2–C3	116.5(3)
C2–C3–H3	119.9
C4–C3–C2	120.2(3)
C4–C3–H3	119.9
C3–C4–H4A	119.1
C3–C4–C5	121.7(3)
C5–C4–H4A	119.1
C4–C5–H5	119.8
C6–C5–C4	120.3(3)
C6–C5–H5	119.8
C5–C6–H6	121.2
C5–C6–C7	117.7(3)
C7–C6–H6	121.2
C2–C7–N2	116.1(3)
C6–C7–N2	120.4(3)
C6–C7–C2	123.6(3)
N4–C8–H8A	108.7
N4–C8–H8B	108.7
N4–C8–C9	114.1(3)
H8A–C8–H8B	107.6
C9–C8–H8A	108.7
C9–C8–H8B	108.7
C8–C9–H9A	109.2
C8–C9–H9B	109.2
C8–C9–C10	112.3(3)

H9A–C9–H9B	107.9
C10–C9–H9A	109.2
C10–C9–H9B	109.2
C9–C10–H10A	108.9
C9–C10–H10B	108.9
H10A–C10–H10B	107.7
C11–C10–C9	113.3(3)
C11–C10–H10A	108.9
C11–C10–H10B	108.9
C10–C11–H11A	108.7
C10–C11–H11B	108.7
C10–C11–C12	114.3(3)
H11A–C11–H11B	107.6
C12–C11–H11A	108.7
C12–C11–H11B	108.7
C11–C12–H12A	108.7
C11–C12–H12B	108.7
H12A–C12–H12B	107.6
C13–C12–C11	114.4(3)
C13–C12–H12A	108.7
C13–C12–H12B	108.7
C12–C13–H13A	108.9
C12–C13–H13B	108.9
C12–C13–C14	113.5(3)
H13A–C13–H13B	107.7
C14–C13–H13A	108.9
C14–C13–H13B	108.9

C13–C14–H14A	109.5
C13–C14–H14B	109.5
C13–C14–H14C	109.5
H14A–C14–H14B	109.5
H14A–C14–H14C	109.5

Symmetry transformations used to generate equivalent atoms:

Table 8. Anisotropic displacement parameters [$Å^2 \times 10^3$]. The anisotropic displacement factor exponent takes the form: $-2\pi^2[h^2a^{*2}U^{11} + \cdots + 2\ h\ k\ a^*\ b^*\ U^{12}\ ]$.

Atom	U^{11}	U^{22}	U^{33}	U^{23}	U^{13}	U^{12}
O1	51(1)	55(2)	51(2)	–4(1)	36(1)	–5(1)
N1	37(2)	38(2)	33(2)	3(1)	16(1)	3(1)
N2	40(2)	47(2)	38(2)	–5(1)	26(2)	–9(2)
N3	39(2)	38(2)	34(2)	–1(1)	21(1)	–2(1)
N4	42(2)	39(2)	40(2)	6(1)	25(2)	5(1)
C1	34(2)	34(2)	32(2)	–2(2)	15(2)	–6(2)
C2	37(2)	40(2)	27(2)	–6(2)	13(2)	–6(2)
C3	41(2)	43(2)	35(2)	1(2)	16(2)	–1(2)
C4	48(2)	37(2)	34(2)	3(2)	14(2)	–4(2)
C5	46(2)	43(2)	35(2)	2(2)	16(2)	–8(2)
C6	42(2)	47(2)	32(2)	0(2)	18(2)	–9(2)
C7	33(2)	36(2)	32(2)	0(2)	12(2)	–1(2)
C8	42(2)	43(2)	38(2)	3(2)	24(2)	5(2)
C9	42(2)	43(2)	41(2)	–5(2)	24(2)	0(2)
C10	38(2)	42(2)	38(2)	2(2)	21(2)	1(2)
C11	39(2)	41(2)	52(2)	–3(2)	25(2)	–2(2)
C12	38(2)	42(2)	42(2)	5(2)	16(2)	3(2)
C13	50(2)	45(2)	72(3)	1(2)	30(2)	–3(2)
C14	51(2)	76(3)	79(3)	10(2)	37(2)	–11(2)

Table 9. Hydrogen coordinates [$\times 10^4$] and isotropic displacement parameters [$Å^2 \times 10^3$].

Atom	*x*	*y*	*z*	U_{eq}	*S.o.f.*
H4	4367(13)	340(30)	5466(17)	45	1
H3	2199	8644	3685	47	1
H4A	2281	11127	2668	48	1
H5	3413	10448	2144	49	1
H6	4478	7167	2637	47	1
H8A	3184	3608	5738	46	1
H8B	3756	1372	6313	46	1
H9A	2735	–1667	5445	48	1
H9B	2143	641	4919	48	1
H10A	2415	–26	6563	45	1
H10B	1745	2038	5976	45	1
H11A	1461	–3353	5819	50	1
H11B	795	–1304	5225	50	1
H12A	1061	–1725	6867	49	1
H12B	384	282	6263	49	1
H13A	134	–5111	6144	64	1
H13B	–543	–3109	5536	64	1
H14A	–1196	–4394	6440	97	1
H14B	–929	–1436	6595	97	1
H14C	–289	–3567	7176	97	1

Table 10. Torsion angles [°].

O1–N2–N3–C1	180.0(2)
O1–N2–C7–C2	179.2(3)
O1–N2–C7–C6	–1.0(4)
N1–C2–C3–C4	179.4(3)
N1–C2–C7–N2	0.7(4)
N1–C2–C7–C6	–179.1(3)
N2–N3–C1–N1	1.2(5)
N2–N3–C1–N4	–178.1(3)
N3–N2–C7–C2	–1.6(4)
N3–N2–C7–C6	178.2(3)
N4–C8–C9–C10	176.0(3)
C1–N1–C2–C3	–179.3(3)
C1–N1–C2–C7	0.9(4)
C1–N4–C8–C9	93.3(3)
C2–N1–C1–N3	–2.0(4)
C2–N1–C1–N4	177.2(3)
C2–C3–C4–C5	0.0(5)
C3–C2–C7–N2	–179.1(2)
C3–C2–C7–C6	1.1(5)
C3–C4–C5–C6	0.6(5)
C4–C5–C6–C7	–0.3(4)
C5–C6–C7–N2	179.6(3)
C5–C6–C7–C2	–0.6(5)
C7–N2–N3–C1	0.8(4)
C7–C2–C3–C4	–0.8(4)

C8–N4–C1–N1	–2.9(5)
C8–N4–C1–N3	176.4(3)
C8–C9–C10–C11	–173.5(2)
C9–C10–C11–C12	–179.3(3)
C10–C11–C12–C13	–179.0(3)
C11–C12–C13–C14	–179.6(3)

Symmetry transformations used to generate equivalent atoms:

Table 11. Hydrogen bonds [Å and °].

D–H···*A*	*d*(*D*–H)	*d*(H···*A*)	*d*(*D*···*A*)	∠(*D*H*A*)
N4–H4···N3^{i}	0.881(2)	2.183(9)	3.041(4)	165(3)

Symmetry transformations used to generate equivalent atoms:

(i) –x+1,–y,–z+1

Compound **161**.

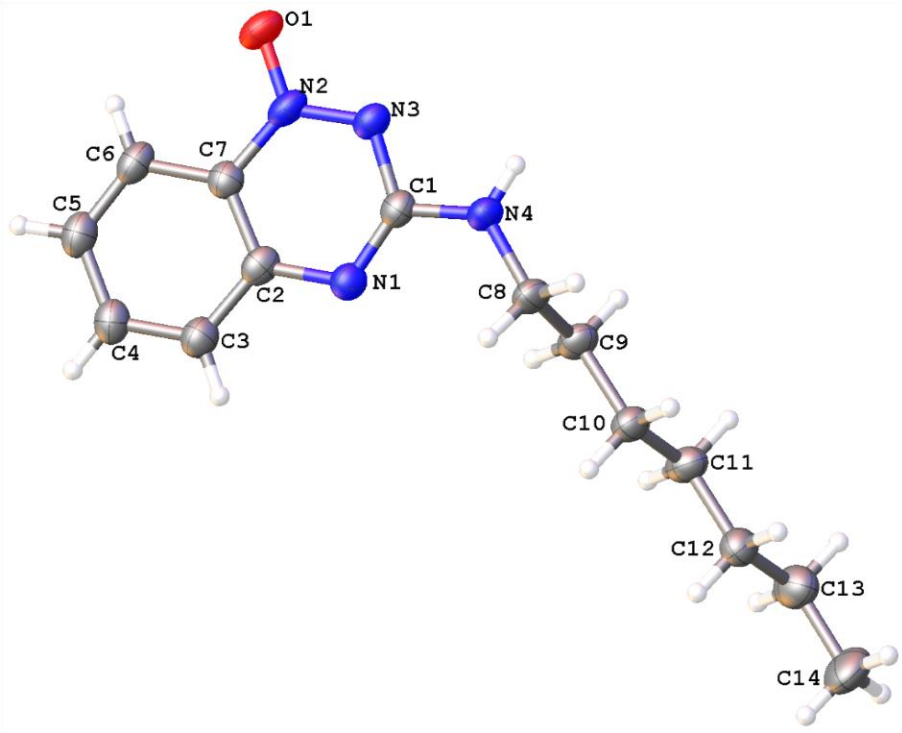

Appendix 2

Anodic oxidation of 1,4-dimethoxy-2,3,5-trimethylbenzene (99)

The anodic oxidation of **99** was performed using a platinum cathode and carbon felt anode. These were in turn connected to an ammeter (Amps), voltmeter (Volts) and a Farnell instruments LTD stabilised power supply, set to maintain a current of 1 Amp. (Figure 50) Both the cathode and anode were submerged in a beaker containing. **99** dissolved in 2% methanolic potassium hydroxide. This was maintained at a temperature of <5 °C and the solution vigorously stirred. (Figure 51)

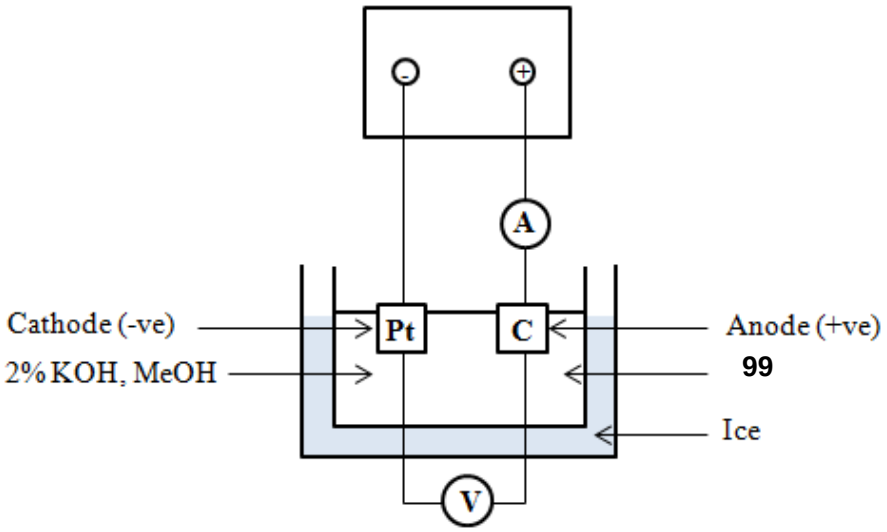

Figure 50. Electrochemical reaction schematic.

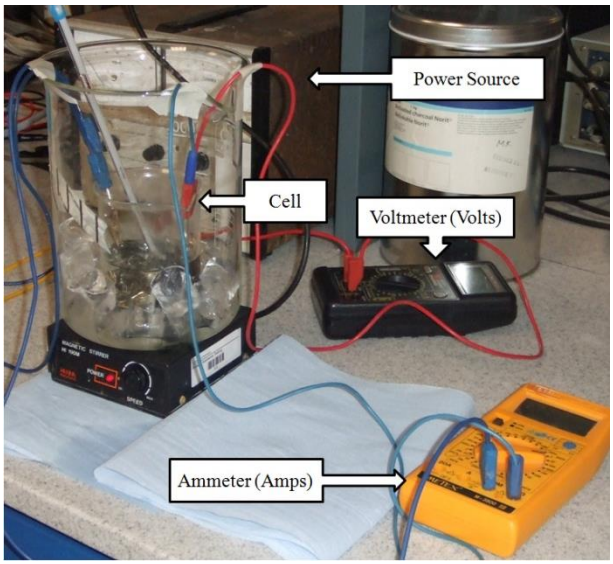

Figure 51. Photograph of the apparatus.

JOURNAL OF NATURAL PRODUCTS

Article

pubs.acs.org/jnp

Anti-parasitic Guanidine and Pyrimidine Alkaloids from the Marine Sponge *Monanchora arbuscula*

Mario F. C. Santos,[†] Philip M. Harper,[‡] David E. Williams,[§] Juliana T. Mesquita,[⊥] Érika G. Pinto,[⊥,∥] Thais A. da Costa-Silva,[⊥] Eduardo Hajdu,[#] Antonio G. Ferreira,[▽] Raquel A. Santos,[⊗] Patrick J. Murphy,[‡] Raymond J. Andersen,[§] Andre G. Tempone,*[,⊥,∥] and Roberto G. S. Berlinck*[,†]

[†]Instituto de Química de São Carlos, Universidade de São Paulo, CP 780, CEP 13560-970 São Carlos, SP, Brazil

[‡]School of Chemistry, Bangor University, Bangor, Gwynedd LL57 2UW, U.K.

[§]Departments of Chemistry and Earth, Ocean & Atmospheric Sciences, University of British Columbia, Vancouver, BC, V6T 1Z1 Canada

[⊥]Centro de Parasitologia e Micologia, Instituto Adolfo Lutz, Av. Dr. Arnaldo 351, 8° andar, Cerqueira Cesar, CEP 01246-000 São Paulo, SP, Brazil

[∥]Instituto de Medicina Tropical de São Paulo, Universidade de São Paulo, Av. Dr. Enéas de Carvalho Aguiar, 470, CEP 05403-000 São Paulo, SP, Brazil

[#]Museu Nacional, Universidade Federal do Rio de Janeiro, Quinta da Boa Vista, s/n, CEP 20940-040 Rio de Janeiro, RJ, Brazil

[▽]Departamento de Química, Universidade Federal de São Carlos, Rod. Washington Luiz, km 235 - SP-310, CEP 13565-905, São Carlos, SP, Brazil

[⊗]Laboratório de Genética e Biologia Molecular, Programa de Pós-Graduação em Ciências, Universidade de Franca, Av. Dr. Armando Salles Oliveira, 201, CEP 14404 600 Franca, SP, Brazil

Supporting Information

ABSTRACT: HPLC-UV-ELSD-MS-guided fractionation of the anti-parasitic extract obtained from the marine sponge *Monanchora arbuscula*, collected off the southeastern coast of Brazil, led to the isolation of a series of guanidine and pyrimidine alkaloids. The pyrimidines monalidine A (**1**) and arbusculidine A (**7**), as well as the guanidine alkaloids batzellamide A (**8**) and hemibatzelladines **9**–**11**, represent new minor constituents that were identified by analysis of spectroscopic data. The total synthesis of monalidine A confirmed its structure. Arbusculidine A (**7**), related to the ptilocaulin/mirabilin/netamine family of tricyclic guanidine alkaloids, is the first in this family to possess a benzene ring. Batzellamide A (**8**) and hemibatzelladines **9**–**11** represent new carbon skeletons that are related to the batzelladines. Evaluation of the anti-parasitic activity of the major known metabolites, batzelladines D (**12**), F (**13**), L (**14**), and nor-L (**15**), as well as of synthetic monalidine A (**1**), against *Trypanosoma cruzi* and *Leishmania infantum* is also reported, along with a detailed investigation of parasite cell-death pathways promoted by batzelladine L (**14**) and norbatzelladine L (**15**).

Leishmaniasis and Chagas disease are neglected diseases affecting over 12 million people worldwide,[1−4] and are considered by the World Health Organization as the neglected diseases with the highest mortality level.[5] Current treatment of leishmaniasis is exclusively based on chemotherapeutics.[1,5] Usual anti-leishmanial chemotherapy relies on antimonium salts, miltefosine, and amphotericin B.[6] Problems are associated with such a narrow choice of anti-leishmanial drugs, including parasite resistance, high toxicity and long-term treatment with sodium stibogluconate, and the high treatment cost with liposomal amphotericin B.[1,3] Similarly, the only two drugs currently used in the treatment of Chagas disease, nifurtimox and benznidazole, also present pronounced adverse effects due to long periods of administration.[7] Therefore, new approaches toward the discovery of new anti-leishmanial and anti-Chagas agents are in need.[1−8]

Marine organisms have been continuously investigated as a source of new anti-parasitic agents during the past two decades.[6,9] Recent examples include the almiramides isolated from the cyanobacterium *Lyngbya majuscula*, active against intracellular *Leishmania donovani* amastigotes,[3] sesquiterpene−

Received: January 24, 2015
Published: April 29, 2015

DOI: 10.1021/acs.jnatprod.5b00070
J. Nat. Prod. 2015, 78, 1101−1112

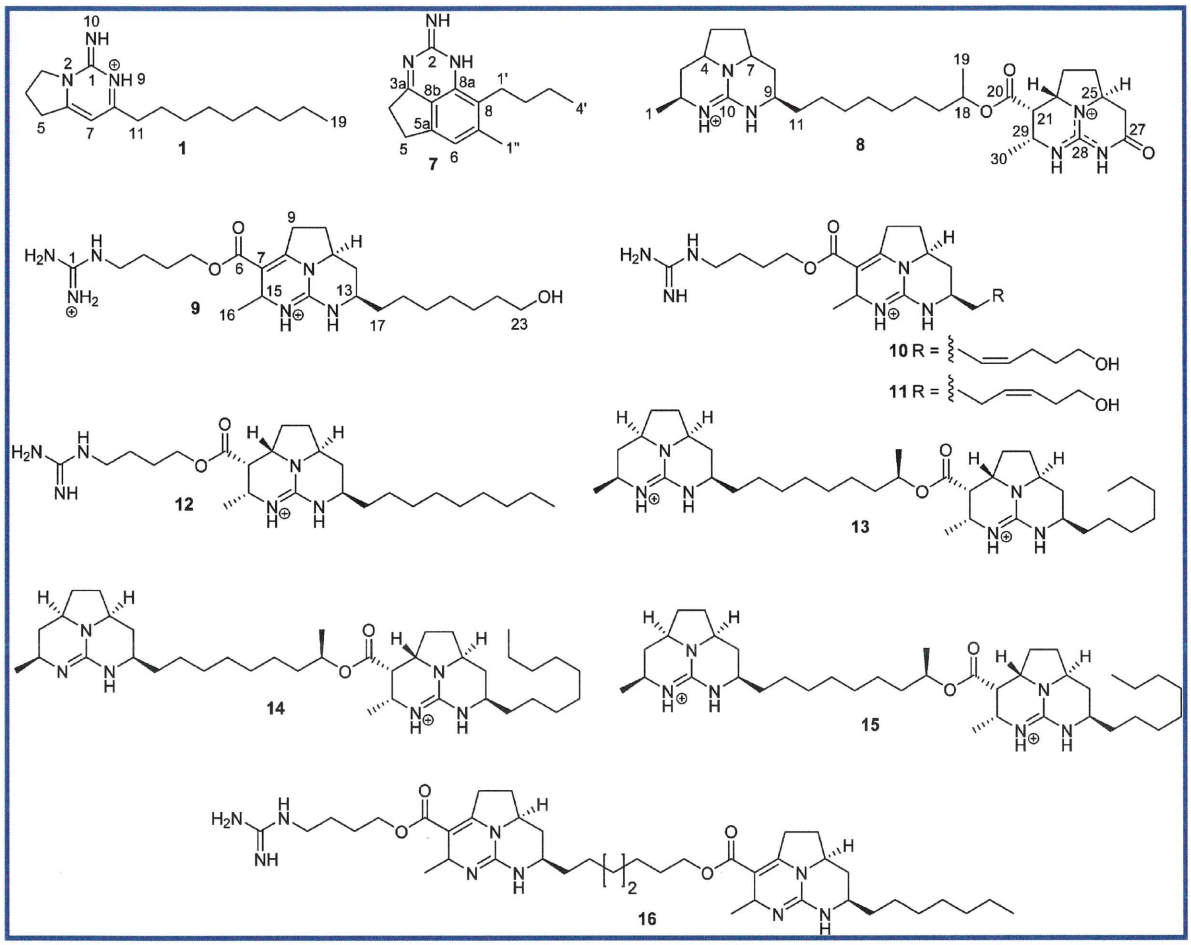

Figure 1. Structures of monalidine A (**1**), arbusculidine (**7**), batzellamide A (**8**), hemibatzelladine J (**9**), hemibatzelladines (**10** and **11**), batzelladines D (**12**), F (**13**), L (**14**), nor-batzelladine L (**15**), and batzelladine J (**16**).

purine conjugates from the sponge *Agelas mauritiana*, active against *L. donovani* promastigotes,[10] and mandanoperoxides, non-cytotoxic potent anti-trypanocidal agents from the sponge *Plakortis lita*.[11] Our continuing interest in the discovery of new anti-parasitic agents from marine organisms[12−14] led us to identify the MeOH extract from the sponge *Monanchora arbuscula* as having a suitable anti-leishmanial and trypanosomicidal activity profile.

Sponges of the genus *Monanchora* are well-known sources of guanidine alkaloids. These alkaloids are frequently found in marine sponges of highly plastic taxa, assigned to several genera in two distinct Demosponge orders (Halichondrida and Poecilosclerida).[15−18] Such guanidine alkaloids belong to four main chemotypes. The first group includes the bicyclic or monocyclic guanidine alkaloids crambescins,[19] of which urupocidin A is the newest and most complex member.[19f] The second group includes the tricyclic guanidines ptilocaulins,[20] mirabilins,[20c,d,21] and netamines.[22] The third group comprises the complex polycyclic alkaloids ptilomycalin A[23] and the crambescidins;[24] monanchocidins and monanchomycalins are variants of this group that present further elaboration on the polyfunctionalized alkyl chains connected to the pentacyclic guanidine core.[25] The fourth group comprises the batzelladines, alkaloids presenting two or three guanidine groups.[24e,26] Such unique alkaloid scaffolds are assumed to be derived from different modes of cyclization of a polyketide-derived chain on a putative guanidine precursor, which leads to structurally complex alkaloid mixtures.[20a,21b] An array of bioactivities have been reported for these guanidine alkaloids and include Na^+-, K^+-, or Ca^{2+}-ATPase inhibition[21c,24b] and anti-viral,[19d,23b,26a,d,27] cytotoxic,[20a,21b,22a,23a,c,25,26b] anti-fungal,[20d,23a,28] and anti-parasitic[20d,22c,29] activities. Moreover, crambescin B carboxylic acid displays inhibitory activity on voltage-gated sodium channels at levels that are only an order of magnitude less than the activity of tetrodotoxin.[30]

A recent collection of *M. arbuscula* as part of our ongoing program in the search for new bioactive metabolites from marine sponges[31] provided us with not only an anti-parasitic extract active against *Leishmania infantum* and *Trypanosoma cruzi* but also enough material to investigate the structures of the minor alkaloids present in the sponge. Herein we report the isolation of six new minor constituents (**1**, **7**−**11**) from the marine sponge *M. arbuscula* along with the known alkaloids batzelladines D (**12**), F (**13**), L (**14**), and nor-L (**15**). The identification and subsequent synthesis of the new monalidine A (**1**) enabled us to evaluate its biological activities as well. A new member of the ptilocaulin/mirabilin/netamine alkaloid family, named arbusculidine A (**7**), along with batzellamide A (**8**) and three new hemibatzelladines A−C (**9**−**11**) are also reported. The anti-leishmanial and anti-trypanosomal activities

DOI: 10.1021/acs.jnatprod.5b00070
J. Nat. Prod. 2015, 78, 1101−1112

of synthetic monalidine A (**1**) and of the major known alkaloids batzelladine D (**12**), F (**13**), L (**14**), and nor-L (**15**) isolated from the same sample of *M. arbuscula* are discussed, including investigations of the mechanism of action of both **14** and **15**. Figure 1 shows the structures of these compounds.

RESULTS AND DISCUSSION

A freeze-dried sample of the sponge *M. arbuscula* was extracted with MeOH. Subsequent solvent partitioning followed by C_{18} reversed-phase column chromatography, adsorption on a 1:1:1 mixture of XAD-2, -4, and -7 resins, Sephadex LH20 column chromatography, and finally repetitive reversed-phase HPLC purifications resulted in the isolation of monalidine A (**1**), arbusculidine (**7**), batzellamide A (**8**), and hemibatzelladines A–C (**9**–**11**), along with the known major alkaloids batzelladines D (**12**), F (**13**), L (**14**), and nor-L (**15**) (Figure 1).

The HR-ESI-MS analysis of monalidine A (**1**) gave an $[M+H]^+$ ion at m/z 262.2247 appropriate for a molecular formula of $C_{16}H_{27}N_3$ requiring five sites of unsaturation. Analysis of the gHSQC, ^{13}C, and ^1H NMR spectra of **1** identified four sp^2 carbons resonating at δ_C 178.5, 163.7, 154.0, and 106.1. The carbon resonance at δ_C 106.1 correlated to a single proton resonating at δ_H 7.00 in the gHSQC spectrum. The other three sp^2 carbons were determined to have no hydrogens attached. Of the remaining 12 carbons of **1**, 11 were assigned as methylenes and the remaining carbon as a terminal methyl CH_3-19 (δ_H 0.84/δ_C 13.9) of an alkyl chain. The gCOSY60, gHSQC, and gHMBC spectra indicated that the three methylenes CH_2-3 (δ_H 4.11/δ_C 51.9), CH_2-4 (δ_H 2.24/δ_C 20.0), and CH_2-5 (δ_H 3.18/δ_C 31.2) were present as a sequential spin system (Figure 2). In the gHMBC spectrum,

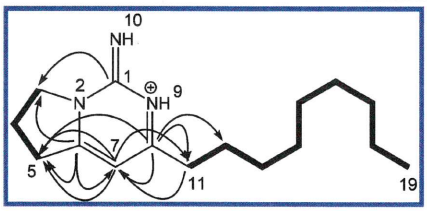

Figure 2. COSY (bold bonds) and key HMBC (arrows) correlations observed for monalidine A (**1**).

the CH_2-3 methylene protons correlated to a carbon at δ_C 163.7 (C-6) and to a likely guanidinium carbon at δ_C 154.0 (C-1). The presence of a guanidine group would account for the three nitrogens required by the molecular formula. The CH_2-4 and CH_2-5 methylene protons similarly correlated to C-6, while CH_2-5 also correlated to the methine carbon at δ_C 106.1 (C-7). In addition, CH_2-4 and CH_2-5 also correlated to a nitrogen resonating at δ_N −215.6 in the g^{15}NlrHMQC experiment, as did H-7 (δ_H 7.00). Analysis of the NMR data suggested that the structure of monalidine A (**1**) contained a disubstituted pyrrolidine ring in which the nitrogen forms part of a guanidine that is adjacent to a trisubstituted olefin residue. The NMR data also indicated that the structure of **1** had to contain a C_9 alkyl chain that terminated with a methyl triplet at δ_H 0.84. The resonances assigned to the CH_2-11 (δ_H 2.66) and CH_2-12 (δ_H 1.63) methylenes, which form the other end of the alkyl chain, both correlated to the sp^2 carbon resonance at δ_C 178.5 in the gHMBC spectrum. Because H-7 also showed HMBC correlations to this resonance, as well as to C-11 (δ_C 37.3) and H_2-11 (δ_H 2.66) correlated with C-7 (δ_C 106.1), the resonance at δ_C 178.5 was assigned to C-8 with the alkyl substituent attached through a C-8/C-11 bond. The chemical shift assigned to C-8 (δ_C 178.5) suggested that this was an aromatic/olefinic conjugated carbon attached to a nitrogen. A ^3J correlation observed between H_2-11 and a nitrogen resonating at δ_N −129.7, in the g^{15}NlrHMQC experiment, confirmed the assignment of N-9. A C-1/N-9 bond to give a 2-aminopyrimidine residue would satisfy the remaining constraints set by the NMR and ESIMS data, where, as suggested earlier, C-1 is a guanidinium carbon. The above assignments lead to the proposal of structure **1** for monalidine A.

In order to confirm the structure of monalidine A (**1**), we undertook its synthesis, starting with a base-catalyzed Claisen condensation between undecan-2-one (**2**) and dihydrofuran-2(3*H*)-one (**3**), to give 1-hydroxypentadecane-4,6-dione (**4**), using NaH and trifluoroethanol (TFE) in a modification of a previously reported procedure,[32] in 34% yield (Scheme 1).

Scheme 1. Synthesis of Monalidine A Hydrochloride (1)[a]

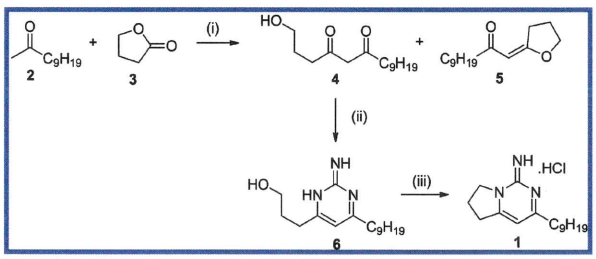

[a]Reagents and conditions: (i) CF_3CH_2OH, NaH, Et_2O, 2-undecanone, 5 °C → rt, 48 h, 34% of **4**; (ii) guanidine hydrochloride, *t*-BuOK, CF_3CH_2OH, 30 min, then **4**, rt, 48 h, 25%; (iii) Ph_3P, imidazole, I_2, CH_2Cl_2, −18 °C, 6 h, 67%.

Yields of **4** were around 6% when using sodium ethoxide, and the major product isolated was **5**. Despite the low yield of **4**, starting materials are inexpensive, and multigram quantities of **4** are accessible. Reaction of guanidine free base generated *in situ* in anhydrous TFE with **4** provided pyrimidine **6** in 25% yield. The product **6** was cyclized using a modified Mitsunobu protocol to give monalidine A (**1**) as its hydrochloride salt in 67% yield. The ^1H, ^{13}C, and HRCIMS spectra of synthetic **1** were indistinguishable from those observed for the natural compound (Supporting Information).

Arbusculidine A (**7**) gave an $[M+H]^+$ ion at m/z 242.1632 in the HR-ESI-MS appropriate for the molecular formula $C_{15}H_{19}N_3$, requiring eight sites of unsaturation. Analysis of the ^1H, ^{13}C, gHSQC, gCOSY60, and gHMBC NMR spectra identified an *n*-butyl chain [CH_2-1′ (δ_H 3.18/δ_C 26.3), CH_2-2′ (δ_H 1.71/δ_C 32.6), CH_2-3′ (δ_H 1.56/δ_C 23.7), and CH_3-4′ (δ_H 0.97/δ_C 14.6)], a two-methylene spin system [CH_2-4 (δ_H 3.10/δ_C 33.3) and CH_2-5 (δ_H 3.03/δ_C 28.2)], an aromatic methine [CH-6 (δ_H 6.86/δ_C 121.0)], and a methyl singlet at δ_H 2.43/δ_C 21.1 (CH_3-1″). Seven additional non-protonated sp^2 carbons were observed at δ_C 183.0 (C-3a), 164.0 (C-2), 146.7 (C-8a), 145.6 (C-7), 145.4 (C-5a), 130.4 (C-8), and 123.5 (C-8b) for a total of 15 carbons, as required by the molecular formula. Two remaining hydrogen atoms, three unaccounted for nitrogen atoms, and the carbon resonating at δ_C 164.0 (C-2) were assigned to a conjugated guanidine fragment. The spectroscopic data described above suggested that the structure of

DOI: 10.1021/acs.jnatprod.5b00070
J. Nat. Prod. 2015, 78, 1101−1112

arbusculidine (7) consisted of a heteroaromatic core with methyl, *n*-butyl, and two methylene chain appendages.

tROESY correlations between the terminal methylene of the *n*-butyl chain at δ_H 3.18 (H_2-1′) and the methyl at δ_H 2.43 (H_3-1″), between this methyl and the aromatic proton resonating at δ_H 6.86 (H-6), and between the aromatic proton and the methylene H_2-5 (δ_H 3.03) revealed that **7** presented a pentasubstituted benzene ring with *n*-butyl, methyl, and methylene substituents. The observed gHMBC correlations illustrated in Figure 3 confirmed this structural fragment, and

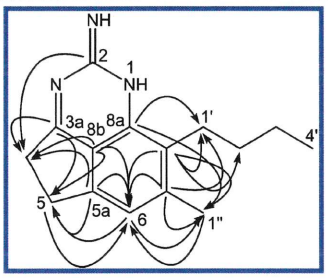

Figure 3. Key HMBC correlations observed for arbusculidine A (7).

the carbon chemical shifts from C-5a to C-8b could be assigned (Table 1). Of the two remaining unassigned carbon resonances (δ_C 183.0 and 164.0), the carbon at δ_C 183.0 showed HMBC correlations to both the H_2-4 (δ_H 3.10) and H_2-5 (δ_H 3.03) methylene protons. With the carbons at δ_C 145.4 and 123.5 already assigned to C-5a and C-8b, respectively, the resonance at δ_C 183.0 was assigned to C-3a, with the two-methylenes chain comprising part of a five-membered ring through C-3a/C-4 and C-5/C-5a carbon−carbon bonds. In order to satisfy the structural constraints required by the NMR and ESIMS data and complete the structure, the two remaining hydrogen atoms and the three nitrogens along with the carbon resonating at δ_C 164.0 (C-2) were, as suggested above, assigned to a conjugated guanidine residue embedded in a 2-aminopyrimidine ring with N-3/C-3a and C-8a/N-1 nitrogen−carbon bonds. The proposed structure for **7** was further confirmed by the observation of a weak four-bond gHMBC correlation between the methylene H-4 protons (δ_H 3.10) and C-2 (δ_C 164.0).

Table 1. NMR Data (^{1}H 600 MHz, ^{13}C 150 MHz, ^{15}N) for Monalidine A (1) (in DMSO-d_6) and Arbusculidine (7) (in Pyridine-d_5)

monalidine A (1)			arbusculidine (7)		
position	δ_C, type[a]	δ_H (J in Hz)[b]	position	δ_C, type[a]	δ_H (J in Hz)[b]
1	154.0, C		1		
2	−215.6 (δ_N)[c]		2	164.0, C	
3	51.9, CH_2	4.11, t (7.6)	3		
4	20.0, CH_2	2.24, qui (7.6)	3a	183.0, C	
5	31.2, CH_2	3.18, t (7.6)	4	33.3, CH_2	3.10, m
6	163.7, C		5	28.2, CH_2	3.03, m
7	106.1, CH	7.00, s	5a	145.4, C	
8	178.5, C		6	121.0, CH	6.86, s
9	−129.7 (δ_N)[c]		7	145.6, C	
10	n.o.[d]		8	130.4, C	
11	37.3, CH_2	2.66, t (7.2)	8a	146.7, C	
12	27.5, CH_2	1.63, tt (7.2, 7.2)	8b	123.5, C	
13	28.8, CH_2	1.24, m	1′	26.3, CH_2	3.18, dd (8.1, 7.9)
14	28.7, CH_2	1.24, m	2′	32.6, CH_2	1.71, m
15	28.6, CH_2	1.24, m	3′	23.7, CH_2	1.56, sex (7.4)
16	28.5, CH_2	1.24, m	4′	14.6, CH_3	0.97, t (7.3)
17	29.0, CH_2	1.24, m	1″	21.1, CH_3	2.43, s
18	22.1, CH_2	1.24, m			
19	13.9, CH_3	0.84, t (6.7)			

[a]125 MHz. [b]600 MHz. [c]^{15}N assignments were not calibrated with an external standard. The δ values have an accuracy of about 1 ppm in reference to CH_3NO_2 (0 ppm) and are assigned on the basis of ^{15}NHSQC and ^{15}NlrHMQC correlations. [d]n.o. = not observed.

Arbusculidine A (**7**) likely exists in equilibrium between several double bond isomers, which would explain why many of the carbon resonances in the ^{13}C NMR spectrum of **7** are not observed or are broad. Although **7** is related to the mirabilins[20c,d,21] and netamines,[22] this is the first such derivative that contains a benzene ring with the distinctive 4,5-dihydrocyclopenta[*de*]quinazoline skeleton.

Batzellamide A (**8**) was isolated as an optically active colorless solid that gave an $[M+H]^+$ ion in the HR-ESI-MS at m/z 541.3878, appropriate for the molecular formula $C_{30}H_{48}N_6O_3$, requiring 10 sites of unsaturation. Some of the resonances in the ^{1}H and ^{13}C NMR spectra recorded for **8** were doubled resulting in complex spectra, even though **8** gave a single clean molecular ion in the HR-ESI-MS spectrum, and at high dilution **8** gave only single sharp well-resolved peaks when analyzed by reversed-phase HPLC using a variety of solvent systems. Ultimately, aquisition of 1D and 2D NMR spectra in the three solvents MeOH-d_4 (Table 2), pyridine-d_5 (Table S1), and DMSO-d_6 (Table S2) allowed us to resolve the NMR complexity and analyze the data obtained for **8**. Comparison of the NMR data of **8** with the data obtained for the concurrently isolated batzelladines F (**13**), L (**14**), and nor-L (**15**) greatly facilitated the structure elucidation of **8**. As illustrated in Figure 1, other than the loss of the C-27 methine resonance along with the associated alkyl side chain, and the observation of an additional amide carbonyl at δ_C 169.3, all other structural features of **8** were the same as those found in **13**−**15**. The placement of a carbonyl at C-27 to give the amide accounted for the additional third oxygen required by the molecular formula of **8** compared with the two oxygens found the structures of **13**-**15**. In the gHMBC spectrum of **8**, the H_2-26 protons correlated to the additional amide carbonyl at δ_C ~169.3. Data collected in DMSO-d_6 (Table S2) showed that both of the resonances at δ_H 11.99 (bs) and 11.88 (bs), assigned to the amide proton on nitrogen atom linking C-27 and C-28, showed HMBC correlations to the resonances assigned to the C-26 methylene carbon at δ_C 36.87/36.84. The two N−H signals of the amide group suggested two different protonated forms of the acyl guanidinium group. The amide hydrogen at δ_H 11.88 correlated weakly to the C-27 amide carbonyl at δ_C 169.3. These HMBC correlations confirmed the structural assignment of **8**. Analysis of the tROESY data obtained for **8**, showed that, at the common stereocenters (C-2, C-4, C-7, and C-9), the relative configuration of **8** was the same as the one re-assigned by Snider and Busuyek to batzelladine F (**13**)[26c] and the same relative configuration assigned to batzelladine L (**14**) and nor-batzelladine L (**15**)[26e] (Figures 1 and 4). The *syn*-fused tricyclic ring system from C-2 to C-9 of **8** presents NMR chemical shifts and coupling constants

DOI: 10.1021/acs.jnatprod.5b00070
J. Nat. Prod. 2015, 78, 1101−1112

Table 2. NMR Data (^{1}H 600 MHz, ^{13}C 150 MHz, MeOH-d_4) for Batzellamide A (8)

position	δ_C, type	δ_H (J in Hz)
1	20.5, CH_3	1.25, d (6.4)
2	47.2, CH	3.54, ddq (2.9, 6.3, 9.6)
3	36.7, CH_2	2.21, m; 1.25, m
4	57.5, CH	3.73, m
5	31.0, CH_2	2.22, m; 1.67, m
6	31.0, CH_2	2.22, m; 1.67, m
7	57.4, CH	3.73, m
8	34.7, CH_2	2.25, m; 1.22, m
9	51.5, CH	3.41, m
10	150.6, CH_2	
11	35.8, CH_2	1.59, m; 1.53, m
12	30.4, CH_2	1.27, m
13	30.5, CH_2	1.27, m
14	30.5, CH_2	1.27, m
15	30.5, CH_2	1.27, m
16	30.3, CH_2	1.27, m
17	36.8, CH_2	1.61, m; 1.53, m
18	73.9/73.8, CH	4.98, m
19	20.7, CH_3	1.27, d (6.4)
20	171.0/170.0, C	
21	44.8/44.5, CH	3.23, dd (7.0, 5.0)
22	58.2/57.9, CH	4.14, m
23	29.2/29.0, CH_2	2.38, ddd (12.0, 6.3, 6.2); 1.68, m
24	31.2, CH_2	2.31, ddd (12.0, 6.0, 5.8); 1.80, m
25	57.0, CH	3.88, m
26	38.1, CH_2	2.92, ddd (13.3, 3.3, 3.3); 2.72, ddd (16.7, 14.0, 2.1)
27	169.3, C	
28	151.1, C	
29	50.7, CH	4.00, m
30	17.6/17.7, CH_3	1.36, d (6.7)

extremely similar to those in the same portion of batzelladine F (**13**), for which the relative configuration has been unambiguously established by synthesis of model compounds and careful NMR and molecular modeling analysis.[26c]

The doubling of some of the resonances observed in the NMR data of **8**, including that of NH-27a (in DMSO-d_6, Table S2), was attributed to the existence of slow equilibria likely involving the exchangeable protons associated with what are probably positively charged guanidine moieties that result from the presence of the TFA utilized in the HPLC purification. Compound **8** was named as batzellamide A, as it constitutes a carbon skeleton related to the batzelladines but devoid of the aliphatic alkyl chain attached to C-27.

The HR-ESI-MS data of hemibatzelladine J (**9**) gave an $[M+H]^+$ ion at m/z 449.3238, appropriate for the molecular formula of $C_{23}H_{40}N_6O_3$, that requires seven sites of unsaturation. Detailed analysis of the ^{1}H, ^{13}C, gHSQC, gCOSY60, and gHMBC NMR spectra of **9** (Table 3) revealed a close structural similarity between **9** and batzelladine D (**12**) (Figure 1). There appeared, however, to be three significant structural differences. First, the side chain no longer possessed a terminal methyl at C-13 as in **12**, but instead terminated with a primary alcohol (δ_H 3.37/δ_C 60.7), and the chain length was C_7 rather than C_9. Second, an additional tetrasubstituted alkene, with resonances at δ_C 100.4 and 148.7, was identified in the structure of **9**, and it accounted for the one additional degree of unsaturation that was required for **9** compared with **12**. These structural differences in **9** were reminiscent of the "western" half of batzelladine J (**16**), previously isolated from the sponge *M. unguifera*.[24e] Third, HMBC correlations between both the H_2-9 methylene protons (δ_H 2.73/3.17) and H-15 (δ_H 4.42), and C-6 (δ_C 164.6, ^4J correlation), C-7 (δ_C 100.4), and C-8 (δ_C 148.7), as well as between Me-16 (δ_H 1.26) and C-7 (δ_C 100.4), confirmed the placement of a tetrasubstituted double bond between carbons C-7 and C-8. Comparison with the NMR data for batzelladine J (**16**)[24e] and analysis of the tROESY data for **9** revealed the same relative configuration in **9** as in the "western" half of **12**, except for the relative configuration at C-15, which could not be assigned due to the absence of any NOE of methyl H_3-16. Because **9** can be considered as the "western moiety" of batzelladine J (**16**), it was named hemibatzelladine J.

Δ^{19}-Hemibatzelladine J (**10**) and Δ^{20}-hemibatzelladine J (**11**) were isolated as an inseparable mixture. The NMR spectra for the 1:2 mixture of **10** and **11** (Table 4) showed a marked resemblance to the spectra obtained for hemibatzelladine J (**9**) except that additional olefinic resonances were observed. The HR-ESI-MS of the mixture gave an $[M+H]^+$ ion at m/z 447.3092 appropriate for the molecular formula of

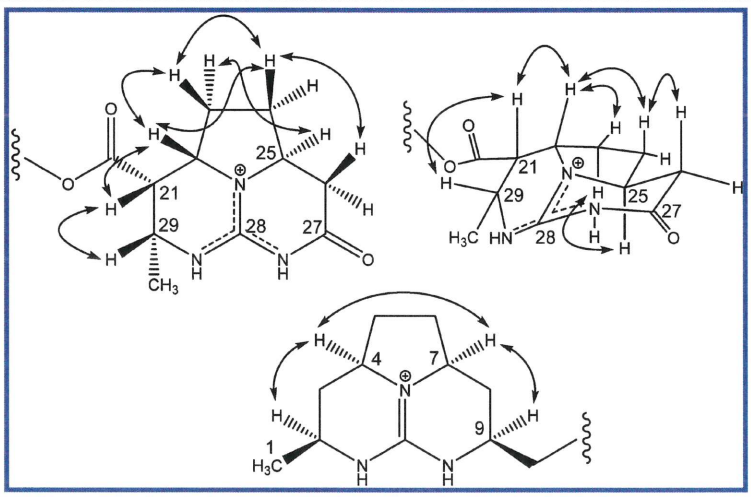

Figure 4. NOE correlations observed for the batzellamide A (**8**) "eastern" (top) and "western" (bottom) tricyclic moieties.

DOI: 10.1021/acs.jnatprod.5b00070
J. Nat. Prod. 2015, 78, 1101−1112

Table 3. NMR Data (^{1}H 600 MHz, ^{13}C 150 MHz, DMSO-d_6) for Hemibatzelladine J (9)

position	δ_C, type	δ_H (J in Hz)
1	156.7, C	
2	40.2, CH_2	3.11, dt (8.0, 8.0)
3	25.4, CH_2	1.53, m
4	25.3, CH_2	1.61, m
5	63.5, CH_2	4.10, m
6	164.6, C	
7	100.4, C	
8	148.7, C	
9	30.1, CH_2	3.17, dd (14.9, 9.1); 2.73, ddd (17.5, 15.3, 5.7)
10	28.6, CH_2	2.23, ddd (10.5, 10.1, 4.4); 1.61, m
11	56.7, CH	3.83, dddd (14.0, 13.0, 8.0, 4.0)
12	31.2, CH_2	2.32, m; 1.40, m
13	51.4, CH	3.52, m
14	147.2, C	
15	46.5, CH	4.42, bd (6.4)
16	24.0, CH_3	1.26, m
17	34.1, CH_2	1.61, m; 1.48, m
18	24.8, CH_2	1.29, m
19	25.4, CH_2	1.53, m
20	24.3, CH_2	1.32, m
21	24.8, CH_2	1.29, m
22	32.4, CH_2	1.39, m
23	60.7, CH_2	3.37[a]
NH-1a	−295 (δ_N)[b]	7.56, bt (5.3)
NH-13a	−285 (δ_N)[b]	8.75, bs
NH-14a	−293 (δ_N)[b]	8.41, bd (4.4)

[a]Partially overlapped. [b]^{15}N assignments were not calibrated with an external standard.

Table 4. NMR Data (^{1}H 600 MHz, ^{13}C 150 MHz, MeOH-d_4) for Δ^{19}-Hemibatzelladine J (10) and Δ^{20}-Hemibatzelladine J (11)

	Δ^{19}-hemibatzelladine J (10)		Δ^{20}-hemibatzelladine J (11)	
position	δ_C, type	δ_H (J in Hz)	δ_C, type	δ_H (J in Hz)
1	158.6, C		158.6, C	
2	42.0, CH_2	3.21, t (6.9)	42.0, CH_2	3.21, t (6.9)
3	26.6, CH_2	1.67, m	26.6, CH_2	1.67, m
4	27.0, CH_2	1.75, m	27.0, CH_2	1.75, m
5	65.0, CH_2	4.20, m	65.0, CH_2	4.20, m
6	166.2, C		166.2, C	
7	102.8, C		102.8, C	
8	149.6, C		149.6, C	
9	31.4, CH_2	3.3, m; 2.83, m	31.4, CH_2	3.3, m; 2.83, m
10	30.2, CH_2	2.3, m; 1.73, m	30.2, CH_2	2.3, m; 1.73, m
11	58.6, CH	3.86, m	58.6, CH	3.86, m
12	32.9, CH_2	2.24, bt (13.6); 1.55, m	32.9, CH_2	2.24, bt (13.6); 1.55, m
13	53.2, CH	3.61, m	53.2, CH	3.61, m
14	149.2, C		149.2, C	
15	48.5, CH	4.51, bq (5.9)	48.5, CH	4.51, bq (5.9)
16	24.5, CH_3	1.36, d (5.9)	24.5, CH_3	1.36, d (5.9)
17	25.9, CH_2	1.50, m	25.9, CH_2	1.50, m
18	35.4, CH_2	1.76, m	35.8, CH_2	1.66, m
19	131.7, CH	5.47, m	23.7, CH_2	2.20, m
20	129.3, CH	5.41, m	131.8, CH	5.47, m
21	24.6, CH_2	2.18, m	127.8, CH	5.45, m
22	33.4, CH_2	1.58, m	31.7, CH_2	2.27, bq (7.2)
23	62.2, CH_2	3.55, t (6.1)	62.5, CH_2	3.54, t (6.1)

$C_{23}H_{38}N_6O_3$, two hydrogens less and one degree of unsaturation more than hemibatzelladine J (**9**). The HRMS and NMR data together indicated that **10** and **11** were unsaturated analogues of **9**. In the major Δ^{20} isomer **11**, the H_2-23 methylene protons (δ_H 3.54) of the terminal primary alcohol were observed coupled to the H_2-22 methylene protons at δ_H 2.27 in the gCOSY60 spectrum, and correlating in the gHMBC spectrum to the olefinic carbons at δ_C 127.8 (C-21) and δ_C 131.8 (C-20). Moreover, the vinylic hydrogens H_2-22 also showed couplings to C-20 and C-21. These results established a Δ^{20} double bond in **11**. In the COSY spectrum, the minor isomer **10** presented a sequential spin system from CH_2-23 (δ_H 3.55) to CH_2-21 (δ_H 2.18) through CH_2-22 (δ_H 1.58), while in the HMBC spectrum the vinylic hydrogens H_2-22 showed couplings to C-20 (δ_C 129.3) and C-19 (δ_C 131.7), indicating a Δ^{19} insaturation. Although the ^{13}C chemical shifts of C-21 (δ_C 24.6) in **10** and of C-19 (δ_C 23.7) in **11** suggested a *Z* configuration for each double bond, the respective vinylic carbons C-18 (δ_C 35.4) in **10** and C-22 (δ_C 31.7) in **11** did not confirm such assignment, which is suggestive only. All the other structural features, including the relative configuration in the tricyclic guanidine portion, were identical to that of **9**. Therefore, compound **10** was named Δ^{19}-hemibatzelladine J and compound **11** Δ^{20}-hemibatzelladine J.

In addition to alkaloids **1** and **7**−**11**, the known batzelladines D (**12**), F (**13**), L (**14**), and norbatzelladine L (**15**)[26b,d,e] were isolated as the major alkaloid constituents of our sample of the sponge *M. arbuscula*. Batzelladine D (**12**)[26b,33] was shown to display activity in an ELISA-based assay to assess the association of soluble CD4 (sCD4) to immobilized recombinant gp120.[26a] Batzelladine F[26b,34] induced the dissociation of p56lck with CD4, an association which is required for antigenic activation.[26b] Batzelladine L (**14**) has been shown to exhibit activity against *Mycobacterium tuberculosis*, along with anti-HIV activity, anti-fungal and anti-bacterial activity, anti-malarial activity, and anti-leishmanial activity, as well as cytotoxicity against a variety of cancer cell lines.[26d] Norbatzelladine L has shown activity against three cancer cell lines and against *Plasmodium falciparum*.[26e] None of the alkaloids **12**−**15** has previously been assayed against *L. infantum*, endemic to Brazil and the etiologic agent of the deadly visceral leishmaniasis, or against *T. cruzi*, the parasite responsible for Chagas disease.

Monalidine A (**1**), batzelladines F (**13**), L (**14**), and norbatzelladine L (**15**) were found to be active against *T. cruzi* trypomastigotes with IC_{50} = 8 μM, 5 μM, 2 μM, and 7 μM, respectively (Table 5), while batzelladine D (**12**) showed the weakest activity at 64 μM. These values compare favorably with the standard drug benznidazole (IC_{50} = 441 μM), with alkaloids **1** and **13**−**15** being at least 54-fold more effective *in vitro*. In addition, alkaloids **14** and **15** demonstrated higher selectivity indices (7 and 12, respectively) when evaluated against monkey kidney cells (LLC-MK2), when compared with positive controls (Table 5). A previous report observed that the structurally less complex merobatzelladines A and B, bearing a single tricyclic guanidine core flanked by two alkyl chains, showed anti-parasitic activity against *T. brucei* with IC_{50} = 0.24 μg/mL.[35]

The guanidine alkaloids **1** and **12**−**15** also displayed activity against *L. infantum* promastigotes (Table 5). However, no activity was observed against intracellular *L. infantum* amastigotes for any of these compounds. This result may well be due to the lack of specific receptors in macrophages, their metabolism by macrophages or the metabolic differences of *L.*

DOI: 10.1021/acs.jnatprod.5b00070
J. Nat. Prod. 2015, 78, 1101−1112

Table 5. Anti-leishmanial, Anti-trypanosomal, and Cytotoxicity Activities of Guanidine Alkaloids 1 and 12–15[a]

compound	*T. cruzi*	*L. infantum*	cytotoxicity[b]
monalidine A (**1**)	8[c] (6.83–9.60)	2[c] (2.28–2.63)	26 (23.67–29.15)
batzelladine D (**12**)	64[c] (31.98–129.4)	2[c] (2.21–3.21)	130 (118.4–142.2)
batzelladine F (**13**)	5[c] (4.42–5.20)	4[c] (3.36–4.61)	10 (8.52–12.39)
batzelladine L (**14**)	2[c] (2.06–2.64)	2[c] (1.96–2.39)	22 (19.89–24.05)
norbatzelladine l (**15**)	7[c] (5.69–8.43)	2[c] (1.58–2.05)	85 (76.01–96.47)
miltefosine	nd	16 (15.45–17.46)	122 (94.78–96.47)
benznidazole	441 (406.16–478.40)	nd	477 (426.82–492.79)

[a]Cell viability was determined using the MTT assay. Data are presented as IC_{50} (95% CI), where IC_{50} is the 50% inhibitory concentration, in μM, and 95% CI is the 95% confidence interval. [b]Measured on LLC-MK2 cells. [c]$p < 0.05$ (compared to standard drug). nd = not determined.

infantum amastigotes.[36] Related guanidine alkaloids have shown anti-parasitic activity against *Leishmania* and *Plasmodium* parasites.[20d,26d,e,35] Mirabilin B showed anti-parasitic activity against *L. donovani*, with IC_{50} = 17 μg/mL.[20d] Crambescidine 800 and a number of batzelladines displayed anti-parasitic activity against *L. donovani*, with IC_{50} values in the range 1.9–8.5 μg/mL, among which batzelladine L (**14**) was the most potent,[26d] with IC_{50} = 1.9 μg/mL, a value that is comparable to the anti-leishmanial activity that we observed for **14** against *L. infantum*.

Investigation into the lethal action of compounds with anti-leishmanial activity may well provide useful information regarding targets and potential metabolic pathways related to anti-parasitic activity. Therefore, we decided to investigate the lethal activity of batzelladine L (**14**) and norbatzelladine L (**15**), two effective anti-leishmanial alkaloids isolated in the present investigation, using three distinct approaches. First, we investigated the potential of **14** and **15** to affect the plasma membrane permeability of *Leishmania* using the fluorescent vital dye SYTOX Green (Figure 5). Both **14** and **15** altered the

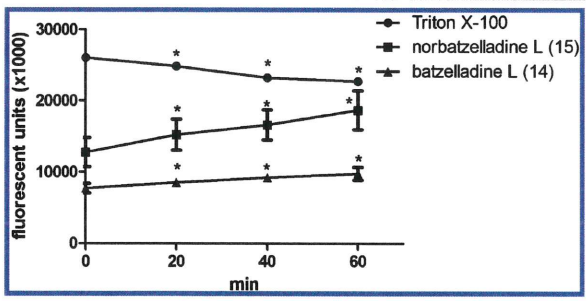

Figure 5. Permeability of *Leishmania* plasma membrane incubated with alkaloids **14** and **15** assessed with the vital dye SYTOX Green. Parasites were treated with Triton X-100 for 100% permeabilization. A control group (untreated) was also included. The fluorescence was determined using a fluorimetric microplate reader with excitation and emission wavelengths of λ_{max} = 485 and 520 nm, respectively. *$p < 0.05$.

plasma membrane permeability of *L. infantum* promastigotes. Norbatzelladine L (**15**) promoted an increase in the fluorescence after the initial incubation period, resulting in 82% of fully permeabilized parasites exposed to Triton X-100 at 60 min (Figure 5). Similarly, batzelladine L (**14**) also altered the permeability of the parasite plasma membranes, though to a lesser extent, resulting in 43% of the permeability of fully permeabilized *L. infantum* membranes. Because the only structural distinction between batzelladine L (**14**) and norbatzelladine L (**15**) is the length of the alkyl side chain, the activity profile of **14** and **15** would appear to be related to the lipophilic nature of the two alkaloids, with the more lipophilic batzelladine L (**14**) being less active than norbatzelladine L (**15**).

The leishmanicidal activity of alkaloids **14** and **15** may be related to cellular metabolic enzymatic activity in mitochondria, which is an indicative of cell viability.[37] Our results indicated that both **14** and **15** mediate a leishmanicidal effect as no oxidation of the MTT by mitochondrial dehydrogenases was observed. A significant loss of mitochondrial membrane potential depletes cell energy and culminates in cell death.[38] Because mitochondrial function is a potential target for batzelladines **14** and **15**, we looked for inhibition of mitochondrial membrane potential in *Leishmania* promastigotes. Both alkaloids induced depolarization of the mitochondrial membrane potential of promastigotes and reduced the fluorescence levels of MitoTracker Red when compared to untreated parasites (Figure 6), with a 30% reduction in the presence of norbatzelladine L (**15**) and 35% reduction with batzelladine L (**14**).

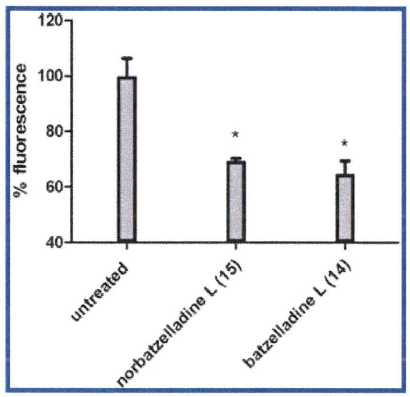

Figure 6. Mitochondrial membrane potential of *L. infantum* incubated with batzelladine alkaloids **14** and **15**. MitoTracker Red was incubated with treated and untreated parasites (control group). The fluorescence was determined using a fluorimetric microplate reader with excitation and emission wavelengths of λ_{max} = 540 and 595 nm, respectively. *$p < 0.05$.

As the susceptibility of many parasites to oxidative stress is a well-known phenomenon, and the generation of reactive oxygen species (ROS) and inhibition of endogenous antioxidant enzymes represent new therapeutic approaches for the development of anti-parasitic drugs,[7,38] batzelladines **14** and **15** were incubated with *L. infantum* and screened for ROS. Batzelladine L (**14**) induced the highest increase in ROS production when compared to untreated parasites, resulting in

DOI: 10.1021/acs.jnatprod.5b00070
J. Nat. Prod. 2015, 78, 1101–1112

approximately a 4000-fold higher fluorescence intensity than that produced by the internal positive control (Figure 7).

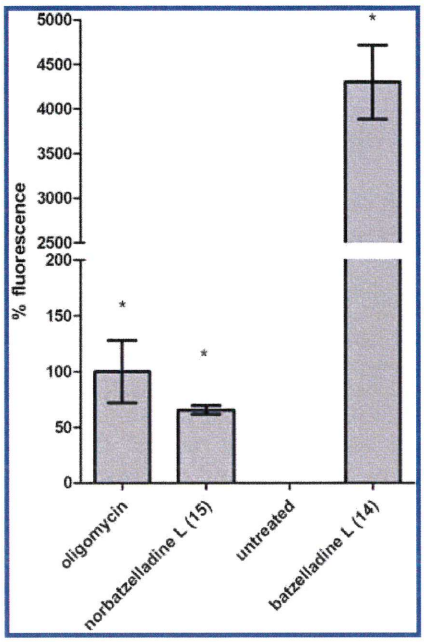

Figure 7. Production of reactive oxygen species (ROS) in *L. infantum* incubated with alkaloids **14** and **15** (tested in the IC_{50} values of 2 μM). 2′,7′-Dichlorodihydrofluorescein diacetate (H_2DCf-DA) was incubated with the cells, and the fluorescence intensity was detected using a fluorimetric microplate reader with excitation and emission wavelengths of λ_{max} = 485 and 520 nm, respectively. Oligomycin (20 μM) was used as positive control. *p < 0.05.

Considering normalized data of oligomycin-treated parasites (100%) and untreated parasites (0%), norbatzelladine L (**15**) also up-regulated ROS in *Leishmania* promastigotes with a 65% increase in fluorescence relative to the untreated group (Figure 7). Many other synthetic compounds kill *Leishmania* by self-generating ROS, such as doxorubicin, mitomycin C, plumbagin, and 2-methoxy-1,4-naphthoquinone.[39] Because elevated levels of ROS produce a lethal effect in protozoan parasites,[40] we suggest that batzelladines **14** and **15** induce oxidative stress in *L. infantum* promastigotes which contributes to parasite cell death.

Monalidine A (**1**) was also tested in cytotoxic assays against three tumor cell lines, A549, HeLa, and MCF-7, and against the normal breast cell line MCF-10A, but was essentially devoid of any cytotoxic activity.

CONCLUSION

HPLC-UV-ELSD-MS-guided investigation of an extract of *M. arbuscula* has led to the isolation of three new classes of metabolites, namely monalidine A (**1**), batzellamide A (**8**), and hemibatzelladines, as well as a new member of the ptilocaulin/mirabilin/netamine family of guanidine/2-aminopyrimidine alkaloids, arbusculidine A (**7**). Monalidine A represents a new scaffold related to crambescins, with an oxidized 2-aminopyrimidine ring, and devoid of the γ-guanidine butyl ester moiety. The synthesis of monalidine A (**1**) not only provided confirmation of its structure but also provided material for biological testing. Batzellamide A (**8**) is the first batzelladine alkaloid devoid of an alkyl chain attached to C-27. The isolation of *M. arbuscula* minor guanidine and pyrimidine alkaloids adds to the diversity of these unique chemotypes.

Recently, arginine was established as the putative precursor of bacterial macrocyclic guanidine polyketides.[41] Although a common biogenetic pathway for bacterial and marine sponge guanidine polyketides remains elusive at this point, there is increasing evidence of prokaryotic origin for many sponge metabolites, particularly those that are PKS or NRPS derived.[42] A similar hypothesis clearly deserves consideration for these marine sponge guanidine alkaloids. The effectiveness of marine sponge guanidine alkaloids as bioactive secondary metabolites[13−18] is herein illustrated by the anti-parasitic activity and the apparent mode of action of batzelladines L (**14**) and norbatzelladine L (**15**). Minor structural differences between these alkaloids result in distinct anti-leishmanial activity profiles. The potential structure−activity relationships observed for the batzelladine series **13**−**15** and batzelladine M, as well as for **12**, batzelladine C, and dehydrobatzelladine C, warrant further investigation, not only to envisage a potential new anti-leishmanial drug lead but also to further unravel cellular death pathways in *Leishmania* parasites.

EXPERIMENTAL SECTION

General Experimental Procedures. Optical rotations were measured using a JASCO P-1010 polarimeter. UV spectra were recorded on a Shimadzu UV-3600 spectrophotometer. IR spectra were obtained on a Shimadzu IRAffinity-1 Fourier transform infrared spectrophotometer on silica plates. NMR spectra were obtained at 25 °C, with TMS as an internal standard, using a Bruker ARX 9.4 T spectrometer operating either at 400.35 MHz (^{1}H) or at 100.10 MHz (^{13}C), and an Agilent Technologies 500/54 Premium Shielded operating either at 499.84 MHz (^{1}H) or at 125.70 MHz (^{13}C). Higher-field NMR analyses were recorded on a Bruker AV-600 spectrometer with a 5 mm CPTCI cryoprobe, for which the ^{1}H chemical shifts are referenced to the residual DMSO-d_6, MeOH-d_4, or pyridine-d_5 signals (δ 2.49, 3.30, and 7.22 ppm, respectively), and ^{13}C chemical shifts are referenced to the DMSO-d_6, MeOH-d_4, or pyridine-d_5 solvent peaks (δ 39.5, 49.0, and 123.9 ppm, respectively). HRMS and direct insertion MS/MS analyses were performed on a Thermo Scientific Velos LTQ Orbitrap (eletrospray), and low- and high-resolution ESI-quadrupole ion trap (QIT)-MS were recorded on a Bruker-Hewlett-Packard 1100 Esquire LC system mass spectrometer. Analytical and semipreparative HPLC separations were performed with a Waters instrument (600 quaternary pump and 2487 double-beam UV detector). HPLC-UV-ELSD-MS analyses were performed using a Waters Alliance 2695 instrument coupled online with a Waters 2996 photodiode array detector and a Waters 2424 evaporative light-scattering detector, followed by a Micromass ZQ 2000 detector with an electrospray interface. The photodiode array scanned the samples at λ_{max} = 230 and 254 nm. The mass spectrometer detector was optimized using the following conditions: capillary voltage, 3.00 kV; source block temperature, 100 °C; desolvation temperature, 350 °C; voltage cone, 25 V; electrospray, positive mode; detection range, 200−550 Da with total ion count extracting acquisition. Cone and desolvation gas flows were set at 50 and 350 L h^{-1}, respectively, with a nitrogen source. HPLC-MS/MS analyses were performed using a system that utilized a Waters Alliance 2695 controller and pump, connected to a Waters 2996 diode-array detector linked in series to a Micromass Quattro LC triple-quadrupole detector, with an API Z-spray ion source and a high-flow electrospray ionization probe, operating in positive mode. HPLC-MS/MS analyses were performed using a Waters Spherisorb ODS2 column (125 mm × 4.0 mm i.d., 5 μm), with a 0.8 mL min^{-1} flow rate and diode array detection in the range of λ_{max} = 215−600 nm, using a gradient of H_2O/MeCN/MeOH, starting at 60:15:25 until 40:15:45 during 8 min, and then to 30:15:55 during 7 min. A post-column split was used to direct 0.25 mL min^{-1} of

DOI: 10.1021/acs.jnatprod.5b00070
J. Nat. Prod. 2015, 78, 1101−1112

the effluent toward the ionization source. Nitrogen was used as the nebulizing (34 L h^{-1}) and desolvation gas (834 L h^{-1}). The ESI capillary probe voltage was set to 3.57 kV, and the sampling and extraction cones were set to 46 and 4 V, respectively. Argon gas was used in the fragmentation experiments, in which precursor ions were accelerated using an energy collision ramp between 5 and 35 eV.

Isolation. The sponge *Monanchora arbuscula* was collected at Cabo Frio (Rio de Janeiro state) in April 2011. A voucher of the collected sponge has been deposited at the Museu Nacional do Rio de Janeiro, Universidade Federal do Rio de Janeiro (MNRJ 11211). A 360 g freeze-dried sample of the sponge was homogenized and extracted with 2 L of MeOH. The solvent was evaporated to 500 mL. The resulting MeOH extract was diluted with 50 mL of H_2O and partitioned with hexane (3 × 500 mL). The MeOH/H_2O fraction was evaporated to dryness, to give 40.5 g of a polar fraction containing mainly alkaloids (TLC analysis using Dragendorff reagent). This fraction was partially desalted in 1:1 MeOH/EtOH. The partially salt-free fraction was separated by C_{18} reversed-phase column chromatography (10 g), with a H_2O/MeOH gradient as the eluent, in portions of approximately 1 g each. Three fractions were obtained: 100% H_2O (1.2 g), 1:1 H_2O/MeOH (MaMe50, 7.9 g), and 100% MeOH (1.6 g).

The 100% H_2O fraction (1.2 g) was dissolved in 200 mL of H_2O, to which was added 21 g of a 1:1:1 mixture of XAD-2/XAD-4/XAD-7. The mixture was left shaking overnight. The resin mixture was collected by filtration and desorbed with 100 mL of MeOH and 100 mL of 1:1 MeOH/acetone. The organic fractions were pooled and evaporated to give 300 mg of an organic extract (MaMeH), which was separated by chromatography on Sephadex LH20 (MeOH), to give 10 fractions. The third (MaMeH-3, 46 mg) was subjected to a semi-preparative HPLC separation with a C8 reversed-phase column (Inertsil, C8-3, 4.6 × 250 mm, 5 μm) using a gradient of MeOH in H_2O+0.1% TFA starting at 45:55 until 75:25 during 37 min, to give three fractions. The third (MaMeH-3C, 3.5 mg) was purified by HPLC with a reversed-phase phenyl column (Inertsil Ph-3, 4.6 × 250 mm, 5 μm) and a gradient of MeCN in H_2O+0.1% TFA starting at 30:70 until 45:55 over 37 min. Pure monalidine (**1**) was obtained from this purification (1.2 mg).

The MaMe50 fraction (7.9 g) was subjected to a separation by chromatography on Sephadex LH20 (MeOH), to give five fractions. The fourth (MaMe50Me-4, 39.7 mg) was separated by HPLC using a C_8 reversed-phase column (Inertsil, C8-3, 4.6 × 250 mm, 5 μm) using a gradient of MeOH in H_2O+0.1% TFA starting at 45:55 until 75:25 over 37 min, to give six fractions. The fourth (MaMe50Me-4D, 9.0 mg) was purified by HPLC using a C8 reversed-phase column (Inertsil, C8-3, 4.6 × 250 mm, 5 μm) using a gradient of MeOH in H_2O+0.1% TFA starting at 50:50 until 70:30 during 37 min, to give pure arbusculidine A (**7**, 1.7 mg).

The 100% MeOH fraction (1.6 g) was separated by chromatography on Sephadex LH-20 (MeOH). Four fractions were obtained and were analyzed by HPLC-ELSD-PDA-MS. The first (MaMe1Me-1, 934 mg) was purified by HPLC using an Inertsil C8-3 column (5 μm, 4.6 × 250 mm) and a gradient of MeOH in H_2O, increasing from 70% MeOH to 75% MeOH over the first 20 min and remaining in this last condition an additional 5 min, with a flow rate of 1.0 mL/min, detected by an ELSD. This separation afforded six fractions: MaMe1Me-1A (391.0 mg), MaMe1Me-1B (38.5 mg), MaMe1Me-1C (25.4 mg), MaMe1Me-1D (148.6 mg), MaMe1Me-1E (45.0 mg), and MaMe1Me-1F (20.0 mg). The purity of fractions MaMe1Me-1B (norbatzelladine L, **15**, 38.5 mg) and MaMe1Me-1D (batzelladine L, **14**, 148.6 mg) was checked by HPLC-ELSD-PDA-MS. Fraction MaMe1Me-1A (391 mg) was separated by HPLC using 6:4 MeOH +0.1% TFA/H_2O+0.1%TFA in an Inertsil C8-4 column (5 μm, 14 × 250 mm) during 80 min. This separation yielded seven fractions: MaMe1Me-1A1 (230.5 mg), MaMe1Me-1A2 (35.1 mg), MaMe1Me-1A3 (40.7 mg) MaMe1Me-1A4 (55.0 mg) MaMe1Me-1A5 (9.8 mg) MaMe1Me-1A6 (5.0 mg), and MaMe1Me-1A7 (8.6 mg). Fraction MaMe1Me-1A1 was further separated using an Inertsil C8-4 column (5 μm, 14 × 250 mm) with a gradient of MeOH+0.1% TFA/H_2O +0.1% TFA from 60:40 to 75:25 over 37 min and 8 mL/min flow rate. A total of five fractions were obtained from this separation: MaMe1Me-1A1A (3.2 mg), MaMe1Me-1A1B (143.0 mg), MaMe1Me-1A1C (10.6 mg), MaMe1Me-1A1D (7.9 mg), and MaMe1Me-1A1E (25.3 mg, batzelladine D, **12**). Fraction MaMe1Me-1A2 (35.1 mg) was separated by HPLC using an Inertsil C8-4 column (5 μm, 14 × 250 mm) and a gradient of MeOH+0.1% TFA/H_2O+0.1% TFA from 60% MeOH to 75% MeOH during 37 min at a 0.8 mL/min flow rate. Two fractions were obtained. The first (MaMe1Me-1A2A, 4.6 mg) was further separated by HPLC using an Inertsil C8-4 column (5 μm, 14 × 250 mm) and 20:80 MeCN/H_2O+0.1% TFA during 25 min, to give 1.2 mg of an impure mixture of Δ^{19}-hemibatzelladine J (**10**) and Δ^{20}-hemibatzelladine J (**11**), as well as 1.2 mg of impure hemibatzelladine J (**9**). A final C_{18} reversed-phase HPLC purification of these two fractions using an InertSustain column (5 μm, 25 × 1.0 cm), with 78% (0.05% TFA/H_2O)/MeCN as eluent gave a pure sample of **9** (0.9 mg) and a clean sample of the mixture of **10** and **11** (0.6 mg).

Fraction MaMe1Me-1A3 was separated using an Inertsil C8-4 column (5 μm, 14 × 250 mm) with a gradient of MeOH+0.1% TFA/H_2O +0.1% TFA from 60:40 to 75:25 during 37 min and 8 mL/min flow rate, to give three fractions: MaMe1Me-1A3A (5.6 mg), MaMe1Me-1A3B (1.5 mg), and MaMe1Me-1A3C (27.2 mg, batzelladine F, **13**). The identities of batzelladines D (**12**), F (**13**), L (**14**), and norbatzelladine L (**15**) were established by analysis of ^{1}H, ^{13}C, COSY, HSQC, and HMBC NMR data, HR-ESI-MS and HPLC-MS/MS analyses, as well as by comparison with literature data.[26a,b,d,e]

Fraction MaMe1Me-1A7 (8.6 mg) was separated by HPLC using an Inertsil C8-4 column (5 μm, 14 × 250 mm) with 55:45 MeOH/H_2O +0.1% TFA during 30 min to give 2.0 mg of impure batzellamide A (**8**). A final C_{18} reversed-phase HPLC purification of this sample using an InertSustain column (5 μm, 25 × 1.0 cm), with 68% (0.05% TFA/H_2O)/MeCN as eluent, gave a pure sample of **8** (1.5 mg).

Monalidine A (1). Colorless glassy solid (1.2 mg); UV (MeOH) λ_{max} (log ε) 205 (4.10), 222 (4.11), 296 (3.56) nm; IR film on Si plate (ν_{max}) 3469, 3298, 3113, 2956, 2924, 2852, 1662, 1643, 1627, 1575, 1463, 1436, 1415, 1394, 1220, 669 cm^{-1}. ^{1}H NMR and ^{13}C NMR, see Table 1; HR-ESI-QIT-MS *m/z* 262.2247 $[M+H]^+$ (calcd for $C_{16}H_{28}N_3$, 262.2283).

Arbusculidine A (7). Colorless glassy solid (1.7 mg); UV (MeOH) λ_{max} (log ε) 208 (4.28), 236 (4.28), 255 (3.90), 307 (2.02) 339 (0.81) nm; ^{1}H NMR and ^{13}C NMR, see Table 1; HR-ESI-QIT-MS *m/z* 242.1632 $[M+H]^+$ (calcd for $C_{15}H_{20}N_3$, 242.1657).

Batzellamide A (8). Colorless glassy solid (1.5 mg); $[\alpha]_D$ −9.5 (*c* 1.0, MeOH); UV (68% (0.05% TFA/H_2O)/MeCN) λ_{max} (log ε) 206 (4.09) nm; ^{1}H NMR and ^{13}C NMR, see Table 2; HR-ESI-QIT-MS *m/z* 541.3878 $[M+H]^+$ (calcd for $C_{30}H_{49}N_6O_3$, 541.3866).

Hemibatzelladine J (9). Colorless glassy solid (0.9 mg); $[\alpha]_D$ −5.8 (*c* 0.6, MeOH); UV (78% (0.05% TFA/H_2O)/MeCN) λ_{max} (log ε) 200 (3.20), 234 (3.23), and 299 (3.23) nm; ^{1}H NMR and ^{13}C NMR, see Table 3; HR-ESI-QIT-MS *m/z* 449.3238 $[M+H]^+$ (calcd for $C_{23}H_{41}N_6O_3$, 449.3240).

Δ^{19}-Hemibatzelladine J (10) and Δ^{20}-Hemibatzelladine J (11). Colorless glassy solid (0.6 mg); $[\alpha]_D$ +38 (*c* 0.4, MeOH) in a 1:2 mixture of **10**/**11**; UV (78% (0.05% TFA/H_2O)/MeCN) λ_{max} (log ε) 231 (3.39) and 299 (3.39) nm; ^{1}H NMR and ^{13}C NMR, see Table 4; HR-ESI-MS *m/z* 447.3092 $[M+H]^+$ (calcd for $C_{23}H_{39}N_6O_3$, 447.3084).

General Experimental Synthesis Procedures. Reactions were mechanically or magnetically stirred and monitored by TLC using Kieselgel 60 F254 silica coated plates which were visualized using I_2, phosphomolybdic acid, vanillin reagents, or under UV light. All anhydrous reactions were carried out in oven-dried glassware and under a static argon atmosphere. Anhydrous Et_2O and CH_2Cl_2 were obtained with a solvent purification system. Trifluoroethanol (TFE) was dried over molecular sieves (3 Å powder). Flash chromatography was carried out on 60A silica gel with the eluting solvent stated in each case. Infrared spectra were obtained on KBr pellets with an FTIR spectrometer.

1-Hydroxypentadecane-4,6-dione (4). Anhydrous TFE (1 mL) was added to a mechanically stirred suspension of NaH (60% dispersion in mineral oil, 4.8 g, 120.0 mmol, 2.40 equiv) in anhydrous

DOI: 10.1021/acs.jnatprod.5b00070
J. Nat. Prod. 2015, 78, 1101−1112

Et_2O (200 mL) taking care to vent pressure as necessary. The resultant suspension was cooled to 5 °C, dihydrofuran-2(3*H*)-one (4.5 g, 4 mL, 52.3 mmol, 1.05 equiv) was added dropwise, and the mixture was stirred for 30 min. Undecan-2-one (8.5 g, 49.9 mmol, 1.0 equiv) was then added dropwise, and stirring was continued at room temperature (rt) for 48 h. After complete consumption of undecan-2-one (TLC, R_f = 0.74, 50% Et_2O in petroleum ether), the mixture was cooled to 0 °C, and a NH_4SO_4 solution (aqueous, 10%, 300 mL) was cautiously added. The pH of the aqueous layer was adjusted to pH 6 by the addition of further NH_4SO_4 solution when necessary, and the organic phase was separated. The aqueous layer was extracted with Et_2O (3 × 150 mL), the combined organic extracts were dried ($MgSO_4$), and the solvent was removed under reduced pressure to give the crude product as a yellow oil. Purification by silica gel chromatography (75% Et_2O in petroleum ether) gave a waxy solid which was recrystallized (Et_2O/hexane) to give **4** (4.29 g, 16.7 mmol) in 34% yield as pale yellow needles; mp 56−57 °C (Et_2O/hexane); TLC R_f = 0.33 (Et_2O:petroleum ether 75:25); IR film on KBr (ν_{max}) 3278, 2954, 2932, 2919, 2873, 2849, 1638, 1598 cm^{-1}; ^1H NMR (400 MHz, DMSO-d_6) 1:1 mixture of enol/keto forms δ 0.86 (t, J = 7.0 Hz, 3H, CH_3), 1.19−1.32 (m, 12H, 6 x CH_2), 1.40−1.56 (m, 2H, CH_2), 1.57−1.71 (m, 2H, CH_2), 2.26−2.35 (2*t*, J = 7.5 Hz, 2H, CH_2 *keto/enol*), 2.44−2.51 (m, 2H, CH_2) 3.32−3.45 (m, 2H, CH_2), 3.66 (s, 1H, CH_2 *keto*), 4.40−4.53 (brm, 1H, OH), 5.69 (s, 0.5 H, CH *enol*), 15.63 (s, 0.5 H, OH *enol*); ^{13}C NMR (100 MHz, DMSO-d_6) *1:1 mixture of enol/keto forms*, δ 13.9, 22.1, 28.4, 28.6, 28.6, 28.7, 28.7, 28.8, 28.9, 31.3, 31.3, 56.3, 59.9, 60.0 99.2, 193.8, 194.6, 205.3. HRCIMS m/z 257.2107 $[M+H]^+$ (calcd for $C_{15}H_{29}O_3$, 257.2111); LRCIMS m/z 257 (23%), 239 ($[M+H-H_2O]^+$, 100%), 133 (19%).

3-(2-Imino-6-nonyl-2,3-dihydropyrimidin-4-yl)propan-1-ol (6). Guanidine hydrochloride (1.27 g, 13.29 mmol, 1.02 equiv) was added to a solution of potassium *t*-butoxide (1.47 g, 13.10 mmol, 1.01 equiv) in anhydrous TFE (10 mL). The resultant suspension was stirred at rt for 30 min, diketone **4** (3.33 g, 13.01 mmol) was added, and stirring was continued at rt for 48 h. After the complete consumption of **4** (TLC, Et_2O/petrol = 75/25, R_f = 0.33) the solvent was removed under reduced pressure to give the crude product as a yellow solid. Purification by silica gel chromatography (10% MeOH in EtOAc) gave **6** (905.0 mg, 3.24 mmol) in 25% yield as an amorphous white solid. TLC R_f = 0.33 ($CHCl_3$:MeOH 90:10); IR film on KBr (ν_{max}) 3470, 3445, 3321, 3174, 2955, 2926, 2919, 2849, 1653, 1639, 1589, 1562; ^1H NMR (400 MHz, DMSO-d_6) δ 6.38 (s, 1H, CH); 5.21 (s, 2H, NH_2); 3.69 (t, J = 6 Hz, 2H, CH_2); 2.69 (t, J = 8 Hz, 2H, CH_2); 2.51 (t, J = 8 Hz, 2H, CH_2); 1.92 (qui, J = 7 Hz, 2H, CH_2); 1.64 (qui, J = 7 Hz, 2H, CH_2); 1.26 (m, 12H, 6 × CH_2); 0.87 (t, J = 8 Hz, 2H, CH_3); ^{13}C NMR (100 MHz, DMSO-d_6) 172.8, 170.9, 162.7, 109.7, 62.3, 38.0, 34.7, 32.1, 31.1, 29.7, 29.7, 29.5, 29.1, 22.9, 14.3; HRCIMS m/z 280.2384 $[M+H]^+$ (calcd for $C_{16}H_{30}O_1N_3$, 280.2383).

Monalidine Hydrochloride (1). A solution of **6** (905 mg, 3.24 mmol) in anhydrous CH_2Cl_2 (80 mL) was cooled to −18 °C using a salt ice bath. Then Ph_3P (1.96 g, 7.47 mmol, 2.31 equiv), imidazole (823 mg, 12.09 mmol, 3.73 equiv), and finally I_2 (820 mg, 3.23 mmol, 1.00 equiv) were added sequentially, and the reaction was stirred and allowed to warm to rt over 6 h. On completion, flash silica (7 g) was added, and the reaction solvent was removed under reduced pressure to give a free-flowing solid which was loaded onto a flash silica column. The column was eluted with EtOAc until the triphenylphosphineoxide byproduct had been eluted (TLC). The product **6** was eluted with 85:15 EtOAc/MeOH. The product-containing fractions were then re-dissolved in $CHCl_3$ and washed with aqueous HCl (1M, 2 × 10 mL), and the organic phase was dried ($MgSO_4$) and evaporated to give **1** (652.0 mg, 2.18 mmol) in 68% yield as an amorphous yellow gum. R_f = 0.33 ($CHCl_3$/MeOH 85:15); IR film on KBr (ν_{max}) 3469 (NH), 3402 (NH) and 3307 (NH), 2957 (CH), 2730 (aromatic CH), 1662, 1579; ^1H NMR (400 MHz, DMSO-d_6) δ 8.99 (s, 1H, NH), 8.33 (s, 1H, NH), 7.03 (s, 1H, CH), 4.14 (t, J = 8 Hz, 2H, CH_2), 3.32 (s, 1H, CH), 3.21 (t, J = 8 Hz, 2H, CH_2), 2.69 (t, J = 8 Hz, 2H, CH_2), 2.26 (qui, J = 8 Hz, 2H, CH_2), 1.65 (m, 2H, CH_2), 1.29 (m, 12H, 6 × CH_2), 0.86 (t, J = 8 Hz, 3H, CH_3); ^{13}C NMR (100 MHz, DMSO-d_6) δ 179.5, 164.8, 154.9, 107.0, 80.1, 59.6, 38.3, 32.2, 32,1, 29.8, 29.7, 29.6, 29.4, 28.5, 23.0, 20.9, 14.9; HRCIMS m/z 262.2271 $[M+H]^+$ (calcd for $C_{16}H_{28}N_3^+$ 262.2271).

Anti-parasitic Assays. *General Analysis Procedure.* Bioassays results are represented as the mean and standard deviation of replicates samples from at least two independent assays. The IC_{50} values were calculated using sigmoidal dose−response curves using GraphPad Prism 5.0 software. The 95% confidence interval is included in parentheses with the analyses. The student t test and ANOVA were used for significance testing ($p < 0.05$).

Bioassays Reagents. Alamar blue (resazurin), SYTOX Green, Mitotracker Red CM-H_2XROS, ROS 2′,7′-dichlorodihydrofluorescein diacetate (H_2DCf-DA), the Annexin-V FITC Apoptosis Kit, M-199 medium, Hank's Balanced Salt Solution (HBSS), phosphate-buffered saline (PBS), oligomycin, and Triton X-100 were obtained from commercial suppliers.

Parasites, Mammalian Cells, and Animals Maintenance. *Leishmania infantum* (MHOM/BR/1972/LD) promastigotes, amastigotes, mammalian cells, and trypomastigotes of *Trypanosoma cruzi* (Y strain) were isolated and maintained as described elsewhere.[43] The amastigotes were obtained from the spleens of previously infected hamsters by differential centrifugation. The macrophages were collected from the peritoneal cavity of BALB/c mice by washing with RPMI-1640 (without phenol red and supplemented with 10% FBS) at 37 °C in a humidified containing 5% CO_2. All assays with BALB/c mice and golden hamsters were performed with the approval of the Research Ethics Commission (project number CTC 70D-2011), in agreement with the Guide for the Care and Use of Laboratory Animals from the National Academy of Sciences.

Anti-parasitic Assay of Leishmania Promastigotes. Batzelladines **12**−**15** were dissolved in DMSO and diluted in M-199 medium in 96-well microplates, at the highest concentration (156 μM), using respective internal controls. After 48 h incubation, the viability was detected by the MTT assay.[44]

Anti-parasitic Assay of Leishmania Intracellular Amastigotes. Mice peritoneal macrophages were infected with *L. infantum* amastigotes at a 1:10 ratio of macrophages to amastigotes. After 120 h incubation, the cells were stained with Giemsa, and the parasite burden was determined by counting the number of infected macrophages out of 500 cells.[7] Miltefosine was used as a standard drug control.

Anti-parasitic Assays of T. cruzi Trypomastigotes. Trypomastigotes were seeded in 96-well microplates, and after 24 h incubation with alkaloids, the viability was determined by the MTT assay.[45,46] Benznidazole was used as the standard drug control.

Cytotoxicity on Mammalian Cells Assay. Rhesus monkey kidney cells (LLC-MK2-ATCC) were seeded at 4 × 10^4 cells per well and incubated with the alkaloids at concentrations up to 200 μM. After 48 h the cell viability was determined using the MTT assay.[46]

Leishmania Mitochondrial Membrane Potential Assay. Promastigotes of *L. infantum* were seeded at 2 × 10^6/well and incubated with batzelladines **14** and **15** at their respective IC_{50} values (2 μM) during 60 min. MitoTracker Red CM-H_2XROS (500 nM) was added, and the fluorescence was determined using a FilterMax F5Multi-Mode Microplate Reader (Molecular Devices) with excitation and emission wavelengths of λ_{max} = 540 and 595 nm, respectively.[47] Internal controls consisted of DMSO, batzelladines, untreated promastigotes, and medium without any cells.

Leishmania Cell Membrane Permeability Assay. Promastigotes of *L. infantum* were seeded at 2 × 10^6/well and incubated with 1 μM SYTOX Green for 15 min, and the batzelladines **14** and **15** were added at their respective IC_{50} values (2 μM to both).[48] Maximum permeabilization was obtained with 0.1% Triton X-100. Fluorescence intensity was determined using the FilterMax F5Multi-Mode Microplate Reader (Molecular Devices) with excitation and emission wavelengths of λ_{max} = 485 and 520 nm, respectively. The internal controls were similar to the above assay.

Reactive Oxygen Species (ROS) Assay. Promastigotes of *L. infantum* were seeded at 2 × 10^6/well and incubated with batzelladines at their respective IC_{50} values (2 μM) for 60 min. Then H_2DCf-DA (5 μM) was added for 15 min, and the fluorescence intensity was

DOI: 10.1021/acs.jnatprod.5b00070
J. Nat. Prod. 2015, 78, 1101−1112

detected with excitation and emission wavelengths of λ_{max} = 485 and 520 nm, respectively. Oligomycin (20 μM) was used as the positive control.[49] The internal controls were similar to the above cited assay.

■ ASSOCIATED CONTENT

Ⓢ Supporting Information

Tables of additional ^{1}H, ^{13}C, and ^{15}N NMR data of batzellamide A (**8**) and hemibatzelladines **10** and **11**, as well as ^{1}H and ^{13}C NMR spectra of **1**, **7**, **8**, **9**, **10**, and **11**. This material is available free of charge via the Internet at http://pubs.acs.org.

■ AUTHOR INFORMATION

Corresponding Authors

*E-mail: atempone@usp.br. Tel.: +55(11)30682974.

*E-mail: rgsberlinck@iqsc.usp.br. Tel: +55(16)33739954. Fax: +55(16)33739952.

Notes

The authors declare no competing financial interest.

■ ACKNOWLEDGMENTS

The authors thank Prof. E. R. Filho (Departamento de Química, Universidade Federal de São Carlos) for the HPLC-MS/MS analyses, D. R. Cardoso (IQSC-USP) for the HRMS analyses, and Prof. J. N. A. Hooper (Queensland Museum) for a taxonomical revision. Financial support was provided by a São Paulo State Funding Agency (FAPESP) BIOTA/BIO*prospec*TA grants (2010/50190-2 and 2013/50228-8) to R.G.S.B. and A.G.T. R.J.A. thanks NSERC (Canada) for financial support. P.J.M. and P.M.H. thank the ERDF BEACON project, KESS program (European Social Fund), and Morvus Technology Ltd. for financial assistance and the EPSRC Mass Spectrometry Centre at Swansea for their assistance in MS analyses. M.F.C.S. and J.T.M. thank CAPES, while E.G.P. and T.A.C.-S. thank FAPESP for scholarships. R.G.S.B. and A.G.T. thank CNPq for investigator awards.

■ DEDICATION

Dedicated to Prof. Larry Overman (University of California, Irvine) for his outstanding contributions to the total synthesis of natural products, in particular guanidine alkaloids.

■ REFERENCES

(1) (a) Aulner, N.; Danckaert, A.; Rouault-Hardoin, E.; Desrivot, J.; Helynck, O.; Commere, P. H.; Munier-Lehmann, H.; Späth, G. F.; Shorte, S. L.; Milon, G.; Prina, E. *PLoS Negl. Trop. Dis.* **2013**, *7*, No. e2154. (b) Hussain, H.; Al-Harrasi, A.; Al-Rawahi, A.; Green, I. R.; Gibbons, S. *Chem. Rev.* **2014**, *114*, 10369−10428.

(2) Richard, J. V.; Werbovetz, K. A. *Curr. Opin. Chem. Biol.* **2010**, *14*, 447−455.

(3) Sanchez, L. M.; Lopez, D.; Vesely, B. A.; Togna, G. D.; Gerwick, W. H.; Kyle, D. E.; Linington, R. G. *J. Med. Chem.* **2010**, *53*, 4187−4197.

(4) Coura, J. R.; Borges-Pereira, J. *Rev. Soc. Bras. Med. Trop.* **2012**, *45*, 286−296.

(5) Cavalli, A.; Bolognesi, M. L. *J. Med. Chem.* **2009**, *52*, 7339−7359.

(6) Watts, K. R.; Tenney, K.; Crews, P. *Curr. Opin. Biotechnol.* **2010**, *21*, 808−818.

(7) Tempone, A. G.; Sartorelli, P.; Mady, C.; Fernandes, F. *Cardiov. Hematol. Agents Med. Chem.* **2007**, *5*, 222−235.

(8) Osorio, Y.; Travi1, B. L.; Renslo, A. R.; Peniche, A. G.; Melby, P. C. *PLoS Negl. Trop. Dis.* **2011**, *5*, No. e962.

(9) Tempone, A.; Oliveira, C. M.; Berlinck, R. G. S. *Planta Med.* **2011**, *77*, 572−585.

(10) Yang, F.; Hamann, M. T.; Zou, Y.; Zhang, M. Y.; Gong, X.-B.; Xiao, J.-R.; Chen, W.-S.; Lin, H.-W. *J. Nat. Prod.* **2012**, *75*, 774−778.

(11) Chianese, G.; Fattorusso, E.; Scala, F.; Teta, R.; Calcinai, B.; Bavestrello, G.; Dien, H. A.; Kaiser, M.; Tasdemir, D.; Taglialatela-Scafati, O. *Org. Biomol. Chem.* **2012**, *10*, 7197−7207.

(12) Gray, C. A.; de Lira, S. P.; Silva, M.; Pimenta, E. F.; Thiemann, O. H.; Oliva, G.; Hajdu, E.; Andersen, R. J.; Berlinck, R. G. S. *J. Org. Chem.* **2006**, *71*, 8685−8690.

(13) Kossuga, M. H.; Nascimento, A. M.; Reimão, J. Q.; Tempone, A. G.; Taniwaki, N. N.; Veloso, K.; Ferreira, A. G.; Cavalcanti, B. C.; Pessoa, C.; Moraes, M. O.; Mayer, A. M. S.; Hajdu, E.; Berlinck, R. G. S. *J. Nat. Prod.* **2008**, *71*, 334−339.

(14) Reimão, J. Q.; Migotto, A. E.; Kossuga, M. H.; Berlinck, R. G. S.; Tempone, A. G. *Parasitol. Res.* **2008**, *103*, 1445−1450.

(15) (a) Berlinck, R. G. S.; Trindade-Silva, A. E.; Santos, M. F. C. *Nat. Prod. Rep.* **2012**, *29*, 1382−1406 and previous reviews in this series. A chemotaxonomic assessment of biogenetically related guanidine alkaloids isolated from sponges assigned to genera *Batzella*, *Crambe*, *Hemimycale*, *Monanchora*, and *Ptilocaulis* suggested that shallow water *Batzella*, *Monanchora*, and *Ptilocaulis* containing cyclic guanidine alkaloids most likely pertain to a single taxon, namely *Monanchora* or *Crambe*. DNA sequencing indicated that *Crambe* and *Monanchora* form a monophyletic group: (b) Hajdu, E.; de Paula, T. S.; Redmond, N.; Cosme, B.; Collins, A. G.; Lôbo-Hajdu, G. *Integr. Comp. Biol.* **2013**, *53*, 462−472. However, taxonomic affinities of *Batzella* from deeper waters and *Hemimycale* with similar guanidines remain elusive: (c) van Soest, R. W. M.; Braekman, J. C.; Faulkner, D. J.; Hajdu, E.; Harper, M. K.; Vacelet, J. *Bull. Inst. R. Sci. Nat. Belg.* **1996**, *66* (suppl.), 89−101. The specimen identified as *Arenochalina mirabilis*[21a] was reassessed by Dr. J. N. A. Hooper, who conceived the possibility of it pertaining instead to Crambeidae (*Monanchora* sp.).

(16) Blunt, J. W.; Copp, B. R.; Keyzers, R. A.; Munro, M. H. G.; Prinsep, M. R. *Nat. Prod. Rep.* **2014**, *31*, 160−258 and previous reviews in this series.

(17) Ebada, S. S.; Proksch, P. *Mini-Rev. Med. Chem.* **2011**, *11*, 225−246.

(18) Heys, L.; Moore, C. G.; Murphy, P. J. *Chem. Soc. Rev.* **2000**, *29*, 57−67.

(19) (a) Berlinck, R. G. S.; Braekman, J. C.; Daloze, D.; Hallenga, K.; Ottinger, R. *Tetrahedron Lett.* **1990**, *31*, 6531−6534. (b) Berlinck, R. G. S.; Braekman, J. C.; Daloze, D.; Bruno, I.; Riccio, R.; Rogeau, D.; Amade, P. *J. Nat. Prod.* **1992**, *55*, 528−532. (c) Jares-Erijman, E. A.; Ingrum, A. A.; Sun, F.; Rinehart, K. L. *J. Nat. Prod.* **1993**, *56*, 2186−2188. (d) Chang, L. C.; Whittaker, N. F.; Bewley, C. A. *J. Nat. Prod.* **2003**, *66*, 1490−1494. (e) Bondu, S.; Genta-Jouve, G.; Leirós, M.; Vale, C.; Guigonis, J.-M.; Botana, L. M.; Thomas, O. P. *RSC Adv.* **2012**, *2*, 2828−2835. (f) Makarieva, T. N.; Ogurtsova, E. K.; Denisenko, V. A.; Dmitrenok, P. S.; Tabakmakher, K. M.; Guzii, A. G.; Pislyagin, E. A.; Es'kov, A. A.; Kozhemyako, V. B.; Aminin, D. L.; Wang, Y. M.; Stonik, V. A. *Org. Lett.* **2014**, *16*, 4292−4295.

(20) (a) Harbour, G. C.; Tymiak, A. A.; Rinehart, K. L., Jr.; Shaw, P. D.; Hughes, R., Jr.; Mizsak, S. A.; Coats, J. H.; Zurenko, G. E.; Li, L. H.; Kuentzel, S. L. *J. Am. Chem. Soc.* **1981**, *103*, 5604−5606. (b) Tavares, R.; Daloze, D.; Braekman, J. C.; Hajdu, E.; Van Soest, R. W. M. *J. Nat. Prod.* **1995**, *58*, 1139−1142. (c) Patil, A. D.; Freyer, A. J.; Offen, P.; Bean, M. F.; Johnson, R. K. *J. Nat. Prod.* **1997**, *60*, 704−707. (d) Hua, H.-M.; Peng, J.; Fronczek, F. R.; Kelly, M.; Hamann, M. T. *Bioorg. Med. Chem.* **2004**, *12*, 6461−6464.

(21) (a) Barrow, R. A.; Murray, L. M.; Lim, T. K.; Capon, R. J. *Aust. J. Chem.* **1996**, *49*, 767−773. (b) Capon, R. J.; Miller, M.; Rooney, F. *J. Nat. Prod.* **2001**, *64*, 643−644. (c) El-Naggar, M.; Conte, M.; Capon, R. J. *Org. Biomol. Chem.* **2010**, *8*, 407−412.

(22) (a) Sorek, H.; Rudi, A.; Gueta, S.; Reyes, F.; Martin, M. J.; Aknin, M.; Gaydou, E.; Vacelet, J.; Kashman, Y. *Tetrahedron* **2006**, *62*, 8838−8843. (b) Yu, M.; Pochapsky, S. S.; Snider, B. B. *J. Org. Chem.* **2008**, *73*, 9065−9074. (c) Gros, E.; Al-Mourabit, A.; Martin, M.-T.; Sorres, J.; Vacelet, J.; Frederich, M.; Aknin, M.; Kashman, Y.; Gauvin-Bialecki, A. *J. Nat. Prod.* **2014**, *77*, 818−823.

DOI: 10.1021/acs.jnatprod.5b00070
J. Nat. Prod. 2015, 78, 1101−1112

(23) (a) Kashman, Y.; Hirsh, S.; McConnell, O. J.; Ohtani, I.; Kusumi, T.; Kakisawa, H. *J. Am. Chem. Soc.* **1989**, *111*, 8925−8926. (b) Ohtani, I.; Kusumi, T.; Kakisawa, H.; Kashman, Y.; Hirsh, S. *J. Am. Chem. Soc.* **1992**, *114*, 8472−8479. (c) Palagiano, E.; De Marino, S.; Minale, L.; Riccio, R.; Zollo, F. *Tetrahedron* **1995**, *51*, 3675−3682. (d) Bensemhoun, J.; Bombarda, I.; Aknin, M.; Vacelet, J.; Gaydou, E. M. *J. Nat. Prod.* **2007**, *70*, 2033−2035. (e) Ohizumi, Y.; Sasaki, S.; Kusumi, T.; Ohtani, I. I. *Eur. J. Pharmacol.* **1996**, *310*, 95−98.

(24) (a) Jares-Erijman, E. A.; Sakai, R.; Rinehart, K. L. *J. Org. Chem.* **1991**, *56*, 5712−5715. (b) Berlinck, R. G. S.; Braekman, J. C.; Daloze, D.; Bruno, I.; Riccio, R.; Ferri, S.; Spampinato, S.; Speroni, E. *J. Nat. Prod.* **1993**, *56*, 1007−1015. (c) Jares-Erijman, E. A.; Ingrum, A. L.; Carney, J. R.; Rinehart, K. L.; Sakai, R. *J. Org. Chem.* **1993**, *58*, 4805−4808. (d) Braekman, J. C.; Daloze, D.; Tavares, R.; Hajdu, E.; Van Soest, R. W. M. *J. Nat. Prod.* **2000**, *63*, 193−196. (e) Gallimore, W. A.; Kelly, M.; Scheuer, P. J. *J. Nat. Prod.* **2005**, *68*, 1420−1423.

(25) (a) Guzii, A. G.; Makarieva, T. N.; Denisenko, V. A.; Dmitrenok, P. S.; Kuzmich, A. S.; Dyshlovoy, S. A.; Krasokhin, V. B.; Stonik, V. A. *Org. Lett.* **2010**, *12*, 4292−4295. (b) Makarieva, T. N.; Tabakmaher, K. M.; Guzii, A. G.; Denisenko, V. A.; Dmitrenok, P. S.; Shubina, L. K.; Kuzmich, A. S.; Lee, H. S.; Stonik, V. A. *J. Nat. Prod.* **2011**, *74*, 1952−1958. (c) Makarieva, T. N.; Tabakmaher, K. M.; Guzii, A. G.; Denisenko, V. A.; Dmitrenok, P. S.; Kuzmich, A. S.; Lee, H. S.; Stonik, V. A. *Tetrahedron Lett.* **2012**, *53*, 4228−4231. (d) Tabakmakher, K. M.; Denisenko, V. A.; Guzii, A. G.; Dmitrenok, P. S.; Dyshlovoy, S. A.; Lee, H. S.; Makarieva, T. N. *Nat. Prod. Commun.* **2013**, *8* (1), 399−1402.

(26) (a) Patil, A. D.; Kumar, N. V.; Kokke, W. C.; Bean, M. F.; Freyer, A. J.; Debrosse, C.; Mai, S.; Truneh, A.; Faulkner, D. J.; Carte, B.; Breen, A. L.; Hertzberg, R. P.; Johnson, R. K.; Westley, J. W.; Potts, B. C. M. *J. Org. Chem.* **1995**, *60*, 1182−1188. (b) Patil, A. D.; Freyer, A. J.; Taylor, P. B.; Carte, B.; Zuber, G.; Johnson, R. K.; Faulkner, D. J. *J. Org. Chem.* **1997**, *62*, 1814−1819. (c) Snider, B. B.; Busuyek, M. V. *J. Nat. Prod.* **1999**, *62*, 1707−1711. (d) Hua, H. M.; Peng, J.; Dunbar, D. C.; Schinazi, R. F.; Andrews, A. G. D. C.; Cuevas, C.; Garcia-Fernandez, L. F.; Kelly, M.; Hamann, M. T. *Tetrahedron* **2007**, *63*, 11179−11188. (e) Laville, R.; Thomas, O. P.; Berrué, F.; Marquez, D.; Vacelet, J.; Amade, P. *J. Nat. Prod.* **2009**, *72*, 1589−1594.

(27) Bewley, C. A.; Ray, S.; Cohen, F.; Collins, S. K.; Overman, L. E. *J. Nat. Prod.* **2004**, *67*, 1319−1324.

(28) Dalisay, D. S.; Saludes, J. P.; Molinski, T. F. *Bioorg. Med. Chem.* **2011**, *19*, 6654−6657.

(29) Lazaro, J. E. H.; Nitcheu, J.; Mahmoudi, N.; Ibana, J. A.; Mangalindan, G. C.; Black, G. P.; Howard-Jones, A. G.; Moore, C. G.; Thomas, D. A.; Mazier, D.; Ireland, C. M.; Concepcion, G. P.; Murphy, P. J.; Diquet, B. *J. Antibiot.* **2006**, *59*, 583−590.

(30) Nakazaki, A.; Ishikawa, Y.; Sawayama, Y.; Yotsu-Yamashita, M.; Nishikawa, T. *Org. Biomol. Chem.* **2014**, *12*, 53−56.

(31) (a) Medeiros, A. I.; Gandolfi, R. C.; Secatto, A.; Falcucci, R. M.; Faccioli, L. H.; Hajdu, E.; Peixinho, S.; Berlinck, R. G. S. *Immunopharm. Immunotox.* **2012**, *34*, 919−924. (b) da Silva, F. R.; Tessis, A. C.; Ferreira, P. F.; Rangel, L. P.; Garcia-Gomes, A. S.; Pereira, F. R.; Berlinck, R. G. S.; Muricy, G.; Ferreira-Pereira, A. *J. Nat. Prod.* **2012**, *74*, 279−282.

(32) Detty, M. R. *J. Org. Chem.* **1978**, *44*, 2073−2077.

(33) Snider, B. B.; Chen, J.; Patil, A. D.; Freyer, A. J. *Tetrahedron Lett.* **1996**, *37*, 6977−6980.

(34) Cohen, F.; Overman, L. E. *J. Am. Chem. Soc.* **2001**, *123*, 10782−10783.

(35) Takishima, S.; Ishiyama, A.; Iwatsuki, M.; Otoguro, K.; Yamada, H.; Omura, S.; Kobayashi, H.; van Soest, R. W. M.; Matsunaga, S. *Org. Lett.* **2009**, *11*, 2655−2658.

(36) Coombs, G. H.; Hart, D. T.; Capaldo, J. *J. Antimicrob. Chemother.* **1983**, *11*, 151−162.

(37) Tada, H.; Shiho, O.; Kuroshima, K.; Koyama, M.; Tsukamoto, K. *J. Immun. Meth.* **1986**, *93*, 157−165.

(38) Pal, C.; Bandyopadhyay, U. *Antiox. Redox Signal.* **2012**, *17*, 555−582.

(39) Shukla, A. K.; Patra, S.; Dubey, V. K. *Mol. Cell. Biochem.* **2011**, *352*, 261−70.

(40) Mehta, A.; Shaha, C. *J. Biol. Chem.* **2004**, *279*, 11798−11813.

(41) Hong, H.; Fill, T.; Leadlay, P. F. *Angew. Chem.* **2013**, *125*, 13334−13337.

(42) Wilson, M. C.; Mori, T.; Rückert, C.; Uria, A. R.; Helf, M. J.; Takada, K.; Gernert, C.; Steffens, U. A. E.; Heycke, N.; Schmitt, S.; Rinke, C.; Helfrich, E. J. N.; Brachmann, A. O.; Gurgui, C.; Wakimoto, T.; Kracht, M.; Crüsemann, M.; Hentschel, U.; Abe, I.; Matsunaga, S.; Kalinowski, J.; Takeyama, H.; Piel, J. *Nature* **2014**, *506*, 58−62.

(43) Corrêa, D. S.; Tempone, A. G.; Reimão, J. Q.; Taniwaki, N. N.; Romoff, P.; Fávero, O. A.; Sartorelli, P.; Mecchi, M. C.; Lago, J. H. G. *Parasitol. Res.* **2011**, *109*, 231−236.

(44) Tada, H.; Shiho, O.; Kuroshima, K.; Koyama, M.; Tsukamoto, K. *J. Immun. Meth.* **1986**, *93*, 157−165.

(45) Lane, J. E.; Rodrigues, R. R.; Suarez, C. C.; Bogitsh, B. J.; Jones, M. M.; Singh, P. K.; Carter, C. E. *Am. J. Trop. Med. Hyg.* **1996**, *55*, 263−266.

(46) Tada, H.; Shiho, O.; Kuroshima, K.; Koyama, M.; Tsukamoto, K. *J. Immun. Meth.* **1986**, *93*, 157−165.

(47) Williams, R. A. M.; Smith, T. K.; Cull, B.; Mottram, J. C.; Coombs, G. H. *PLoS Pathog.* **2012**, *8*, No. e1002695.

(48) Mangoni, M. L.; Saugar, J. M.; Dellisanti, M.; Barra, D.; Simmaco, M.; Rivas, L. *J. Biol. Chem.* **2005**, *280*, 984−990.

(49) Ribeiro, G. A.; Cunha, E. F.; Pinheiro, R. O.; Da-Silva, S. A. G.; Canto-Cavalheiro, M. M.; Silva, A. J. M.; Costa, P. R. R.; Netto, C. D.; Melo, R. C. N.; Almeida-Amaral, E. E.; Torres-Santos, E. C. *J. Antimicrob. Chemother.* **2013**, *68*, 789−799.

DOI: 10.1021/acs.jnatprod.5b00070
J. Nat. Prod. 2015, 78, 1101−1112

JOURNAL OF NATURAL PRODUCTS

Article

pubs.acs.org/jnp

Analogues of Marine Guanidine Alkaloids Are *in Vitro* Effective against *Trypanosoma cruzi* and Selectively Eliminate *Leishmania* (*L.*) *infantum* Intracellular Amastigotes

Ligia F. Martins,[†] Juliana T. Mesquita,[†] Erika G. Pinto,[†,‡] Thais A. Costa-Silva,[†] Samanta E. T. Borborema,[†] Andres J. Galisteo Junior,[‡] Bruno J. Neves,[§] Carolina H. Andrade,[§] Zainab Al Shuhaib,[⊥] Elliot L. Bennett,[⊥] Gregory P. Black,[⊥] Philip M. Harper,[⊥] Daniel M. Evans,[⊥] Hisham S. Fituri,[⊥] John P. Leyland,[⊥] Claire Martin,[⊥] Terence D. Roberts,[⊥] Andrew J. Thornhill,[⊥] Stephen A. Vale,[⊥] Andrew Howard-Jones,[⊥] Dafydd A. Thomas,[⊥] Harri L. Williams,[⊥] Larry E. Overman,[∥] Roberto G. S. Berlinck,[¶] Patrick J. Murphy,[⊥] and Andre G. Tempone[*,†,#]

[†]Centre for Parasitology and Mycology, Instituto Adolfo Lutz, Avenida Dr. Arnaldo, 351, 8° andar, 01246-000 São Paulo, SP, Brazil

[‡]Instituto de Medicina Tropical, Universidade de São Paulo, Avenida Dr. Enéas de Carvalho Aguiar, 470, 05403-000 São Paulo, SP, Brazil

[§]LabMol, Laboratory for Molecular Modeling and Drug Design, Faculdade de Farmácia, Universidade Federal de Goiás, Goiânia, Brazil

[⊥]School of Chemistry, Bangor University, Bangor, Gwynedd, Wales, U.K. LL57 2UW

[∥]University of California, Irvine, 4042A Frederick Reines Hall, Irvine, California 92697, United States

[¶]Instituto de Química de São Carlos, Universidade de São Paulo, CP 780, CEP 13560-970, São Carlos, SP, Brazil

Supporting Information

ABSTRACT: Synthetic analogues of marine sponge guanidine alkaloids showed *in vitro* antiparasitic activity against *Leishmania* (*L.*) *infantum* and *Trypanosoma cruzi*. Guanidines **10** and **11** presented the highest selectivity index when tested against *Leishmania*. The antiparasitic activity of **10** and **11** was investigated in host cells and in parasites. Both compounds induced depolarization of mitochondrial membrane potential, upregulation of reactive oxygen species levels, and increased plasma membrane permeability in *Leishmania* parasites. Immunomodulatory assays suggested an NO-independent effect of guanidines **10** and **11** on macrophages. The same compounds also promoted anti-inflammatory activity in *L.* (*L.*) *infantum*-infected macrophages cocultived with splenocytes, reducing the production of cytokines MCP-1 and IFN-γ. Guanidines **10** and **11** affect the bioenergetic metabolism of *Leishmania*, with selective elimination of parasites via a host-independent mechanism.

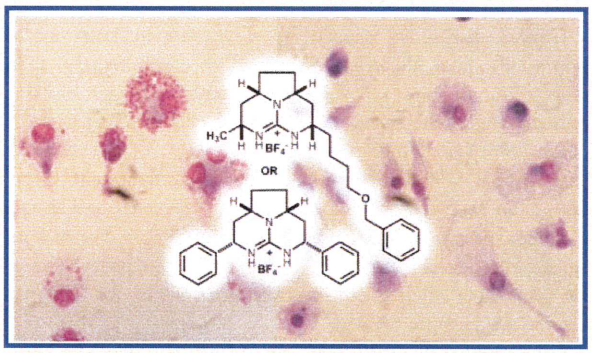

Considerable attention has been raised to address the effective cure of neglected tropical diseases (NTDs) in the past decade, which globally impact mainly economically disfavored nations. These infectious pathogenies, of which most have parasites as the causative agents, have spread and now affect populations in developed countries as well. Most drugs to treat NTDs were developed decades ago and show harmful, even deadly, adverse effects. Therefore, the search for new drugs or vaccines to treat human neglected diseases is a priority for the World Health Organization and other organizations.[1,2]

Two of the deadliest NTDs are leishmaniasis and Chagas disease. Leishmaniasis affects 12 million people in 98 countries mainly in Africa, Asia, and Latin America.[3,4] Two distinct human pathological conditions are observed for leishmaniasis, cutaneous and visceral. *Leishmania* (*L.*) *infantum* is the etiologic agent of visceral leishmaniasis (VL) in South America and southern Europe countries, while *Leishmania* (*L.*) *donovani* is in Asian and African countries. Visceral leishmaniasis promoted by *L.* (*L.*) *infantum* is fatal, with a mortality rate of 100% if untreated.[4] Leishmaniasis is included as a target disease by DNDi (Drugs for Neglected Diseases Initiative) and iOWH (Institute for One World Health).

Received: March 21, 2016

DOI: 10.1021/acs.jnatprod.6b00256
J. Nat. Prod. XXXX, XXX, XXX−XXX

Table 1. Antileishmanial/Antitrypanosomal Activities and Mammalian Cytotoxicity of Guanidines and the Standard Drugs Benznidazole and Miltefosine

	T. cruzi trypomastigotes[a]	*L. (L.) infantum* promastigotes[b]	*L. (L.) infantum* amastigotes	NCTC cells	selectivity index[e]	
compound	IC_{50}[c] (μM) 95% CI[f]	IC_{50} (μM) 95% CI	IC_{50} (μM) 95% CI	CC_{50}[d] (μM) 95% CI	*Leishmania* amastigotes	*Trypanosoma cruzi* trypomastigotes
1	8 (7–9)	42 (36–49)	5 (2–14)	42 (35–51)	8	5
2	88 (65–119)	NA[g]	NA	>150	ND[h]	>2
3	49 (43–56)	NA	NA	>150	ND	>2
4	22 (21–24)	109 (97–123)	NA	>150	ND	>7
5	8 (8–8)	53 (45–64)	NA	100 (93–107)	ND	12
6	4 (2–9)	59 (47–74)	NA	84 (80–88)	ND	28
7	4 (4–7)	48 (39–61)	NA	57 (45–71)	ND	19
8	NA	NA	NA	>150	ND	ND
9	4 (4–5)	7 (4–10)	18 (15–21)	65 (58–73)	4	16
10	41 (36–47)	57 (50–65)	5 (4–7)	138 (115–164)	25	3
11	9 (8–10)	34 (30–39)	2 (1–4)	45 (42–49)	20	5
12	NA	NA	8 (6–12)	>150	>19	ND
13	NA	NA	NA	>150	ND	ND
14	35 (31–41)	9 (9–10)	19 (6–56)	116 (105–128)	6	3
15	79 (31–197)	57 (50–65)	24 (23–25)	70 (57–85)	3	0.9
16	69 (55–86)	47 (40–54)	NA	60 (46–79)	ND	0.9
17	0.9 (0.9–10)	NA	0.8 (0.3–2)	2 (2–3)	3	2
18	NA	NA	49 (34–72)	>150	>3.0	ND
benznidazole	16 (14–20)	ND	ND	>150	ND	>9
miltefosine	ND	16 (15–17)	17 (12–24)	122 (95–157)	7	ND

[a]Cell viability was determined using the resazurin assay. [b]Cell viability was determined using the MTT assay. [c]IC_{50}: 50% inhibitory concentration: concentration of compound required to reduce 50% of parasites. [d]CC_{50}: 50% cytotoxic concentration: concentration of compound that reduces the viability of mammalian cells by 50%. All data represent mean values for at least two separate experiments. [e]Selectivity index: ratio of CC_{50}/IC_{50}. [f]95% CI: 95% confidence interval. [g]NA: not active to the highest concentration of 100 μM. [h]ND: not determined.

Chagas disease is caused by *Trypanosoma cruzi* as a potentially fatal disorder resulting in cardiomegaly and megacolon in about 30% of the patients.[5] Chagas disease remains one of the most severe public-health problems in 21 countries of Latin America, causing more than 7000 deaths per year without early and successful antiparasitic treatment. Over 25 million people are at risk of infection by *T. cruzi*, and about 7 million people are infected worldwide.[1] Chagas disease has spread into several European countries and Japan, probably due to population migration. Effective treatments for Chagas disease are urgently needed.[6]

Large drug screening campaigns to find new drugs to treat NTDs are currently being developed. New criteria for improving the success of clinical drug candidates with potential use in NTDs have been recently reviewed.[7] While most hit compounds for infectious diseases were discovered using phenotypic assays, subsequent optimization efforts need to establish the drug target.[7] Among various classes of natural and synthetic compounds that present antiparasitic activity, guanidines have shown to be of particular interest because of their potent activity and suitable pharmacokinetic profile.[8−11] On the basis of the findings recently reported by some of us showing potent and selective antileishmanial and antitrypanosomal activity for marine sponge-derived guanidine alkaloids,[11] herein we report the results of the investigation of 18 synthetic guanidines as antiparasitic agents against *Leishmania* and *Trypanosoma* parasites. The two most selective synthetic guanidines active against *L. (L.) infantum* were further investigated for the mechanism of action on the parasites and for their immunomodulatory activity.

RESULTS

Antileishmanial Activity and Antitrypanosomal Activity. *L. (L.) infantum* promastigotes were incubated for 48 h with guanidines **1**−**18**, and the viability of cells was determined by the MTT colorimetric assay. Compounds **1**−**18** showed IC_{50} values in the range between 6.6 and 110 μM. Intracellular *L. (L.) infantum* amastigotes were also treated with compounds **1**−**18**. The observed IC_{50} values were in the range between 0.8 and 49 μM. Miltefosine was used as a standard drug (IC_{50} of 16 μM). *T. cruzi* trypomastigotes were incubated with the same series of compounds for 24 h, and the cell viability was determined by the resazurin assay. Guanidines **1**−**18** displayed antitrypanosomal activity with IC_{50} values in the range between 0.9 and 88.5 μM. These results are presented in Table 1. Benznidazole was used as standard drug (IC_{50} of 16 μM) (Table 1).

Determination of the 50% Cytotoxic Concentration (CC_{50}) in Mammalian Cells. Aiming to evaluate the mammalian cytotoxicity of compounds **1**−**19**, NCTC cells (clone 929) were incubated for 48 h, and the cell viability was determined by the MTT colorimetric assay method. Guanidines **1**−**19** showed toxicity, with CC_{50} values in the range between 2.4 and >150 μM. Miltefosine and benznidazole were used as standard drugs and showed CC_{50} values of 122 and >150 μM, respectively (Table 1).

Immunomodulatory Potential of Compounds. Quantification of Nitric Oxide (NO). Guanidines **10** and **11** showed the highest selectivity index (25 and 20, respectively) as antileishmanial agents (Table 1, selectivity index) and were selected for further mechanism of action assays. Compounds **10** and **11** were incubated with peritoneal macrophages, and the

DOI: 10.1021/acs.jnatprod.6b00256
J. Nat. Prod. XXXX, XXX, XXX−XXX

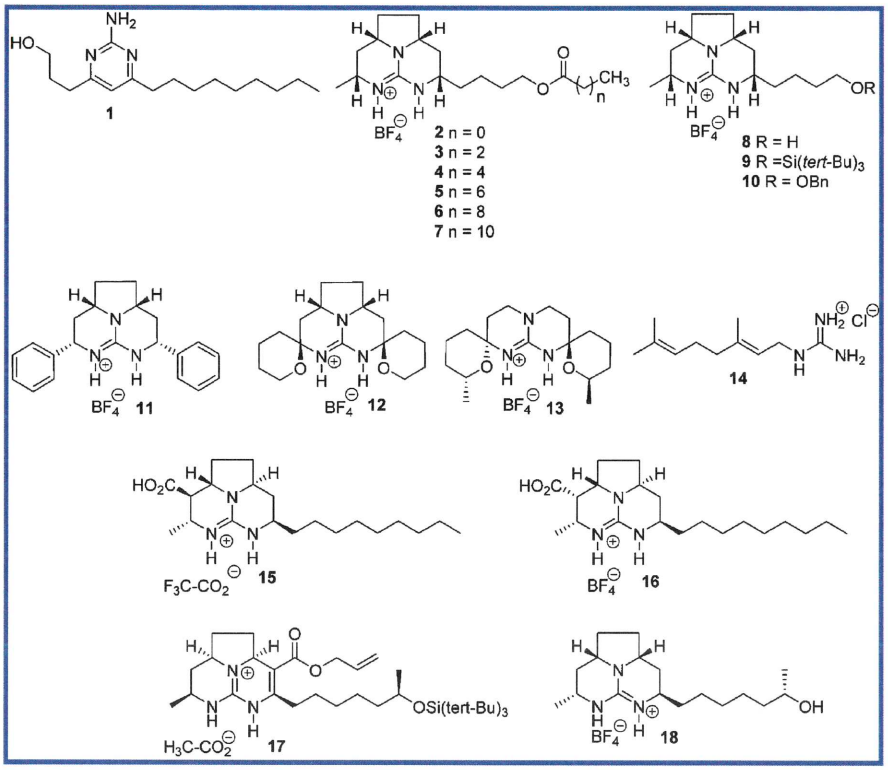

NO content was evaluated after 24 h. Both compounds revealed no capacity to upregulate NO production (Figure 1). Bacterial lipopolysaccharide (LPS) was used as the positive control.

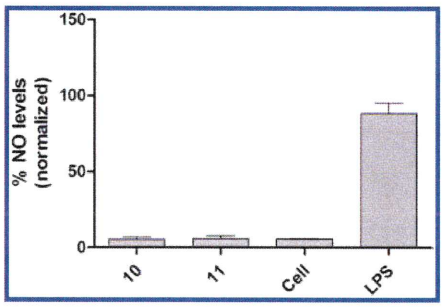

Figure 1. Evaluation of nitric oxide levels of peritoneal macrophages incubated with compounds **10** and **11** at the respective IC_{50} values (intracellular amastigote assay = 5 and 2 μM, respectively) for 24 h. The Griess reaction was used to measure the concentration of nitrite (NO_2^-). *$p < 0.05$.

Cellular Immune Response of *L.* (*L.*) *infantum*-Infected Macrophages Cocultivated with Splenocytes. Non-infected and *L.* (*L.*) *infantum*-infected macrophages were treated for 48 h with guanidines **10** and **11** and were cocultivated with or without splenocytes. The production of cytokines MCP-1, IL-6, IL-10, TNF, and IFN-γ was detected by flow cytometry analysis. Compound **10** decreased the production of cytokines MCP-1 ($p < 0.05$) and IFN-γ ($p < 0.05$) in both noninfected and *L.* (*L.*) *infantum*-infected macrophages. The same result was observed when macrophages were cocultivated with or without splenocytes. A similar downregulation effect ($p < 0.001$) of MCP-1 was also observed in splenocytes incubated with guanidines **10** and **11**. However, compounds **10** and **11** did not promote alteration of cytokines TNF, IL-6, and IL-10 levels (data not shown). The production of cytokine IFN-γ was negatively modulated by **10** and **11** in noninfected as well as in *L.* (*L.*) *infantum*-infected macrophages cocultivated with splenocytes (Figure 2).

Evaluation of Lethal Action of Guanidines 10 and 11 on *L.* (*L.*) *infantum*. Permeability of Plasma Membrane. Guanidines **10** and **11** (57 and 34 μM, respectively) promoted a slight alteration in plasma membrane permeability of *L.* (*L.*) *infantum* promastigotes, measured using the fluorescent probe SYTOX Green. Compounds **10** and **11** promoted approximately 25% and 10% higher fluorescence intensity (Figure 3) after 60 min when compared to untreated parasites ($p < 0.05$) (Figure 3). Triton X-100 was used for normalization as 100% permeabilization.

Evaluation of Mitochondrial Membrane Potential. Alteration of *L.* (*L.*) *infantum* mitochondrial membrane potential was investigated in the presence of **10** and **11** (57 and 34 μM, respectively). Promastigotes were incubated with both compounds separately for 60 min, and the mitochondrial membrane potential was monitored using the fluorescent probe rhodamine 123. Both compounds induced a significant reduction ($p < 0.001$) of the fluorescence intensity of rhodamine 123 when compared to untreated *L.* (*L.*) *infantum* promastigotes. The 70% depolarization intensity caused by both compounds was similar to the level observed with the positive control sodium azide (Figure 4).

Reactive Oxygen Species (ROS) Regulation. Production of ROS by *L.* (*L.*) *infantum* promastigotes in the presence of guanidines **10** and **11** was determined using the fluorescent probe H_2DCF-DA. After 120 min of incubation, guanidine **10** promoted significant alteration in *L.* (*L.*) *infantum* ROS levels ($p < 0.001$), resulting in a 3-fold higher content than the

DOI: 10.1021/acs.jnatprod.6b00256
J. Nat. Prod. XXXX, XXX, XXX−XXX

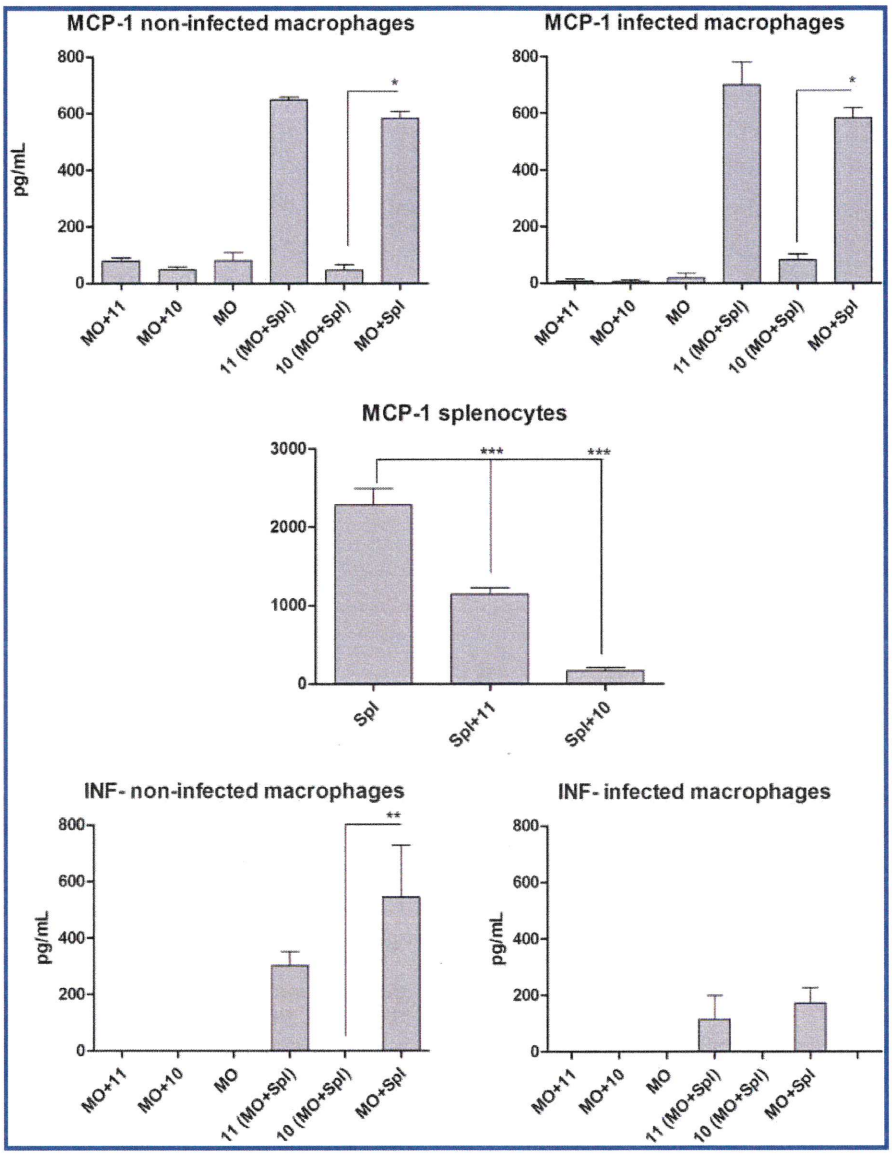

Figure 2. Immunomodulatory effect of compounds **10** (30 μM) and **11** (15 μM) on the production of MCP-1 and IFN-γ by uninfected macrophages, lymphocytes (LY), and *L.* (*L.*) *infantum*-infected macrophages cocultivated or not with lymphocytes. Results are expressed in pg/mL. Cytokines were measured with a CBA (cytometric bead array). *Escherichia coli* lipopolysaccharide for macrophages and concanavalin A (ConA) for lymphocytes (1 μM) were used as controls. *$p < 0.05$, **$p < 0.01$, ***$p < 0.001$.

sodium azide positive control. Compound **11** also promoted alteration of ROS levels in *L.* (*L.*) *infantum*, 60% higher than in untreated parasites ($p < 0.05$) (Figure 5).

DISCUSSION

Several guanidine compounds have been evaluated as antiparasitic compounds and showed significant *in vitro* antileishmanial and antitrypanosomal activity when compared to standard drugs.[11−18] On the basis of our recent discovery of a series of alkaloids from the sponge *Monanchora arbuscula*, active against *L.* (*L.*) *infantum* and *T. cruzi* parasites,[11] we evaluated an additional series of 18 synthetic guanidine derivatives against *L.* (*L.*) *infantum* and *T. cruzi*.

Among 18 guanidine compounds tested against *T. cruzi* trypomastigotes, 14 (77%) showed activity below 100 μM, of which compounds **1**, **5**, **6**, **7**, **9**, **11**, and **17** presented IC_{50} values below 10 μM. Guanidines **5**, **6**, **7**, and **9** showed low cytotoxicity and the highest selectivity indexes (SI), between 12 and 28. Guanidine **17** was approximately 17-fold more effective than the standard drug benznidazole. Guanidines **6** and **7** were about 4-fold more effective, presenting a trypanocidal activity observed by the lack of mitochondrial activity measured by resazurin. Other guanidine compounds were tested against *T. cruzi* and showed potent activity, in the range between 1 and 10 μM,[13] similarly as observed for compounds **1**, **5**, **6**, **7**, **9**, **11** and **17**. Compound **17** displayed potent antitrypanosomal activity, with an IC_{50} value of 0.9 μM. However, the selectivity index was below 10 and therefore does not meet an important criterion for the hit stage.

DOI: 10.1021/acs.jnatprod.6b00256
J. Nat. Prod. XXXX, XXX, XXX−XXX

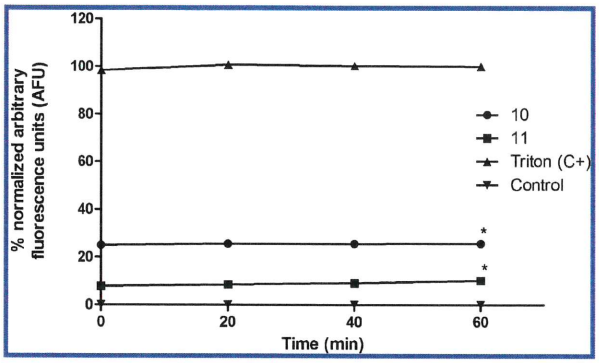

Figure 3. Permeability of *L. (L.) infantum* plasma membrane incubated with compounds **10** (57 μM) and **11** (34 μM), assessed with the vital dye SYTOX Green. Promastigotes were treated with Triton X-100 and used as 100% permeabilization. A control group (untreated) was also included. Fluorescence was determined using a fluorimetric microplate reader (FilterMax F5 multi-mode microplate reader) with excitation and emission wavelengths of 485 and 520 nm, respectively. $*p < 0.05$.

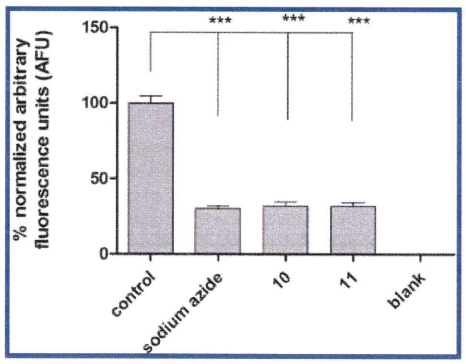

Figure 4. Evaluation of the mitochondrial membrane potential of *L. (L.) infantum* promastigotes incubated with compounds **10** (57 μM) and **11** (34 μM). Untreated parasites were also incubated with rhodamine 123 (control group). Fluorescence was determined using a fluorimetric microplate reader (FilterMax F5 multi-mode microplate reader) with excitation and emission wavelengths of 488 and 525 nm, respectively. Sodium azide (10 mM) was used as positive control. $***p < 0.001$.

Guanidine compounds isolated as natural products and synthetic derivatives have also shown potent antileishmanial activity.[14−18] Eleven (61%) out of 18 synthetic guanidines herein evaluated displayed antileishmanial activity against promastigotes, nine of which were active against *L. (L.) infantum* intracellular amastigotes below 100 μM. Five of these displayed IC_{50} values below 10 μM (**1**, **10**, **11**, **12**, and **18**). Considering the recommendations of the DNDi for anti-leishmanial agents,[19] an IC_{50} < 10 μM and SI ≥ 10 are determinant features for antileishmanial compounds at the hit stage.[19,20] Guanidines **10** and **11** presented SIs of 25 and 20, respectively, and were selected for investigation of the lethal mechanism of action against *Leishmania* parasites.

Due to the complexity of intracellular amastigote defenses, an antileishmanial suitable hit compound needs to specifically target the parasite that lives in the acidic parasitophorous vacuole inside the macrophage.[21] Guanidines **10** and **11** showed more potent antiparasitic activity against intracellular amastigotes than to extracellular promastigotes. In order to investigate if the antileishmanial activity of **10** and **11** against

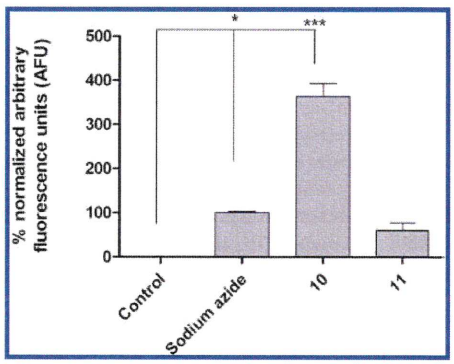

Figure 5. Evaluation of reactive oxygen species levels in *L. (L.) infantum* promastigotes incubated with compounds **10** (57 μM) and **11** (34 μM). The parasites were incubated with the probe H_2DCf-DA, and the fluorescence intensity was detected using a fluorimetric microplate reader (FilterMax F5 multi-mode microplate reader) with excitation and emission wavelengths of 485 and 520 nm, respectively. Sodium azide (10 mM) was used as positive control. $*p < 0.05$, $***p < 0.001$.

intracellular amastigotes could be ascribed to an immunomodulatory effect in host cells, we evaluated cytokine production by macrophages in the presence of guanidines **10** and **11**. This approach enables differentiating compounds that are directly active in the parasite from those that exert an antiparasitic effect by an immunomodulatory response.[22]

Immunomodulators have been investigated as drugs for the clinical treatment of leishmaniasis, but with limited efficacy when administered alone.[23,24] Guanidines **10** and **11** caused no upregulation of NO in macrophages. Flow cytometry analysis indicated that **10** and **11** significantly suppressed the production of IFN-γ and MCP-1 cytokines in the host cell, causing no significant alteration of TNF, IL-6, and IL-10 levels. Cytokines play different roles during a *Leishmania* infection in macrophages. In *L. (L.) infantum*-infected human macrophages, treatment with monocyte chemotactic protein chemokine (MCP-1) enhances NO production and the antileishmanial activity.[25] MCP-1 is a leukocyte activator, related to the production of proinflammatory cytokines and microbicidal molecules. It promotes NO release and increased parasite killing by *T. cruzi*-infected macrophages. Upregulation of cytokine IL-6 has been associated with a lethal outcome of the disease, preceding death in patients with visceral leishmaniasis.[26] High levels of IFN-γ, IL-10, and IL-6 are associated with human visceral leishmaniasis and with leishmaniasis persistence.[27,28]

In addition to the downregulation of inflammatory cytokines induced by guanidines **10** and **11** in *Leishmania*-infected macrophages cocultived with splenocytes, both compounds promoted the death of intracellular amastigotes. Attenuation of immune response by immunomodulators, such as pentoxyfylline associated with pentavalent antimony, decreases tissue inflammation in patients, leading to a curative therapy associated with the decrease of TNF and IFN-γ levels.[29] These results suggest that guanidines **10** and **11** exert antileishmanial activity by a direct effect on parasites, promoting anti-inflammatory modulation in host cells, which might contribute to a beneficial prognosis of the disease.

Because the antileishmanial activity of guanidines **10** and **11** was associated with other mechanisms than merely macrophage activation, we investigated possible intracellular targets in

DOI: 10.1021/acs.jnatprod.6b00256
J. Nat. Prod. XXXX, XXX, XXX−XXX

Leishmania. Damage to the plasma membrane and mitochondria was then evaluated using different fluorescent probes, as mitochondria are unique machinery in protozoan parasites and have been shown as a potential target for antiparasitic drugs.[30−33] The permeability of the *L.* (*L.*) *infantum* plasma membrane was observed using green-fluorescent nuclear and chromosome counter stain, which enters live cells and exhibits >500-fold fluorescence enhancement after binding nucleic acids.[34] Both guanidines **10** and **11** increased fluorescence levels, indicating a slight membrane permeabilization within 60 min of incubation.

The mitochondrial membrane potential is crucial for ATP generation in the respiratory chain.[33] In contrast to mammalian cells, where the presence of multiple mitochondria ensures compensation for functionally impaired ones, trypanosomatids present a single mitochondrion.[30] We investigated the effects of **10** and **11** on *Leishmania* mitochondria at initial contact. Both compounds **10** and **11** induced rapid depolarization of the mitochondrial membrane potential to levels similar to the positive control. Amphotericin B, used in the treatment of leishmaniasis, also increases permeability of the *Leishmania* plasma membrane, followed by a rapid decrease in the mitochondrial membrane potential.[35] Paromomycin significantly decreases the mitochondrial membrane potential of *Leishmania*, indicating that this organelle might be the ultimate drug target.[31,32]

Leishmania parasites present various defense mechanisms to cope with oxidative stress, including expression of antioxidant enzymes such as trypanothione,[36] superoxide dismutase,[37] peroxidases,[38] trypanothione S-transferase,[39] and 6-phosphogluconate dehydrogenase.[40] These enzymes, including iron superoxide dismutase and peroxiredoxin, are located in the mitochondria.[41] During oxidative stress, excessive amounts of ROS are produced in the mitochondria. These oxidant components, including superoxide radical ($O_2^{\bullet-}$), hydrogen peroxide (H_2O_2), hydroxyl radical ($HO^{\bullet}$), hypochlorite (OCl^-), and peroxynitrite ($ONOO^-$), are reactive signaling chemicals that accumulate under pathological conditions and lead to oxidative stress caused by dysfunction of the *Leishmania* mitochondrial respiratory chain.[42] Guanidine **10** was the most effective compound at enhancing ROS levels in *Leishmania*, while **11** showed a similar effect but to a lesser extent when compared to the positive control (sodium azide). Our results are in agreement with the mechanism of action (MoA) of other guanidines in protozoa. The antimalarial guanidine proguanil collapse the mitochondrial membrane potential of the parasite *Plasmodium*, the etiologic agent of malaria.[43] Considering similar effects in mitochondria, it seems probable that the guanidines herein investigated affect the respiratory system of *Leishmania*, leading to parasite death. This outcome may be a useful strategy to kill protozoans, as these microorganisms present a single mitochondrion. The capacity of these compounds to induce parasite death in the intracellular form without host cell activation is another significant outcome, important to provide new drug candidates useful to treat immunodeficient patients.

A series of 18 guanidines tested against *T. cruzi* and *L.* (*L.*) *infantum* parasites provided an elevated number of selective hits, with IC_{50} values below 10 μM. The two most active antileishmanial guanidines, compounds **10** and **11**, induce depolarization of the mitochondrial membrane potential, promoting a strong alteration of ROS levels in *Leishmania* parasites. Despite an effective detoxification system of these parasites, if not rapidly scavenged, the accumulated ROS are able to induce strong cellular damage. This effect might contribute to oxidative stress induced by guanidines **10** and **11**, leading to *L.* (*L.*) *infantum* elimination. A computational study was performed to predict pan-assay interference compounds (PAINS), but none of the compounds were predicted as PAINS (Supporting Information). The *in silico* studies, the *in vitro* potency of guanidines **10** and **11** (<10 μM), a selectivity index > 10, and the respective MoA against *Leishmania* parasites without affecting host cells allow us to select these compounds as possible hits for future investigations. Further experiments are in progress in order to gather information about ADMET properties and *in vivo* efficacy of compounds **10** and **11**. Results will be reported in due time.

EXPERIMENTAL SECTION

Chemicals. 3-(4,5-Dimethylthiazol-2-yl)-2,5-diphenyltetrazolium bromide (thiazolyl blue; MTT), resazurin (AlamarBlue), SYTOX Green, rhodamine 123, and H_2DCFDA were purchased from Molecular Probes. Giemsa stain, DMSO, and MeOH were obtained from Merck. RPMI-1640 medium, M-199 medium, Hank's balanced salts, phosphate-buffered saline (PBS), trypan blue stain, and miltefosine were obtained from Sigma. Other reagents were purchased from Sigma-Aldrich. The cytometric beads array (CBA, mouse inflammation kit, Biosciences) was from Becton Dixon.

Synthesis of Substrate Compounds. Guanidines **1**−**18** were tested as antileishmanial and antitrypanosomal compounds. Pyrimidine **1**, tricyclic guanidines **2**−**11** and **15**−**18**, tetracyclic guanidine **13**, and pentacyclic guanidine **12** were prepared as previously described.[17,44−54] The naturally occurring guanidine alkaloid nitensidine D (**14**)[50] was prepared as its hydrochloride salt in 53% yield by the reaction of geranylamine with 1*H*-pyrazole-1-carboxamidine hydrochloride (see Supporting Information).

General Bioassay Procedures. Golden hamsters and BALB/c mice were obtained by the animal breeding facility at the Adolfo Lutz Institute-SP, Brazil. The animals were maintained in sterilized cages under a controlled environment and received water and food *ad libitum*. Animal procedures were performed with the approval of the Research Ethics Commission (project number CEUA IAL/Pasteur 02/2011), in agreement with the Guide for the Care and Use of Laboratory Animals from the National Academy of Sciences.

Parasites and Mammalian Cell Maintenance. *L.* (*L.*) *infantum* (MHOM/BR/1972/LD) was maintained in golden hamsters (*Mesocricetus auratus*) up to approximately 60−70 days postinfection. Promastigotes were maintained in M-199 medium supplemented with 10% fetal calf serum (FBS) and 0.25% hemin at 24 °C. Amastigotes were obtained from the spleen of previously infected hamsters and purified by differential centrifugation. Macrophages were collected from the peritoneal cavity of BALB/c mice by washing them with RPMI-1640 medium supplemented with 10% FBS and were maintained at 37 °C in a 5% CO_2-humidified incubator. Trypomastigotes of *T. cruzi* (Y strain) were maintained in Rhesus-monkey kidney cells (LLC-MK2-ATCC CCL 7), cultivated in RPMI-1640 medium supplemented with 2% FBS at 37 °C in a 5% CO_2-humidified incubator. The murine conjunctive cells (NCTC clone 929, ATCC) were maintained in RPMI-1640 supplemented with 10% FBS at 37 °C in a humidified atmosphere containing 5% CO_2. NCTC-clone 929 cells were cultivated in M-199 medium, supplemented with 10% FBS at 37 °C in a 5% CO_2-humidified incubator.

Determination of the 50% Inhibitory Concentration (IC_{50}). Promastigotes in late growth phase (nonstationary at 3 × 10^7/mL, passage 5) were counted in a hemocytometer chamber and seeded at 1 × 10^6/well, with a final volume of 150 μL. The compounds were dissolved in DMSO and diluted in M-199 medium in 96-well microplates, with the highest concentration of 100 μM for 48 h at 24 °C. The parasite viability was determined using the MTT colorimetric assay.[55] The optical density was read at 570 nm (FilterMax F5 multimode microplate reader, Molecular Devices) using control wells

DOI: 10.1021/acs.jnatprod.6b00256
J. Nat. Prod. XXXX, XXX, XXX−XXX

without drugs (100% viability) and without cells (blank). The control group consisted of promastigotes incubated with 0.5% DMSO. Miltefosine was used as a standard drug. Compounds were tested to the highest concentration of 100 μM and were reported as NA (not active) when the IC_{50} value was above this concentration. For amastigotes, Peritoneal macrophages were collected from the peritoneal cavity of BALB/c mice, and the macrophages were seeded at 1×10^5/well for 24 h in a 16-well slide. Amastigotes were prepared as described previously in a 1:10 ratio of macrophages to amastigotes for 24 h at 37 °C in a 5% CO_2-humidified incubator. The compounds were incubated with infected macrophages for 120 h. Miltefosine was used as standard drug. Subsequently, the cells were fixed with MeOH, stained with Giemsa, and observed using a light microscope. The parasite burden was determined by the number of infected macrophages out of 400 cells.[20] Compounds were tested to the highest concentration of 100 μM and were reported as NA when the IC_{50} value was above this concentration.

Trypomastigotes of *T. cruzi*. Free trypomastigotes were counted in a hemocytometer chamber and seeded at 1×10^6 cells per well in 96-well microplates. The compounds were diluted in RPMI-1640 medium and incubated in highest concentrations to 150 μM for 24 h at 37 °C in a 5% CO_2-humidified incubator. The parasite viability was determined using resazurin (0.011% in PBS).[56] The optical density was read at 570 nm using control wells without drugs (100% viability) and without cells (blank). The control group consisted of trypomastigotes incubated with 0.5% DMSO. Benznidazole was used as a standard drug. Compounds were tested to the highest concentration of 100 μM and were reported as NA when the IC_{50} value was above this concentration.

Cytotoxicity in Mammalian Cells. NCTC cells were counted in a hemocytometer chamber, seeded at 6×10^4/well, and incubated in highest concentrations to 150 μM for 48 h at 37 °C in a 5% CO_2-humidified incubator. The cell viability was determined using the MTT assay.[55] Miltefosine was used as standard drug. The selectivity index was determined using the relationship CC_{50} against NCTC/IC_{50} against parasites.

Evaluation of Plasma Membrane Permeability. Late growth-phase (nonstationary at 3×10^7/mL, passage 7) promastigotes were washed in PBS, seeded at 2×10^6/well, and incubated with 1 μM SYTOX Green for 15 min at 24 °C.[34] The compounds **10** and **11** were added at their respective IC_{50} values (57 and 34 μM, respectively), and the fluorescence was measured every 20 min for 60 min total. The maximum permeabilization was obtained with 0.1% Triton X-100. Fluorescence intensity was determined using a fluorimetric microplate reader (FilterMax F5 multi-mode microplate reader, Molecular Devices) with excitation and emission wavelengths of 485 and 520 nm, respectively. The following internal controls were used in the evaluation: (i) the background fluorescence of test compounds, (ii) the possible interference of DMSO, (iii) untreated promastigotes, and (iv) medium without any cells. Samples were tested in triplicate.[57]

Evaluation of Mitochondrial Membrane Potential. The change in mitochondrial membrane potential in intact promastigotes was estimated by measuring rhodamine-123 accumulation.[58] Parasites (2×10^6 promastigotes/mL) were resuspended in Hank's balanced salt solution–glucose (HBSS-Glc) and incubated with **10** and **11** at the respective IC_{50} values (57 and 34 μM, respectively) for 60 min at 25 °C. Subsequently parasites were incubated with rhodamine-123 for 10 min (0.3 μg/mL, 5 min, 37 °C), washed by centrifugation, and resuspended in HBSS-Glc, and the fluorescence was determined using a fluorimetric microplate reader with excitation and emission wavelengths of 485 and 520 nm, respectively. Sodium azide (10 mM) was used as the positive control.[59] The following internal controls were used in the evaluation: (i) the background fluorescence of test compound, (ii) the possible interference of DMSO, (iii) untreated promastigotes, and (iv) medium without any cells. Samples were tested in triplicate.

Detection of ROS. Promastigotes (2×10^6/well) were washed with HBSS and incubated with **10** and **11** at the respective IC_{50} values (57 and 34 μM, respectively) for 60 min. H_2DCFDA was added (5 μM), and the cells were incubated for 15 min. Fluorescence intensity was evaluated using a fluorimetric microplate reader with excitation and emission wavelengths of 485 and 520 nm, respectively. Sodium azide (10 mM) was used as the positive control.[60−62] The following internal controls were used in the evaluation: (i) the background fluorescence of test compounds, (ii) the possible interference of DMSO, (iii) untreated promastigotes, and (iv) medium without any cells. Samples were tested in triplicate.

Quantification of Nitric Oxide. NO content was measured in the culture supernatants from peritoneal macrophages treated with compounds **10** and **11** at the respective IC_{50} values (intracellular amastigote assay = 5 and 2 μM, respectively) for 24 h and analyzed by Griess assay.[63] Results obtained were extrapolated from a standard curve prepared with $NaNO_2$ at different concentrations (0 to 400 μM). Bacterial LPS (1 μg/mL) was used as a positive control. Samples were tested in triplicate.

Cellular Immune Response Assay. Peritoneal Macrophages Cocultived with Splenocytes and *in Vitro* Infection. Peritoneal macrophages were isolated from BALB/c mice and seeded into the 24-well plate at 1.5×10^5 cells/well. After 24 h *L.* (*L.*) *infantum* amastigotes were used to infect the cells at a 1:10 ratio (macrophage/amastigotes).[20] After 24 h infected macrophages were cocultivated with splenocytes at a concentration of 6:1. Preparations were obtained by crushing spleens in PBS (pH 7.2). Subsequently, splenocyte suspensions were washed twice with PBS and erythrocytes were lysed with ammonium-chloride-potassium (ACK) buffer (0.15 M NH_4Cl; 10 mM $KHCO_3$; 0.1 M Na_2EDTA) for 5 min. After washing two times with PBS by centrifugation at 4 °C for 10 min, the cells were resuspended in RPMI 1640 medium and 10% heat-inactivated FBS. The viability of the cells used in the experiments was always higher than 85%, as measured by trypan blue exclusion. After 48 h with compounds **10** (30 μM) and **11** (15 μM), supernatants were collected to perform the cytokine assay. Proteins levels were determined using an inflammatory CBA kit according to the manufacturer's instructions. The concentrations of the released mediators were measured: interleukin-6 (IL-6), interleukin-10 (IL-10), monocyte chemotactic protein-1 chemokine (MCP-1), interferon-γ (IFN-γ), tumor necrosis factor (TNF), and interleukin-12p70 (IL-12p70) using flow cytometry. Sham-treated macrophages infected with *L.* (*L.*) *infantum* were used as controls.

Statistical Analysis. The results are represented as the mean and standard deviation of replicate samples from at least two independent assays. The IC_{50} values were calculated using sigmoidal dose–response curves using GraphPad Prism 5.0 software. The 95% confidence interval is included in parentheses with the analyses. The *t* test was used for significance testing ($p < 0.05$).

■ ASSOCIATED CONTENT

Supporting Information

The Supporting Information is available free of charge on the ACS Publications website at DOI: 10.1021/acs.jnatprod.6b00256.

Procedure for preparation of compound **14**; ^{1}H and ^{13}C NMR spectra for compounds **1**−**14** (not previously published) and **16**−**18**; PAINS analysis for guanidines (PDF)

■ AUTHOR INFORMATION

Corresponding Author

*Tel: (55 + 11) 3068-2974. Fax: (55 + 11) 3068-2890. E-mail: atempone@usp.br.

Present Address

#(A.G.T.) Center for Parasitology and Mycology, Instituto Adolfo Lutz, Avenida Dr. Arnaldo, 351, 8° andar, 01246-000 São Paulo, Brazil.

Notes

The authors declare no competing financial interest.

DOI: 10.1021/acs.jnatprod.6b00256
J. Nat. Prod. XXXX, XXX, XXX−XXX

■ ACKNOWLEDGMENTS

The authors thank the São Paulo Research Foundation (FAPESP) for financial support (grants 2012/18756-1 and 2013/50228-8 for A.G.T. and R.G.S.B., respectively; scholarships 2011/23703-1 and 2013/07275-5). A.G.T., R.G.S.B., and C.H.A. thank the Conselho Nacional de Desenvolvimento Científico e Tecnológico for scientific awards. ERDF BEACON project (P.J.M.), the European Social Fund KESS project (E.L.B.), the EPSRC (G.P.B., D.A.T., D.M.E.), AstraZeneca (D.A.T.), Pfizer (G.P.B.), and the Libyan Authority for Research, Science & Technology are also gratefully acknowledged. The authors would like to thank Goias Research Foundation (FAPEG) and ACD/I-Laboratories for providing credits to use their server.

■ REFERENCES

(1) World Health Organization. *Investing to overcome the global impact of neglected tropical diseases: third WHO report on neglected diseases*; World Health Organization: Geneva, 2015.
(2) Barrett, M. P.; Croft, S. L. *Parasitology* **2014**, *141*, 1−7.
(3) Da Silva Filho, A. A.; Resende, D. O.; Fukui, M. J.; Santos, F. F.; Pauletti, P. M.; Cunha, W. R.; Silva, M. L.; Gregório, L. E.; Bastos, J. K.; Nanayakkara, N. P. *Fitoterapia* **2009**, *80*, 478−482.
(4) World Health Organization. *Control of the Leishmaniases*; WHO Technical Report Series; WHO: Geneva, 2010.
(5) Tempone, A. G.; Sartorelli, P.; Mady, C.; Fernandes, F. *Cardiovasc. Hematol. Agents Med. Chem.* **2007**, *5*, 222−235.
(6) World Health Organization. *Chagas disease (American trypanosomiasis) fact sheet. Wkly Epidemiol Rec.*, WHO Technical Report Series; WHO: Geneva, 2010.
(7) Katsuno, K.; Burrows, J. N.; Duncan, K.; van Huijsduijnen, R. H.; Kaneko, T.; Kita, K.; Mowbray, C. E.; Schmatz, D.; Warner, P.; Slingsby, B. T. *Nat. Rev. Drug Discovery* **2015**, *14*, 751−758.
(8) Saczewski, F.; Balewski, L. *Expert Opin. Ther. Pat.* **2009**, *19*, 1417−1448.
(9) Sączewski, F.; Balewski, L. *Expert Opin. Ther. Pat.* **2013**, *23*, 965−995.
(10) Agarwal, K. C.; Sharma, V.; Shakya, N.; Gupta, S. *Bioorg. Med. Chem. Lett.* **2009**, *15*, 5474−5477.
(11) Santos, M. F.; Harper, P. M.; Williams, D. E.; Mesquita, J. T.; Pinto, E. G.; da Costa-Silva, T. A.; Hajdu, E.; Ferreira, A. G.; Santos, R. A.; Murphy, P. J.; Andersen, R. J.; Tempone, A. G.; Berlinck, R. G. *J. Nat. Prod.* **2015**, *22*, 1101−1111.
(12) Coleman, R. E.; Edman, J. D.; Semprevivo, L. H. *Ann. Trop. Med. Parasitol.* **1989**, *83*, 339−344.
(13) Espírito Santo, R. D.; Machado, M. G. M.; dos Santos, J. L.; González, E. R. P.; Chin, C. M. *Curr. Org. Chem.* **2014**, *18*, 2572−2602.
(14) Barrosa, K. H.; Pinto, E. G.; Tempone, A. G.; Martins, E. G.; Lago, J. H. *Planta Med.* **2014**, *80*, 1310−1314.
(15) Gonzalez, J. L.; Stephens, C. E.; Wenzler, T.; Brun, R.; Tanious, F. A.; Wilson, W.; Barszcz, T.; Werbovetz, K. A.; Boykin, D. W. *Eur. J. Med. Chem.* **2007**, *42*, 552−557.
(16) Ahmed, N.; Brahmbhatt, K. G.; Khan, S. I.; Jacob, M.; Tekwani, B. L.; Sabde, S.; Mitra, D.; Singh, I. P.; Khan, I. A.; Bhutani, K. K. *Chem. Biol. Drug Des.* **2013**, *81*, 491−498.
(17) Hua, H. M.; Peng, J.; Fronczek, F. R.; Kelly, M.; Hamann, M. T. *Bioorg. Med. Chem.* **2004**, *12*, 6461−6464.
(18) Stephens, C. E.; Brun, R.; Salem, M. M.; Werbovetz, K. A.; Tanious, F.; Wilson, W. D.; Boykin, D. W. *Bioorg. Med. Chem. Lett.* **2003**, *16*, 2065−2069.
(19) Don, R.; Ioset, J. R. *Parasitology* **2014**, *140*, 140−146.
(20) Tempone, A. G.; de Oliveira, C. M.; Berlinck, R. G. S. *Planta Med.* **2011**, *77*, 572−585.
(21) Aulner, N.; Danckaert, A.; Rouault-Hardoin, E.; Desrivot, J.; Helynck, O.; Commere, P. H.; Munier-Lehmann, H.; Späth, G. F.; Shorte, S. L.; Milon, G.; Prina, E. *PLoS Neglected Trop. Dis.* **2013**, *47*, e2154.
(22) Kedzierski, L.; Evans, K. J. *Parasitology* **2014**, *30*, 1−19.
(23) Santarem, A. A.; Greggianin, G. F.; Debastiani, R. G.; Ribeiro, J. B.; Polli, D. A.; Sampaio, R. N. *Rev. Soc. Bras. Med. Trop.* **2014**, *47*, 517−520.
(24) de Sá Oliveira, T.; Capp Neto, M.; Martins, B. J.; Rodrigues, H. A.; Antonino, R. M.; Magalhães, A. V. *Mem. Inst. Osw. Cruz.* **2000**, *95*, 477−482.
(25) Brandonisio, O.; Panaro, M. A.; Fumarola, I.; Sisto, M.; Leogrande, D.; Acquafredda, A.; Spinelli, R.; Mitolo, V. *Clin. Exp. Med.* **2002**, *2*, 2125−2129.
(26) Costa, D. L.; Rocha, R. L.; Carvalho, R. M.; Lima-Neto, A. S.; Harhay, M. O.; Costa, C. H.; Barral-Neto, M.; Barral, A. P. *Pathog. Global Health* **2013**, *107*, 78−87.
(27) Ansari, N. A.; Saluja, S.; Salotra, P. *Clin. Immunol.* **2006**, *119*, 339−345.
(28) Verma, S.; Kumar, R.; Katara, G. K.; Singh, L. C.; Negi, N. S.; Ramesh, V.; Salotra, P. *PLoS One* **2010**, *9*, e10107.
(29) Brito, G.; Dourado, M.; Polari, L.; Celestino, D.; Carvalho, L. P.; Queiroz, A.; Carvalho, E. M.; Machado, P. R.; Passos, S. *Am. J. Trop. Med. Hyg.* **2014**, *90*, 617−620.
(30) Fidalgo, L. M.; Gille, L. *Pharm. Res.* **2011**, *28*, 2758−70.
(31) Jhingran, A.; Chawla, B.; Saxena, S.; Barrett, M. P.; Madhubala, R. *Mol. Biochem. Parasitol.* **2009**, *164*, 111−117.
(32) Croft, S. L.; Sundar, S.; Fairlamb, A. H. *Clin. Microbiol. Rev.* **2006**, *19*, 111−126.
(33) Joshi, D. C.; Bakowska, J. C. *J. Visualized Exp.* **2011**, *23*, pii2704.
(34) Mangoni, M. L.; Saugar, J. M.; Dellisanti, M.; Barra, D.; Simmaco, M.; Rivas, L. *J. Biol. Chem.* **2005**, *280*, 984−990.
(35) Lee, N.; Bertholet, S.; Debrabant, A.; Muller, J.; Duncan, R.; Nakhasi, H. L. *Cell Death Differ.* **2002**, *9*, 53−64.
(36) Olin-Sandoval, V.; Moreno-Sánchez, R.; Saavedra, E. *Curr. Drug Targets* **2010**, *11*, 1614−1630.
(37) Mehlotra, R. K. *Crit. Rev. Microbiol.* **1996**, *22*, 295−314.
(38) Krauth-Siegel, L. R.; Comini, M. A.; Schlecker, T. *Subcell. Biochem.* **2007**, *44*, 231−251.
(39) Vickers, T. J.; Fairlamb, A. H. *J. Biol. Chem.* **2004**, *279*, 27246−27256.
(40) Dardonville, C.; Rinaldi, E.; Hanau, S.; Barrett, M. P.; Brun, R.; Gilbert, I. H. *Bioorg. Med. Chem.* **2003**, *11*, 3205−3214.
(41) Castro, H.; Teixeira, F.; Romao, S.; Santos, M.; Cruz, T.; Flórido, M.; Appelberg, R.; Oliveira, P.; Ferreira-da-Silva, F.; Tomás, A. M. *PLoS Pathog.* **2011**, *7*, e1002325.
(42) Mesquita, J. T.; Pinto, E. G.; Taniwaki, N. N.; Galisteo, A. J., Jr; Tempone, A. G. *Acta Trop.* **2013**, *128*, 666−673.
(43) Bridges, H. R.; Jones, A. J.; Pollak, M. N.; Hirst, J. *Biochem. J.* **2014**, *15*, 475−487.
(44) Black, G. P.; Murphy, P. J.; Walshe, N. D. A.; Hibbs, D. E.; Hursthouse, M. B.; Malik, K. M. A. *Tetrahedron Lett.* **1996**, *37*, 6943−6946.
(45) Black, G. P.; Murphy, P. J.; Walshe, N. D. A. *Tetrahedron* **1998**, *54*, 9481−9488.
(46) Caukett, P.; Howard-Jones, A.; Murphy, P. J.; Thomas, D. *J. Org. Chem.* **1999**, *64*, 1039−1041.
(47) Black, G. P.; Coles, S. J.; Hizi, A.; Howard-Jones, A. G.; Hursthouse, M. B.; McGown, A. T.; Loya, S.; Moore, C. G.; Murphy, P. J.; Smith, N. K.; Walshe, N. D. A. *Tetrahedron Lett.* **2001**, *42*, 3377−3381.
(48) Allingham, M. T.; Howard-Jones, A.; Murphy, P. J.; Thomas, D. A.; Caulkett, P. W. R. *Tetrahedron Lett.* **2003**, *44*, 8677−8680.
(49) Bennett, F. E. L.; Black, G. P.; Browne, P.; Hizi, A.; Jaffar, M.; Leyland, J. P.; Martin, C.; Oz-Gleenberg, I.; Murphy, P. J.; Roberts, T. D.; Thornhill, A. J.; Vale, S. A. *Tetrahedron* **2013**, *69*, 3061−3066.
(50) Regasini, L. O.; Gamboa, I. C.; Silva, D. H. S.; Furlan, M.; Barreiro, E. J.; Ferreira, P. M. P.; Pessoa, C.; Lotufo, L. V. C.; Moraes, M. O.; Young, M. C. M.; Bolzani, V. S. *J. Nat. Prod.* **2009**, *72*, 473−476.

DOI: 10.1021/acs.jnatprod.6b00256
J. Nat. Prod. XXXX, XXX, XXX−XXX

(51) Cohen, F.; Overman, L. E. *J. Am. Chem. Soc.* **2006**, *128*, 2594–2603.
(52) Cohen, F.; Overman, L. E. J. *J. Am. Chem. Soc.* **2006**, *128*, 2604–2608.
(53) Franklin, A. S.; Ly, S. K.; Mackin, G. H.; Overman, L. E.; Shaka, A. J. *J. Org. Chem.* **1999**, *64*, 1512–1519.
(54) Cohen, F.; Overman, L. E.; Sakata, S. K. L. *Org. Lett.* **1999**, *1*, 2169–2172.
(55) Tada, H.; Shiho, O.; Kuroshima, K.; Koyama, M.; Tsukamoto, K. J. *J. Immunol. Methods* **1986**, *93*, 157–165.
(56) Mikus, J.; Steverding, D. *Parasitol. Int.* **2000**, *3*, 265–269.
(57) Kulkarni, M. M.; Reddy, N.; Gude, T.; McGwire, B. S. *Parasitol. Res.* **2013**, *5*, 2095–2099.
(58) Luque-Ortega, J. R.; Rivero-Lezcano, O. M.; Croft, S. L.; Rivas, L. *Antimicrob. Agents Chemother.* **2001**, *45*, 1121–1125.
(59) Luque-Ortega, J. R.; Rivas, L. *Methods Mol. Biol.* **2010**, *25*, 393–491.
(60) Coimbra, E. S.; Gonçalves-da-Costa, S. C.; Corte-Real, S.; De Freitas, F. G.; Durão, A. C.; Souza, C. S.; Silva-Santos, M. I.; Vasconcelos, E. G. *Parasitology* **2002**, *124*, 137–143.
(61) al Tuwaijri, A. S.; al Mofleh, I. A.; Mahmoud, A. A. *J. Med. Microbiol.* **1990**, *32*, 189–193.
(62) Saraiva, E. M.; Vannier-Santos, M. A.; Silva-Filho, F. C.; de Souza, W. *J. Cell. Sci.* **1989**, *93*, 481–489.
(63) Lezama-Dávila, C. M.; Isaac-Márquez, A. P.; Barbi, J.; Cummings, H. E.; Lu, B.; Satoskar, A. R. *Immunol. Cell Biol.* **2008**, *86*, 539–543.

DOI: 10.1021/acs.jnatprod.6b00256
J. Nat. Prod. XXXX, XXX, XXX–XXX